frontiers | Research Topics

Primary and acquired resistance in lung cancer

Edited by
Rossella Bruno, Michele Simbolo and Iacopo Petrini

Published in
Frontiers in Oncology

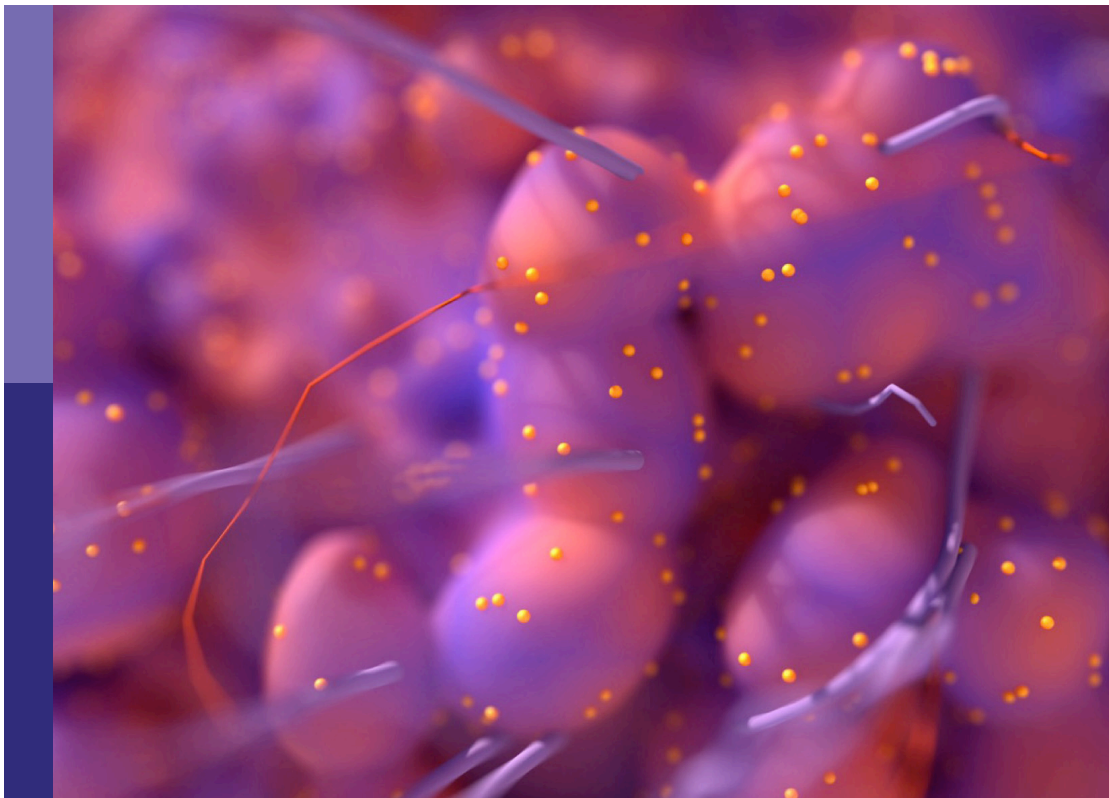

ISSN 1664-8714
ISBN 978-2-8325-3939-2
DOI 10.3389/978-2-8325-3939-2

About Frontiers

Frontiers is more than just an open access publisher of scholarly articles: it is a pioneering approach to the world of academia, radically improving the way scholarly research is managed. The grand vision of Frontiers is a world where all people have an equal opportunity to seek, share and generate knowledge. Frontiers provides immediate and permanent online open access to all its publications, but this alone is not enough to realize our grand goals.

Frontiers journal series

The Frontiers journal series is a multi-tier and interdisciplinary set of open-access, online journals, promising a paradigm shift from the current review, selection and dissemination processes in academic publishing. All Frontiers journals are driven by researchers for researchers; therefore, they constitute a service to the scholarly community. At the same time, the *Frontiers journal series* operates on a revolutionary invention, the tiered publishing system, initially addressing specific communities of scholars, and gradually climbing up to broader public understanding, thus serving the interests of the lay society, too.

Dedication to quality

Each Frontiers article is a landmark of the highest quality, thanks to genuinely collaborative interactions between authors and review editors, who include some of the world's best academicians. Research must be certified by peers before entering a stream of knowledge that may eventually reach the public - and shape society; therefore, Frontiers only applies the most rigorous and unbiased reviews. Frontiers revolutionizes research publishing by freely delivering the most outstanding research, evaluated with no bias from both the academic and social point of view. By applying the most advanced information technologies, Frontiers is catapulting scholarly publishing into a new generation.

What are Frontiers Research Topics?

Frontiers Research Topics are very popular trademarks of the *Frontiers journals series*: they are collections of at least ten articles, all centered on a particular subject. With their unique mix of varied contributions from Original Research to Review Articles, Frontiers Research Topics unify the most influential researchers, the latest key findings and historical advances in a hot research area.

Find out more on how to host your own Frontiers Research Topic or contribute to one as an author by contacting the Frontiers editorial office: frontiersin.org/about/contact

Primary and acquired resistance in lung cancer

Topic editors

Rossella Bruno — University Hospital of Pisa, Italy
Michele Simbolo — University of Verona, Italy
Iacopo Petrini — University of Pisa, Italy

Citation

Bruno, R., Simbolo, M., Petrini, I., eds. (2023). *Primary and acquired resistance in lung cancer*. Lausanne: Frontiers Media SA. doi: 10.3389/978-2-8325-3939-2

Table of contents

frontiers | Frontiers in Oncology

TYPE Editorial
PUBLISHED 01 November 2023
DOI 10.3389/fonc.2023.1310331

OPEN ACCESS

EDITED AND REVIEWED BY
Lizza E.L. Hendriks,
Maastricht University Medical Centre,
Netherlands

*CORRESPONDENCE
Rossella Bruno
rossella.bruno@for.unipi.it

RECEIVED 09 October 2023
ACCEPTED 12 October 2023
PUBLISHED 01 November 2023

CITATION
Bruno R, Simbolo M and Petrini I (2023) Editorial: Primary and acquired resistance in lung cancer.
Front. Oncol. 13:1310331.
doi: 10.3389/fonc.2023.1310331

Editorial: Primary and acquired resistance in lung cancer

Rossella Bruno[1]*, Michele Simbolo[2] and Iacopo Petrini[3]

[1]Unit of Pathological Anatomy, University Hospital of Pisa, Pisa, Italy, [2]Department of Diagnostics and Public Health, Section of Pathology, University of Verona, Verona, Italy, [3]Medical Oncology, Department of Translational Research and New Technologies in Medicine and Surgery, University of Pisa, Pisa, Italy

KEYWORDS

lung cancer, targeted therapy, immunotherapy, predictive biomarkers, primary resistance, acquired resistance

Editorial on the Research Topic
Primary and acquired resistance in lung cancer

Targeted therapies and immunotherapy have significantly enhanced treatment of patients with advanced and metastatic non-small cell lung cancer (NSCLC), which accounts for about 85% of all lung cancer cases (1). The molecular characterization of non-squamous tumors is necessary to identify patients harboring targetable alterations (2). Despite the continuous advances of precision medicine, primary and acquired drug resistance remains a challenge (2).

The articles featured in this Research Topic mainly focus on *EGFR* and *KRAS* addicted tumors, collectively accounting for approximately 45% of NSCLC. The authors describe resistance mechanisms to tyrosine-kinase inhibitors (TKIs) and immune-checkpoint inhibitors. Additionally, this Research Topic includes a study exploring the predictive role of genetic alterations in small cell lung cancer (SCLC).

In NSCLC, *EGFR* exhibits somatic mutations of the intracellular tyrosine-kinase domain mainly between exons 18-21. The majority of these mutations are predictive of TKI response, while a minority confers resistance to specific treatments (2). Resistance mechanisms vary depending on drugs and include on-target (secondary alterations within the same gene) and off-target mechanisms (alternative pathway activation, histological transformation). The acquisition of the T790M mutation within *EGFR* exon 20 is the most common resistance mechanism to first (gefitinib, erlotinib) and second-generation (afatinib) TKIs. Hsieh et al. reported a higher T790M mutation rate with first compared to second-generation TKIs. Tumors carrying T790M mutation respond to the third-generation EGFR inhibitor, osimertinib, which was initially approved for patients with this acquired resistance mechanism. Currently, osimertinib is the preferred drug for the first-line therapy of tumors with *EGFR* common activating mutations (3). There are not predominant resistance mutations for third-generation TKIs (4). Mahfoudhi et al. reviewed preclinical studies evaluating acquired resistance to third-generation EGFR TKIs across all treatment lines. Secondary *EGFR* mutations, like C797S, occur in approximately 10% of patients. In contrast, most tumors activate alternative pathways bypassing EGFR inhibition (i.e. *MET* amplification). Recent studies, as reported by Fabrizio et al., explored the influence of epigenetic alterations (DNA methylation and miRNA deregulation) on treatment resistance. There is an emerging evidence for a role of multi-gene and

genome-wide global methylation profile, particularly when liquid biopsy is employed. In the same context, Lee et al. showed how platelet activation can confer acquired resistance to EGFR TKIs, thus suggesting new therapeutic strategies.

Mutations affecting *KRAS* gene are the most frequent in lung cancer, those specific to codon 12 are especially related to smokers. To date, only *KRAS* G12C inhibitors are approved for the second-line treatment of NSCLC patients who progress to a first-line immunotherapy or chemo-immunotherapy (2). KRAS inhibitors specific for G12D mutation are under evaluation in preliminary clinical trials (5). Therefore, the initial treatment for NSCLC patients carrying *KRAS* mutations is immunotherapy or chemo-immunotherapy, according to PD-L1 expression levels. Alternatively, chemotherapy is considered for patients with contraindication for immunotherapy. As described by Fancelli et al., different *KRAS* mutations have distinct characteristics and behaviors. Improved outcomes are observed with immunotherapy alone or in combination with chemotherapy when compared with chemotherapy alone, especially for mutations G12C, G12D and G12A, while a poorer prognosis is associated with G12V mutation. In clinical trials KRAS G12C inhibitors obtain objective responses between 30-50%, with a median progression free survival (PFS) of 5.6-6.5 months (6, 7). Resistance mechanisms to KRAS G12C inhibitors are poorly characterized. Ning et al. reviewed non-genetic mechanisms, including epithelial to mesenchymal transition, which are responsible of adaptive drug resistance and treatment failure. Considering the relative low response rate and PFS of KRAS inhibitors, identification of factors impacting response is crucial. Strategies promoting mesenchymal-to-epithelial transition, as well as the inhibition of YAP (oncoprotein acting downstream Hippo pathway) should be further investigated.

As mentioned before, immunotherapy is an important option for patients without targetable alterations (8) not only in the advanced settings, but also in early stages as neoadjuvant or adjuvant treatment (9). Neoadjuvant chemo-immunotherapy improved overall survival compared to chemotherapy in phase III clinical trials (10, 11). Alì et al. showed that neoadjuvant chemo-immunotherapy improved pathological responses compared to chemotherapy alone, and correlated with a better overall survival and event free survival in resectable NSCLC. However, a substantial percentage of patients do not respond to neoadjuvant chemo-immunotherapy. Consequently, there is an urgent need for predictive biomarkers. PD-L1, predictive of response for stage IV patients, has a limited utility in the neoadjuvant setting. In the same study authors observed that after chemo-immunotherapy residuals tumors showed enhanced expression levels of *YAP/TAZ* and *CTLA4* genes opening new interesting scenarios.

When the first-line chemo-immunotherapy or immunotherapy alone fails, chemotherapy becomes the standard second-line option, but it is often associated with toxicity and limited effectiveness. The combination of anti-angiogenetic drugs with taxane has improved patients' outcome: for example, the addition of ramucirumab to docetaxel slightly increased overall survival after progression to a first-line chemotherapy (12). The effect of this combination after immunotherapy remains poorly characterized. Nevertheless, in preclinical studies it has been demonstrated that anti-angiogenic drugs can modulate tumor microenvironment enhancing the activity of immune check-point inhibitors (13). Kareff et al. evaluated the use of ramucirumab and docetaxel following disease progression on chemotherapy and immunotherapy combination. Their data support the advantageous effect of a combined chemotherapy and anti-angiogenic therapy after first-line immunotherapy exposure.

Precision medicine perfectly suits NSCLC, whereas therapeutic options are still limited for SCLC (15% of all cases). SCLC patients typically achieve tumor shrinkage with the first-line of chemotherapy, but, thereafter, they often rapidly experience disease progression (14). SCLC genetic landscape could help to understand how to stratify tumors improving prognosis definition. In their study Tang et al. used whole exome sequencing data to identify significant genetic differences, developing a classifier capable of predicting chemoresistance, chemosensitivity, and the risk of recurrence in SCLC.

Comprehensive genome profiling is providing valuable insights into resistance mechanisms to lung cancer treatments. However, it is important to recognize that various resistance alterations can coexist within the same tumor or between primary tumors and metastatic sites. It is essential to thoroughly evaluate resistance at molecular levels to track the genetic evolution of cancer and optimize treatment.

Author contributions

RB: Writing – original draft, Writing – review & editing. MS: Writing – original draft, Writing – review & editing. IP: Writing – original draft, Writing – review & editing.

Funding

The author(s) declare that no financial support was received for the research, authorship, and/or publication of this article.

Acknowledgments

We acknowledge all the Authors who contributed to this Research Topic.

Conflict of interest

The authors declare that the research was conducted in the absence of any commercial or financial relationships that could be construed as a potential conflict of interest.

Publisher's note

References

1. Villaruz LC, Socinski MA, Weiss J. Guidance for clinicians and patients with non-small cell lung cancer in the time of precision medicine. *Front Oncol* (2023) 13:1124167. doi: 10.3389/fonc.2023.1124167

2. Hendriks LE, Kerr KM, Menis J, Mok TS, Nestle U, Passaro A, et al. Oncogene-addicted metastatic non-small-cell lung cancer: ESMO Clinical Practice Guideline for diagnosis, treatment and follow-up. *Ann Oncol* (2023) 34:339–57. doi: 10.1016/j.annonc.2022.12.009

3. Ramalingam SS, Vansteenkiste J, Planchard D, Cho BC, Gray JE, Ohe Y, et al. Overall survival with osimertinib in untreated, *EGFR* -mutated advanced NSCLC. *N Engl J Med* (2020) 382:41–50. doi: 10.1056/NEJMoa1913662

4. Leonetti A, Sharma S, Minari R, Perego P, Giovannetti E, Tiseo M. Resistance mechanisms to osimertinib in EGFR-mutated non-small cell lung cancer. *Br J Cancer* (2019) 121:725–37. doi: 10.1038/s41416-019-0573-8

5. Christensen JG, Hallin J. The KRASG12D inhibitor MRTX1133 elucidates KRAS-mediated oncogenesis. *Nat Med* (2022) 28:2017–8. doi: 10.1038/s41591-022-02008-6

6. de Langen AJ, Johnson ML, Mazieres J, Dingemans A-MC, Mountzios G, Pless M, et al. Sotorasib versus docetaxel for previously treated non-small-cell lung cancer with KRASG12C mutation: a randomised, open-label, phase 3 trial. *Lancet* (2023) 401:733–46. doi: 10.1016/S0140-6736(23)00221-0

7. Jänne PA, Riely GJ, Gadgeel SM, Heist RS, Ou S-HI, Pacheco JM, et al. Adagrasib in non-small-cell lung cancer harboring a KRASG12C mutation. *N Engl J Med* (2022) 387:120–31. doi: 10.1056/NEJMoa2204619

8. Gridelli C, Peters S, Mok T, Forde PM, Reck M, Attili I, et al. First-line immunotherapy in advanced non-small-cell lung cancer patients with ECOG performance status 2: results of an International Expert Panel Meeting by the Italian Association of Thoracic Oncology. *ESMO Open* (2022) 7:100355. doi: 10.1016/j.esmoop.2021.100355

9. De Scordilli M, Michelotti A, Bertoli E, De Carlo E, Del Conte A, Bearz A. Targeted therapy and immunotherapy in early-stage non-small cell lung cancer: current evidence and ongoing trials. *IJMS* (2022) 23:7222. doi: 10.3390/ijms23137222

10. Wakelee H, Liberman M, Kato T, Tsuboi M, Lee S-H, Gao S, et al. Perioperative pembrolizumab for early-stage non-small-cell lung cancer. *N Engl J Med* (2023) 389:491–503. doi: 10.1056/NEJMoa2302983

11. Forde PM, Spicer J, Lu S, Provencio M, Mitsudomi T, Awad MM, et al. Neoadjuvant nivolumab plus chemotherapy in resectable lung cancer. *N Engl J Med* (2022) 386:1973–85. doi: 10.1056/NEJMoa2202170

12. Garon EB, Ciuleanu T-E, Arrieta O, Prabhash K, Syrigos KN, Goksel T, et al. Ramucirumab plus docetaxel versus placebo plus docetaxel for second-line treatment of stage IV non-small-cell lung cancer after disease progression on platinum-based therapy (REVEL): a multicentre, double-blind, randomised phase 3 trial. *Lancet* (2014) 384:665–73. doi: 10.1016/S0140-6736(14)60845-X

13. Subramanian M, Kabir AU, Barisas D, Krchma K, Choi K. Conserved angio-immune subtypes of the tumor microenvironment predict response to immune checkpoint blockade therapy. *Cell Rep Med* (2023) 4:100896. doi: 10.1016/j.xcrm.2022.100896

14. Rudin CM, Brambilla E, Faivre-Finn C, Sage J. Small-cell lung cancer. *Nat Rev Dis Primers* (2021) 7:3. doi: 10.1038/s41572-020-00235-0

frontiers | Frontiers in Oncology

REVIEW
published: 07 April 2022
doi: 10.3389/fonc.2022.853501

Preclinical Models for Acquired Resistance to Third-Generation EGFR Inhibitors in NSCLC: Functional Studies and Drug Combinations Used to Overcome Resistance

Emna Mahfoudhi[1], *Charles Ricordel*[1,2], *Gwendoline Lecuyer*[1], *Cécile Mouric*[1], *Hervé Lena*[1,2] *and Rémy Pedeux*[1]*

[1] Univ Rennes, Institut Nationale de la Santé et de la Recherche Médicale (INSERM), COSS (Chemistry Oncogenesis Stress Signaling), UMR_S 1242, Centre de Lutte Contre le Cancer (CLOC) Eugène Marquis, Rennes, France, [2] Centre Hospitalier Universitaire de Rennes, Service de Pneumologie, Université de Rennes 1, Rennes, France

Epidermal growth factor receptor (EGFR)-tyrosine kinase inhibitors (TKIs) are currently recommended as first-line treatment for advanced non-small-cell lung cancer (NSCLC) with *EGFR*-activating mutations. Third-generation (3rd G) EGFR-TKIs, including osimertinib, offer an effective treatment option for patients with NSCLC resistant 1st and 2nd EGFR-TKIs. However, the efficacy of 3rd G EGFR-TKIs is limited by acquired resistance that has become a growing clinical challenge. Several clinical and preclinical studies are being carried out to better understand the mechanisms of resistance to 3rd G EGFR-TKIs and have revealed various genetic aberrations associated with molecular heterogeneity of cancer cells. Studies focusing on epigenetic events are limited despite several indications of their involvement in the development of resistance. Preclinical models, established in most cases in a similar manner, have shown different prevalence of resistance mechanisms from clinical samples. Clinically identified mechanisms include EGFR mutations that were not identified in preclinical models. Thus, NRAS genetic alterations were not observed in patients but have been described in cell lines resistant to 3rd G EGFR-TKI. Mainly, resistance to 3rd G EGFR-TKI in preclinical models is related to the activation of alternative signaling pathways through tyrosine kinase receptor (TKR) activation or to histological and phenotypic transformations. Yet, preclinical models have provided some insight into the complex network between dominant drivers and associated events that lead to the emergence of resistance and consequently have identified new therapeutic targets. This review provides an overview of preclinical studies developed to investigate the mechanisms of acquired resistance to 3rd G EGFR-TKIs, including osimertinib and rociletinib, across all lines of therapy. In fact, some of the models described were first generated to be resistant to first- and second-generation EGFR-TKIs and often carried the T790M mutation, while others had never been exposed to TKIs. The review further describes the therapeutic opportunities to overcome resistance, based on preclinical studies.

Keywords: preclinical models, 3rd G EGFR-TKI, resistance mechanism, osimertinib, lung cancer

OPEN ACCESS

Edited by:
Iacopo Petrini,
University of Pisa, Italy

Reviewed by:
Jih-Hsiang Lee,
National Taiwan University, Taiwan
Elena Levantini,
Harvard Medical School, United States

***Correspondence:**
Rémy Pedeux
remy.pedeux@univ-rennes1.fr

Specialty section:
This article was submitted to Thoracic Oncology, a section of the journal Frontiers in Oncology

Received: *12 January 2022*
Accepted: *02 March 2022*
Published: *07 April 2022*

Citation:
Mahfoudhi E, Ricordel C, Lecuyer G, Mouric C, Lena H and Pedeux R (2022) Preclinical Models for Acquired Resistance to Third-Generation EGFR Inhibitors in NSCLC: Functional Studies and Drug Combinations Used to Overcome Resistance. Front. Oncol. 12:853501. doi: 10.3389/fonc.2022.853501

INTRODUCTION

Epidermal growth factor receptor (*EGFR*)-activating mutations in non-small-cell lung cancer (NSCLC) are an important predictor of treatment efficacy with EGFR tyrosine kinase inhibitors (TKIs). EGFR-TKIs have been shown to prolong the survival of patients with tumors harboring *EGFR*-activating mutations from less than 1 year to approximately 20 to 30 months (1, 2). Despite the initial benefits, almost all tumors develop resistance leading to disease progression. Acquired resistance against the first- and second-generation EGFR-TKIs is primarily caused by the development of the secondary $EGFR^{T790M}$ mutation (3, 4). Several third-generation EGFR-TKIs have been developed to overcome T790M-induced resistance. AZD9291 (osimertinib), CO-1686 (rociletinib), HM61713 (olmutinib), EGF816 (nazartinib), ASP8273 (naquotinib), lazertinib (YH25448), PF06747775, and AC0010 (avitinib) are third-generation (3rd G) EGFR-TKIs, which selectively and irreversibly inhibit EGFR with the common activating mutations, exon 19 deletion (Del19) and exon 21 L858R mutation, and the T790M mutation while sparing wild-type EGFR (5, 6). Currently, osimertinib is the standard of care for EGFR-positive advanced NSCLC with T790M mutation. It has been shown to have remarkably positive results as a first-line treatment for EGFR-mutated advanced NSCLC, with a median progression-free survival (PFS) of 18.9 months (7), leading to its approval for first-line treatment of metastatic EGFR-mutated NSCLC.

Preclinical modeling and analysis of tumor tissue obtained from patients after disease progression have led to the identification of many mechanisms involved in resistance. Contrary to 1st- and 2nd-generation TKIs, no predominant gatekeeper-resistant gene mutations have been observed (8). In clinical studies, mechanisms responsible for resistance include the emergence of mutations in exon 20 of EGFR (e.g., C797S) (9), MET and HER2 amplification, gene fusion, altered cell cycle genes, and *de novo* mutations in KRAS (10).

The pattern of resistance mechanisms differs in the reported clinical and preclinical studies. The vast majority of preclinical models developed to date to identify the mechanisms underlying resistance to 3rd G EGFR-TKIs have used sensitive cell line models exposed to the drug until resistance emerges. The drug concentrations and exposure duration vary from study to study. However, despite the large number of models available, 40% to 50% of the genetic mechanisms associated with disease progression during osimertinib treatment are still unknown (11). This raises the question of whether continuing to generate preclinical models on a recurrent basis would really help to better decipher the mechanisms involved in resistance acquisition and discover biomarkers of relapse. Resistance to EGFR-TKIs therapy is associated with high tumor heterogeneity (12). Such heterogeneity requires tools that mimic the real world for the discovery and evaluation of new therapeutic strategies.

Recent published reviews on resistance mechanisms have focused, in particular, on clinical studies (13–18). Only one review specifically addressed preclinical models, but only those generated from cell lines resistant to first-line osimertinib (19). In this review, we describe reported preclinical models established to identify mechanisms responsible for or involved in resistance to 3rd G EGFR-TKIs and the combinatorial approaches used to circumvent this resistance. We also highlight whether the identified mechanism has been reported in clinical studies. In **Table 1**, the models are listed in the order in which they are cited in the review. Drug doses or the duration of treatment are not listed if not reported in the original articles or references. Models based on modified cell lines generated by transfection, transduction, and/or site-directed mutagenesis are not included in **Table 1**, but are mentioned in the review.

EPIGENETICS IN EGFR-TKIs RESISTANCE IN NSCLC

Resistance to EGFR-TKIs may be related to the presence of preexisting drug-resistant subclones that will be selected under treatment pressure (52) or to the expansion of persistent cells (with or without an acquired resistance mechanism) after the initial response to targeted therapy (53–55). The question that arises is how, in the absence of a genetic mechanism triggering the development of resistance, persister cells manage to escape EGFR-TKI therapy. Previous studies have suggested that entering into a drug-tolerant (DT) persister state is an alternative strategy towards acquiring resistance. It has been reported that small cell populations undergo non-genetic adaptations that allow survival in the presence of the drug from which a fraction of cells can grow into the drug (53, 56). The first attempt to characterize the drug-tolerant cells was reported in 2010 by Sharma et al.; DT persister PC9 cells generated by lethal exposure to erlotinib showed upregulation of histone demethylase KDM5A associated with impaired histone deacetylase (HDAC) activity. Interestingly, the cells returned to spontaneous sensitivity after drug withdrawal (57). Subsequent studies identified other targets related to persister DT cells including IGF1-R (58), and Axl (59), in addition to modulation of apoptosis involving Mcl-1 (60) and Aurora kinases (61). In addition to this, sensitivity to 3rd G EGFR-TKIs had been restored in resistant cell lines generated after drug withdrawal (47, 49), suggesting a non-genetic adaptation. Taken together, these studies indicate a potential role for epigenetics in the adaptation persister drug-tolerant cells. Epigenetic modulations are changes that affect cellular phenotype without affecting the DNA sequence. These changes include DNA methylation, post-translational modifications of histones, and small and long non-coding RNA sequences, all of which may be reversible and heritable modifications. While the mechanisms of genetic resistance to 3rd G EGFR-TKIs, in particular osimertinib, are widely investigated in clinical and preclinical studies, the epigenetic involvement is not well characterized and remains poorly understood. Nevertheless, some published data show a strong epigenetic involvement in this phenomenon and invite further investigations. First, the methylcytosine dioxygenase TET2 and the methyltransferase DNMT3A appeared in the mutational profile of NSCLC patients on post-osimertinib

TABLE 1 | Preclinical models of resistance to third-generation EGFR-TKIs.

Model generation method	Cell line	3rd G TKI	Genetic alteration	Therapy	Method/ approach	References
On-target EGFR-dependent mechanisms						
Dose escalation method (0.3 to 1 μM) for several months	PC9	Rocilitinib	EGFR amplification	Cetuximab + rocilitinib Afatinib + rocilitinib	FISH, Exome sequencing, DNA qPCR	Nukaga et al. (20)
MAPK/PI3K implication						
- Chronic treatment with osimertinib single dose 160 nM for several months -Dose escalation method until 160 nM osimertinib -Dose escalation method until 1500 nM WZ4002 or osimertinib	PC9 and H1975	Osimertinib WZ4002	- NRAS gain - NRAS Q61K, NRAS E63K and NRAS G12V/R - KRAS gain - MAPK1 gain - CRKL1 gain	Selumetinib (MEK inhibitor) + osimertinib	SnaPshot mutation analysis, targeted and whole exome sequencing	Eberlein et al. (21)
Dose-escalation exposure (0.01 to 1.0 μmol/L) for 7.8 months followed by single-cell cloning	Gefetinib resistant PC9 (T790M +)	Naquotinib	NRAS amplification in all sub-clones	Selumetinib/Trametinib (MEK inhibitor) + naquotinib	RNA kinome sequencing, WB, qPCR, and NRAS-GTP pull-down	Ninomiya et al. (22)
Escalation dose steps (0.3 to 1 μM)	PC9	Osimertinib	KRAS G13D	ND	Whole-exome sequencing (WES)	Nukaga et al. (20)
Exposure to increasing concentration (10 nM to 1 μM)	PC9	Osimertinib	HRAS G13R with increased MET expression	ND	NGS	Ku et al. (23)
Exposure to increasing concentration (10 to 500 nM) followed by cloning	PC9	Osimertinib	BRAF G469	Selumetinib/Trametinib + osimertinib	NGS	La Monica et al. (24)
Dose escalation method (0.3 to 1 μM)	H1975	Osimertinib	Integrin β1 and phospho-Src upregulation with EMT	Dasatinib/bosutinib (src inhibitor) + osimertinib	WB and Q-PCR	Nukaga et al. (20)
MET alterations						
- PC9 mice xenograft tumors collected after 100 days of rociletinib administration (150 mg/kg BID) - L858R-positive patient-derived xenograft	–	Rocilitinib	MET amplification	Crizotinib + rocilitinib	CAPP-Seq profiling, NGS, RTK array, FISH	Chabon et al. (25)
Exposure to increasing concentrations (10 nM to 500 nM) for approximately 6 months	HCC827	Osimertinib Cross resist to CO-1686 and erlotinib	MET copy gain	ARQ179/ SGX523 / crizotinib (MET inhibitors) + osimertinib	WB, qPCR	Shi et al. (26)
Resistant clones were generated by cloning of Resistant cell populations established from resistant xenograft tumors obtained after a series of continuous drug exposure for 115 days.	H1975	AC0010 Cross- resist to CO-1686 and to osimertinib	MET upregulation	Crizotinib + AC0010	RNA-sequencing, WB	Xu et al. (27)
Exposure to increasing concentrations (0.01 to 1.0 μmol/L) during 5.2 months	PC9	Naquotinib	MET amplification	Crizotinib/SGX523 + naquotinib	Phospho-RTK arrays, WB, FISH	Ninomiya et al. (22)
AXL						
Resistant cells were established from subcutaneous tumors collected from mice treated for 29 days with osimertinib	PC9	Osimertinib	AXL overexpression	ONO-7475 (AXL inhibitor) + osimertinib	WB	Okura et al. (28)
Stepwise escalation up to 3 μM	H1975	Osimertinib	STC2 upregulation AXL overexpression	R428 (AXL inhibitor) + osimertinib	WB, qPCR, phospho-RTK array	Liu et al. (29)
Exposure to escalating doses (0.001–0.5 μM)	HCC827	Osimertinib	GAS6 overexpression AXL overexpression	YD (degrader) + osimertinib	WB, IHC	Kim et al. (30)
- Exposure to stepwise escalation (10 nmol/L to 2 μmol/L) over 6 months - Exposure intermittently to 2 μmol/L over 6 months	HCC827, HCC4006, PC-9, H1975	Osimertinib	AXL upregulation AXL upregulation+ EMT+ EGFR copy loss+ ALDHA1 upregulation AXL upregulation + MET amplification	Cabozantinib (TKIs inhibitor including AXL) + osimertinib	WB, NGS, qPCR	Namba et al. (31)
Exposure to increasing doses up to 1 μM for more than 6 months	HCC827	Osimertinib	AXL upregulation associated with MET amplification	CB469 (dual MET and AXL inhibitor) + osimertinib	Phospho-RTK-array	Yang et al. (32)

(Continued)

TABLE 1 | Continued

Model generation method	Cell line	3rd G TKI	Genetic alteration	Therapy	Method/ approach	References
Stepwise dose escalation	Gefitinib-resistant PC9 (T790M+)	Osimertinib	AXL overexpression AXL overexpression with MET activation FGFR1 upregulation	-Foretinib (RTK and AURKB inhibitor) -Barasertib (AURKB-specific inhibitor) -Tozasertib	WB, IHC and Q-PCR	Bertran-Alamillo et al. (33)
IGF1-R						
Exposure to increasing concentrations	Gefitinib-resistant PC9	WZ4002	IGF1-R activation with IGFBP3 decreased expression	AG-1024 (IGF1-R inhibitor) or BI836845 (monoclonal anti-IGF1/2 blocking antibody) + WZ4002	RTK-array	Park et al. (34)
Stepwise escalation method from 150 nmol/L to 1 μmol/L over 6 months - Chronic exposure to 1 μmol/L over 3 months	- Gefitinib-resistant PC9 (T790M+) - H1975	Osimertinib	IGF1R activation	Linsitinib (IGF1R inhibitor) + osimertinib	RTK array	Hayakawa et al. (35)
Dose escalation method (0.03 to 1 μmol/L) for several months followed by cloning	PC9	Osimertinib	IGF1-R activation mediated by IGF2 overexpression	Linsitinib + osimertinib	Phospho-RTK array, ELISA	Manabe et al. (36)
EMT and stemness						
Stepwise escalation (0.1 μM to 1 μM) within 6 months	HCC827	Osimertinib	Zeb1 upregulation	JMF3086 (HDAC inhibitor) + osimertinib	WB	Weng et al. (37)
Stepwise dose escalation (0.03 to 1 μmol/L) followed by limiting dilution	H1975	Osimertinib	Zeb1 upregulation with miR-200c downregulation	LY2090314 (GSK-3 inhibitor) + osimertinib	WB, miRNA array	Fukuda et al. (38)
Stepwise method over 6 months	PC9, HCC827	Osimertinib	ANKRD1 overexpression with miR-200 family downregulation	Imatinib + osimertinib	WES, cDNA microarray	Takahashi et al. (39)
Stepwise-dose escalation (500 nm to 1.5 μM) followed by single-cell dilution	H1975	Osimertinib	Downregulation of SQSTM1/p62 and up regulation of LC3	–	WB	Verusingam et al. (40)
Mesenchymal-resistant cell line derived from biopsies of NSCLC patients who progressed on 3rd-generation EGFR TKIs	–	EGF816	Hight expression of FGFR1 and FGF2	BGJ39 (FGFR1/2/3 inhibitor) with EGF816 (nazartinib)	Whole-genome CRISPR screening	Crystal et al. (41); Raoof et al. (42)
Exposure to increasing doses	PC9	Osimertinib	HES1 upregulation ALDH1A1 upregulation	–	WB	Codony-Servat et al. (43)
Apoptosis modulators						
Gradually increasing concentrations (10 nM to 500 nM) for approximately 6 months	-PC9; Gefitinib-resistantT790M+ PC9; HCC827	Osimertinib	Bim downregulation with Mcl-1 upregulation	MEK inhibitors (PD0325901; AZD6244; GSK1120212) + osimertinib HDAC inhibitors (SAHA and LBH589) + osimertinib	WB	Shi et al. (44); Zang et al. (45)
Escalating dose exposure (20 nM to 5 μM) for 12–16 weeks followed by single-cell cloning for 12–16 weeks	H1975	AC0010 cross-resist to rociletinib and osimertinib.	BCL-2 upregulation	ABT263 (navitoclax) + AC0010	RNA sequencing, WB	Xu et al. (27)
Stepwise increased concentration (5 μM to 15 μM) over 11 months	H1975	Osimertinib	BCL-2 upregulation	BCL- 2 inhibitors (ABT263/ABT199) + osimertinib	WB, qPCR	Liu et al. (46)
NF-KB						
Exposure to escalating concentrations up to 1 μM for 8 to 10 months	H1975	CNX-2006 cross-resist to rociletinib	Overexpression of p105 and of p50	TPCA-1 + CNX-2006 Bortezomib + of CNX-2006 BEZ-235 + of CNX-2006	WB, phospho-kinase array	Galvani et al. (47)
Gradually increasing concentrations: -from 30 nM to 4 μM, for 10 months -from 200 nM up to 4 μM	Gefitinib-resistant PC9 H1975	Rociletinib	Overexpression of p50, p65, IKKα/β and KBα	-Rociletinib + TPCA-1 -Rociletinib + metformin	WB	Pan et al. (48)

(Continued)

TABLE 1 | Continued

Model generation method	Cell line	3rd G TKI	Genetic alteration	Therapy	Method/ approach	References
Escalating dose exposure (20 nM to 5 μM) for 12–16 weeks followed by single-cell cloning for 12–16 weeks	H1975	AC0010	NFKB1 upregulation	–	RNA sequencing, WB	Xu et al. (27)
Other mechanism						
Stepwise dose escalation (50 nM to 1 μM)	PC9, HCC827, H1975, and HCC4006	Rociletinib or osimertinib	AURKA activation with TPX2 overexpression	Alisertib + osimertinib	Drug screening, WB	Shah et al. (49)
Increased concentrations (5 nM to 1.5 μM) over 22 weeks	H1975	Osimertinib	Upregulation of CDK4, CDK6 and CCND1 and hyperphosphorylation of Rb	Palbociclib + osimertinib	Cell cycle analysis, qPCR, WB	Qin et al. (50)
–	HCC827	Osimertinib	IRE1α upregulation	STF-083010 (IRE1α inhibitor)	WB	Tang et al. (51)

therapy (62). Second, HDAC inhibitors have shown synergy with osimertinib in reversing epithelial–mesenchymal transition (EMT)-related resistance linked to stemness, in preclinical models (37, 38). In addition, analysis of circular microRNAs (crmiR) in established osimertinib-resistant cell lines revealed 16,000 differentially expressed crmiRs compared to non-resistant cells (63). MicroRNAs such as the miR-200 family have previously been shown to play a role in acquired resistance to osimertinib (39). Finally, recently, long non-coding RNAs (lncRNAs), CRNDE and DGCR5, have been reported to induce resistance to afatinib and osimertinib *via* downregulation of eIF4A (64).

Notably, a recent report showed that the emergence of EGFR inhibitor resistance in NSCLC may also be nonheritable and attributed to stochastic variations (65).

PRECLINICAL MODELS FOR ACQUIRED RESISTANCE TO 3RD G EGFR-TKIs

EGFR-Dependent Mechanisms

The mechanisms of on-target EGFR resistance consist of genetic alterations in EGFR occurring during progression under 3rd G EGFR-TKIs. In clinical studies, EGFR-dependent resistance is related to additional somatic EGFR mutations and to gene amplification (9, 27). EGFR point mutations occur in the kinase domain and affect the osimertinib covalent binding residue (C797S/G, exon 20), the EGFR solvent-front (G796S/R, exon 20), the hinge region (L792H/F), and residues inducing steric interaction (L718Q/V, G719C/S/A and G724S, exon 18) (62, 66, 67).

In preclinical models, EGFR amplification was reported in an established rociletinib-resistant cell line (**Table 1**) and sensitivity to rociletinib was restored by cetuximab, a specific anti-EGFR monoclonal antibody, or by afatinib (20). Somatic EGFR mutations, however, have not been identified, which could be explained by the efficacy of 3rd G EGFR-TKIs in inhibiting EGFR protein. Thus, to better understand the involvement of EGFR aberrations in the induction of resistance, studies have been limited to ectopic overexpression of the wild-type (25) or mutated protein or to site-directed mutagenesis replicating mutations described in relapsed patients. The C797S mutation, engineered with a deletion within exon 19 in Ba/F3 cells, conferred significant resistance against osimertinib compared to other EGFR variants such as L718V, L792F/H, and G724S. However, when associated with L858R, C797S/G and L718Q/V conferred comparable resistance, which was greater than in a Del19 background. L792F/H, in contrast, induced significantly less resistance with L858R (68). This indicates that the initial activating mutation may play a role in the potency of resistance to osimertinib. Consistent with this finding, it was reported in the FLAURA study that patients with the L858R mutation have a worse prognosis than those with Del19 (7). Importantly, as observed in the clinic (69–72), earlier-generation EGFR-TKIs may be effective against osimertinib resistance; this may depend not only on the position of the mutation but also on its allelic context. Afatinib inhibited EGFR phosphorylation and cell growth in osimertinib-resistant Ba/F3 cells that exogenously express the G724S mutation, alone or with Del19 (67). The S724 variant induced conformational changes that are incompatible with EGFR-TKIs 3rd G and 1st G binding but not with 2nd G (67). Ba/F3 cells expressing $EGFR^{L858R/C797S}$ by N-ethyl-N-nitrosurea mutagenesis were found to be sensitive to gefitinib (73). A recent study showed that sensitivity and response to EGFR-TKIs are also heterogeneous within the same EGFR exon and proposes a new classification rather based on the structure function of the mutation to determine potential future therapeutic approaches (74).

In clinical studies, emergence of the $EGFR^{C797X}$ mutation is the most common mechanism of resistance to EGFR-dependent osimertinib regardless of treatment line. It was detected in 15% of patients progressing to second-line osimertinib therapy (75) and in only 7% of disease progression when osimertinib is administrated in first-line therapy (76). C797S occurred more frequently in association with Del19 than with L858R mutation (77, 78). Otherwise, C797S was observed in less than 3% of cases in rociletinib-resistant patients (25) and was not observed in patients who progressed after AC0010 treatment (79), suggesting that the resistance mechanism might be drug dependent.

EGFR-Independent Mechanisms

Resistance to osimertinib mediated by EGFR-independent mechanisms can be acquired through activation of alternative bypass pathways, aberrant downstream signaling or histologic transformation. **Figure 1** illustrates the involved pathways described in the review.

MAPK and PI3K Pathways Implication

MAPK and AKT are common downstream modulators of receptor tyrosine kinases (RTKs). Activation of the MAPK pathway *via* ERK activation is a common feature of nearly all preclinical models of resistance to 3rd G EGFR-TKIs. However, alterations of other upstream effectors have also been identified as a driving event in the occurrence of resistance. Copy number gains of MAPK1, CRKL, NRAS, and KRAS as well as single mutations in NRAS (G12V/R, Q61K and E63K) were identified in resistant populations established from PC9 and H1975 cells after chronic exposure to osimertinib or WZ4002 (**Table 1**). Combination with MEK inhibitor Selumetinib prevented the emergence of resistant PC9 cells after 34 days at which time resistant cells appeared in the presence of osimertinib alone, and delayed resistance in H1975 from 17 days in the presence of osimertinib alone to 40 days in the presence of selumetinib. Interestingly, combination therapy induced regression in osimertinib-resistant tumors in transgenic mice carrying $EGFR^{L858R/T790M}$ (21). NRAS amplification was also reported, in a subsequent study, in naquotinib-resistant PC9 cells harboring the T790M mutation (**Table 1**). Either selumetinib or trametinib, a second MEK inhibitor, resensitized naquotinib-resistant cells (22). Single KRAS mutations have also been described in resistance to 3rd G EGFR-TKIs. First, to assess the relevance of $KRAS^{G12S}$ identified in a patient with acquired osimertinib resistance, Ortiz-Cuaran et al. showed that exogenous expression of $KRAS^{G12S}$ in PC9 and HCC827 cells reduced sensitivity to osimertinib and rociletinib, indicating that expression of an activated KRAS allele is sufficient to drive resistance to 3rd-generation TKI (10). In a second study, $KRAS^{G13D}$ mutation was reported as a potential resistance mechanism in osimertinib-resistant PC9 cells (20) (**Table 1**). Another variant, $HRAS^{G13R}$, in association with increased MET expression was reported in osimertinib-resistant PC9 cells (23) (**Table 1**). Moreover, $BRAF^{G469A}$ mutation occurred in osimertinib-resistant PC9 clones (**Table 1**). Similar to the models mentioned, dual therapy using selumetinib or trametinib with osimertinib was effective in overcoming resistance and enhancing cell death in mutated cells (24). To our knowledge, no NRAS alteration has been reported in clinical studies. Alterations in KRAS, however, are widely reported in clinical data. The $KRAS^{G12S}$ mutation was identified in the lymph node biopsy, collected after relapse of osimertinib treatment, but not in plasma sample. Interestingly, $EGFR^{C797S}$ variant, which in turn appeared after relapse, had been found in the patient's plasma but not in the lymph node biopsy, indicating that different resistance mechanisms may develop at the same

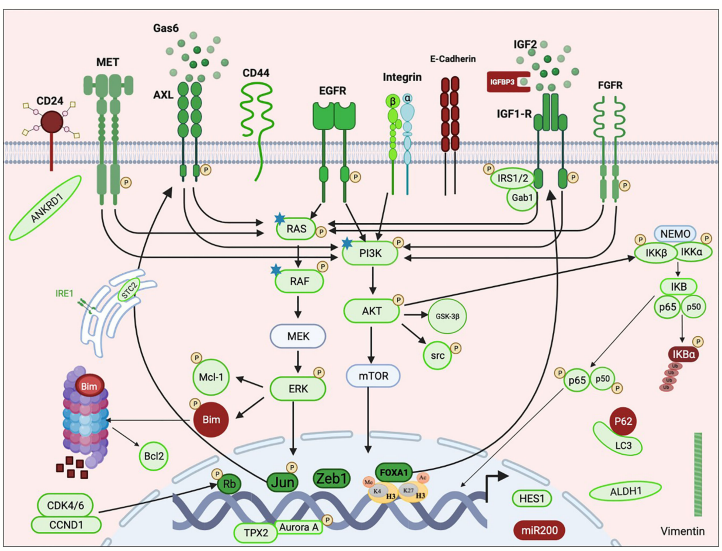

FIGURE 1 | Schematic representation of an overview of pathways implicated in resistance emergence to third-generation EGFR-TKIs. Mechanisms of resistance to third-generation EGFR-TKIs include aberrant activation of receptor tyrosine kinases (MET, AXL, IGF1-R, FGFR, and EGFR) and/or the downstream pathways (PI3K/AKT, RAS/MAPK, and NFKB) and histological transformation. RTK activation is due to overexpression of the protein with or without copy number gain, through its transactivation involving transcription factors (e.g., Jun and FOXA1) or consequently to the overexpression of its specific ligand (e.g., IGF2 and GAS6). Activation of the downstream cascades can also be due to somatic mutations (e.g., RAS, RAF, and PI3K). Histological transformations consist of EMT and EMT-related stemness features including downregulation of E-cadherin and miR200 family, upregulation of Vimentin, Zeb1 and ANKRD1, enrichment in $CD44^{hight}/CD24^{low}$ and $ALDHA1^{hight}$ populations, HES1 overexpression, and autophagy activity. Resistance also required apoptosis modulation through Bim degradation and Bcl-1 upregulation. Non-classified resistance mechanisms include activation of AURKA and its coactivator TPX2 and upregulation of CDK4/6 and IRE1. Green color indicates activation or overexpression; red indicates down-regulation. P: phosphorylation. Star: point mutation. This figure was created using the free version of the Biorender website.

time (10). In another study, the $KRAS^{G12D}$ mutation detected in patient's plasma relapsing on first-line osimertinib therapy was associated with the $CTNNB1^{S37F}$ mutation. Notably, the initial Del19 has not been detected in the post-therapy plasma sample (11). Clearance of the Del19 subpopulation may be due to different sources of the pre- and post-therapy samples or to selection of $EGFR^{WT}$ cells during the development of resistance. The $KRAS^{Q61R}$ variant has also been reported in the occurrence of osimertinib resistance (78). KRAS G12A, Q61H, and A146T variants were found in patients treated with rociletinib that were not detected in their pre-treatment plasma specimens (25). KRAS amplification has also been involved in osimertinib resistance. Molecular profiling of patients who relapsed on osimertinib therapy showed one case of KRAS/MDM2/CDK4 co-amplification (78). Finally, the $BRAF^{V600E}$ mutation has been reported as a mechanism of resistance to osimertinib treatment, both alone (80) and in combination with MET amplification (81). The variant was also identified in a liquid biopsy sample from a patient undergoing treatment with ASP8273, a Japanese 3rd G EGFR-TKI (82). Combination therapies with 3rd G EGFR-TKIs and MEK inhibitors have been developed for lung cancers with EGFR mutations (NCT02143466).

As with ERK, maintained AKT activation is shown in the majority of preclinical models resistant to 3rd G TKIs and its restoration to normal status often required dual therapy. Shigenari et al. reported Src-AKT pathway activation, through Integrin β1 overexpression, as a resistance mechanism in established osimertinib- and rociletinib-resistant H1975 cells (**Table 1**). Either dasatinib or bosutinib, both Src inhibitors, suppressed Src phosphorylation and restored sensitivity to 3rd G EGFR-TKIs. Finally, to understand if the co-occurring of $PIK3CA^{G106V}$ with $CTNNB1^{S37F}$ mutations observed in a patient that had progressed on rociletinib treatment had a role in acquired resistance, HCC827 cells were engineered with single or both mutations. While $PIK3CA^{G106V}$ expression promoted invasion and migration, $CTNNB1^{S37F}$ activated the wnt/beta-catenin pathway, promoted cellular invasion and suppressed apoptosis in response to rociletinib. Authors suggested a non-redundant cooperation of CTNNB1 with PI3CA alterations to promote tumor metastasis or limit EGFR inhibitor response (83). β-catenin has been shown to play an important role in acquired resistance to EGFR-TKIs and EMT in NSCLC cells (84, 85).

In patients, PIK3CA mutations, including E542K, E545K, and E418K, are frequently observed in resistance to 3rd G EGFR-TKIs (25, 62, 78, 83). They accounted for 7% of the resistance mechanisms to first-line osimertinib therapy (76).

ALTERNATIVE RECEPTOR TYROSINE KINASE ACTIVATION

MET

Activation of C-mesenchymal–epithelial transition factor (c-MET) appears to be a common resistance mechanism to third-generation EGFR-TKIs, and has been found to be associated with resistance to osimertinib, to rociletinib (10), and to AC0010 (86). In preclinical studies, MET activation is due to gene copy gain or protein overexpression. No MET point mutations have been reported as observed in patients. In an preclinical, *in vivo*, model, rociletinib-resistant tumors were collected from mice bearing PC9 tumors (**Table 1**). Genomic and biochemical analysis revealed MET amplification and activation as the only mechanism of acquired resistance. The combination of rociletinib with crizotinib, a kinase inhibitor with multiple targets including MET, reduced significantly the viability of cell lines derived from rociletinib-resistant tumors. Dual therapy effectively decreased growth on mice of patient-derived xenograft tumors harboring L858R and MET copy gain (25). In a second original model, established by Wanhong et al., AC0010-resistant H1975 cells were generated in two steps first, *in vivo*, and then after selection, *in vitro* (**Table 1**). The derived cells were cross-resistant to EGFR-TKIs of other generations and showed upregulation of MET. Consistent with the above mentioned, double inhibition of EGFR and MET with AC0010 and crizotinib, respectively, prevented colony formation and suppressed MET activation in resistant cell lines and reduced significantly tumor growth in xenograft, compared with single therapy (86). MET activation has also been reported in cell line-based models generated by exposure to progressively increasing concentrations of 3rd G EGFR-TKI. Increased MET copy number was observed in osimertinib-resistant HCC827 cells (**Table 1**), which were also cross-resistant to rociletinib and the 1st-generation EGFR-TKI, erlotinib. MET inhibitors such as crizotinib, ARQ179, or SGX523 sensitized osimertinib-resistant cells (26). In a second model, increased MET phosphorylation was reported to be responsible for acquired resistance in naquotinib-resistant PC9 cells (**Table 1**). Interestingly, dual therapy by naquotinib with crizotinib or SGX-523 had a limited effect on bulk resistant cells, while drastically reducing the proliferation of monoclonal resistant cells, suggesting that heterogeneity may underlie the resistance to a specific TKI target. Notably, the one clone that overexpressed MET protein showed an increase in MET copy number, which was not observed in the resistant parental cells arguing for clonal evolution in the development of resistance. In addition, naquotinib administrated with crizotinib induced robust regression in mice bearing monoclonal resistant cell tumors without apparent cytotoxicity (22).

In clinical studies, MET copy number gains are the most common alternative bypass mechanisms for osimertinib resistance, regardless of treatment line (76, 78). In a recent report, MET amplification was found in 66% (n = 6/9) of patients treated with first-line osimertinib (12). Besides osimertinib, MET amplification has also been reported in tumor biopsies from patients with lung adenocarcinoma who developed resistance to rociletinib (10). Point mutations, such as MET P97Q, I865F, and H1094Y, have also been identified in patients with lung cancer progressing on osimertinib (62, 77). The efficacy of MET inhibitors alone or in combined therapy with 3rd G EGFR-TKIs has been reported in clinical studies (87, 88). Recently, the feasibility of combining osimertinib with

savolitinib, a potent and selective MET inhibitor, has been tested in clinical trials (89).

AXL

In NSCLC, it has been reported that anexelekto (AXL) plays a role in resistance to many anti-cancer drugs including EGFR inhibitors (90). Indeed, Tanguichi et al. showed that PC9 cells do not have basal AXL activity as it is the case for MET and HER3 and that AXL phosphorylation appears shortly (4 h) after exposure to osimertinib and increases throughout the exposure period. They also observed a concomitant increase in MET, HER3, and EGFR phosphorylation, suggesting that AXL activation may accelerate the emergence of tolerant cells (59). In addition, drug-tolerant cells isolated from PC9, HCC4011, or H1975, 9 days after high-dose osimertinib treatment (3 μmol/L) expressed a higher level of AXL than parental cells and were highly sensitive to the AXL inhibitor, ONO-7475, in contrast to parental cells (28). Moreover, initial combined treatment with osimertinib and ONO-7475 had more effective effect on tumor regression PC9-derived xenograft when used as the initial treatment than as an alternative therapy once resistance to osimertinib developed (28). Since PC9 cells are enriched in AXL, this indicates that AXL expression level may be a predictor of response to osimertinib. Moreover, primary PE2988 cells, established from the pleural effusion of a patient who developed resistance to osimertinib showed high level of total and phosphorylated AXL and of stanniocalcin (STC2) and responded to the combination of AXL inhibitors and osimertinib (29). STC2 is involved in EGFR-TKIs resistance and was found upregulated in established gefitinib-resistant PC9 and osimertinib-resistant H1975 cells (**Table 1**). Indeed, exogenous overexpression of STC2 activated AXL and increased c-jun level and phosphorylation. In fact, c-jun forms with c-Fos the transcription factor, activation protein-1 (AP-1), which binds to AXL promoter (91), suggesting the involvement of the STC2-JUN-AXL axis in EGFR-TKI resistance (29, 92). Another mechanism of resistance to osimertinib and gefitinib, involving AXL, was described by Kim et al. in osimertinib-resistant HCC827 cells (**Table 1**). The model showed increased expression level of GAS6, a ligand of AXL, and prolonged protein degradation rates in parallel with AXL overexpression. Thus, YD-mediated AXL degradation synergized with osimertinib to restore osimertinib sensitivity *in vitro* and *in vivo* (30). AXL activation was identified as the mechanism of resistance in different established osimertinib-resistant cell lines, despite different EGFR mutational profiles (**Table 1**). It has been observed alone, with an EMT phenotype, or with MET amplification (31–33). Cabozantinib, a multiple TKI including AXL (31), or CB469, a dual inhibitor of MET and AXL, with osimertinib (32) overcame resistance. Notably, resistant clones generated with AXL upregulation lost the T790M subpopulation and some the Del19 population, indicating that clonal evolution leads to heterogeneity in resistance mechanisms. In testing a library of drugs, foretinib, a type II inhibitor targeting a panel of RTKs including MET and AXL, showed the lowest IC_{50} in resistant cell lines, which were T790M-negative (33), indicating that clonal heterogeneity is very likely to impair the efficacy of targeted therapy.

In clinical data, high AXL expression was associated with low RR to osimertinib in patients with EGFR-mutated NSCLC (59). Furthermore, PFS and ORR were inversely correlated with AXL mRNA expression in patients with EGFR-mutated NSCLC (93). Results of phase 1 clinical trials to assess the safety and tolerability of DS-1205c, a specific AXL inhibitor, when combined with osimertinib in metastatic or unresectable subjects with EGFR-mutant NSCLC (NCT03255083) are not yet published.

IGF1-R

Insulin-like growth factor receptor (IGF-R) activation is involved in EGFR-TKIs resistance in NSCLC cell lines (94) and patients (95). Regarding its implication in resistance to 3rd G EGFR-TKIs, it was shown that drug-tolerant cells obtained 72 h after osimertinib treatment expressed elevated levels of total and phosphorylated IGF1-R without changes in the expression of its ligands, IGF1 and IGF2. This activation in the presence of osimertinib was due to epigenetic activation of its own transcription, mediated by the transcription factor FOX1. Moreover, osimertinib treatment enhanced the association of IGF1-R with its adaptor proteins Gab1 and IRS1, thereby promoting cell survival (58). Indeed, WZ4002-resistant PC9 cells (**Table 1**) showed activated IGF1-R associated with IGFBP3 downregulation. Chemical inhibition of IGF1-R with AG-1024 or the blocking monoclonal anti-IGF1/2 antibody, BI836845, restored sensitivity to WZ4002, *in vitro*, and in xenograft mice (34). Loss of IGFBP3 was shown to induce activation of IGF1-R signaling and enhance resistance to WZ4002 in gefitinib-resistance cell line. Reciprocally, addition of recombinant IGFBP3 was sufficient to restore sensitivity to the 3rd G EGFR-TKI (96). In osimertinib-resistant cell line models, IGF1-R activation was observed in the presence (35) or absence of T790M (**Table 1**). Indeed, a protein phosphorylation array performed in PC9 osimertinib cells (**Table 1**) detected high activity of the "p-Y-IRS1 p-IRS2 bind PI3K" pathway, which is involved in IGF1-R signaling. Interestingly, the pathway was not activated in gefitinib- or erlotinib-resistant PC9, suggesting a mechanism specific to third-generation EGFR inhibitors. In contrast to the above models, the resistant cells did not show IGFBP3 downregulation but did show increased IGF2 expression. The IGF1-R inhibitor linsitinib overcame osimertinib resistance in resistant cell lines and in the patient-derived KOLK43 cells [established from pleural effusion of a erlotinib- and osimertinib-resistant patient with high IGF1-R phosphorylation (36)]. Increased phosphorylation of IGF1-R was observed, by immunohistochemistry, in the tumor sample of an EGFR-mutated NSCLC patient who acquired resistance to osimertinib (35).

HISTOLOGICAL TRANSFORMATION

Histological and phenotypic transformations in preclinical models of resistance to 3rd-generation EGFR-TKIs correspond

mainly to epithelial–mesenchymal transition (EMT) and to EMT-related stemness. In contrast to clinical data, transformation into small cell lung cancer has not been reported in preclinical models to date. Features of EMT, including decreased E-cadherin and increased vimentin expression, were reported in the generated osimertinib-resistant cell lines. The phenotype was observed in association with upregulation of the zinc finger transcription factor ZEB1 and the formation of spheroids, a feature of stemness (**Table 1**). Reversal of EMT by dual HDAC and the 3-hydroxy-3-methylglutaryl coenzyme A reductase inhibitor, JMF3086, successfully restored sensitivity to osimertinib (37). In fact, ZEB1 could recruit HDAC1 or DNMT1 to the E-cadherin promoter leading to E-cadherin silencing and EMT induction (97). A similar model (**Table 1**) had shown, in addition, a decrease in microRNA-200c expression (38). In fact, the EMT process is governed by a mutually inhibitory miR-200/ZEB feedback loop (98). Glycogen synthase kinase-3-beta (GSK-3β) inhibitor (LY2090314) that emerged in drug screening with significant inhibition of resistant cell growth, in combination with osimertinib, bypassed resistance by suppressing AKT signaling and restoring apoptosis in resistant cells (38). GSK-3β inhibition has been shown to decrease mesenchymal markers and to reduce the associated properties of cancer stem cells (CSC) in aggressive breast cancer (99). A third preclinical model of osimertinib-resistant cells (**Table 1**) reported that the EMT phenotype and downregulation of the miR-200 family were associated with overexpression of Ankyrin Repeat Domain1 (ANKRD1) (39). Indeed, when upregulated, ZEB1 forms a transactivation complex of ANKRD1 with YAP and JUN (100). Imatinib, by inhibiting ANKRD1 and ZEB1, restored apoptosis in resistant cells by increasing levels of Bcl-2 and cleaved PARP (39). Recently, established osimertinib-resistant H1975 clones (**Table 1**) had exhibited EMT characteristics and autophagy activity by downregulating of p62 and upregulation of LC3 (40). Notably, autophagy has been shown to play an important role in promoting cancer metastasis, and inhibition of autophagy might be an effective treatment strategy for malignant cancer (101). Interestingly, whole-genome CRISPR screening in a resistant mesenchymal cell line established from biopsies of NSCLC patients who progressed on 3rd G EGFR-TKIs (41) identified FGFR1 as the top sensitization target of EGF816-resistant cells. Dual EGFR/FGFR inhibition by combining EGF816 with BGJ398, a selective FGFR1–3 inhibitor, induced mesenchymal cell death but had no effect on patient-derived epithelial cell lines (42). In accordance with this, *in vitro* analysis demonstrated that FGF2 supplementation conferred resistance to osimertinib in EGFR mutant NSCLC cells. The same study reported FGFR amplification in patients after progression on osimertinib (102).

Anticancer drug resistance and EMT have been associated with CSCs. However, there are no suitable CSC markers for NSCLC-associated drug resistance and EMT. Upregulation of aldehyde dehydrogenase ALDH1A1, a widely used cancer stem cell marker, was observed in osimertinib-resistant HCC827 cells with EMT features and MET amplification (31) (**Table 1**). EGFR-TKIs, including osimertinib, have been shown to induce enrichment of ALDH positive subpopulations in EGFR-mutated NSCLC models (103, 104), suggesting that specific dual targeting could overcome this adverse effect. Furthermore, osimertinib-resistant PC9 clones (**Table 1**) showed ALDH1A1 or Hairy and enhancer of split homolog-1 (HES1) overexpression (43). HES1 is a transcriptional factor that plays a critical role in gaining and retaining stemness capacity (105). Clinical studies showed HES1 protein levels increased during relapse and were negatively correlated with PFS in EGFR-mutated patients treated with TKIs including osimertinib (43, 106).

APOPTOSIS MODULATORS

Bcl2-like 11 (BIM) has emerged as a key modulator of EGFR-TKI induced apoptosis. Low levels of *BIM* expression in primary tumors are reported to be associated with shorter PFS in patients treated with EGFR-TKI (107). In preclinical studies, osimertinib-resistant PC9 and HCC827 cells (**Table 1**) showed Bim downregulation and Mcl-1 upregulation in association with ERK activation (44). Bim and Mcl-1 are known to be regulated by ERK (108, 109). MEK inhibitors such as PD0325901, AZD6244, or GSK1120212 suppressed phosphorylation of ERK, Bim, and Mcl-1 in cell lines and effectively decreased the growth of osimertinib-resistant xenografts (44). Alternatively, HDAC inhibitors (SAHA and LBH589) plus osimertinib induced significant growth inhibition of osimertinib-resistant cells and xenografts through Bim stabilization (45). Furthermore, a drug screen performed in gefitinib-resistant cells in which WZ4002 failed to restore Bim expression identified ABT-263 (navitoclax), a dual inhibitor of BCL-XL and BCL-2 at the head of compounds that achieve maximal growth inhibition in combination with WZ4002, suggesting a role for BCL-2 in the occurrence of resistance against 3rd G EGFR-TKIs (55). Indeed, RNA sequencing of AC0010-resistant H1975 cells generated *in vitro* (**Table 1**) revealed an overexpression of BCL-2 (8.6-fold compared to parental cells). Dual therapy with ABT263 and AC0010 enhanced apoptosis in resistant cells and reduced colony formation (86). In another model of osimertinib-resistant H1975 cells (**Table 1**) with BCL-2 upregulation, ABT263 as well as ABT199 (BCL-2 inhibitor) synergized with osimertinib to overcome resistance through downregulation of p21or downregulation of SQSTM1 and Survivin (46). Clinical trials studying oral combination therapy with navitoclax and osimertinib in advanced EGFR-mutant NSCLC with prior TKI treatment have reported an ORR of up to 100% and a median PFS of 16.8 months. However, thrombocytopenia and lymphopenia were the most common adverse events (37%) observed in the study (110). Finally, it was found that C-FLIP knockdown restored osimertinib-induced apoptosis in resistant cells (**Table 1**), suggesting that C-FLIP depletion may be an effective strategy to overcome osimertinib resistance in NSCLC

(44, 111). Moreover, silencing of C-FLIP had sensitized EGFR-mutant NSCLC to erlotinib and, conversely, its overexpression rescued EGFR-mutant lung cancer cells from erlotinib treatment, presumably through modulation of NF-κB activity (112).

NF-KB PATHWAY

Enhanced nuclear factor binding near the κ light chain gene in *B* cells (NF-κB) signaling activity has been implicated as a possible mechanism of resistance to EGFR-TKIs since patients with EGFR mutations who had developed resistance to erlotinib showed low expression of the NF-κB inhibitor, IκBα (112). Activation of NF-κB by overexpression of NF-κB1 (p50) and its precursor (p105), without altering the expression level of p65, has been reported as a mechanism of acquired resistance against CNX-2006, a prototype for rociletinib, in resistant H1975 cells (**Table 1**). Notably, resistant cells showed a variety of differences compared to parental cells, but the involvement of NF-κB was the most studied. Bortezomib, TPCA-1, or BEZ-235, all inhibitors of the NF-κB pathway, synergized with CNX-2006 to inhibit cell growth, but with different efficiencies (47). A similar phenotype was observed in established rociletinib-resistant cells (**Table 1**) that expressed higher levels of p50, p65, phospho-IKKα/β, and phospho-KBα proteins than the parental cells. As in the previous model, combination treatment of rociletinib with TPCA-1 or with Metformin, which is known to inhibit the NF-κB activity (113), overcame resistance (48). More recently, NF-κB1 was identified among the top ten upregulated gene in AC0010-resistant H1975 generated *in vitro* (**Table 1**), but no further investigations have been conducted to understand the mechanism involved in acquired resistance (86).

Others

AURKA

Aurora kinase A (AURKA) is a serine/threonine kinase that plays a key role during cell division particularly in the process of chromosome segregation (114). The Aurora kinase inhibitors, barasertib and VX680, were identified at the top of the list of drugs that synergized with osimertinib or rociletinib to reduce the growth of generated resistant cell lines, respectively (**Table 1**). Mechanistically, phosphorylation of AURKA was associated with increasing TPX2 protein level following abolition of its CDH1-dependent degradation due to CDH1 sequestration in the cytosol (49). Moreover, barasertib and tozasertib, a second AURK inhibitor, showed a significant antiproliferative effect on osimertinib-resistant cells with no observed difference in AURK expression level (33). Recently, the importance of AURK inhibition in enhancing BIM- and PUMA-mediated apoptosis upon EGFR-TKI therapy in EGFR-mutated lung cancer cells has been described (61). TPX2 expression was significantly increased in tumor tissue samples obtained from patients with advanced EGFR-mutant NSCLC after erlotinib treatment failure compared with results from pre-treatment samples (49).

A Phase 1/1b clinical trial of AURKA inhibitor, Alisertib, with osimertinib in *EGFR*-mutant stage IV metastatic lung cancer is currently recruiting participants (NCT04085315).

CDK4/6

Upregulation of CDK4 and CDK6 together with hyperphosphorylation of Rb have been reported as a mechanism of resistance to osimertinib in H1975-resistant cells (**Table 1**). The combination of palbociclib, a selective and potent inhibitor of CDK4/6, with osimertinib overcomes the resistance (50). Acquired alterations in cell cycle genes, including amplification of CDK4/6, CCND1, CCND2, and CCNE1, account for 10% of the acquired resistance mechanisms detected in patients who relapsed after first-line treatment with osimertinib (76).

IRE1

Zheng-Hai Tang et al. suggested an increase in Inositol requiring enzyme 1α (IRE1α) expression as a mechanism of resistance to osimertinib in resistant HCC827established *in vitro* (**Table 1**). Indeed, IRE1α knockdown or STF-083010, an inhibitor of IRE1α, reduces cell viability in resistant cells (51).

CONCLUSION AND PERSPECTIVES

In preclinical studies, resistance to 3rd G EGFR-TKIs is mainly due to genetic alterations that increase activity of receptor tyrosine kinases (such as MET, IGF1-R, and AXL) and downstream signaling cascades (such as RAS/MAPK and PI3K/AKT). Histological transformations are limited to EMT and EMT-related stemness. Multiple mechanisms of resistance could be observed in the same population highlighting the heterogeneity of the process, which may be explained in part by clonal evolution, and suggesting that combination therapies will be required to overcome acquired resistance. At this stage, we cannot conclude which of the mechanisms identified in the *in vitro* or *in vivo* models are the closest to what is described in the clinic because of limited data on *in vivo* studies. In general, the developed models do not really reflect the diversity of mechanisms observed in the clinic. Somatic alterations in EGFR, HER2 amplification, and gene fusions (e.g., ALK, RET, and BRAF fusions) are not identified as mechanisms of resistance to 3rd G EGFR-TKIs in the preclinical models. Nevertheless, the models described highlight the utility of early dual therapy and provide insights into possible combination therapies to optimize treatment lines. They also allow the identification of potential biomarkers in pre-existing resistant cells that will emerge under selective pressures, hence the need to develop new relevant preclinical models. NSCLC organoids derived from primary patient tumors or patient-derived xenograft tumors have been shown to maintain the histologic and tumorigenic properties of the parental cancer cells and reflect the drug responses of the parental tumor (115). Such models as well as murine models of patient-derived xenograft and syngeneic lung cancer may be suitable to further investigate resistance mechanisms that are not identified *in vitro*, such as

EGFR mutations, or small cell or squamous cell transformation, while preserving the authenticity of the tumor. They could also allow the anticipation of investigations on new-generation therapeutic strategies.

AUTHOR CONTRIBUTIONS

RP conceived and supervised the project direction. EM and GL inquired and collected the literature. EM read the literature, wrote the manuscript, and prepared the figure and table. CR and CM revised the manuscript. RP and HL read and approved the final draft. All authors contributed to the article and approved the submitted version.

FUNDING

This work was funded by post-doctoral fellowship from Association pour la recherche contre le cancer (ARC), Ligue contre le cancer Grand Ouest, Institut National de la Santé et de la Recherche Médicale (INSERM).

REFERENCES

1. Mok TS, Wu Y-L, Thongprasert S, Yang C-H, Chu D-T, Saijo N, et al. Gefitinib or Carboplatin–Paclitaxel in Pulmonary Adenocarcinoma. *N Engl J Med* (2009) 361:947–57. doi: 10.1056/NEJMoa0810699
2. Sequist LV, Yang JC-H, Yamamoto N, O'Byrne K, Hirsh V, Mok T, et al. Phase III Study of Afatinib or Cisplatin Plus Pemetrexed in Patients With Metastatic Lung Adenocarcinoma With EGFR Mutations. *J Clin Oncol* (2013) 31:3327–34. doi: 10.1200/JCO.2012.44.2806
3. Kobayashi S, Boggon TJ, Dayaram T, Jänne PA, Kocher O, Meyerson M, et al. EGFR Mutation and Resistance of Non-Small-Cell Lung Cancer to Gefitinib. *N Engl J Med* (2005) 352:786–92. doi: 10.1056/NEJMoa044238
4. Kosaka T, Yatabe Y, Endoh H, Yoshida K, Hida T, Tsuboi M, et al. Analysis of Epidermal Growth Factor Receptor Gene Mutation in Patients With Non-Small Cell Lung Cancer and Acquired Resistance to Gefitinib. *Clin Cancer Res* (2006) 12:5764–9. doi: 10.1158/1078-0432.CCR-06-0714
5. Pirker R. Third-Generation Epidermal Growth Factor Receptor Tyrosine Kinase Inhibitors in Advanced Nonsmall Cell Lung Cancer. *Curr Opin Oncol* (2016) 28:115–21. doi: 10.1097/CCO.0000000000000260
6. Barnes TA, O'Kane GM, Vincent MD, Leighl NB. Third-Generation Tyrosine Kinase Inhibitors Targeting Epidermal Growth Factor Receptor Mutations in Non-Small Cell Lung Cancer. *Front Oncol* (2017) 7:113:113. doi: 10.3389/fonc.2017.00113
7. Soria J-C, Ohe Y, Vansteenkiste J, Reungwetwattana T, Chewaskulyong B, Lee KH, et al. Osimertinib in Untreated *EGFR* -Mutated Advanced Non–Small-Cell Lung Cancer. *N Engl J Med* (2018) 378:113–25. doi: 10.1056/NEJMoa1713137
8. Zhang Q, Zhang X-C, Yang J-J, Yang Z-F, Bai Y, Su J, et al. EGFR L792H and G796R: Two Novel Mutations Mediating Resistance to the Third-Generation EGFR Tyrosine Kinase Inhibitor Osimertinib. *J Thorac Oncol* (2018) 13:1415–21. doi: 10.1016/j.jtho.2018.05.024
9. Thress KS, Paweletz CP, Felip E, Cho BC, Stetson D, Dougherty B, et al. Acquired EGFR C797S Mutation Mediates Resistance to AZD9291 in Non–Small Cell Lung Cancer Harboring EGFR T790M. *Nat Med* (2015) 21:560–2. doi: 10.1038/nm.3854
10. Ortiz-Cuaran S, Scheffler M, Plenker D, Dahmen L, Scheel AH, Fernandez-Cuesta L, et al. Heterogeneous Mechanisms of Primary and Acquired Resistance to Third-Generation EGFR Inhibitors. *Clin Cancer Res* (2016) 22:4837–47. doi: 10.1158/1078-0432.CCR-15-1915
11. Ramalingam SS, Yang JC-H, Lee CK, Kurata T, Kim D-W, John T, et al. Osimertinib As First-Line Treatment of *EGFR* Mutation–Positive Advanced Non–Small-Cell Lung Cancer. *JCO* (2018) 36:841–9. doi: 10.1200/JCO.2017.74.7576
12. Roper N, Brown A-L, Wei JS, Pack S, Trindade C, Kim C, et al. Clonal Evolution and Heterogeneity of Osimertinib Acquired Resistance Mechanisms in EGFR Mutant Lung Cancer. *Cell Rep Med* (2020) 1:100007. doi: 10.1016/j.xcrm.2020.100007
13. Leonetti A, Sharma S, Minari R, Perego P, Giovannetti E, Tiseo M. Resistance Mechanisms to Osimertinib in EGFR-Mutated Non-Small Cell Lung Cancer. *Br J Cancer* (2019) 121:725–37. doi: 10.1038/s41416-019-0573-8
14. Schmid S, Li JJN, Leighl NB. Mechanisms of Osimertinib Resistance and Emerging Treatment Options. *Lung Cancer* (2020) 147:123–9. doi: 10.1016/j.lungcan.2020.07.014
15. Lazzari C, Gregorc V, Karachaliou N, Rosell R, Santarpia M. Mechanisms of Resistance to Osimertinib. *J Thorac Dis* (2020) 12:2851–8. doi: 10.21037/jtd.2019.08.30
16. Piper-Vallillo AJ, Sequist LV, Piotrowska Z. Emerging Treatment Paradigms for EGFR-Mutant Lung Cancers Progressing on Osimertinib: A Review. *JCO* (2020) 38:2926–36. doi: 10.1200/JCO.19.03123
17. Passaro A, Jänne PA, Mok T, Peters S. Overcoming Therapy Resistance in EGFR-Mutant Lung Cancer. *Nat Cancer* (2021) 2:377–91. doi: 10.1038/s43018-021-00195-8
18. Ricordel C, Friboulet L, Facchinetti F, Soria J-C. Molecular Mechanisms of Acquired Resistance to Third-Generation EGFR-TKIs in EGFR T790M-Mutant Lung Cancer. *Ann Oncol* (2018) 29:i28–37. doi: 10.1093/annonc/mdx705
19. Ohara S, Suda K, Mitsudomi T. Cell Line Models for Acquired Resistance to First-Line Osimertinib in Lung Cancers—Applications and Limitations. *Cells* (2021) 10:354. doi: 10.3390/cells10020354
20. Nukaga S, Yasuda H, Tsuchihara K, Hamamoto J, Masuzawa K, Kawada I, et al. Amplification of EGFR Wild-Type Alleles in Non–Small Cell Lung Cancer Cells Confers Acquired Resistance to Mutation-Selective EGFR Tyrosine Kinase Inhibitors. *Cancer Res* (2017) 77:2078–89. doi: 10.1158/0008-5472.CAN-16-2359
21. Eberlein CA, Stetson D, Markovets AA, Al-Kadhimi KJ, Lai Z, Fisher PR, et al. Acquired Resistance to the Mutant-Selective EGFR Inhibitor AZD9291 Is Associated With Increased Dependence on RAS Signaling in Preclinical Models. *Cancer Res* (2015) 75:2489–500. doi: 10.1158/0008-5472.CAN-14-3167
22. Ninomiya K, Ohashi K, Makimoto G, Tomida S, Higo H, Kayatani H, et al. MET or NRAS Amplification is an Acquired Resistance Mechanism to the Third-Generation EGFR Inhibitor Naquotinib. *Sci Rep* (2018) 8:1955. doi: 10.1038/s41598-018-20326-z
23. Ku BM, Choi MK, Sun J-M, Lee S-H, Ahn JS, Park K, et al. Acquired Resistance to AZD9291 as an Upfront Treatment Is Dependent on ERK Signaling in a Preclinical Model. *PloS One* (2018) 13:e0194730. doi: 10.1371/journal.pone.0194730
24. La Monica S, Minari R, Cretella D, Bonelli M, Fumarola C, Cavazzoni A, et al. Acquired BRAF G469A Mutation as a Resistance Mechanism to First-Line Osimertinib Treatment in NSCLC Cell Lines Harboring an EGFR Exon 19 Deletion. *Targ Oncol* (2019) 14:619–26. doi: 10.1007/s11523-019-00669-x
25. Chabon JJ, Simmons AD, Lovejoy AF, Esfahani MS, Newman AM, Haringsma HJ, et al. Circulating Tumour DNA Profiling Reveals Heterogeneity of EGFR Inhibitor Resistance Mechanisms in Lung Cancer Patients. *Nat Commun* (2016) 7:11815. doi: 10.1038/ncomms11815
26. Shi P, Oh Y-T, Zhang G, Yao W, Yue P, Li Y, et al. Met Gene Amplification and Protein Hyperactivation Is a Mechanism of Resistance to Both First and Third Generation EGFR Inhibitors in Lung Cancer Treatment. *Cancer Lett* (2016) 380:494–504. doi: 10.1016/j.canlet.2016.07.021
27. Xu H, Shen J, Xiang J, Li H, Li B, Zhang T, et al. Characterization of Acquired Receptor Tyrosine–Kinase Fusions as Mechanisms of Resistance to

EGFR Tyrosine–Kinase Inhibitors. *CMAR* (2019) 11:6343–51. doi: 10.2147/CMAR.S197337
28. Okura N, Nishioka N, Yamada T, Taniguchi H, Tanimura K, Katayama Y, et al. ONO-7475, a Novel AXL Inhibitor, Suppresses the Adaptive Resistance to Initial EGFR-TKI Treatment in *EGFR* -Mutated Non–Small Cell Lung Cancer. *Clin Cancer Res* (2020) 26:2244–56. doi: 10.1158/1078-0432.CCR-19-2321
29. Liu Y, Tsai M, Wu S, Chang T, Tsai T, Gow C, et al. Acquired Resistance to EGFR Tyrosine Kinase Inhibitors Is Mediated by the Reactivation of STC2/JUN/AXL Signaling in Lung Cancer. *Int J Cancer* (2019) 145:1609–24. doi: 10.1002/ijc.32487
30. Kim D, Bach D-H, Fan Y-H, Luu T-T-T, Hong J-Y, Park HJ, et al. AXL Degradation in Combination With EGFR-TKI can Delay and Overcome Acquired Resistance in Human Non-Small Cell Lung Cancer Cells. *Cell Death Dis* (2019) 10:361. doi: 10.1038/s41419-019-1601-6
31. Namba K, Shien K, Takahashi Y, Torigoe H, Sato H, Yoshioka T, et al. Activation of AXL as a Preclinical Acquired Resistance Mechanism Against Osimertinib Treatment in *EGFR* -Mutant Non–Small Cell Lung Cancer Cells. *Mol Cancer Res* (2019) 17:499–507. doi: 10.1158/1541-7786.MCR-18-0628
32. Yang Y-M, Jang Y, Lee SH, Kang B, Lim SM. AXL/MET Dual Inhibitor, CB469, has Activity in Non-Small Cell Lung Cancer With Acquired Resistance to EGFR TKI With AXL or MET Activation. *Lung Cancer* (2020) 146:70–7. doi: 10.1016/j.lungcan.2020.05.031
33. Bertran-Alamillo J, Cattan V, Schoumacher M, Codony-Servat J, Giménez-Capitán A, Cantero F, et al. AURKB as a Target in Non-Small Cell Lung Cancer With Acquired Resistance to Anti-EGFR Therapy. *Nat Commun* (2019) 10:1812. doi: 10.1038/s41467-019-09734-5
34. Park JH, Choi YJ, Kim SY, Lee J-E, Sung KJ, Park S, et al. Activation of the IGF1R Pathway Potentially Mediates Acquired Resistance to Mutant-Selective 3rd-Generation EGF Receptor Tyrosine Kinase Inhibitors in Advanced Non-Small Cell Lung Cancer. *Oncotarget* (2016) 7:22005–15. doi: 10.18632/oncotarget.8013
35. Hayakawa D, Takahashi F, Mitsuishi Y, Tajima K, Hidayat M, Winardi W, et al. Activation of Insulin-Like Growth Factor-1 Receptor Confers Acquired Resistance to Osimertinib in Non-Small Cell Lung Cancer With *EGFR* T790M Mutation. *Thorac Cancer* (2020) 11:140–9. doi: 10.1111/1759-7714.13255
36. Manabe T, Yasuda H, Terai H, Kagiwada H, Hamamoto J, Ebisudani T, et al. IGF2 Autocrine-Mediated IGF1R Activation Is a Clinically Relevant Mechanism of Osimertinib Resistance in Lung Cancer. *Mol Cancer Res* (2020) 18:549–59. doi: 10.1158/1541-7786.MCR-19-0956
37. Weng C-H, Chen L-Y, Lin Y-C, Shih J-Y, Lin Y-C, Tseng R-Y, et al. Epithelial-Mesenchymal Transition (EMT) Beyond EGFR Mutations Per Se Is a Common Mechanism for Acquired Resistance to EGFR TKI. *Oncogene* (2019) 38:455–68. doi: 10.1038/s41388-018-0454-2
38. Fukuda K, Takeuchi S, Arai S, Kita K, Tanimoto A, Nishiyama A, et al. Glycogen Synthase Kinase-3 Inhibition Overcomes Epithelial-Mesenchymal Transition-Associated Resistance to Osimertinib in *EGFR* -Mutant Lung Cancer. *Cancer Sci* (2020) 111:2374–84. doi: 10.1111/cas.14454
39. Takahashi A, Seike M, Chiba M, Takahashi S, Nakamichi S, Matsumoto M, et al. Ankyrin Repeat Domain 1 Overexpression Is Associated With Common Resistance to Afatinib and Osimertinib in EGFR-Mutant Lung Cancer. *Sci Rep* (2018) 8:14896. doi: 10.1038/s41598-018-33190-8
40. Verusingam ND, Chen Y-C, Lin H-F, Liu C-Y, Lee M-C, Lu K-H, et al. Generation of Osimertinib-Resistant Cells From Epidermal Growth Factor Receptor L858R/T790M Mutant Non-Small Cell Lung Carcinoma Cell Line. *J Chin Med Assoc* (2021) 84:248–54. doi: 10.1097/JCMA.0000000000000438
41. Crystal AS, Shaw AT, Sequist LV, Friboulet L, Niederst MJ, Lockerman EL, et al. Patient-Derived Models of Acquired Resistance can Identify Effective Drug Combinations for Cancer. *Science* (2014) 346:1480–6. doi: 10.1126/science.1254721
42. Raoof S, Mulford IJ, Frisco-Cabanos H, Nangia V, Timonina D, Labrot E, et al. Targeting FGFR Overcomes EMT-Mediated Resistance in EGFR Mutant Non-Small Cell Lung Cancer. *Oncogene* (2019) 38:6399–413. doi: 10.1038/s41388-019-0887-2
43. Codony-Servat J, Codony-Servat C, Cardona AF, Giménez-Capitán A, Drozdowskyj A, Berenguer J, et al. Cancer Stem Cell Biomarkers in EGFR-Mutation-Positive Non-Small-Cell Lung Cancer. *Clin Lung Cancer* (2019) 20:167–77. doi: 10.1016/j.cllc.2019.02.005
44. Shi P, Oh Y-T, Deng L, Zhang G, Qian G, Zhang S, et al. Overcoming Acquired Resistance to AZD9291, A Third-Generation EGFR Inhibitor, Through Modulation of MEK/ERK-Dependent Bim and Mcl-1 Degradation. *Clin Cancer Res* (2017) 23:6567–79. doi: 10.1158/1078-0432.CCR-17-1574
45. Zang H, Qian G, Zong D, Fan S, Owonikoko TK, Ramalingam SS, et al. Overcoming Acquired Resistance of Epidermal Growth Factor Receptor-Mutant Non–Small Cell Lung Cancer Cells to Osimertinib by Combining Osimertinib With the Histone Deacetylase Inhibitor Panobinostat (LBH589). *Cancer* (2020) 126:2024–33. doi: 10.1002/cncr.32744
46. Liu Z, Gao W. Synergistic Effects of Bcl-2 Inhibitors With AZD9291 on Overcoming the Acquired Resistance of AZD9291 in H1975 Cells. *Arch Toxicol* (2020) 94:3125–36. doi: 10.1007/s00204-020-02816-0
47. Galvani E, Sun J, Leon LG, Sciarrillo R, Narayan RS, Tjin Tham Sjin R, et al. NF-κb Drives Acquired Resistance to a Novel Mutant-Selective EGFR Inhibitor. *Oncotarget* (2015) 6:42717–32. doi: 10.18632/oncotarget.3956
48. Pan Y-H, Lin C-Y, Lu C-H, Li L, Wang Y-B, Chen H-Y, et al. Metformin Synergistically Enhances the Antitumor Activity of the Third-Generation EGFR-TKI CO-1686 in Lung Cancer Cells Through Suppressing NF-κb Signaling: Pan Et al. *Clin Respir J* (2018) 12:2642–52. doi: 10.1111/crj.12970
49. Shah KN, Bhatt R, Rotow J, Rohrberg J, Olivas V, Wang VE, et al. Aurora Kinase A Drives the Evolution of Resistance to Third-Generation EGFR Inhibitors in Lung Cancer. *Nat Med* (2019) 25:111–8. doi: 10.1038/s41591-018-0264-7
50. Qin Q, Li X, Liang X, Zeng L, Wang J, Sun L, et al. CDK4/6 Inhibitor Palbociclib Overcomes Acquired Resistance to Third-Generation EGFR Inhibitor Osimertinib in Non-Small Cell Lung Cancer (NSCLC). *Thorac Cancer* (2020) 11:2389–97. doi: 10.1111/1759-7714.13521
51. Tang Z, Su M-X, Guo X, Jiang X-M, Jia L, Chen X, et al. Increased Expression of IRE1α Associates With the Resistant Mechanism of Osimertinib (AZD9291)-Resistant Non-Small Cell Lung Cancer HCC827/OSIR Cells. *ACAMC* (2018) 18:550–5. doi: 10.2174/1871520617666170719155517
52. Wang J, Wang B, Chu H, Yao Y. Intrinsic Resistance to EGFR Tyrosine Kinase Inhibitors in Advanced Non-Small-Cell Lung Cancer With Activating EGFR Mutations. *Oncol Targets Ther* (2016) 9:3711–26. doi: 10.2147/OTT.S106399
53. Ramirez M, Rajaram S, Steininger RJ, Osipchuk D, Roth MA, Morinishi LS, et al. Diverse Drug-Resistance Mechanisms can Emerge From Drug-Tolerant Cancer Persister Cells. *Nat Commun* (2016) 7:10690. doi: 10.1038/ncomms10690
54. Oxnard GR. The Cellular Origins of Drug Resistance in Cancer. *Nat Med* (2016) 22:232–4. doi: 10.1038/nm.4058
55. Hata AN, Niederst MJ, Archibald HL, Gomez-Caraballo M, Siddiqui FM, Mulvey HE, et al. Tumor Cells can Follow Distinct Evolutionary Paths to Become Resistant to Epidermal Growth Factor Receptor Inhibition. *Nat Med* (2016) 22:262–9. doi: 10.1038/nm.4040
56. De Conti G, Dias MH, Bernards R. Fighting Drug Resistance Through the Targeting of Drug-Tolerant Persister Cells. *Cancers* (2021) 13:1118. doi: 10.3390/cancers13051118
57. Sharma SV, Lee DY, Li B, Quinlan MP, Takahashi F, Maheswaran S, et al. A Chromatin-Mediated Reversible Drug-Tolerant State in Cancer Cell Subpopulations. *Cell* (2010) 141:69–80. doi: 10.1016/j.cell.2010.02.027
58. Wang R, Yamada T, Kita K, Taniguchi H, Arai S, Fukuda K, et al. Transient IGF-1R Inhibition Combined With Osimertinib Eradicates AXL-Low Expressing EGFR Mutated Lung Cancer. *Nat Commun* (2020) 11:4607. doi: 10.1038/s41467-020-18442-4
59. Taniguchi H, Yamada T, Wang R, Tanimura K, Adachi Y, Nishiyama A, et al. AXL Confers Intrinsic Resistance to Osimertinib and Advances the Emergence of Tolerant Cells. *Nat Commun* (2019) 10:259. doi: 10.1038/s41467-018-08074-0
60. Song K-A, Hosono Y, Turner C, Jacob S, Lochmann TL, Murakami Y, et al. Increased Synthesis of MCL-1 Protein Underlies Initial Survival of *EGFR* -Mutant Lung Cancer to EGFR Inhibitors and Provides a Novel Drug Target. *Clin Cancer Res* (2018) 24:5658–72. doi: 10.1158/1078-0432.CCR-18-0304
61. Tanaka K, Yu HA, Yang S, Han S, Selcuklu SD, Kim K, et al. Targeting Aurora B Kinase Prevents and Overcomes Resistance to EGFR Inhibitors in

Lung Cancer by Enhancing BIM- and PUMA-Mediated Apoptosis. *Cancer Cell* (2021) 39:1245–61.e6. doi: 10.1016/j.ccell.2021.07.006
62. Yang Z, Yang N, Ou Q, Xiang Y, Jiang T, Wu X, et al. Investigating Novel Resistance Mechanisms to Third-Generation EGFR Tyrosine Kinase Inhibitor Osimertinib in Non–Small Cell Lung Cancer Patients. *Clin Cancer Res* (2018) 24:3097–107. doi: 10.1158/1078-0432.CCR-17-2310
63. Chen T, Luo J, Gu Y, Huang J, Luo Q, Yang Y. Comprehensive Analysis of Circular RNA Profiling in AZD9291-Resistant Non-Small Cell Lung Cancer Cell Lines. *Thorac Cancer* (2019) 10:930–41. doi: 10.1111/1759-7714.13032
64. Takahashi S, Noro R, Seike M, Zeng C, Matsumoto M, Yoshikawa A, et al. Long Non-Coding RNA CRNDE Is Involved in Resistance to EGFR Tyrosine Kinase Inhibitor in EGFR-Mutant Lung Cancer *via* Eif4a3/MUC1/EGFR Signaling. *IJMS* (2021) 22:4005. doi: 10.3390/ijms22084005
65. Hayford CE, Tyson DR, Robbins CJ, Frick PL, Quaranta V, Harris LA. An *In Vitro* Model of Tumor Heterogeneity Resolves Genetic, Epigenetic, and Stochastic Sources of Cell State Variability. *PloS Biol* (2021) 19:e3000797. doi: 10.1371/journal.pbio.3000797
66. Klempner S, Mehta P, Schrock A, Ali S, Ou S-HI. Cis-Oriented Solvent-Front EGFR G796S Mutation in Tissue and ctDNA in a Patient Progressing on Osimertinib: A Case Report and Review of the Literature. *LCTT* (2017) 8:241–7. doi: 10.2147/LCTT.S147129
67. Fassunke J, Müller F, Keul M, Michels S, Dammert MA, Schmitt A, et al. Overcoming EGFRG724S-Mediated Osimertinib Resistance Through Unique Binding Characteristics of Second-Generation EGFR Inhibitors. *Nat Commun* (2018) 9:4655. doi: 10.1038/s41467-018-07078-0
68. Nishino M, Suda K, Kobayashi Y, Ohara S, Fujino T, Koga T, et al. Effects of Secondary EGFR Mutations on Resistance Against Upfront Osimertinib in Cells With EGFR-Activating Mutations *In Vitro*. *Lung Cancer* (2018) 126:149–55. doi: 10.1016/j.lungcan.2018.10.026
69. Peled N, Roisman LC, Miron B, Pfeffer R, Lanman RB, Ilouze M, et al. Subclonal Therapy by Two EGFR TKIs Guided by Sequential Plasma Cell-Free DNA in EGFR -Mutated Lung Cancer. *J Thorac Oncol* (2017) 12:e81–4. doi: 10.1016/j.jtho.2017.02.023
70. Niederst MJ, Hu H, Mulvey HE, Lockerman EL, Garcia AR, Piotrowska Z, et al. The Allelic Context of the C797S Mutation Acquired Upon Treatment With Third-Generation EGFR Inhibitors Impacts Sensitivity to Subsequent Treatment Strategies. *Clin Cancer Res* (2015) 21:3924–33. doi: 10.1158/1078-0432.CCR-15-0560
71. Wang Z, Yang J-J, Huang J, Ye J-Y, Zhang X-C, Tu H-Y, et al. Lung Adenocarcinoma Harboring EGFR T790M and In Trans C797S Responds to Combination Therapy of First- and Third-Generation EGFR TKIs and Shifts Allelic Configuration at Resistance. *J Thorac Oncol* (2017) 12:1723–7. doi: 10.1016/j.jtho.2017.06.017
72. Arulananda S, Do H, Musafer A, Mitchell P, Dobrovic A, John T. Combination Osimertinib and Gefitinib in C797S and T790M EGFR-Mutated Non-Small Cell Lung Cancer. *J Thorac Oncol* (2017) 12:1728–32. doi: 10.1016/j.jtho.2017.08.006
73. Rangachari D, To C, Shpilsky JE, VanderLaan PA, Kobayashi SS, Mushajiang M, et al. EGFR-Mutated Lung Cancers Resistant to Osimertinib Through EGFR C797S Respond to First-Generation Reversible EGFR Inhibitors But Eventually Acquire EGFR T790M/C797S in Preclinical Models and Clinical Samples. *J Thorac Oncol* (2019) 14:1995–2002. doi: 10.1016/j.jtho.2019.07.016
74. Robichaux JP, Le X, Vijayan RSK, Hicks JK, Heeke S, Elamin YY, et al. Structure-Based Classification Predicts Drug Response in EGFR-Mutant NSCLC. *Nature* (2021) 597:732–7. doi: 10.1038/s41586-021-03898-1
75. Papadimitrakopoulou VA, Wu Y-L, Han J-Y, Ahn M-J, Ramalingam SS, John T, et al. Analysis of Resistance Mechanisms to Osimertinib in Patients With EGFR T790M Advanced NSCLC From the AURA3 Study. *Ann Oncol* (2018) 29:viii741. doi: 10.1093/annonc/mdy424.064
76. Ramalingam SS, Cheng Y, Zhou C, Ohe Y, Imamura F, Cho BC, et al. Mechanisms of Acquired Resistance to First-Line Osimertinib: Preliminary Data From the Phase III FLAURA Study. *Ann Oncol* (2018) 29:viii740. doi: 10.1093/annonc/mdy424.063
77. Schoenfeld AJ, Chan JM, Kubota D, Sato H, Rizvi H, Daneshbod Y, et al. Tumor Analyses Reveal Squamous Transformation and Off-Target Alterations As Early Resistance Mechanisms to First-Line Osimertinib in *EGFR* -Mutant Lung Cancer. *Clin Cancer Res* (2020) 26:2654–63. doi: 10.1158/1078-0432.CCR-19-3563
78. Le X, Puri S, Negrao MV, Nilsson MB, Robichaux J, Boyle T, et al. Landscape of EGFR-Dependent and -Independent Resistance Mechanisms to Osimertinib and Continuation Therapy Beyond Progression in *EGFR* -Mutant NSCLC. *Clin Cancer Res* (2018) 24:6195–203. doi: 10.1158/1078-0432.CCR-18-1542
79. Ma Y, Zheng X, Zhao H, Fang W, Zhang Y, Ge J, et al. First-In-Human Phase I Study of AC0010, a Mutant-Selective EGFR Inhibitor in Non–Small Cell Lung Cancer: Safety, Efficacy, and Potential Mechanism of Resistance. *J Thorac Oncol* (2018) 13:968–77. doi: 10.1016/j.jtho.2018.03.025
80. Ho C-C, Liao W-Y, Lin C-A, Shih J-Y, Yu C-J, Yang JC-H. Acquired BRAF V600E Mutation as Resistant Mechanism After Treatment With Osimertinib. *J Thorac Oncol* (2017) 12:567–72. doi: 10.1016/j.jtho.2016.11.2231
81. Minari R, Bordi P, La Monica S, Squadrilli A, Leonetti A, Bottarelli L, et al. Concurrent Acquired BRAF V600E Mutation and MET Amplification as Resistance Mechanism of First-Line Osimertinib Treatment in a Patient With EGFR-Mutated NSCLC. *J Thorac Oncol* (2018) 13:e89–91. doi: 10.1016/j.jtho.2018.03.013
82. Bearz A, De Carlo E, Doliana R, Schiappacassi M. Acquired BRAF V600E Mutation as Resistant Mechanism After Treatment With Third-Generation EGFR Tyrosine Kinase Inhibitor. *J Thorac Oncol* (2017) 12:e181–2. doi: 10.1016/j.jtho.2017.07.017
83. Blakely CM, Watkins TBK, Wu W, Gini B, Chabon JJ, McCoach CE, et al. Evolution and Clinical Impact of Co-Occurring Genetic Alterations in Advanced-Stage EGFR-Mutant Lung Cancers. *Nat Genet* (2017) 49:1693–704. doi: 10.1038/ng.3990
84. Fang X, Gu P, Zhou C, Liang A, Ren S, Liu F, et al. β-Catenin Overexpression Is Associated With Gefitinib Resistance in Non-Small Cell Lung Cancer Cells. *Pulm Pharmacol Ther* (2014) 28:41–8. doi: 10.1016/j.pupt.2013.05.005
85. Togashi Y, Hayashi H, Terashima M, de Velasco MA, Sakai K, Fujita Y, et al. Inhibition of β-Catenin Enhances the Anticancer Effect of Irreversible EGFR-TKI in EGFR-Mutated Non–Small-Cell Lung Cancer With a T790M Mutation. *J Thorac Oncol* (2015) 10:93–101. doi: 10.1097/JTO.0000000000000353
86. Xu W, Tang W, Li T, Zhang X, Sun Y. Overcoming Resistance to AC0010, a Third Generation of EGFR Inhibitor, by Targeting C-MET and BCL-2. *Neoplasia* (2019) 21:41–51. doi: 10.1016/j.neo.2018.11.004
87. Ou S-HI, Cui J, Schrock AB, Goldberg ME, Zhu VW, Albacker L, et al. Emergence of Novel and Dominant Acquired EGFR Solvent-Front Mutations at Gly796 (G796S/R) Together With C797S/R and L792F/H Mutations in One EGFR (L858R/T790M) NSCLC Patient Who Progressed on Osimertinib. *Lung Cancer* (2017) 108:228–31. doi: 10.1016/j.lungcan.2017.04.003
88. Sequist LV, Han J-Y, Ahn M-J, Cho BC, Yu H, Kim S-W, et al. Osimertinib Plus Savolitinib in Patients With EGFR Mutation-Positive, MET-Amplified, Non-Small-Cell Lung Cancer After Progression on EGFR Tyrosine Kinase Inhibitors: Interim Results From a Multicentre, Open-Label, Phase 1b Study. *Lancet Oncol* (2020) 21:373–86. doi: 10.1016/S1470-2045(19)30785-5
89. Oxnard GR, Yang JC-H, Yu H, Kim S-W, Saka H, Horn L, et al. TATTON: A Multi-Arm, Phase Ib Trial of Osimertinib Combined With Selumetinib, Savolitinib, or Durvalumab in EGFR-Mutant Lung Cancer. *Ann Oncol* (2020) 31:507–16. doi: 10.1016/j.annonc.2020.01.013
90. Zhang Z, Lee JC, Lin L, Olivas V, Au V, LaFramboise T, et al. Activation of the AXL Kinase Causes Resistance to EGFR-Targeted Therapy in Lung Cancer. *Nat Genet* (2012) 44:852–60. doi: 10.1038/ng.2330
91. Mudduluru G, Leupold JH, Stroebel P, Allgayer H. PMA Up-Regulates the Transcription of Axl by AP-1 Transcription Factor Binding to TRE Sequences *via* the MAPK Cascade in Leukaemia Cells. *Biol Cell* (2011) 103:21–33. doi: 10.1042/BC20100094
92. Liu Y-N, Chang T-H, Tsai M-F, Wu S-G, Tsai T-H, Chen H-Y, et al. IL-8 Confers Resistance to EGFR Inhibitors by Inducing Stem Cell Properties in Lung Cancer. *Oncotarget* (2015) 6:10415–31. doi: 10.18632/oncotarget.3389
93. Karachaliou N, Chaib I, Cardona AF, Berenguer J, Bracht JWP, Yang J, et al. Common Co-Activation of AXL and CDCP1 in EGFR-Mutation-Positive Non-Small Cell Lung Cancer Associated With Poor Prognosis. *EBioMedicine* (2018) 29:112–27. doi: 10.1016/j.ebiom.2018.02.001

94. Peled N, Wynes MW, Ikeda N, Ohira T, Yoshida K, Qian J, et al. Insulin-Like Growth Factor-1 Receptor (IGF-1R) as a Biomarker for Resistance to the Tyrosine Kinase Inhibitor Gefitinib in Non-Small Cell Lung Cancer. *Cell Oncol (Dordr)* (2013) 36:277–88. doi: 10.1007/s13402-013-0133-9
95. Yeo CD, Park KH, Park CK, Lee SH, Kim SJ, Yoon HK, et al. Expression of Insulin-Like Growth Factor 1 Receptor (IGF-1R) Predicts Poor Responses to Epidermal Growth Factor Receptor (EGFR) Tyrosine Kinase Inhibitors in non-Small Cell Lung Cancer Patients Harboring Activating EGFR Mutations. *Lung Cancer* (2015) 87:311–7. doi: 10.1016/j.lungcan.2015.01.004
96. Cortot AB, Repellin CE, Shimamura T, Capelletti M, Zejnullahu K, Ercan D, et al. Resistance to Irreversible EGF Receptor Tyrosine Kinase Inhibitors Through a Multistep Mechanism Involving the IGF1R Pathway. *Cancer Res* (2013) 73:834–43. doi: 10.1158/0008-5472.CAN-12-2066
97. Aghdassi A, Sendler M, Guenther A, Mayerle J, Behn C-O, Heidecke C-D, et al. Recruitment of Histone Deacetylases HDAC1 and HDAC2 by the Transcriptional Repressor ZEB1 Downregulates E-Cadherin Expression in Pancreatic Cancer. *Gut* (2012) 61:439–48. doi: 10.1136/gutjnl-2011-300060
98. Brabletz S, Brabletz T. The ZEB/miR-200 Feedback Loop—A Motor of Cellular Plasticity in Development and Cancer? *EMBO Rep* (2010) 11:670–7. doi: 10.1038/embor.2010.117
99. Vijay GV, Zhao N, Den Hollander P, Toneff MJ, Joseph R, Pietila M, et al. Gsk3β Regulates Epithelial-Mesenchymal Transition and Cancer Stem Cell Properties in Triple-Negative Breast Cancer. *Breast Cancer Res* (2019) 21:37. doi: 10.1186/s13058-019-1125-0
100. Feldker N, Ferrazzi F, Schuhwerk H, Widholz SA, Guenther K, Frisch I, et al. Genome-Wide Cooperation of EMT Transcription Factor ZEB 1 With YAP and AP -1 in Breast Cancer. *EMBO J* (2020) 39(17):e103209. doi: 10.15252/embj.2019103209
101. DeNardo DG, Barreto JB, Andreu P, Vasquez L, Tawfik D, Kolhatkar N, et al. CD4(+) T Cells Regulate Pulmonary Metastasis of Mammary Carcinomas by Enhancing Protumor Properties of Macrophages. *Cancer Cell* (2009) 16:91–102. doi: 10.1016/j.ccr.2009.06.018
102. Kim TM, Song A, Kim D-W, Kim S, Ahn Y-O, Keam B, et al. Mechanisms of Acquired Resistance to AZD9291. *J Thorac Oncol* (2015) 10:1736–44. doi: 10.1097/JTO.0000000000000688
103. Arasada RR, Amann JM, Rahman MA, Huppert SS, Carbone DP. EGFR Blockade Enriches for Lung Cancer Stem–like Cells Through Notch3-Dependent Signaling. *Cancer Res* (2014) 74:5572–84. doi: 10.1158/0008-5472.CAN-13-3724
104. Codony-Servat C, Codony-Servat J, Karachaliou N, Molina MA, Chaib I, Ramirez JL, et al. Activation of Signal Transducer and Activator of Transcription 3 (STAT3) Signaling in EGFR Mutant non-Small-Cell Lung Cancer (NSCLC). *Oncotarget* (2017) 8:47305–16. doi: 10.18632/oncotarget.17625
105. Goto N, Ueo T, Fukuda A, Kawada K, Sakai Y, Miyoshi H, et al. Distinct Roles of HES1 in Normal Stem Cells and Tumor Stem-Like Cells of the Intestine. *Cancer Res* (2017) 77:3442–54. doi: 10.1158/0008-5472.CAN-16-3192
106. Bousquet Mur E, Bernardo S, Papon L, Mancini M, Fabbrizio E, Goussard M, et al. Notch Inhibition Overcomes Resistance to Tyrosine Kinase Inhibitors in EGFR-Driven Lung Adenocarcinoma. *J Clin Invest* (2019) 130:612–24. doi: 10.1172/JCI126896
107. Faber AC, Corcoran RB, Ebi H, Sequist LV, Waltman BA, Chung E, et al. BIM Expression in Treatment-Naïve Cancers Predicts Responsiveness to Kinase Inhibitors. *Cancer Discov* (2011) 1:352–65. doi: 10.1158/2159-8290.CD-11-0106
108. Ley R, Balmanno K, Hadfield K, Weston C, Cook SJ. Activation of the ERK1/2 Signaling Pathway Promotes Phosphorylation and Proteasome-Dependent Degradation of the BH3-Only Protein, Bim. *J Biol Chem* (2003) 278:18811–6. doi: 10.1074/jbc.M301010200
109. Domina AM, Vrana JA, Gregory MA, Hann SR, Craig RW. MCL1 is Phosphorylated in the PEST Region and Stabilized Upon ERK Activation in Viable Cells, and at Additional Sites With Cytotoxic Okadaic Acid or Taxol. *Oncogene* (2004) 23:5301–15. doi: 10.1038/sj.onc.1207692
110. Bertino EM, Gentzler RD, Clifford S, Kolesar J, Muzikansky A, Haura EB, et al. Phase IB Study of Osimertinib in Combination With Navitoclax in *EGFR* -Mutant NSCLC Following Resistance to Initial *EGFR* Therapy (ETCTN 9903). *Clin Cancer Res* (2021) 27:1604–11. doi: 10.1158/1078-0432.CCR-20-4084
111. Shi P, Zhang S, Zhu L, Qian G, Ren H, Ramalingam SS, et al. The Third-Generation EGFR Inhibitor, Osimertinib, Promotes C-FLIP Degradation, Enhancing Apoptosis Including TRAIL-Induced Apoptosis in NSCLC Cells With Activating EGFR Mutations. *Trans Oncol* (2019) 12:705–13. doi: 10.1016/j.tranon.2019.02.006
112. Bivona TG, Hieronymus H, Parker J, Chang K, Taron M, Rosell R, et al. FAS and NF-κb Signalling Modulate Dependence of Lung Cancers on Mutant EGFR. *Nature* (2011) 471:523–6. doi: 10.1038/nature09870
113. Moiseeva O, Deschênes-Simard X, St-Germain E, Igelmann S, Huot G, Cadar AE, et al. Metformin Inhibits the Senescence-Associated Secretory Phenotype by Interfering With IKK / NF -κ B Activation. *Aging Cell* (2013) 12:489–98. doi: 10.1111/acel.12075
114. Tang A, Gao K, Chu L, Zhang R, Yang J, Zheng J. Aurora Kinases: Novel Therapy Targets in Cancers. *Oncotarget* (2017) 8:23937–54. doi: 10.18632/oncotarget.14893
115. Shi R, Radulovich N, Ng C, Liu N, Notsuda H, Cabanero M, et al. Organoid Cultures as Preclinical Models of Non-Small Cell Lung Cancer. *Clin Cancer Res* (2020) 26:1162–74. doi: 10.1158/1078-0432.CCR-19-1376

Conflict of Interest: RP received a grant from AstraZeneca to conduct a project in the laboratory but it was not used to fund this review.

The remaining authors declare that the research was conducted in the absence of any commercial or financial relationships that could be construed as a potential conflict of interest.

frontiers | Frontiers in Oncology

ORIGINAL RESEARCH
published: 08 June 2022
doi: 10.3389/fonc.2022.876051

Platelet Activation in High D-Dimer Plasma Plays a Role in Acquired Resistance to Epidermal Growth Factor Receptor Tyrosine Kinase Inhibitors in Patients with Mutant Lung Adenocarcinoma

Meng-Jung Lee[1,2†], *Chih-Ming Weng*[2,3†], *Wei Chao*[2], *Yueh-Fu Fang*[4], *Fu-Tsai Chung*[4], *Chien-Huang Lin*[1,2] *and Han-Pin Kuo*[2,5*]

[1] Graduate Institute of Medical Sciences, College of Medicine, Taipei Medical University, Taipei, Taiwan, [2] Thoracic Medicine Research Center, Taipei Medical University, Taipei, Taiwan, [3] School of Respiratory Therapy, College of Medicine, Taipei Medical University, Taipei, Taiwan, [4] Department of Thoracic Medicine, Chang Gung Medical Foundation, Chang Gung University College of Medicine, Taipei, Taiwan, [5] Department of Thoracic Medicine, Taipei Medical University Hospital, Taipei, Taiwan

OPEN ACCESS

Edited by:
Iacopo Petrini,
University of Pisa, Italy

Reviewed by:
Fang-Ju Cheng,
China Medical University, Taiwan
Chin-Chou Wang,
Kaohsiung Chang Gung Memorial Hospital, Taiwan

***Correspondence:**
Han-Pin Kuo
q8828@tmu.edu.tw;
hpk8828@gmail.com

[†]These authors have contributed equally to this work and share first authorship

Specialty section:
This article was submitted to Thoracic Oncology, a section of the journal Frontiers in Oncology

Received: 15 February 2022
Accepted: 09 May 2022
Published: 08 June 2022

Citation:
Lee M-J, Weng C-M, Chao W, Fang Y-F, Chung F-T, Lin C-H and Kuo H-P (2022) Platelet Activation in High D-Dimer Plasma Plays a Role in Acquired Resistance to Epidermal Growth Factor Receptor Tyrosine Kinase Inhibitors in Patients with Mutant Lung Adenocarcinoma. Front. Oncol. 12:876051. doi: 10.3389/fonc.2022.876051

Objective: Platelet activation and adhesion to cancer cells increase the release of multiple factors that contribute to EMT and chemoresistance. Elevated levels of D-dimer have been associated with poor clinical outcomes in lung cancer. Platelets in high D-dimer plasma may be activated and implicated in acquired resistance to EGFR TKI in advanced lung adenocarcinoma with mutant EGFR.

Materials and Methods: Clinical responsive rate (RR), progression-free survival (PFS), and overall survival (OS) were prospectively measured in treatment-naïve lung adenocarcinoma patients with activation mutation. Plasma or platelets from patients with high or low D-dimer level were obtained to investigate the cytotoxic effects of TKIs on mutant cancer cells, and the mechanistic pathways were also explored.

Results: Patients with high D-dimer had worse RR, PFS, and OS. High D-dimer plasma induced resistance to gefitinib, erlotinib, afatinib, or osimertinib in EGFR mutant lung cancer cells. Depletion of platelets in high D-dimer plasma reversed the resistance to TKI. Platelets of high D-dimer plasma had higher adherence capacity to cancer cells, and induced EGFR and Akt activation as well as EMT through Src activation. Inhibition of platelet adherence or activation of Src or Akt conquered the resistance to TKI. The acquired resistance to TKI by high D-dimer plasma was less attributed to secondary gene mutation.

Conclusion: Increased platelet activation in the high D-dimer plasma may contribute to first-line acquired EGFR TKI resistance. Thus, therapeutic strategy against platelet activation in patients with high D-dimer levels may improve the efficacy of first-line treatment with EGFR TKI.

Keywords: epidermal growth factor receptor, tyrosine kinase inhibitor, lung adenocarcinoma, platelet, epithelial–mesenchymal transition, D-dimer, Src, Akt

INTRODUCTION

Blockage of dysregulated EGFR with tyrosine kinase inhibitors (EGFR-TKI) has played a central role in the treatment of advanced non-small cell lung cancer (NSCLC) with a significant improvement in clinical outcome: a response rate as high as 80%, especially for lung cancer patients with exon 19 deletions or an L858R mutation. However, acquired resistance and secondary progression are seen in almost all the patients with a median of 10–14 months of progression-free survival (PFS) (1–3). Molecular mechanism analysis reveals that the T790M point mutation, which lowers TKI binding affinity to the ATP pocket, is the most frequent underlying mechanism (4, 5), though it is more frequent with reversible TKI (gefitinib and erlotinib) than irreversible afatinib (6). Less frequent resistance mechanisms include ERBB2 and MET amplifications (7, 8) and mutations within the downstream signaling molecules BRAF, KRAS, PIK3CA, and CTNNB1 (9). Nevertheless, the efficacy differs a lot among patients with the same EGFR-sensitive mutations (10). The histological transformation into small cell or sarcomatoid lung cancer phenotypes, aberrations of drug transporters, or lysosomal sequestration (11) has been reported for the mechanisms underlying the diminished efficacy of EGFR TKI. However, given the multiple possible escape strategies, it remains a big challenge to predict the future mechanism of resistance of a specific tumor and target it from the beginning.

Increasing evidence has demonstrated that platelets play an important role in cancer survival, growth, and metastasis (12, 13). Within the blood circulation, tumor cells can aggregate with platelets and avoid cytotoxicity of natural killer cells (14, 15), indicating that platelet adhesion to tumor cells is a crucial step for tumor cell survival within the blood circulation. Direct contact of platelets with tumor cells also results in activation (16). Platelet–tumor cell aggregates form through binding of platelet integrin αIIbβ3 to tumor cell integrin αvβ3 *via* RGD-containing proteins including fibrinogen, von Willebrand factor, and fibronectin, a process known as tumor cell-induced platelet aggregation (TCIPA) (10). Once activated, platelets release an array of biologically active molecules that can modulate tumor growth, angiogenesis, and metastasis, including transforming growth factor beta (TGF-β1), vascular endothelial growth factor (VEGF), and platelet-derived growth factor (PDGF), inducing epithelial mesenchymal transit (12, 13). The roles of platelets in tumor development have also been shown to contribute to chemoresistance (17, 18).

D-dimer is a dimerized fragment from fibrinogen and a marker of thrombin activity and fibrin turnover, and represents both hemostasis and fibrinolysis (19). A variety of cancers have association between D-dimer and clinical manifestations such as tumor stage, metastasis and growth, and progression of cancers, as well as thromboembolic events (20, 21). D-dimer levels are a useful predictor for survival independent of clinical stage, histologic tumor type, and performance status of lung cancer patients (22). The mechanism underlying the relationship between D-dimer levels and lung cancer prognosis remains unknown. It is well known that platelet activation and blood coagulation are complementary, mutually dependent processes in hemostasis and thrombosis (23). Platelets interact with several coagulation factors, while the coagulation product thrombin is a potent platelet-activating agonist (23). Thus, the platelets in patients with high D-dimer may be further activated. On the other hand, the enhanced fibrin formation and fibrinolysis in cancer patients with high D-dimer may be secondary to platelet activation and aggregation (24).

This study addressed the question whether platelets in high D-dimer plasma of patients with mutant adenocarcinoma conferred EGFR-TKI acquired resistance. The results of this prospective study revealed that platelets were more activated in patients with high plasma D-dimer levels contributing to the development of phosphorylation of EGFR and Akt, as well as epithelial–mesenchymal transition (EMT) through Src activation, resulting in poor PFS and overall survival (OS). The acquired resistance to EGFR TKI in high D-dimer plasma was less attributed to secondary gene mutation. Thus, therapeutic strategy against platelet activation in patients with high D-dimer levels may improve the efficacy of first-line treatment with EGFR TKI.

MATERIALS AND METHODS

Subjects' Characteristics

During 2016 to 2018, 102 late-stage (Stage IV) treatment-naïve, non-smoking patients with mutant adenocarcinoma (Exon19 deletion or exon 21 point-mutation) without primary T790M or *ERBB2* and *MET* amplifications or ALK and ROS1 rearrangement intending to receive EGFR TKI treatment (gefitinib, erlotinib, or afatinib) were recruited from the outpatient department of Chang Gung Memorial Hospital and Taipei Medical University Hospital (both were tertiary referral hospitals in Northern Taiwan) into this 2-year prospective observational study. The biopsied specimens of naïve lung cancer that were routinely screened for mutation analysis of EGFR (exon18-21) were analyzed, including exon 19 deletions and L858R and T790M missense mutations by PCR assays with the Cobas EGFR mutation test. ERBB2 amplification and MET fusion or variant transcript were detected by RNA sequencing, and ALK and ROS1 rearrangement was confirmed by immunohistochemistry (IHC) assay with anti-ALK and anti-ROS1 rabbit monoclonal primary antibodies (VENTANA). The levels of D-dimer were measured before treatment. Patients with evident deep vein thrombosis, under anti-coagulant and/or anti-platelet treatment, with symptomatic heart failure (>NYHA II), with prior or coexistence of other malignancies, or with GOLD stage III-IV COPD were excluded from the recruitment. The existence of deep vein thrombosis in patients with high D-dimer levels was systemically assessed, using duplex ultrasonography and CT angiography. Clinical responses were assessed by response rate, PFS, and OS. Re-biopsy of tumors after disease progression was performed in most patients. Genetic analysis of the

mechanisms for secondary resistance to EGFR TKI was also done. Because osimertinib was not reimbursed by the National Health Insurance in Taiwan during this study period, most patients received platinum-based doublet chemotherapy after disease progression, while 10 patients in the low D-dimer group and 6 patients in the high D-dimer group received self-pay osimertinib treatment for disease progression with the 2nd T790M mutation. Since osimertinib has been shown to be effective in counteracting with resistance T790M, those patients with osimertinib treatment were excluded from the OS assessment. All patients provided informed consent to participate in this study, which was approved by the local ethics committee [IRB was provided by the TMU-Joint Institutional Review Board (no. N201808072)].

Proteomic Analysis of High D-Dimer Plasma

The proteomic analysis of patient's plasma was performed by Biotools service (Biotools Co., Ltd., Taiwan) according to the manufacturer's instructions.

Preparation of Platelet-Rich Plasma and Platelet-Poor Plasma

Plasma was separated from the whole blood of high or low D-dimer patients. In brief, after centrifugation, the yellow upper phase containing the plasma component was transferred to new tubes with great care and then centrifuged again. The lower one-third was the platelet-rich plasma (PRP) and the upper two-thirds was the platelet-poor plasma (PPP). At the bottom of the tube, platelet pellets were formed (25).

Cell Lines and Cell Viability Assay

HCC827 (Cat# CRL-2868) and NCI-H1975 (Cat# CRL-5908) were purchased from the American Type Culture Collection (ATCC), and PC9 (Cat# 90071810) was purchased from Sigma-Aldrich Corporation (St. Louis, MO). The cancer cells were cultured in high-glucose RPMI with 10% FBS and antibiotics in a humidified 37°C incubator, and seeded onto 96 wells for cell viability assay and onto 6-cm dishes for transfection and immunoblotting.

Surface Protein Analysis of Platelet

PRP was isolated from normal, low, or high D-dimer lung cancer patients and then stained with CD42b-PE and glycoprotein VI-AF647 for 30 min. After washing, the percentage of $CD42b^+$/$GPVI^+$ cells was analyzed by a FACSLyrics flow cytometer and FACSuite software (Becton Dickinson, Mountain View, CA, USA).

Platelet Adherence to Cancer Cells

The PRP of patients with low and high D-dimer levels was added to cultured HCC827 cells for 2 h in the presence or absence of PGI2 or dasatinib. Platelets were labeled with CD42b-PE, and non-adherent platelets were washed with PBS. The adherent platelets were counted under high-power fields of fluorescence microscopy for a total of 5 fields.

Transfection of E-Cadherin siRNA

E-cadherin (GenBank no. NM_004360) siRNAs were generated, following the sequence of siRNA1: 5'-GGGUUAAGC ACAACAGCAA-3' and siRNA2: 5'-CAGACAAAGACCAGG ACUA-3'. HCC827 cells were transfected with siRNA against E-cadherin using the DharmaFect 1 transfection reagent for 6 h, and cells were then measured with MTT assay or Western blot analysis.

Western Blot Analysis

Western blot analyses were performed as described previously (26). Briefly, whole-cell lysates (50 μg) were subjected to SDS-PAGE and transferred onto a polyvinylidene difluoride (PVDF) membrane. Proteins were visualized by specific antibodies and the immunoreactivity was detected using enhanced chemiluminescence (ECL) following the manufacturer's instructions. Quantitative data were obtained using a computing densitometer with scientific imaging systems (Kodak, Rochester, NY).

Statistical Analysis

The receiver operating characteristic (ROC) curve was used to estimate the D-dimer levels in predicting disease progression with EGFR TKI treatment. The Kaplan–Meier method was used to estimate the distribution of survival curves, and log-rank tests were used to compare the distributions between groups. One-way analysis of variance (ANOVA) followed by Dunnett's test, where appropriate, was used to determine the statistical significance of the difference between means for the results of *in vitro* cell line studies. Values of p less than 0.05 were considered statistically significant.

RESULTS

The ROC curve for the D-dimer assay in the prediction of disease progression is shown in **Supplementary Figure S1**. The cutoff values for the D-dimer levels were determined to be 0.82 μg/ml based on the ROC curve. The area under the curve was 0.8063 ± 0.0472, $p < 0.0001$ ($N = 40$). Based on the cutoff values from the ROC curve, patients were divided into two groups, high and low D-dimer groups.

Clinical Characteristics

There was no significant difference in clinical characteristics between the high ($N = 52$) and the low ($N = 50$) D-dimer groups of patients, but there was a significantly higher level of fibrinogen in the high D-dimer group (**Table 1**). Patients in the high D-dimer group had a lower clinical response rate (34.6%, $N = 52$, $p < 0.02$) and a worse PFS (median 5.6 months, $p < 0.0001$, $N = 52$) to TKI treatment compared to the low D-dimer group (76%, $N = 50$; median 29.8 months, respectively, $N = 50$) (**Table 1**, **Figure 1A**) with a hazard ratio (HR) of 4.506 (95% CI: 2.729 to 7.438, Log-rank). The disease control rate was also favored in the low D-dimer group of patients (100% vs. 25%). Cox proportional HR analysis of clinical variables showed that high and low D-dimer levels and clinical response rate were independent variables

for patients' PFS (**Supplementary Table 1A**). Patients in the high D-dimer group had a worse OS (median 18.6 months, $N = 42$) compared with those in the low D-dimer group (median 41.3 months, $N = 41$, $p < 0.0001$) with an HR of 3.837 (95% CI: 2.143 to 6.870) (**Figure 1B**). Cox proportional HR analysis of clinical variables showed that high and low D-dimer levels and performance status were independent variables for patients' OS (**Supplement Table 1B**).

There was no significant difference between patients with the exon19 or L858R genotype in the proportion of patients with high D-dimer (**Table 1**) or PFS of EGFR TKI treatment (**Figures 1C, D**). There was no significant difference in PFS between exon19 and L858R genotypes of patients in the high D-dimer groups (median 4.27 months, $N = 28$; vs. median 5.35 months, $N = 24$, $p = 0.192$) or in the low D-dimer groups (median 24.1 months, $N = 31$ vs. 19.2 months, $N = 19$, $p = 0.158$) (**Figures 1C, D**). Neither was there a significant difference in PFS or OS between 1st-generation TKI (Tarceva and Iressa) and 2nd-generation TKI (afatinib) treatment groups (**Supplementary Figure S2**).

Re-biopsy of tumor in patients with disease progression revealed that a higher proportion of patients in the low D-dimer group had the T790M mutation (61.9%, $N = 21$) compared to patients in the high D-dimer group (19.4%, $N = 31$, $p = 0.018$, Chi-square test). In contrast, EGFR mutation persisted their genotypes in patients in the high D-dimer group (80.6%, $N = 31$) compared to patients in the low D-dimer group (38.1%, $N = 21$) (**Supplementary Figure S3**). Among those with the 2nd T790M mutation, 10 from the low D-dimer group and 6 from the high D-dimer group received self-pay osimertinib treatment. One from the low D-dimer group lost to follow-up. Nine from the low D-dimer group and 3 from the high D-dimer group had clinical response to osimertinib, while 3 from the high D-dimer group failed to significantly respond to the treatment ($p = 0.044$, Fisher's exact test, **Supplementary Figure S4**). Patients in the low D-dimer group had better survival benefit to osimertinib treatment in terms of PFS (median 21.0 months, $N = 9$, $p = 0.0109$) and OS (median 36.2 months, $N = 8$, $p = 0.0288$), compared with the high D-dimer group (median 7.0 months, $N = 6$ and 20.5 months, $N = 6$, respectively) (**Supplement S4**).

Plasma From the High D-Dimer Patients Induced Resistance to TKI in Mutant Non-Small Cell Lung Cancer Cells

Plasma collected from patients in either the high or the low D-dimer group was diluted as indicated with culture medium before incubation with HCC827 cells. The plasma from patients of the high D-dimer group induced more than 90% resistance to gefitinib treatment (up to 1 μM) after incubation for 72 h at the concentrations ≥20% (**Figure 2A**), but not those from the low D-dimer group (**Figure 2B**). The following studies adopted 20% plasma for experiments. The 20% plasma of the high D-dimer group also induced HCC827 cells >90% resistance to either erlotinib or afatinib treatment (**Figures 2C, D**). In contrast to the 1st- and 2nd-generation EGFR TKI, the 3rd-generation TKI, osimertinib, could still induce cytotoxicity approximately 50% in the presence of high D-dimer plasma (**Figure 2E**). High D-dimer plasma also induced resistance to gefitinib in PC9 and H1975 cells (**Supplementary Figure S5**).

Platelets in High D-Dimer Plasma Induced Resistance to EGFR TKI

Proteomic analysis of the pooled high and low D-dimer plasma revealed an increase in pro-coagulation factors (factors V, IX, and XI) that led to thrombin, fibrin clot formation, and cross-link (XIIIa); factors that promote platelet aggregation and adherence (fibronectin, von Willebrand factor, platelet glycoprotein Ib, thrombospondin-1, and leucine-rich alpha 2 glycoprotein); and factors released from activated platelets (platelet factor 4 and platelet basic protein) (**Figures 3A, B**). Sera of the high D-dimer group failed to induce resistance to gefitinib in HCC827 cells (**Figure 3C**). To determine the role of platelets in inducing TKI resistance, plasma of the high D-dimer group was prepared as PRP and PPP. PPP failed to induce resistance to gefitinib, erlotinib, or afatinib, compared with PRP

TABLE 1 | Clinical Characteristics of lung cancer patients.

	High D-dimer ($N = 52$)	Low D-dimer ($N = 50$)	p-value
Age (years)	66.9 ± 2.0	60.5 ± 1.5	0.153[¶]
Gender (M/F)	18/34	15/35	0.675[§]
Mutation	28	31	NS[§]
L858R	24	19	
Exon 19			
TKI	8	2	0.123[§]
Iressa	18	23	
Tarceva	26	25	
Afatinib			
Performance status	0.42 ± 0.10	0.27 ± 0.12	0.329[¶]
Response	18	38	<0.001[§]
PR+CR	34	12	
SD+PD			
D-dimer level (ng/dl)	2477.0 ± 436.6	312.2 ± 28.2	0.0006[¶]
Fibrinogen (mg/dl)	429.8 ± 28.7	329.5 ± 28.2	0.019[¶]
Thrombin time (s)	17.37 ± 0.32	17.9 ± 0.40	0.312[¶]
Platelet count (count $\times 10^3$/ml)	245.8 ± 21.4	259.2 ± 14.6	0.66[¶]

Data are means ± SEM. [§]Chi-square test. [¶]Unpaired t-test.

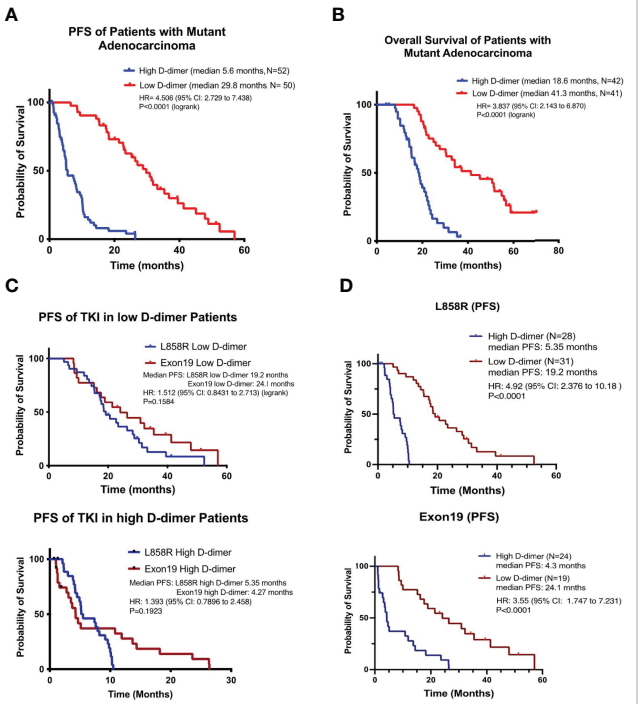

FIGURE 1 | NSCLC patients with high D-dimer have poor free survival rate. The Kaplan–Meier survival curves of progression-free survival **(A)** and overall survival **(B)** or L858R **(C)** or exon19 del **(D)** genotypes of patients with high or low level of D-dimer in target therapy. *p*-value was compared to the low D-dimer group.

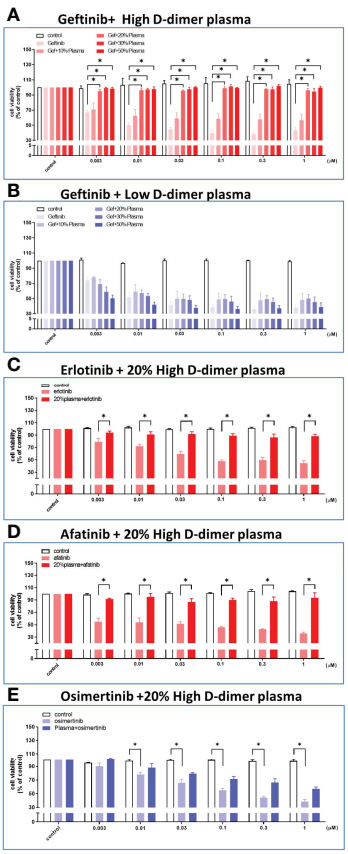

FIGURE 2 | Plasma from high D-dimer NSCLC patients induced tyrosine kinase inhibitor resistance in HCC827 cells. The HCC827 cells in 96-well plates were treated with different concentrations of the patient's plasma from the high D-dimer level **(A)** and the low D-dimer level **(B)** for 6 h, and then incubated with different concentrations of gefitinib for 72 (h) After incubation, the MTT was added in culture medium for 2 h, and the absorbance was read at 570 nm. Data represent the mean ± SEM of five experiments, with the vehicle control as the 100% reference. The HCC827 cells in 96-well plates were preincubated with 20% high D-dimer plasma for 6 h, and then treated with different concentrations of erlotinib **(C)** or afatinib **(D)** or osimertinib **(E)** for 72 h, and MTT was added in culture medium for another 2 (h) The absorbance was read at 570 nm. Data represent the mean ± SEM of three experiments, with the vehicle control as the 100% reference. *p < 0.05 compared to corresponding vehicle control or gefitinib group.

(**Figures 3D–G**). To further exclude the influence of humoral factors on high D-dimer plasma induced TKI resistance, platelets of the high D-dimer plasma were replaced by concentrated platelets from the low D-dimer plasma (LD platelet/HD PPP), or platelets of the low D-dimer plasma were replaced by concentrated platelets from the high D-dimer plasma (HD platelet/LD PPP). **Figure 3H** reveals that HD platelet/LD PPP induced resistance to gefitinib to the same extent as the high D-dimer plasma. In contrast, LD platelet/HD PPP failed to induce any resistance.

Isolated platelets from the high D-dimer plasma were found to increase the expression of surface protein GPIb-V-XI (CD42b) (**Figure 4A**) and adherence to tumor cells, compared with platelets from the low D-dimer plasma (**Figure 4B**). The GPVI-Alexa 647 MFI and the proportion of $GPVI^+$ of $CD42b^+$ platelets were higher in the high D-dimer plasma, compared to the low D-dimer plasma (**Figure 4A**). Pretreatment with prostacyclin to inhibit platelet adherence (**Figure 4C**) almost completely reversed the high D-dimer plasma-induced resistance to gefitinib (**Figure 4D**).

Signaling Pathways Underlying High D-Dimer Plasma-Induced EGFR-TKI Resistance

To examine the role of platelets in high D-dimer plasma in inducing EGFR-TKI resistance, platelet depletion in high D-dimer plasma (high D-dimer PPP) acted as the negative control for high D-dimer PRP, in which platelets were enriched. Low D-dimer PRP also examined the effects of enriched platelets in comparison with high D-dimer PRP. The PRP of the high D-dimer plasma, but not those from PRP of the low D-dimer plasma or PPP of the high D-dimer plasma, induced phosphorylation of EGFR and Src, and the downstream signal pathways, ERK and Akt (**Figure 5A**). In the presence of gefitinib, phosphorylation of EGFR was suppressed in PRP of the low D-dimer plasma or PPP of the high D-dimer plasma-treated HCC827 cells (**Figure 5A**). Gefitinib also almost completely inhibited ERK phosphorylation (**Figure 5A**). However, gefitinib failed to suppress EGFR or Src or Akt phosphorylations induced by the PRP of the high D-dimer plasma group (**Figure 5A**). An Src inhibitor (dasatinib) completely suppressed EGFR, Akt, and

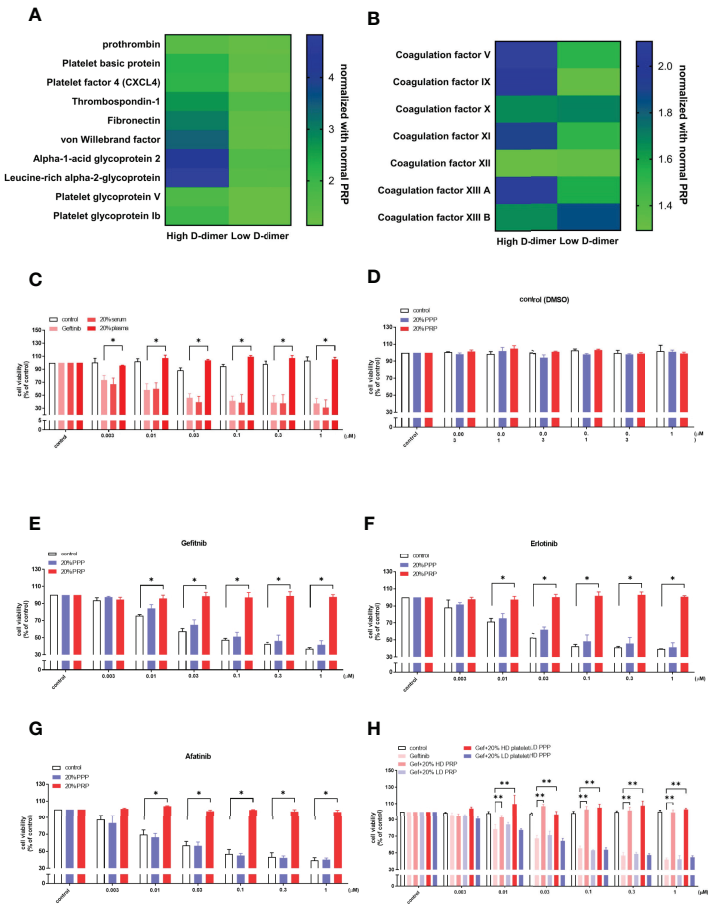

FIGURE 3 | Platelets play a crucial role in plasma-induced TKI resistance in HCC827. Heatmap showing the proteomic results of platelet-rich plasma from high D-dimer or low D-dimer NSCLC patients was analyzed for platelet activation factors and coagulation factors **(A, B)**. Columns indicate biological replicates from the experiments (blue, high; yellow, low). **(C)** The HCC827 cells in 96-well plates were treated with 20% of the patient's plasma or serum from the high D-dimer level for 6 h, and then incubated with different concentrations of gefitinib for 72 h, the MTT was added in the culture medium for 2 h, and the absorbance was read at 570 nm. The HCC827 cells in 96-well plates were preincubated with 20% high D-dimer platelet-rich plasma (PRP) or platelet-poor plasma (PPP) for 6 h, and then treated with DMSO as the controls **(D)** or with different concentrations of gefitinib **(E)**, erlotinib **(F)**, or afatinib **(G)** ($N = 3$, respectively) for 72 h; the MTT was added in culture medium for 2 h, and the absorbance was read at 570 nm. **(H)** The HCC827 cells in 96-well plates were treated with 20% high or low D-dimer plasma, or high or low D-dimer platelets for 6 h, and then incubated with different concentrations of gefitinib ($N = 3$) for 72 h. The MTT was added in culture medium for 2 h, and the absorbance was read at 570 nm. Data represent the mean ± SEM of three experiments, with the vehicle control as the 100% reference. $^{*}p < 0.05$; $^{**}p < 0.01$ compared with the corresponding TKI treatment group.

ERK phosphorylation induced by high D-dimer plasma (**Figure 5B**) and also significantly inhibited platelets of the high D-dimer plasma adherence to HCC827 cells (**Figure 5C**). PRP of the high D-dimer-induced TKI resistance was also reversed by dasatinib (**Figure 5D**).

The high D-dimer plasma also time-dependently induced a decrease in epithelial cell markers, and an increase in mesenchymal cell markers in HCC827 cells (**Figure 6A**). The EMT-transformed HCC827 cells increased their migratory activities compared to the controls (**Figures 6A, B**). Dasatinib significantly reversed the high D-dimer plasma-induced EMT (**Figure 6C**). To explore whether a loss of E-cadherin would induce EGFR activation, the E-cadherin siRNA was used to knock down E-cadherin. The E-cadherin defective cells showed upregulated EGFR phosphorylation (**Figure 7A**) and developed partial resistance to gefitinib (**Figure 7B**).

DISCUSSION

In the present study, we demonstrated that patients with mutant lung adenocarcinoma with high D-dimer levels in their peripheral blood were less responsive to EGFR TKI, were more vulnerable to develop early disease progression, and had shorter survival. Most of the secondary resistance in those patients was beyond secondary gene mutation. The platelets in high D-dimer plasma were activated and conferred resistance to EGFR TKI *via* Src activation to trans-activate EGFR and the Akt signal pathway. These results indicated

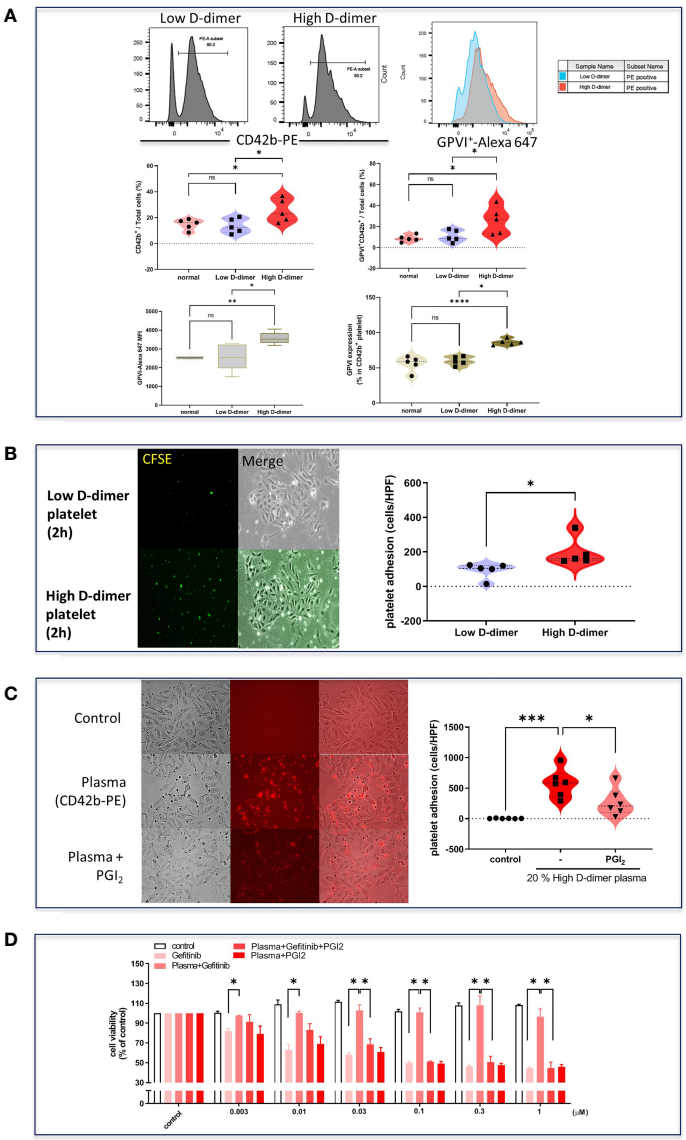

FIGURE 4 | Increased cell adhesion and surface protein glycoprotein VI in high D-dimer platelets. **(A)** Isolated platelets from low D-dimer and high D-dimer patients were stained with specific antibodies for CD42b-PE and glycoprotein VI-AF647 and then analyzed by flow cytometry. The histogram of flow cytometry analysis for surface protein expression and MFI in platelets isolated from patients with low or high D-dimer. Data represent the mean ± SEM of five patients. *$p < 0.05$, **$p < 0.01$, ***$p < 0.005$, ****$p < 0.001$ compared to the corresponding vehicle control or low D-dimer group. ns, not significant. **(B)** Isolated platelets from low D-dimer and high D-dimer patients were labeled with CFSE-DA and then incubated with HCC827 for 2 h, followed by washing twice with PBS. The images of platelet adhesion were recorded by a fluorescence microscope, and the statistical results were calculated as the average of five HPF from five patients. Data represent the mean ± SEM of five patients. *$p < 0.05$ compared to the low D-dimer group. **(C)** Isolated platelets from high D-dimer patients were treated with or without prostacyclin (PGI_2) for 30 min and then labeled with CD42b-PE. After labeling, isolated platelets were incubated with tumor cells for another 1 h, and washed three times with PBS. The images of platelet adhesion were recorded by a fluorescence microscope, and the statistical results were calculated as the average of five HPF from six patients. *$p < 0.05$, ***$p < 0.005$ compared to the corresponding vehicle control or high D-dimer group. **(D)** The isolated platelets were treated with PGI_2 for 30 min and then incubated with HCC827 cells for 6 h in 96-well plates. After incubation, cells were treated with different concentrations of gefitinib for 72 h, and the MTT was added in culture medium for 2 h, and the absorbance was read at 570 nm. Data represent the mean ± SEM of three experiments. *$p < 0.05$ compared to the corresponding gefitinib or high D-dimer group.

that the D-dimer plasma levels could be a good predictor for early development of acquired resistance to EGFR TKI in the beginning of therapy. The platelets of the high D-dimer plasma may become a therapeutic target to improve the efficacy of EGFR TKI in patients with mutant lung adenocarcinoma.

Cancer cells through TCIPA can confer an advantage to the survival and growth of cancer cells, metastatic potential, evading the body's immune system and shielding it from high shearing force (15, 27, 28). Proteomic analysis of the high and low D-dimer plasma revealed that the high D-dimer plasma contained

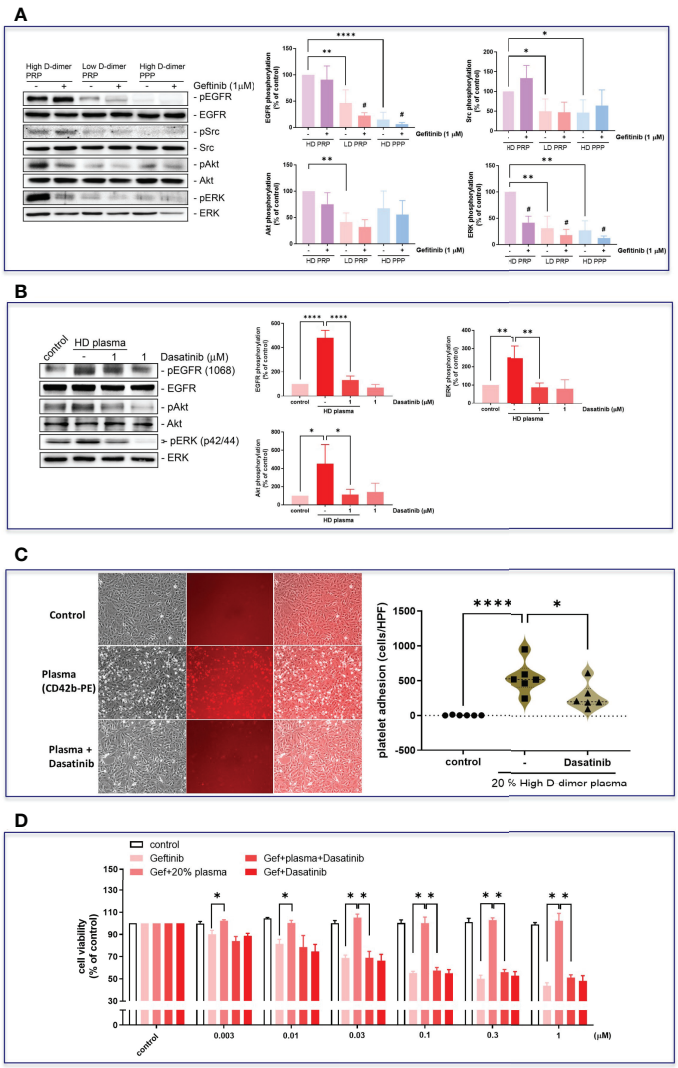

FIGURE 5 | Plasma induced EGFR-related signal activation in HCC827 *via* Src. **(A)** The HCC827 cells in 6-cm dishes were treated with or without 1 μM gefitinib for 30 min and then incubated with 20% high D-dimer PRP, low D-dimer PRP, or high D-dimer PPP for 24 h; Western blot analysis was performed, and proteins were detected by specific antibodies for the phosphorylation form of EGFR, Src, Akt, or ERK. Data represent the mean ± SEM of four experiments.*$p < 0.05$, **$p < 0.01$, ****$p < 0.001$ compared to the HD PRP group as the 100% reference; $^{\#}p < 0.05$ compared with the corresponding control. The exposure time of the bands of Western blot was reduced to avoid overexposure of the bands of high D-dimer PRP, resulting in a reduced expression in low D-dimer PRP group and high D-dimer PPP. **(B)** HCC827 cells were pretreated with dasatinib (1 μM) and then cells were treated with 20% high D-dimer plasma for 24 h. Western blot analysis was performed, and proteins were detected by specific antibodies for the phosphorylation form of EGFR, Akt, or ERK. Data represent the mean ± SEM of three experiments. *$p < 0.05$, **$p < 0.01$, ****$p < 0.001$ compared to the corresponding vehicle control or HD plasma group. The exposure time of the bands of Western blot was reduced to avoid overexposure of the bands of high D-dimer plasma, resulting in a reduced expression in the control. **(C)** Isolated platelets from high D-dimer patients were treated with or without dasatinib for 30 min and then labeled with CD42b-PE. After labeling, isolated platelets were incubated with tumor cells for another 1 h, and washed three times with PBS. The images of platelet adhesion were recorded by a fluorescence microscope, and the statistical results were calculated as the average of five HPF from six patients. *$p < 0.05$, ****$p < 0.001$ compared to the corresponding vehicle control or HD plasma group. **(D)** The isolated platelets were treated with dasatinib for 30 min and then incubated with HCC827 cells for 6 h in 96-well plates. After incubation, cells were treated with different concentrations of gefitinib for 72 h, the MTT was added in culture medium for 2 h, and the absorbance was read at 570 nm. Data represent the mean ± SEM of three experiments. *$p < 0.05$ compared to the gefitinib or HD plasma group.

increased levels of proteins that promote platelet aggregation and adherence, factors released from activated platelets, and increased levels of coagulation factors that led to thrombin, fibrin clot formation, and cross-link. Thus, the high D-dimer plasma provided a good environment for platelet aggregation and adherence. The expression of platelet GPIb-IX-V, GPIIb/IIIa, and P-selectin on the tight inter-junction between platelet and cancer cells is crucial for TCIPA (29, 30). In this study, platelets of the high D-dimer plasma were found with the upregulated expression of GPIb-IX-V and GPIIb/IIIa,

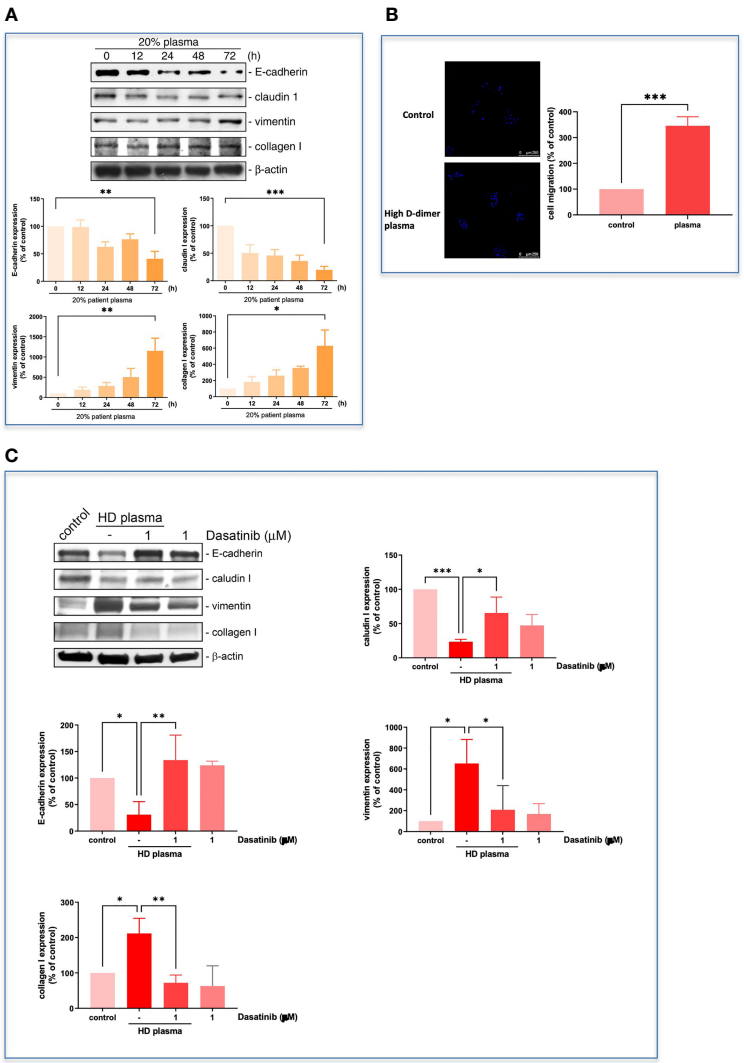

FIGURE 6 | Plasma induced EMT progression in HCC827. **(A)** The HCC827 cells in 6-cm dishes were incubated with 20% high D-dimer plasma for different time intervals. Western blot analysis was performed, and proteins were detected by specific antibodies for EMT markers. The data were calculated and represent the mean ± SEM of three experiments shown in statistical figures. *$p < 0.05$, **$p < 0.01$, ***$p < 0.005$ compared to the corresponding vehicle control as the 100% reference. **(B)** HCC827 cells in 8 μM transwells were incubated with 20% high D-dimer plasma for 24 (h) The membrane of transwells was cut, stained with Hoechst33342, and then counted for positive cells under fluorescence microscopy. The data were calculated and represent the mean ± SEM of three experiments shown in statistical figures. ***$p < 0.005$ compared to the corresponding vehicle control as the 100% reference. **(C)** HCC827 cells were pretreated with dasatinib (1 μM) and then cells were treated with 20% high D-dimer plasma for 24 h. Western blot analysis was performed, and proteins were detected by specific antibodies for EMT markers. Data represent the mean ± SEM of three experiments. *$p < 0.05$, **$p < 0.01$, ***$p < 0.005$ compared to the corresponding vehicle control or HD plasma treatment group.

indicating that those platelets were activated by TCIPA and ready for aggregation and adherence. Another surface glycoprotein expression of activated platelets, GPVI, a surface receptor belonging to the immunoglobulin superfamily, which principally binds collagen (31), was also upregulated on platelets of the high D-dimer plasma. Prostacyclin is the most potent known inhibitor of platelet aggregation (32) and has been shown to inhibit TCIPA (33). In this study, treatment with prostacyclin inhibited platelet adherence to tumor cells, and completely reversed platelets of the high D-dimer plasma-induced TKI resistance. These results suggested that platelet activation and adherence to tumor cells contributed to EGFR TKI resistance. The surface receptors of platelets may be a potential therapeutic target to conquer the resistance development in EGFR mutant lung cancer patients.

When platelets aggregate around cancer cells, clustering of these surface receptors in activated platelets may activate Src family kinases (SFKs) to release a variety of cytokines and growth factors, which have been implicated in cancer growth, progression, and escape from apoptosis when challenged with

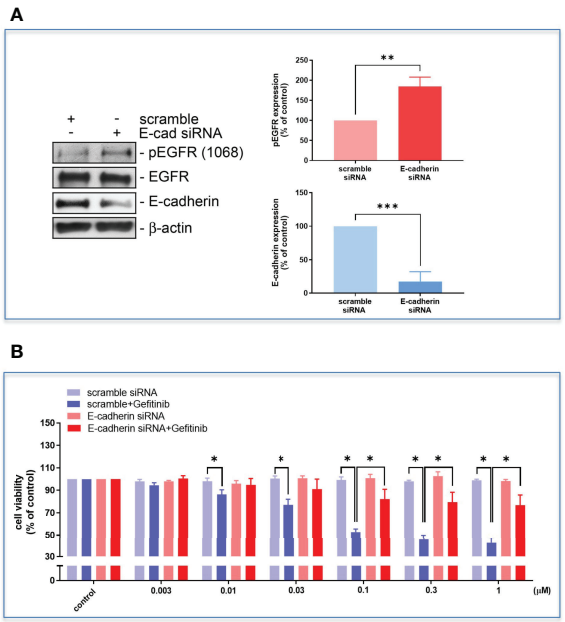

FIGURE 7 | The HCC827 cells in 96-well plates were transfected with E-cadherin siRNA and then incubated with different concentrations of gefitinib, the Western blot **(A)** and MTT assay **(B)** were performed, and the absorbance was read at 570 nm. Data represent the mean ± SEM. $*p < 0.05$, $**p < 0.01$, $***p < 0.005$ compared to the corresponding vehicle control or treated group.

chemotherapy (18, 34, 35). In the present study, depletion of platelets from the high D-dimer plasma failed to cause EGFR TKI resistance, suggesting that the humoral factors in the high D-dimer plasma was not directly contributory to induce TKI resistance. In contrast, enriched platelets of the high D-dimer plasma (PRP) induced gefitinib-resistant phosphorylation of Src, EGFR, and Akt signaling pathways in HCC827 cells. Src binds to EGFR, resulting in a variety of downstream effects and an induction of survival and migration signaling pathways (36). This downstream pathway activation may provide a synergism with EGFR (37) for tumor cells to escape from EGFR TKI inhibition (11). The present study demonstrated that treatment with dasatinib inhibited platelet adherence to tumor cells, phosphorylation of EGFR and Akt, as well as ERK, resulting in complete reversal of the high D-dimer plasma-induced TKI resistance. These results suggest that Src activation through platelet interaction with HCC827 cells plays a central role in platelets of high D-dimer plasma-induced TKI resistance.

The PI3K/Akt signaling pathway plays an important role in regulating cell proliferation and maintaining the biological characteristics of malignant cells (38), and also mediates EMT (39). Although Akt activation *via* PI3K and ERK *via* Ras are the two principal downstream signaling pathways mediating the oncogenic effects of EGFR (40), the high D-dimer plasma-induced Akt phosphorylation was not inhibited by EGFR TKI or gefitinib, but by the Src inhibitor, dasatinib, suggesting that Akt phosphorylation was mostly beyond EGFR activation, but resulted from a direct involvement with SFKs (41). Akt activation has been shown to be a convergent, resistance-driving signaling event across a spectrum of EGFR-mutant NSCLCs with acquired resistance to EGFR TKIs caused by diverse underlying mechanisms, such as amplification, overexpression, and activation of MET, FGFR, EphA2, Mer, and AXL or the T790M mutation (42). Akt phosphorylation has also been shown to increase in the majority of EGFR-mutant patients prior to EGFR-TKI treatment and correlates with poor initial therapeutic responses (42). In the present study, Akt inhibitors significantly reversed the high D-dimer plasma-induced TKI resistance, indicating that Akt activation played an important role in SFK-mediated acquired EGFR inhibitor resistance.

The activation of SFK has also been shown to induce E-cadherin deregulation and associated EMT, which acquired resistance to TKIs (43–45). In NSCLC, clinical cancer specimens with acquired gefitinib resistance showed a decrease in E-cadherin and an increase in Hakai expression (46). The dual HDAC and HMGR inhibitor reverses E-cadherin expression, attenuates vimentin and stemness, and restores gefitinib sensitivity through an inhibition of the Src/Hakai and Hakai/E-cadherin interaction (46). Here, we showed that the high D-dimer plasma induced EMT in HCC827 cells by decreasing the expression of E-cadherin and claudin 1, and increasing the expression of vimentin and collagen 1. The high D-dimer plasma also increased HCC827 cell migratory activity. Dasatinib was also shown to inhibit the high D-dimer-induced EMT and HCC827 cell migration. Disruption of E-cadherin alone may result in reduced suppression of EGFR-dependent signaling pathways (47, 48), since E-cadherin has been shown to suppress intracellular signaling pathways, which regulate cell activation, proliferation, and differentiation (49). Our results also showed that E-cadherin knockdown by siRNA transactivated EGFR and became resistant to gefitinib treatment. E-cadherin loss may further exacerbate Src-induced aberrant EGFR activation. Thus, the reversal effect on EMT may cast an important role in the efficiency of dasatinib in restoring EGFR TKI responsiveness.

Disruption of the SFK pathway may therefore provide a method to overcome EGFR TKI resistance. However, several clinical trials with dasatinib in combination with EGFR TKI failed to overcome acquired TKI resistance (50, 51). The lack of clinical benefits of combined therapies is attributed to an incomplete abrogation of c-Src hyper-activation and the enrolment of molecular uncharacterized patients (51). The heterogeneity of lung cancer cells in expressing Src kinase activity and dependence of Src activation in regulation of cell growth may be differentially responsive to Src inhibition and also differentially vulnerable to Src activation and development of EGFR TKI resistance. Src activation by platelet adherence to tumor cells in patients with mutant adenocarcinoma may be a predictive biomarker of responses to Src inhibitors in conquering acquired TKI resistance.

Based on our cell line *in vitro* studies, osimertinib could induce cytotoxicity approximately 50% in the presence of high D-dimer plasma (**Figure 2E**). We propose that osimertinib as a first-line treatment for patients in the high D-dimer group may have a significant survival benefit compared with comparator EGFR TKI. However, whether the 50% resistance to osimertinib in *in vitro* studies could be clinically translated into a significant difference in survival benefit deserves further studies if the superior efficacy of

osimertinib in lung adenocarcinoma with activating EGFR mutation (52, 53) would conquer the induction of resistance by high D-dimer plasma. As shown in the second-line treatment for resistance T790M in our limited number of patients, the efficacy of osimertinib was hindered by high D-dimer plasma in terms of response rate, PFS, and OS.

In conclusion, our study demonstrated that platelets in the high D-dimer plasma were activated and induced EGFR TKI resistance through Src-mediated EGFR transactivation, Akt activation, and EMT in patients with mutant lung adenocarcinoma. Platelet activation in high D-dimer plasma might play a role in acquired resistance to TKI and poor clinical outcomes. Inhibiting platelet or/and Src activation may be a potential therapeutic direction to improve the efficacy of EGFR TKI in patients with high D-dimer plasma levels.

DATA AVAILABILITY STATEMENT

The original contributions presented in the study are included in the article/**Supplementary Material**. Further inquiries can be directed to the corresponding author.

ETHICS STATEMENT

The studies involving human participants were reviewed and approved by the TMU-Joint Institutional Review Board. The patients/participants provided their written informed consent to participate in this study.

AUTHOR CONTRIBUTIONS

Conception and design: M-JL, C-MW, and H-PK. Supervising the research: C-HL and H-PK. Performing the experiments including quality control: M-JL, C-MW, and WC. Clinical resource: Y-FF, F-TC, and H-PK. Analysis and interpretation: all authors. Drafting the manuscript: M-JL, C-MW, C-HL, and H-PK. All authors contributed to the article and approved the submitted version.

FUNDING

This work is supported by Taiwan Ministry of Science and Technology grants 110-2314-B-038-150 and 110-2314-B-038-145.

SUPPLEMENTARY MATERIAL

The Supplementary Material for this article can be found online at: https://www.frontiersin.org/articles/10.3389/fonc.2022.876051/full#supplementary-material

REFERENCES

1. Maemondo M, Inoue A, Kobayashi K, Sugawara S, Oizumi S, Isobe H, et al. Gefitinib or Chemotherapy for Non-Small-Cell Lung Cancer With Mutated EGFR. *New Engl J Med* (2010) 362(25):2380–8. doi: 10.1056/NEJMoa0909530
2. Wu YL, Zhou C, Hu CP, Feng J, Lu S, Huang Y, et al. Afatinib Versus Cisplatin Plus Gemcitabine for First-Line Treatment of Asian Patients With Advanced non-Small-Cell Lung Cancer Harbouring EGFR Mutations (LUX-Lung 6): An Open-Label, Randomised Phase 3 Trial. *Lancet Oncol* (2014) 15 (2):213–22. doi: 10.1016/S1470-2045(13)70604-1
3. Zhou C, Wu YL, Chen G, Feng J, Liu XQ, Wang C, et al. Erlotinib Versus Chemotherapy as First-Line Treatment for Patients With Advanced EGFR Mutation-Positive Non-Small-Cell Lung Cancer (OPTIMAL, CTONG-0802): A Multicentre, Open-Label, Randomised, Phase 3 Study. *Lancet Oncol* (2011) 12(8):735–42. doi: 10.1016/S1470-2045(11)70184-X
4. Nagano T, Tachihara M, Nishimura Y. Mechanism of Resistance to Epidermal Growth Factor Receptor-Tyrosine Kinase Inhibitors and a Potential Treatment Strategy. *Cells* (2018) 7(11):212–28. doi: 10.3390/cells7110212
5. Pao W, Miller VA, Politi KA, Riely GJ, Somwar R, Zakowski MF, et al. Acquired Resistance of Lung Adenocarcinomas to Gefitinib or Erlotinib Is Associated With a Second Mutation in the EGFR Kinase Domain. *PloS Med* (2005) 2(3):e73. doi: 10.1371/journal.pmed.0020073
6. Wagener-Ryczek S, Heydt C, Suptitz J, Michels S, Falk M, Alidousty C, et al. Mutational Spectrum of Acquired Resistance to Reversible Versus Irreversible EGFR Tyrosine Kinase Inhibitors. *BMC Cancer* (2020) 20(1):408. doi: 10.1186/s12885-020-06920-3
7. Takezawa K, Pirazzoli V, Arcila ME, Nebhan CA, Song X, de Stanchina E, et al. HER2 Amplification: A Potential Mechanism of Acquired Resistance to EGFR Inhibition in EGFR-Mutant Lung Cancers That Lack the Second-Site EGFRT790M Mutation. *Cancer Discovery* (2012) 2(10):922–33. doi: 10.1158/2159-8290.CD-12-0108
8. Yamaoka T, Ohmori T, Ohba M, Arata S, Murata Y, Kusumoto S, et al. Distinct Afatinib Resistance Mechanisms Identified in Lung Adenocarcinoma Harboring an EGFR Mutation. *Mol Cancer Res* (2017) 15(7):915–28. doi: 10.1158/1541-7786.MCR-16-0482
9. Kohler J, Schuler M. Afatinib, Erlotinib and Gefitinib in the First-Line Therapy of EGFR Mutation-Positive Lung Adenocarcinoma: A Review. *Onkologie* (2013) 36(9):510–8. doi: 10.1159/000354627
10. Goubran HA, Burnouf T, Radosevic M, El-Ekiaby M. The Platelet-Cancer Loop. *Eur J Intern Med* (2013) 24(5):393–400. doi: 10.1016/j.ejim.2013.01.017
11. Van Der Steen N, Giovannetti E, Carbone D, Leonetti A, Rolfo CD, Peters GJ. Resistance to Epidermal Growth Factor Receptor Inhibition in Non-Small Cell Lung Cancer. *Cancer Drug Resist* (2018) 1:230–49. doi: 10.20517/cdr.2018.13
12. Janowska-Wieczorek A, Wysoczynski M, Kijowski J, Marquez-Curtis L, Machalinski B, Ratajczak J, et al. Microvesicles Derived From Activated Platelets Induce Metastasis and Angiogenesis in Lung Cancer. *Int J Cancer* (2005) 113(5):752–60. doi: 10.1002/ijc.20657
13. Labelle M, Begum S, Hynes RO. Direct Signaling Between Platelets and Cancer Cells Induces an Epithelial-Mesenchymal-Like Transition and Promotes Metastasis. *Cancer Cell* (2011) 20(5):576–90. doi: 10.1016/j.ccr.2011.09.009
14. Egan K, Cooke N, Kenny D. Living in Shear: Platelets Protect Cancer Cells From Shear Induced Damage. *Clin Exp Metastasis* (2014) 31(6):697–704. doi: 10.1007/s10585-014-9660-7
15. Palumbo JS, Talmage KE, Massari JV, La Jeunesse CM, Flick MJ, Kombrinck KW, et al. Platelets and Fibrin(Ogen) Increase Metastatic Potential by Impeding Natural Killer Cell-Mediated Elimination of Tumor Cells. *Blood* (2005) 105(1):178–85. doi: 10.1182/blood-2004-06-2272
16. Menter DG, Tucker SC, Kopetz S, Sood AK, Crissman JD, Honn KV. Platelets and Cancer: A Casual or Causal Relationship: Revisited. *Cancer Metastasis Rev* (2014) 33(1):231–69. doi: 10.1007/s10555-014-9498-0

17. Chen H, Lan X, Liu M, Zhou B, Wang B, Chen P. Direct TGF-Beta1 Signaling Between Activated Platelets and Pancreatic Cancer Cells Primes Cisplatin Insensitivity. *Cell Biol Int* (2013) 37(5):478–84. doi: 10.1002/cbin.10067
18. Radziwon-Balicka A, Medina C, O'Driscoll L, Treumann A, Bazou D, Inkielewicz-Stepniak I, et al. Platelets Increase Survival of Adenocarcinoma Cells Challenged With Anticancer Drugs: Mechanisms and Implications for Chemoresistance. *Br J Pharmacol* (2012) 167(4):787–804. doi: 10.1111/j.1476-5381.2012.01991.x
19. Adam SS, Key NS, Greenberg CS. D-Dimer Antigen: Current Concepts and Future Prospects. *Blood* (2009) 113(13):2878–87. doi: 10.1182/blood-2008-06-165845
20. Blackwell K, Haroon Z, Broadwater G, Berry D, Harris L, Iglehart JD, et al. Plasma D-Dimer Levels in Operable Breast Cancer Patients Correlate With Clinical Stage and Axillary Lymph Node Status. *J Clin Oncol* (2000) 18 (3):600–8. doi: 10.1200/JCO.2000.18.3.600
21. Kim HK, Song KS, Lee KR, Kang YH, Lee YJ, Lee ES. Comparison of Plasma D-Dimer and Thrombus Precursor Protein in Patients With Operable Breast Cancer as a Potential Predictor of Lymph Node Metastasis. *Blood Coagul Fibrinolysis* (2004) 15(1):9–13. doi: 10.1097/00001721-200401000-00002
22. Komurcuoglu B, Ulusoy S, Gayaf M, Guler A, Ozden E. Prognostic Value of Plasma D-Dimer Levels in Lung Carcinoma. *Tumori* (2011) 97(6):743–8. doi: 10.1177/030089161109700611
23. Heemskerk JW, Bevers EM, Lindhout T. Platelet Activation and Blood Coagulation. *Thromb Haemost* (2002) 88(2):186–93.
24. Repetto O, De Re V. Coagulation and Fibrinolysis in Gastric Cancer. *Ann N Y Acad Sci* (2017) 1404(1):27–48. doi: 10.1111/nyas.13454
25. Dhurat R, Sukesh M. Principles and Methods of Preparation of Platelet-Rich Plasma: A Review and Author's Perspective. *J Cutan Aesthet Surg* (2014) 7 (4):189–97. doi: 10.4103/0974-2077.150734
26. Weng CM, Yu CC, Kuo ML, Chen BC, Lin CH. Endothelin-1 Induces Connective Tissue Growth Factor Expression in Human Lung Fibroblasts by ETAR-Dependent JNK/AP-1 Pathway. *Biochem Pharmacol* (2014) 88 (3):402–11. doi: 10.1016/j.bcp.2014.01.030
27. Gasic GJ. Role of Plasma, Platelets, and Endothelial Cells in Tumor Metastasis. *Cancer Metastasis Rev* (1984) 3(2):99–114. doi: 10.1007/BF00047657
28. Plantureux L, Crescence L, Dignat-George F, Panicot-Dubois L, Dubois C. Effects of Platelets on Cancer Progression. *Thromb Res* (2018) 164 Suppl 1: S40–S7. doi: 10.1016/j.thromres.2018.01.035
29. Alonso-Escolano D, Strongin AY, Chung AW, Deryugina EI, Radomski MW. Membrane Type-1 Matrix Metalloproteinase Stimulates Tumour Cell-Induced Platelet Aggregation: Role of Receptor Glycoproteins. *Br J Pharmacol* (2004) 141(2):241–52. doi: 10.1038/sj.bjp.0705606
30. Oleksowicz L, Dutcher JP. Adhesive Receptors Expressed by Tumor Cells and Platelets: Novel Targets for Therapeutic Anti-Metastatic Strategies. *Med Oncol* (1995) 12(2):95–102. doi: 10.1007/BF01676709
31. Watson SP, Auger JM, McCarty OJ, Pearce AC. GPVI and Integrin alphaIIb Beta3 Signaling in Platelets. *J Thromb Haemost* (2005) 3(8):1752–62. doi: 10.1111/j.1538-7836.2005.01429.x
32. Moncada S, Gryglewski R, Bunting S, Vane JR. An Enzyme Isolated From Arteries Transforms Prostaglandin Endoperoxides to an Unstable Substance That Inhibits Platelet Aggregation. *Nature* (1976) 263(5579):663–5. doi: 10.1038/263663a0
33. Jurasz P, Stewart MW, Radomski A, Khadour F, Duszyk M, Radomski MW. Role of Von Willebrand Factor in Tumour Cell-Induced Platelet Aggregation: Differential Regulation by NO and Prostacyclin. *Br J Pharmacol* (2001) 134 (5):1104–12. doi: 10.1038/sj.bjp.0704343
34. Lee M, Rhee I. Cytokine Signaling in Tumor Progression. *Immune Netw* (2017) 17(4):214–27. doi: 10.4110/in.2017.17.4.214
35. Musolino C, Allegra A, Innao V, Allegra AG, Pioggia G, Gangemi S. Inflammatory and Anti-Inflammatory Equilibrium, Proliferative and Antiproliferative Balance: The Role of Cytokines in Multiple Myeloma. *Mediators Inflamm* (2017) 2017:1852517. doi: 10.1155/2017/1852517
36. Matsuoka H, Nada S, Okada M. Mechanism of Csk-Mediated Down-Regulation of Src Family Tyrosine Kinases in Epidermal Growth Factor Signaling. *J Biol Chem* (2004) 279(7):5975–83. doi: 10.1074/jbc.M311278200
37. Ishizawar R, Parsons SJ. C-Src and Cooperating Partners in Human Cancer. *Cancer Cell* (2004) 6(3):209–14. doi: 10.1016/j.ccr.2004.09.001
38. Ye B, Jiang LL, Xu HT, Zhou DW, Li ZS. Expression of PI3K/AKT Pathway in Gastric Cancer and its Blockade Suppresses Tumor Growth and Metastasis. *Int J Immunopathol Pharmacol* (2012) 25(3):627–36. doi: 10.1177/039463201202500309
39. Xu W, Yang Z, Lu N. A New Role for the PI3K/Akt Signaling Pathway in the Epithelial-Mesenchymal Transition. *Cell Adh Migr* (2015) 9(4):317–24. doi: 10.1080/19336918.2015.1016686
40. Sordella R, Bell DW, Haber DA, Settleman J. Gefitinib-Sensitizing EGFR Mutations in Lung Cancer Activate Anti-Apoptotic Pathways. *Science* (2004) 305(5687):1163–7. doi: 10.1126/science.1101637
41. Jiang T, Qiu Y. Interaction Between Src and a C-Terminal Proline-Rich Motif of Akt is Required for Akt Activation. *J Biol Chem* (2003) 278(18):15789–93. doi: 10.1074/jbc.M212525200
42. Jacobsen K, Bertran-Alamillo J, Molina MA, Teixido C, Karachaliou N, Pedersen MH, et al. Convergent Akt Activation Drives Acquired EGFR Inhibitor Resistance in Lung Cancer. *Nat Commun* (2017) 8(1):410. doi: 10.1038/s41467-017-00450-6
43. Avizienyte E, Fincham VJ, Brunton VG, Frame MC. Src SH3/2 Domain-Mediated Peripheral Accumulation of Src and Phospho-Myosin Is Linked to Deregulation of E-Cadherin and the Epithelial-Mesenchymal Transition. *Mol Biol Cell* (2004) 15(6):2794–803. doi: 10.1091/mbc.e03-12-0879
44. Sequist LV, Waltman BA, Dias-Santagata D, Digumarthy S, Turke AB, Fidias P, et al. Genotypic and Histological Evolution of Lung Cancers Acquiring Resistance to EGFR Inhibitors. *Sci Trans Med* (2011) 3(75):75ra26. doi: 10.1126/scitranslmed.3002003
45. Thiery JP, Acloque H, Huang RY, Nieto MA. Epithelial-Mesenchymal Transitions in Development and Disease. *Cell* (2009) 139(5):871–90. doi: 10.1016/j.cell.2009.11.007
46. Weng CH, Chen LY, Lin YC, Shih JY, Lin YC, Tseng RY, et al. Epithelial-Mesenchymal Transition (EMT) Beyond EGFR Mutations Per Se Is a Common Mechanism for Acquired Resistance to EGFR TKI. *Oncogene* (2019) 38(4):455–68. doi: 10.1038/s41388-018-0454-2
47. Fedor-Chaiken M, Hein PW, Stewart JC, Brackenbury R, Kinch MS. E-Cadherin Binding Modulates EGF Receptor Activation. *Cell Commun Adhes* (2003) 10(2):105–18. doi: 10.1080/cac.10.2.105.118
48. Rubsam M, Mertz AF, Kubo A, Marg S, Jungst C, Goranci-Buzhala G, et al. E-Cadherin Integrates Mechanotransduction and EGFR Signaling to Control Junctional Tissue Polarization and Tight Junction Positioning. *Nat Commun* (2017) 8(1):1250. doi: 10.1038/s41467-017-01170-7
49. Pece S, Gutkind JS. Signaling From E-Cadherins to the MAPK Pathway by the Recruitment and Activation of Epidermal Growth Factor Receptors Upon Cell-Cell Contact Formation. *J Biol Chem* (2000) 275(52):41227–33. doi: 10.1074/jbc.M006578200
50. Creelan BC, Gray JE, Tanvetyanon T, Chiappori AA, Yoshida T, Schell MJ, et al. Phase 1 Trial of Dasatinib Combined With Afatinib for Epidermal Growth Factor Receptor- (EGFR-) Mutated Lung Cancer With Acquired Tyrosine Kinase Inhibitor (TKI) Resistance. *Br J Cancer* (2019) 120(8):791–6. doi: 10.1038/s41416-019-0428-3
51. Gold KA, Lee JJ, Harun N, Tang X, Price J, Kawedia JD, et al. A Phase I/II Study Combining Erlotinib and Dasatinib for Non-Small Cell Lung Cancer. *Oncologist* (2014) 19(10):1040–1. doi: 10.1634/theoncologist.2014-0228
52. Ramalingam SS, Vansteenkiste J, Planchard D, Cho BC, Gray JE, Ohe Y, et al. Overall Survival With Osimertinib in Untreated, EGFR-Mutated Advanced NSCLC. *New Engl J Med* (2020) 382(1):41–50. doi: 10.1056/NEJMoa1913662
53. Soria JC, Ohe Y, Vansteenkiste J, Reungwetwattana T, Chewaskulyong B, Lee KH, et al. Osimertinib in Untreated EGFR-Mutated Advanced Non-Small-Cell Lung Cancer. *New Engl J Med* (2018) 378(2):113–25. doi: 10.1056/NEJMoa1713137

Conflict of Interest: The authors declare that the research was conducted in the absence of any commercial or financial relationships that could be construed as a potential conflict of interest.

this article, or claim that may be made by its manufacturer, is not guaranteed or endorsed by the publisher.

frontiers | Frontiers in Oncology

SYSTEMATIC REVIEW
published: 28 June 2022
doi: 10.3389/fonc.2022.869390

Comparison of T790M Acquisition After Treatment With First- and Second-Generation Tyrosine-Kinase Inhibitors: A Systematic Review and Network Meta-Analysis

Po-Chun Hsieh[1], *Yao-Kuang Wu*[2,3], *Chun-Yao Huang*[2,3], *Mei-Chen Yang*[2,3], *Chan-Yen Kuo*[4], *I-Shiang Tzeng*[4] *and Chou-Chin Lan*[2,3]*

[1] Department of Chinese Medicine, Taipei Tzu Chi Hospital, Buddhist Tzu Chi Medical Foundation, New Taipei City, Taiwan, [2] Division of Pulmonary Medicine, Taipei Tzu Chi Hospital, Buddhist Tzu Chi Medical Foundation, New Taipei City, Taiwan, [3] School of Medicine, Tzu-Chi University, Hualien, Taiwan, [4] Department of Research, Taipei Tzu Chi Hospital, Buddhist Tzu Chi Medical Foundation, New Taipei City, Taiwan

OPEN ACCESS

Edited by:
Iacopo Petrini,
University of Pisa, Italy

Reviewed by:
Francesco Pepe,
University of Naples Federico II, Italy
Lorenzo Belluomini,
University of Verona, Italy

***Correspondence:**
Chou-Chin Lan
bluescopy@yahoo.com.tw

Specialty section:
This article was submitted to Thoracic Oncology, a section of the journal Frontiers in Oncology

Received: 04 February 2022
Accepted: 30 May 2022
Published: 28 June 2022

Citation:
Hsieh P-C, Wu Y-K, Huang C-Y, Yang M-C, Kuo C-Y, Tzeng I-S and Lan C-C (2022) Comparison of T790M Acquisition After Treatment With First- and Second-Generation Tyrosine-Kinase Inhibitors: A Systematic Review and Network Meta-Analysis. Front. Oncol. 12:869390. doi: 10.3389/fonc.2022.869390

Background: Lung adenocarcinoma is a common disease with a high mortality rate. Epidermal growth factor receptor (*EGFR*) mutations are found in adenocarcinomas, and oral EGFR-tyrosine kinase inhibitors (EGFR-TKIs) show good responses. EGFR-TKI therapy eventually results in resistance, with the most common being T790M. T790M is also a biomarker for predicting resistance to first- and second-generation EGFR-TKIs and is sensitive to osimertinib. The prognosis was better for patients with acquired T790M who were treated with osimertinib than for those treated with chemotherapy. Therefore, T790M mutation is important for deciding further treatment and prognosis. Previous studies based on small sample sizes have reported very different T790 mutation rates. We conducted a meta-analysis to evaluate the T790M mutation rate after EGFR-TKI treatment.

Methods: We systematic reviewed the electronic databases to evaluate the T790M mutation rate after treatment with first-generation (gefitinib, erlotinib, and icotinib) and second-generation (afatinib and dacomitinib) EGFR-TKIs. Random-effects network meta-analysis and single-arm meta-analysis were conducted to estimate the T790M mutation rate of the target EGFR-TKIs.

Results: A total of 518 studies were identified, of which 29 were included. Compared with afatinib, a higher odds ratio (OR) of the T790M mutation rate was observed after erlotinib [OR = 1.48; 95% confidence interval (CI):1.09–2.00] and gefitinib (OR = 1.45; 95% CI: 1.11–1.90) treatments. An even OR of the T790M mutation rate was noted after icotinib treatment (OR = 0.91, 95% CI: 0.46–1.79) compared with that after afatinib. The T790M mutation rate was significantly lower with afatinib (33%) than that with gefitinib (49%) and erlotinib treatments (47%) ($p < 0.001$). The acquired T790M mutation rate in all participants was slightly lower in Asians (43%) than that in Caucasians (47%).

Conclusions: Erlotinib and gefitinib had a higher OR for the T790M mutation than afatinib. The T790M mutation rate was significantly lower in afatinib than in gefitinib and erlotinib. T790M is of great significance because osimertinib shows a good prognosis in patients with T790M mutation.

Systematic Review Registration: PROSPERO, identifier CRD42021257824.

Keywords: non-small cell lung cancer, adenocarcinoma, epidermal growth factor receptor, tyrosine kinase inhibitors, T790M acquisition

1 INTRODUCTION

Lung cancer is associated with significant mortality rates worldwide. Non-small-cell lung cancer (NSCLC) accounts for approximately 80% of all lung cancer cases, and its treatment depends on the stage and gene profiles of the tumors (1). Most patients with NSCLC are at an advanced stage at the time of diagnosis, have unresectable tumors, and usually present with a poor prognosis (1). Therefore, targeted therapy and chemotherapy are major treatments for these patients (1).

Traditionally, chemotherapy has been the standard treatment for patients with NSCLC. However, chemotherapy often causes serious adverse reactions and complications that can render patients unable to receive a complete course of treatment. Adenocarcinomas account for 80% of all NSCLC cases (1). Epidermal growth factor receptor (*EGFR*) mutations occur in approximately 50% of Asian and 20% of Caucasian patients with lung adenocarcinoma (2). Oral EGFR-tyrosine kinase inhibitors (EGFR-TKIs) have become promising treatments for patients with adenocarcinoma because of their good curative effects and few adverse reactions.

EGFR is a tyrosine kinase receptor that plays a key role in tumor cell proliferation and vascularization. Hence, it is an important molecular target in cancer treatment. Previous studies have shown that EGFR-TKIs are superior to paclitaxel/carboplatin in NSCLC patients with *EGFR*-sensitizing gene mutations. This finding implies that the effective treatment of NSCLC consists of EGFR-TKIs. Currently, the available EGFR-TKIs for NSCLC are first- (gefitinib, erlotinib, and icotinib), second- (afatinib and dacomitinib), and third-generation TKIs (osimertinib) (3).

Gefitinib was approved for patients with advanced NSCLC and sensitive *EGFR* mutations in July 2015 (4). Gefitinib as the first line of treatment for NSCLC patients with sensitive *EGFR* mutations showed an objective response rate (ORR) of 62–71%, progression-free survival (PFS) of 8–13 months, and overall survival (OS) of 21–30 months (4). Erlotinib was approved in 2004 for patients harboring EGFR exon 21 L858R mutations and exon 19 deletions (5). Erlotinib as the first line of treatment for NSCLC patients with sensitive *EGFR* gene mutations revealed an ORR of 58–83%, PFS of 9.7–13 months, and OS of 23–33 months (5). Afatinib is an irreversible covalent inhibitor of the ErbB receptor family, which includes EGFR, ErbB2/HER2, and ErbB4/HER4 (6). It was approved by the FDA for treating NSCLC patients with exon 21 L858R substitutions and exon 19 deletions in 2013 and for uncommon *EGFR* mutations such as L861Q in exon 21 and G719X in exon 18 in 2018 (6). Afatinib, as the first line of treatment for NSCLC patients with sensitive *EGFR* gene mutations, showed an ORR of 70%–81.8%, PFS of 13.4–15.2 months, and OS of 27.9–49 months (6).

Predictive biomarkers are important for the treatment of NSCLC. In previous studies, PDL-1 expression was found to be a predictive biomarker for the therapeutic response to immunotherapy (7). The clinical outcomes of patients with higher PDL-1 expression were better PFS and OS associated with immunotherapy (7). However, evidence shows that patients with metastatic squamous cell lung cancer tend to benefit from immunotherapy, regardless of PD-L1 status (7). Tumor mutational burden (TMB) also serves as a predictive biomarker for immunotherapy, and OS was in favor of chemotherapy for patients with low TMB and immunotherapy for patients with high TMB (7). Previous evidence suggests that micro RNAs may serve as biomarkers of response to cancer treatment and enable better management decisions (8). Furthermore, micro RNAs can be used as biomarkers for lung cancer screening and are associated with OS (8). *EGFR* mutations are the most important biomarkers for predicting treatment response to EGRF-TKIs. *EGFR* gene mutations mainly occur in the 18–21 exon and classical mutations refer to deletions in exon 19 and point mutation L858R in exon 21, which account for approximately 85% of all *EGFR* mutations (9). These mutations are associated with sensitivity to EGFR-TKIs such as gefitinib, erlotinib, afatinib, and icotinib (9, 10). EGFR-TKIs have better outcomes than chemotherapy as the first line of treatment in patients with *EGFR*-mutant NSCLC (10).

Although these EGFR-TKIs show good responses in NSCLC patients with *EGFR*-sensitizing genes (3), all treated patients eventually develop acquired resistance. The mechanisms of acquired resistance to first- or second-generation EGFR-TKIs include the T790M mutation, ERBB2 amplification, MET amplification, and transformation to small-cell lung cancer, of which T790M mutations are the most common resistance mechanism (11). The main process of developing T790M is a single nucleotide transition mutation in *EGFR*, a cytosine to thymine (C>T) mutation at position 2369, causing a threonine to methionine amino acid change at codon 790 (12). The T790M mutation leads to steric hindrance, increased binding affinity for ATP, and downstream signal transduction. When encountering patients with T790M, physicians can choose osimertinib as further therapy. As second-line therapy for NSCLC patients with acquired T790M mutations, osimertinib has better outcomes than platinum-based chemotherapy (13). Therefore, research on T790M mutation rate is of great significance because it may be related to further treatment strategies and prognosis.

Therefore, T790M also serves as a biomarker for resistance to first- and second-generation EGFR-TKIs and sensitivity to osimertinib (14). The prognosis was better for patients with acquired T790M who were treated with osimertinib than for those treated with chemotherapy (13, 15–17). In patients without acquired T790M, PFS with chemotherapy is worse (13, 17). Therefore, T790M mutation is a prognostic factor.

It is important to understand the T790M mutation rate in patients with NSCLC after treatment with EGFR-TKIs. Many studies have been conducted on the T790M mutation rate after treatment with EGFR-TKIs. These studies suggest that the acquired T790M mutation rate is approximately 50%–60% (11), and the acquired T790M mutation rate with afatinib is lower than that with gefitinib or erlotinib (11). However, the range of positive rates for acquired T790M was considerably wide in these studies. In addition, many of these data come from studies with very small sample sizes, some even fewer than ten patients. Therefore, such statistics produce significant errors and no definite conclusions can be obtained.

Due to the very small number of subjects in these studies and the wide range of T790M mutation rates, it is difficult to determine whether the T790M mutation rate after afatinib treatment is lower than that after first-generation EGFR-TKIs. To solve this problem, we conducted a meta-analysis to analyze the T790M mutation rate after treatment with first- and second-generation EGFR-TKIs using direct and indirect comparisons.

2 MATERIALS AND METHODS

2.1 Study Design and Participants

This study was performed in accordance with the Preferred Reporting Items for Systematic Reviews and Meta-Analyses (PRISMA) extension guidelines for network meta-analysis (18). A prospective protocol was created in advance and registered on the International Prospective Register of Systematic Reviews PROSPERO website (registration number: CRD42021257824).

2.2 Search Strategy

We performed a comprehensive literature search of electronic databases, including Embase, Cochrane Library, PubMed, and ClinicalTrials.gov, from their inception until May 31, 2021, without language restrictions. We aimed to compare the acquired T790M acquisition rates after treatment with different first-generation (gefitinib, erlotinib, and icotinib) and second-generation (afatinib and dacomitinib) EGFR-TKIs in patients with NSCLC. The detailed definitions of PICOS are listed in **Table S1**. The full details of the search strategy are listed in **Table S2**.

2.3 Study Selection Criteria

Studies were included under the following conditions: (1) observational studies, including prospective and retrospective cohort studies; (2) patients with NSCLC treated with only one EGFR-TKI during the study; (3) reported acquired T790M acquisition rates in separate EGFR-TKI groups; and (4) published as full-length articles. The exclusion criteria were (1) case-control studies or case reports; (2) T790M acquisition detected before EGFR-TKI treatment; (3) patients administered more than one EGFR-TKI; (4) EGFR-TKIs combined with chemotherapy or anti-vascular endothelial growth factor therapy; and (5) published articles, posters, or abstracts with limited information that could not be used for analysis. Bibliographies of the included studies and related systematic review articles were manually reviewed for relevant references. Two reviewers (PCH and YKW) independently reviewed the titles and abstracts of identified articles. Discrepancies or issues between reviewers were resolved by consulting a third reviewer (CCL) as an arbiter.

2.4 Data Extraction

A predetermined form was used by two reviewers (PCH and YKW) independently for data extraction of the following information: (1) publication year, (2) authors, (3) countries where the research was conducted, (4) NSCLC stages, (5) EGFR-TKIs, (6) number of patients with acquired resistance, (7) baseline characteristics and outcomes (sex, age, L858R mutation, exon 19 deletion, PFS, and OS); (8) biopsy sample types for examination; and (9) detection methods of T790M acquisition.

2.5 Outcome Measurement

The outcome was the acquired T790M acquisition rate in the research cohort after first- or second-generation EGFR-TKI treatment.

2.6 Data Synthesis and Statistical Analyses

We summarized the odds ratio (OR) with a 95% confidence interval (CI) as the effective size for measuring the acquired T790M acquisition rate. All graph generation and statistical analyses were performed using the statistical software RStudio (version 1.4.1106) (19). To compare the acquired T790M acquisition rate between the target EGFR-TKIs, network meta-analyses were conducted using "netmeta", "ggplot2", and "reshape2" packages. A random-effects network meta-analysis was performed using a consistency model. Single-arm meta-analyses with random-effects models were conducted using "meta" and "metafor" packages to estimate the specific acquired T790M acquisition rate of the target EGFR-TKIs. Subgroup analyses with Asian or Caucasian populations were conducted because of the varying characteristics of different races. Q and I^2 statistics were used to quantify heterogeneity among the included studies.

2.7 Publication Bias, Direct Evidence Plot, Inconsistency Assessment, Meta-Regression, and Influence Analysis

If more than 10 studies were included in the analysis, a funnel plot was used to examine publication bias. We performed Egger's test to assess the existence of bias in small-sample studies. Within the network meta-analysis results, a plot of direct evidence

proportions was constructed to quantify the percentage of direct and indirect evidence proportions for each network estimate (20). Inconsistent assumptions were assessed using a node-splitting model and design-by-treatment interaction model. Within the single-arm meta-analysis, a meta-regression analysis was performed to explore the potential associations between the effect size and target EGFR-TKIs. If more than two studies were included in the single-arm meta-analysis, an influence analysis was performed using the leave-one-out method.

2.8 Risk of Bias Assessment

Two reviewers (PCH and YKW) independently assessed the methodological quality of the retrieved multi-cohort studies using the ROBINS-I tool (21), and discrepancies were resolved by a third reviewer (CCL).

3 RESULTS

3.1 Study Identification

The review process is illustrated in **Figure 1**. A total of 518 studies were identified using the search terms in the electronic databases, with 200 studies on PubMed, 265 on Embase, 31 on Cochrane Library, and 22 on ClinicalTrials.gov (**Table S2**). After removing duplicate studies and excluding titles and abstracts, 56 studies were considered for full-text evaluation, and 27 studies were excluded for different reasons (**Table S3**). Finally, 29 studies [including 23 multi-cohort studies (5, 11, 22–42) and six single-cohort studies (43–48)] were included in the risk of bias assessment and single-arm meta-analysis, and 20 multi-cohort studies were included in the network meta-analysis. Among the studies identified in the search results, acquired T790M acquisition rates after treatment with gefitinib, erlotinib, icotinib, or afatinib were noted. To our knowledge, no study has reported the acquired T790M acquisition rate after dacomitinib treatment. A summary of the retrieved studies is shown in **Table 1**.

3.2 Characteristics of the Included Participants

The characteristics of the participants are presented in **Tables 1** and **S4**. The final quantitative analysis included 3385 participants (age: 27–93-years-old), with stages I–IV and advanced, recurrent, or metastatic NSCLC. Twenty-four studies were conducted in Asia (12 in Japan, 5 in Korea, 4 in China, and 3 in Taiwan; with 2883 Asian participants), and 5 studies were conducted in Europe and North America (2 in Italy, 1 in Germany, and 2 in the USA; with 502 Caucasian participants).

3.3 Outcome: Acquired T790M Mutation Rate

3.3.1 Risk of Acquired T790M Mutation Rate in All Participants

In terms of the acquired T790M acquisition rate following treatment with gefitinib, erlotinib, icotinib, and afatinib, 20 multi-cohort studies (5, 22–37, 39–41) were included in the

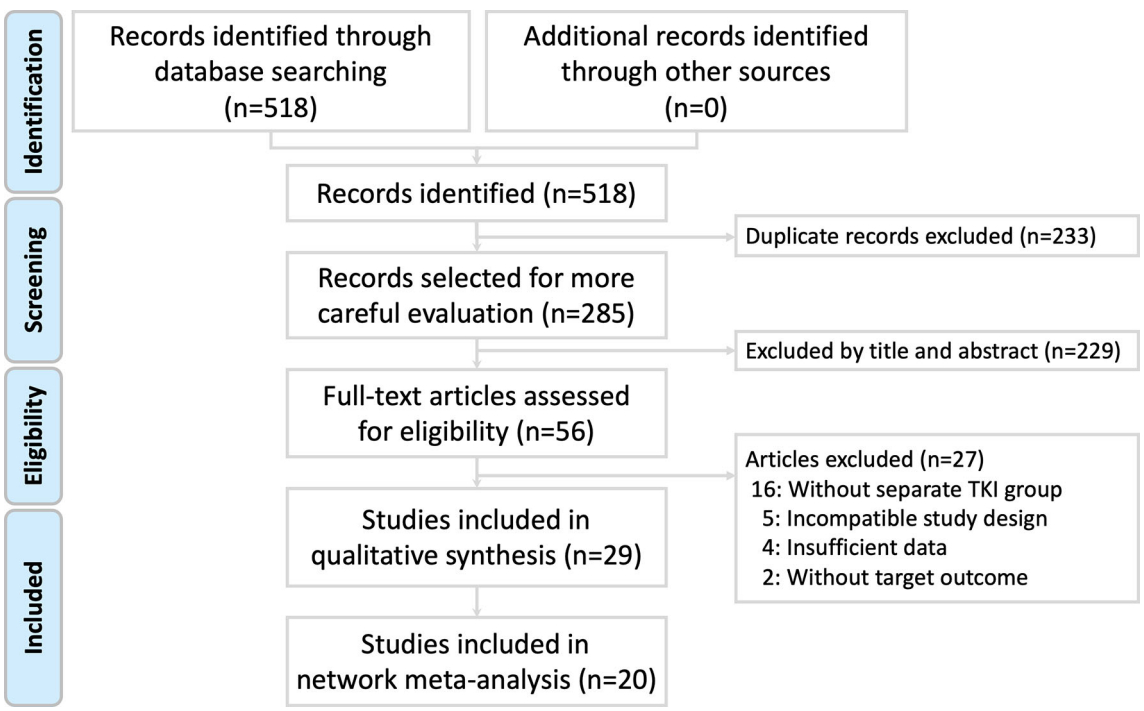

FIGURE 1 | Study flow diagram.

TABLE 1 | Summary of the retrieved studies.

Author, year	Study design	Country	Stage	EGFR-TKIs	Patientwith AR, n	Female, n (%)	Age, median (range),mean ± SD, y	Re-biopsysample	Detection method	Ref.
Single-cohort study										
Onitsuka 2010	Pro	Japan	IA-IV	G	10	7 (70.0)	61.5 (53-85)	Tissue	PCR	(43)
Uramoto 2012	Retro	Japan	IA-IV	G	19	14 (73.7)	65.0 (52-87)	Tissue	PCR	(44)
Ji 2013	Retro	Korea	N/A	G	26	16 (61.5)	58.0 (40-80)	Tissue	multiplexed PCR	(45)
Campo 2016	Pro	USA	advanced or recurrent	A	24	18 (75.0)	57 (27-83)	Tissue	PCR	(46)
Liang 2017	Retro	Taiwan	IIIB-IV	A	140	87 (62.1)	61 (28–87)	Tissue	MALDI-TOF MS	(47)
Tanaka 2017	Retro	Japan	advanced or recurrent	A	37	15 (40.5)	65 (34-79)	Tissue, Fluid	PNA-LNA PCR, Cycleave PCR, dPCR, ARMS, Cobas	(48)
Multi-cohort study										
Sequist 2011	Retro	USA	N/A	G E	37	22 (59.5)	59.0 (37-88)	Tissue	multiplexed PCR	(22)
Yano 2011	Retro	Japan	N/A	G E	22	14 (63.6)	59.5 (32-85)	Tissue	PCR	(23)
Hata 2013	Retro	Japan	N/A	G E	78	54 (69.2)	N/A	Tissue	PNA-LNA PCR	(24)
Sun 2013	Pro	Korea	advanced or recurrent	G E	70	52 (74.3)	N/A	Tissue	PCR	(25)
Li 2014	Pro	China	IV	G E I	54	25 (46.3)	51.2 (45.9-67.3)	Tissue	PCR	(26)
Jin 2016	Retro	China	IV	G E I	83	47 (56.6)	61 (29-85)	Tissue, Fluid	targeted pan-cancer NGS	(27)
Ko 2016	Retro	Japan	N/A	G E A	61	44 (72.1)	64 (39-84)	Tissue, Fluid	PCR	(28)
Matsuo 2016	Retro	Japan	advanced or recurrent	G E A	73	57 (78.1)	67 (48-82)	Tissue	dPCR	(29)
Nosaki 2016	Retro	Japan	advanced or metastatic	G E A	395	241 (61.0)	63 (27-84)	Tissue	N/A	(30)
Takahama 2016	Pro	Japan	IIIB-IV	G E A	260	182 (70.0)	68 (36–90)	Plasma	ddPCR	(31)
Tseng 2016	Retro	Taiwan	advanced	G E A	98	61 (62.2)	57.5 (30–83)	Tissue, Fluid	MALDI-TOF MS	(32)
Lee 2017	Retro	Korea	IIIA-IV	G E	19	12 (63.2)	58 (36-72)	Tissue	NGS	(33)
Oya 2017	Retro	Japan	III-IV	G E A	181	110 (60.8)	65 (35-85)	Tissue	PCR	(34)
Wang 2017	Pro	China	advanced or recurrent	G E I	108	53 (49.1)	57 (28–79)	Tissue, Plasma	ddPCR, ARMS	(35)
Zhang 2017	Retro	China	IIIB-IV	G E	51	32 (62.8)	58 (30-87)	Tissue	Sanger, ARMS	(36)
Kaburagi 2018	Retro	Japan	III-IV	G E A	233	144 (61.8)	70 (32-93)	Tissue, Plasma	allele-specific PCR, Cobas	(37)
Lee 2019	Retro	Korea	N/A	G E A	116	52 (44.8)	55.8	Tissue	PNA-mediated PCR clamping	(38)
Lin 2019	Retro	Taiwan	advanced or recurrent	G	134	98 (73.1)	71 (IQR: 60–80)	Tissue	RT-PCR	(5)
				E	68	46 (67.7)	67 (IQR: 61–73)	Tissue		
				A	99	61 (61.6)	60 (IQR: 53–71)	Tissue		
Yoon 2019	Retro	Korea	IIIB-IV	G	123	58 (47.2)	60.9 ± 11.5	Tissue	PNA-mediated PCR clamping	(39)
				A	41	20 (48.8)	59.2 ± 12.3	Tissue		
Dal Maso 2020	Retro	Italy	IIIB-IV	G E A	235	154 (65.5)	66 (33-92)	Tissue	Pyrosequencing, PCR, MS, NGS	(41)

(Continued)

TABLE 1 | Continued

Author, year	Study design	Country	Stage	EGFR-TKIs	Patientwith AR, n	Female, n (%)	Age, median (range),mean ± SD, y	Re-biopsysample	Detection method	Ref.
Del Re 2020	Retro	Italy	IIIB-IV	G E	42	29 (69.1)	64.1 ± 8.6	Plasma	ddPCR	s (40)
				A	41	20 (48.8)	70.5 ± 11.3	Plasma		
Wagener-Ryczek 2020	Retro	Germany	N/A	G E A	123	70 (56.9)	68 (40-87)	Tissue	multiplexed PCR	(11)
Oya 2021	Pro	Japan	III-IV	G E A	62	33 (53.2)	67 (36-80)	Tissue, Plasma	ddPCR, Cobas	(42)

A, afatinib; AR, acquired resistance; ARMS, Amplification Refractory Mutation System; Cobas, Cobas® EGFR Mutation Test; dPCR, digital PCR; ddPCR, droplet digital PCR; E, erlotinib; EGFR-TKI, epidermal growth factor receptor-tyrosine kinase inhibitor; G, gefitinib; I, Icotinib; MALDI-TOF MS, matrix-assisted laser desorption ionization-time of flight mass spectrometry; MS, mass spectrometry; NGS, Next Generation Sequencing; PCR, polymerase chain reaction; PNA-LNA PCR, peptide nucleic acid-locked nucleic acids PCR; PNA-mediated PCR clamping, peptide nucleic acid-mediated PCR clamping; Pro, prospective cohort; Retro, retrospective cohort; Sanger, Sanger sequencing.

network meta-analysis. The structure of the network is shown in **Figure 2A**. A forest plot of the network meta-analysis is shown in **Figure 2B**. There was no statistical heterogeneity among the included studies, with an I^2 of 0% (95% CI: 0–32.6), and the Q statistic was 25.04% (p = 0.57) for within-design and 1.56 (p = 0.66) for between-designs, indicating no heterogeneity and consistency in the model used. Compared with afatinib, a higher OR of acquired T790M acquisition rate was observed after erlotinib (OR = 1.48; 95% CI: 1.09–2.00) and gefitinib (OR = 1.45; 95% CI: 1.11–1.90) treatments. The results also indicated an even OR of acquired T790M acquisition rate after treatment with icotinib (OR = 0.91, 95% CI: 0.46–1.79) compared with that after afatinib treatment in NSCLC patients. According to the league table (**Table 2**) and P-scores (**Table S5**), erlotinib was associated with the highest risk of acquired T790M acquisition rate, followed by gefitinib.

3.3.2 Risk of Acquired T790M Mutation Rate in Asian Patients

In terms of the acquired T790M acquisition rates in Asian patients following treatment with gefitinib, erlotinib, icotinib, and afatinib, 18 multi-cohort studies (5, 23–37, 39, 41) were included in the subgroup network meta-analysis. The structure of the network is shown in **Figure 2C**. A forest plot of the network meta-analysis is shown in **Figure 2D**. There was no statistical heterogeneity among the included studies, with I^2 0% (95% CI: 0–34.8), and the Q statistic was 22.35 (p = 0.55) for within-design and 1.70 (p = 0.63) for between-designs, indicating no heterogeneity and consistency in the model used. The results indicated a higher OR of acquired T790M acquisition rate after treatment with gefitinib (OR = 1.52; 95% CI: 1.13–2.05) and erlotinib (OR = 1.47; 95% CI: 1.05–2.05) than that after afatinib treatment in patients with NSCLC. Furthermore, an even OR of acquired T790M acquisition rate was observed after icotinib treatment (OR = 0.94; 95% CI: 0.47–1.86) compared with that in afatinib-treated patients with NSCLC. According to the league table (**Table 3**) and P-scores (**Table S5**), gefitinib was associated with the highest risk of acquired T790M acquisition rate, followed by erlotinib.

3.3.3 Risk of Acquired T790M Mutation Rate in Caucasian Patients

In terms of the acquired T790M acquisition rate in Caucasian patients following treatment with gefitinib, erlotinib, and afatinib, two multi-cohort studies (22, 40) were included in the subgroup network meta-analysis. The structure of the network is shown in **Figure 2E**. No statistical heterogeneity was observed among the included studies, with an I^2 value of 0%. The Q statistic was 0.11 (p = 0.91) for between-designs, indicating no heterogeneity and consistency in the model used. A forest plot of the network meta-analysis is shown in **Figure 2F**. The results indicated an even OR of acquired T790M acquisition rate after treatment with erlotinib (OR = 1.85; 95% CI: 0.84–4.05) and gefitinib (OR = 1.12, 95% CI: 0.60–2.07) compared with that in afatinib-treated patients with NSCLC. According to the league table (**Table 4**) and P-scores (**Table S5**), gefitinib, erlotinib, and afatinib were associated with an even risk of an acquired T790M acquisition rate.

3.3.4 Acquired T790M Mutation Rate in All Participants

In terms of specific acquired T790M acquisition rates with EGFR-TKIs following treatment with gefitinib, erlotinib, icotinib, and afatinib, 29 studies (5, 11, 22–48) were included in the single-arm meta-analysis. A forest plot of the analysis is shown in **Figure 3**. The overall rate of acquired T790M acquisition was 44% (95% CI: 40–47; I^2 = 71%). The specific acquired T790M acquisition rates were 49% for gefitinib (95% CI: 44–54; I^2 = 74%), 47% for erlotinib (95% CI: 43–52; I^2 = 16%), 37% for icotinib (95% CI: 0–46; I^2 = 0%), and 33% for afatinib (95% CI, 24–41; I^2 = 76%). The meta-regression results indicated potential associations between the acquired T790M acquisition rate and different EGFR-TKIs, with statistical significance (p < 0.0001) (**Table S6**).

3.3.5 Acquired T790M Mutation Rate in Asian Patients

In terms of specific acquired T790M acquisition rates in Asian patients following treatment with gefitinib, erlotinib, icotinib, and afatinib, 24 studies (5, 23–39, 42–45, 47, 48) were included in the single-arm meta-analysis. A forest plot of the analysis is shown in

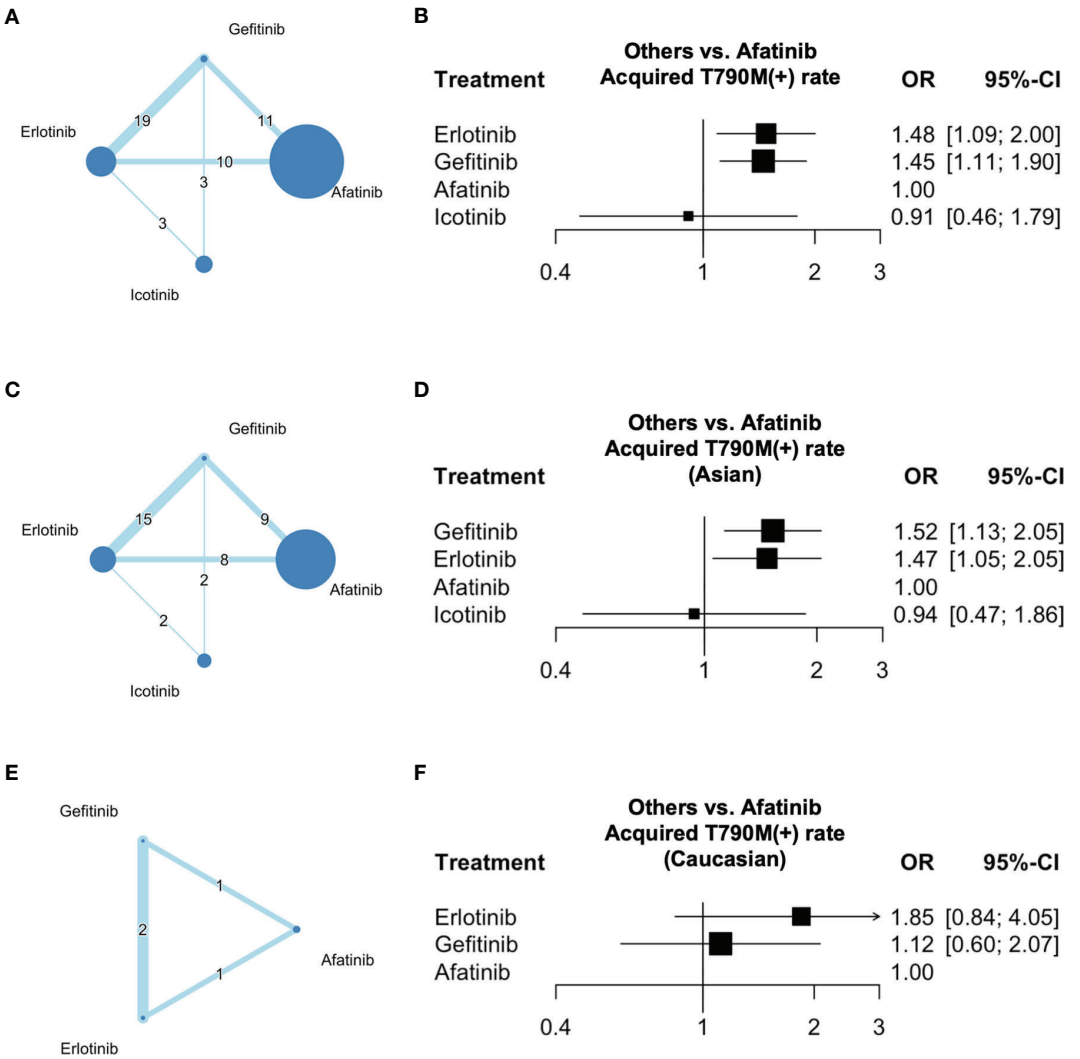

FIGURE 2 | Network of the comparisons and forest plot for the network meta-analysis. Networks of eligible EGFR-TKIs comparisons for outcomes of acquired T790M mutation rate for **(A)** all participants, **(C)** Asians, and **(E)** Caucasians. Forest plots of eligible EGFR-TKI comparisons for outcomes of acquired T790M mutation rate for **(B)** all participants, **(D)** Asians, and **(F)** Caucasians. Network: The size of the nodes corresponds to the number of studies for each treatment. The lines between nodes represent a direct comparison of the trials and the thickness of the lines linking nodes corresponds to the number of trials included.

Figure 4. The overall acquired T790M acquisition rate was 43% (95% CI: 39–47; $I^2 = 73\%$). The specific acquired T790M acquisition rates were 49% for gefitinib (95% CI: 43–52; $I^2 = 76\%$), 46% for erlotinib (95% CI: 41–50; $I^2 = 5\%$), 37% for icotinib (95% CI: 0–46; $I^2 = 0\%$), and 30% for afatinib (95% CI: 0–41; $I^2 = 80\%$). Meta-regression results indicated potential associations between the acquired T790M acquisition rate and different EGFR-TKIs in Asians, with statistical significance ($p < 0.0001$) (**Table S6**).

TABLE 2 | League table with network meta-analysis estimates of acquired T790M mutation rate in all participants.

Erlotinib	1.04 (0.84 to 1.28)	1.54 (1.08 to 2.19)*	1.86 (0.78 to 4.46)
1.02 (0.83 to 1.26)	**Gefitinib**	1.44 (1.10 to 1.90)*	1.42 (0.70 to 2.91)
1.48 (1.09 to 2.00)*	1.45 (1.11 to 1.90)*	**Afatinib**	–
1.62 (0.86 to 3.05)	1.59 (0.85 to 2.98)	1.10 (0.56 to 2.15)	**Icotinib**

*Pairwise (upper-right portion) and network (lower-left portion) meta-analysis results are presented as estimated effect sizes as mean difference (MD) and 95% confidence interval for the outcome of the acquired T790M mutation rate. An MD > 0 favors treatment in the column for the acquired T790M mutation rate. *Statistically significant.*

TABLE 3 | League table with network meta-analysis estimates of acquired T790M mutation rate in Asian patients.

Gefitinib	1.02 (0.81 to 1.27)	1.54 (1.13 to 2.09) *	1.42 (0.70 to 2.91)
1.04 (0.83 to 1.29)	**Erlotinib**	1.47 (0.99 to 2.18)	1.86 (0.78 to 4.46)
1.52 (1.13 to 2.05)*	1.47 (1.05 to 2.05)*	**Afatinib**	–
1.62 (0.87 to 3.04)	1.57 (0.83 to 2.96)	1.07 (0.54 to 2.12)	**Icotinib**

*Pairwise (upper-right portion) and network (lower-left portion) meta-analysis results are presented as estimated effect sizes as mean difference (MD) and 95% confidence interval for the outcome of the acquired T790M mutation rate. An MD > 0 favors treatment in the column for the acquired T790M mutation rate. *Statistically significant.*

3.3.6 Acquired T790M Mutation Rate in Caucasian Patients

In terms of the acquired T790M acquisition rate of EGFR-TKIs in Caucasian patients following treatment with gefitinib, erlotinib, and afatinib, five studies (11, 22, 40, 41, 46) were included in the single-arm meta-analysis. A forest plot of the analysis is shown in **Figure 5**. The overall acquired T790M acquisition rate was 47% (95% CI: 42–53; I^2 = 12%). The specific acquired T790M acquisition rates were 49% for gefitinib (95% CI: 40–57; I^2 = 0%), 57% for erlotinib (95% CI: 45–68; I^2 = 0%), and 42% for afatinib (95% CI: 35–50; I^2 = 0%). Meta-regression results indicated no potential association between the acquired T790M acquisition rate and different EGFR-TKIs in Caucasians (p = 0.6621) (**Table S6**).

3.3.7 Meta-Regression Analysis of Gefitinib, Erlotinib, and Afatinib in Asians/Caucasians

We also conducted a meta-regression analysis to investigate the potential associations between gefitinib, erlotinib, and afatinib treatments and Asians/Caucasians. In terms of the acquired T790M acquisition rate of gefitinib, the results indicated potential associations between the acquired T790M acquisition rate and Asian/Caucasian populations (p < 0.0001). In terms of the acquired T790M acquisition rate of erlotinib, the results indicated no potential association between the acquired T790M acquisition rate and Asians/Caucasians (p = 0.3941). In terms of the acquired T790M acquisition rate of afatinib, the results indicated potential associations between the acquired T790M acquisition rate and Asian/Caucasian populations (p < 0.0001). Gefitinib and afatinib treatments had different effects on the acquired T790M acquisition rates in Asians and Caucasians (**Table S7**).

3.3.8 Detection of Acquired T790M Mutation Between Tissue or Plasma Biopsy

We conducted single-arm meta-analyses and meta-regression analyses to evaluate the rate of acquired T790M acquisition in tissue or plasma biopsy samples. Forest plots of the analyses are shown in **Figure S1**. The results showed that after treatment with gefitinib, the acquired T790M acquisition rate was 52% (95% CI: 48–56; I^2 = 30%) in tissue biopsy samples, whereas the acquired T790M acquisition rate was 27% (95% CI: 21–33) in plasma biopsy samples. After treatment with erlotinib, the acquired T790M acquisition rate was 46% (95% CI: 40–52; I^2 = 22%) in tissue biopsy samples, whereas the acquired T790M acquisition rate was 40% (95% CI: 26–54) in plasma biopsy samples. Furthermore, after treatment with afatinib, the acquired T790M acquisition rate was 39% (95% CI: 34–45; I^2 = 0%) in tissue biopsy samples, whereas the acquired T790M mutation rate was 33% (95% CI: 23–42; I^2 = 65%) in plasma biopsy samples. Meta-regression analysis results showed potential associations between the acquired T790M mutation rate and tissue/plasma biopsy after treatment with gefitinib, erlotinib, or afatinib (**Table S8**). After treatment with gefitinib, erlotinib, or afatinib, the detection rate of the acquired T790M mutation was significantly lower in plasma biopsy samples than that in tissue biopsy samples.

3.4 Publication Bias

Among the network meta-analyses of all Asian patients, funnel plots of publication bias showed general symmetry. Egger's test showed no significant publication bias among the included studies (**Figures S2A, B**). Because only two studies were included in the network meta-analysis for Caucasians, no further assessment of publication bias was performed.

In the single-arm meta-analysis of all participants, funnel plots of publication bias showed general symmetry (**Figure S3A**). Because the intercept was close to zero, the small study bias was not significant (**Figure S3B**). In the single-arm meta-analysis for Asians, funnel plots of publication bias showed a general symmetry (**Figure S3C**). Because the intercept was significantly close to zero, the small study bias was not significant (**Figure S3D**). As only three studies were included in the single-arm meta-analysis for Caucasians, no further assessment of publication bias was performed.

3.5 Direct Evidence Plots and Inconsistency Assessment

In the network meta-analyses, direct evidence plots for all patients, Asian and Caucasian are presented in **Figure S4**. We found no

TABLE 4 | League table with network meta-analysis estimates of acquired T790M mutation rate in Caucasian patients.

Erlotinib	1.65 (0.85 to 3.23)	1.87 (0.83 to 4.19)
1.65 (0.85 to 3.23)	**Gefitinib**	1.11 (0.60 to 2.07)
1.85 (0.84 to 4.05)	1.12 (0.60 to 2.07)	**Afatinib**

Pairwise (upper-right portion) and network (lower-left portion) meta-analysis results are presented as estimated effect sizes as mean difference (MD) and 95% confidence interval for the outcome of the acquired T790M mutation rate. An MD > 0 favors treatment in the column for the acquired T790M mutation rate.

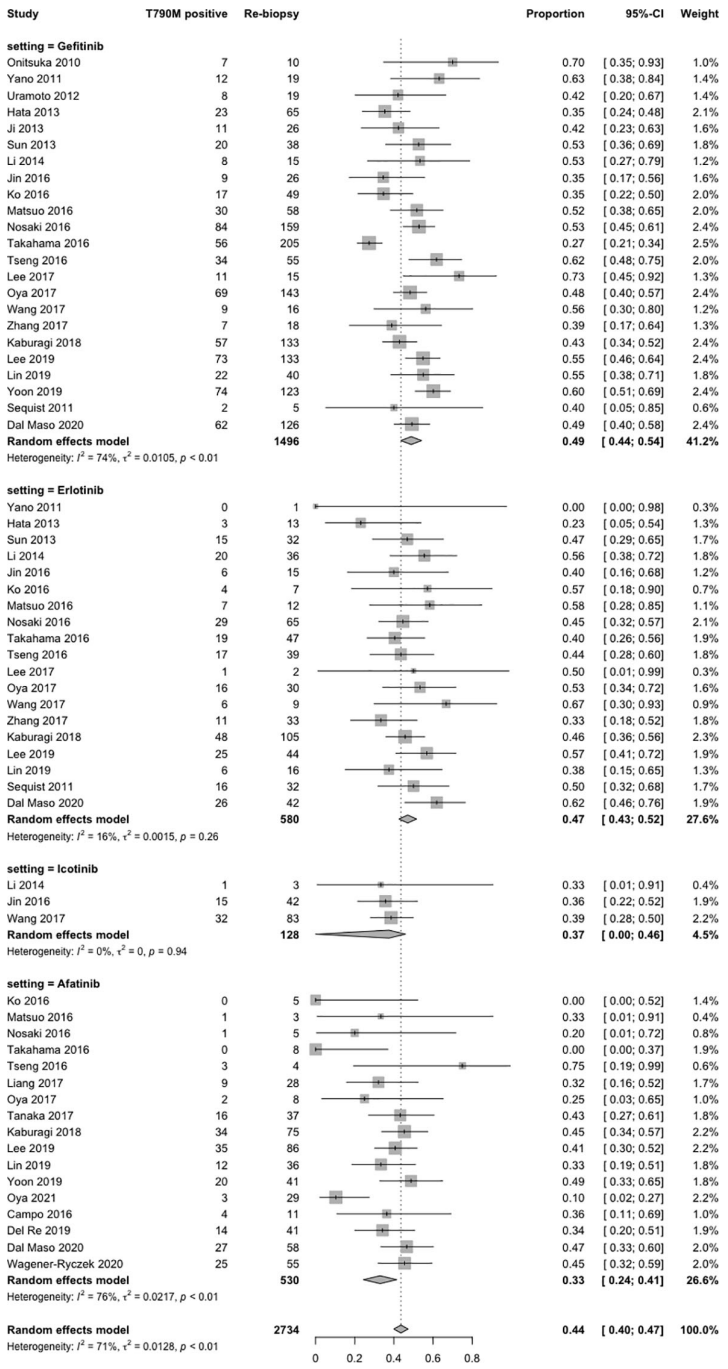

FIGURE 3 | Forest plot of subgroup single-arm meta-analysis of all participants.

evidence of inconsistencies using either node-splitting (**Figure S5**) or design-by-treatment interaction model approaches (**Figure S6**).

3.6 Influence Analysis

In the single-arm meta-analysis for gefitinib, erlotinib, icotinib, and afatinib treatment in Asian patients, the results indicated no significant changes in the integrated or after eliminating each study individually (**Figure S7**). For the single-arm meta-analysis of afatinib in Caucasians, the results indicated no significant changes in the integrated OR while eliminating each study individually (**Figure S8**).

3.7 Risk of Bias Assessment: ROBINS-I

The ROBINS-I results are presented in **Table S9**. Most of the studies had a moderate risk of overall bias. There were three main reasons. (1) For baseline *EGFR* mutation types, the number of patients with L858R mutations or exon 19 deletions was not

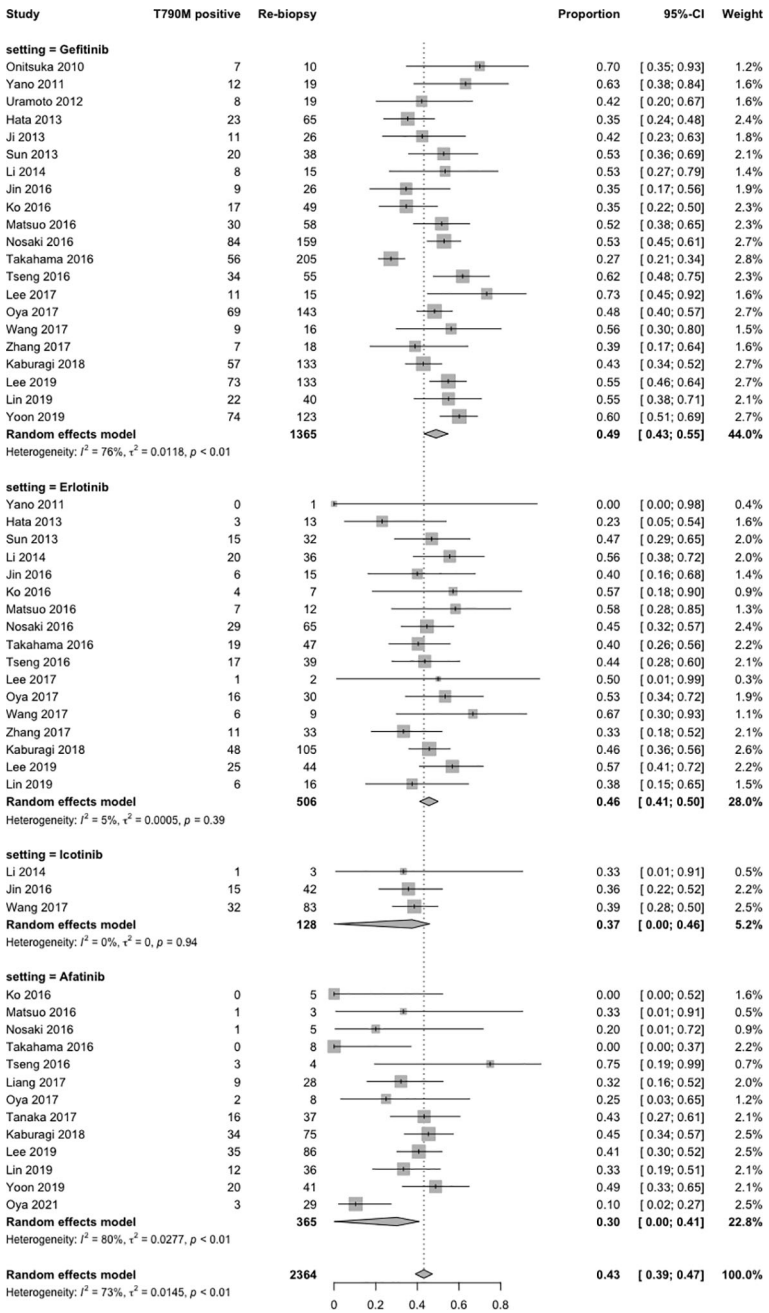

FIGURE 4 | Forest plot of subgroup single-arm meta-analysis of Asian patients.

balanced or adjusted for different EGFR-TKI-treated groups. Hence, we propose a moderate risk of bias owing to confounding factors. (2) For the detection of T790M mutation, five studies used multiple methods (**Table 1**) (35–37, 41, 42). As the detection accuracy differed according to the detection method (49, 50), we proposed a moderate risk of bias in the measurement of outcomes. (3) For the re-biopsy samples, six studies used multiple types of samples, including tissue, plasma, and fluid (**Table 1**) (27, 28, 32, 35, 37, 42). As the detection accuracy differed according to the type of examination sample (50), we proposed a moderate risk of bias in the measurement of outcomes.

4 DISCUSSION

This is the first meta-analysis of the acquired T790M mutation rate associated with treatment using different EGFR-TKIs, and it has revealed that the acquired T790M mutation rate was

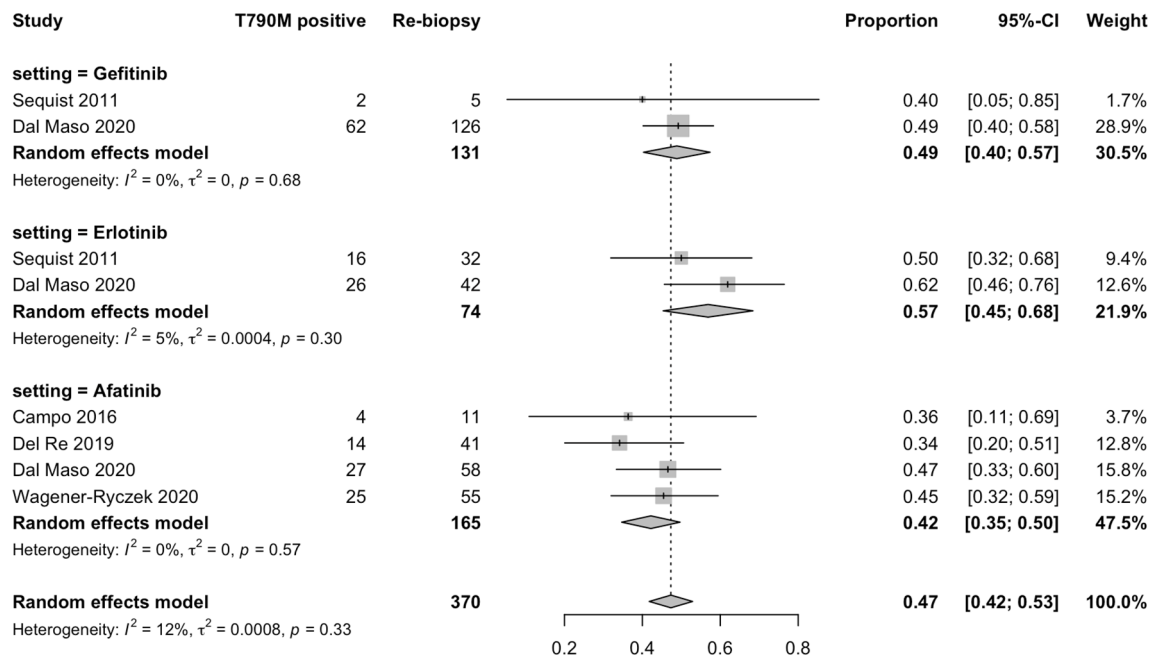

FIGURE 5 | Forest plot of subgroup single-arm meta-analysis of Caucasian patients.

significantly lower with afatinib (33%) than that with gefitinib (49%) and erlotinib (47%) ($p < 0.05$) treatments in the overall population. The first- and second-generation EGFR-TKIs are different. The mechanisms underlying the lower T790M mutation rate after afatinib treatment are unclear; several hypotheses can explain this result.

Initially, gefitinib, erlotinib, and afatinib were considered similar EGFR-TKIs. However, gefitinib and erlotinib are reversible EGRF-TKIs with similar activities in *in vitro* and xenograft assays. In our analysis, the incidence of acquired T790M mutations was similar following treatment with gefitinib and erlotinib. In contrast, afatinib is an irreversible EGFR-TKI that inhibits the ErbB receptor family and causes rare *EGFR* mutations, including exon 18 p.G719X and exon 21 p.L861Q point mutations (6). Afatinib has pharmacological characteristics that differ from those of gefitinib and erlotinib.

El Kadi et al. found that acquired *EGFR* T790M occurs mainly through activation-induced cytidine deaminase (AICDA)-mediated deamination of 5-methylcytosine following TKI treatment (12). They reported that EGFR-TKI treatment leads to activation of the nuclear factor-kappa B pathway, which in turn induces the expression of AICDA, further causing deamination of 5-methylcytosine to thymine at position c.2369 to generate the T790M mutation. The different pharmacological characteristics of these EGFR-TKIs may lead to different rates of acquired T790M mutation. Gefitinib and erlotinib showed higher AICDA expression than afatinib (12). Therefore, it is rational to understand the higher frequencies of the T790M mutation rates following treatment with gefitinib and erlotinib.

Another hypothesis is that clonal selection during different EGFR-TKI treatments may lead to different clonality of the acquired resistance. Previous studies have shown that afatinib suppresses the growth of lung cancer cells harboring T790M cells (51, 52). Furthermore, afatinib exerts a 100-fold potent activity against T790M cell lines than first-generation EGFR-TKIs (51). Afatinib was initially considered a potential salvage therapy after first-generation TKIs. However, the clinical use of afatinib as salvage therapy after first-generation TKIs has been disappointing (52) because of the difficulty in increasing the clinical dose of afatinib to reach the afatinib concentration in the human body in an *in vitro* study (52). Although afatinib cannot effectively overcome T790M at a clinically achievable dose, it may reduce the occurrence of T790M colonies. Therefore, T790M subclonies are likely to be enriched under the different effects of gefitinib, erlotinib, and afatinib (39). Previous studies have shown that prolonged exposure to EGFR-TKIs promotes selective survival of T790M-positive cells (5, 53, 54). These results support the hypothesis of clonal selection for EGFR-TKI therapy.

Interestingly, we found that the rate of acquired T790M mutation was slightly lower in Asians (43%) than that in Caucasians (47%). Asian and Caucasian patients with lung cancer have different genetic susceptibilities (2). For example, common *EGFR* mutations in adenocarcinoma occur in approximately 50% of Asian patients and 20% of Caucasian patients (2). In contrast, the incidence of *KRAS* mutations in European populations (30%) is higher than that in Asian populations (<10%) (2). The exact mechanisms for the different *EGFR* or *KRAS* mutations in Asian and Caucasian populations remain unclear. In this meta-analysis, we found that the rate of acquired T790M mutation was higher in Caucasian patients than that in Asian patients. However, the reason for this difference remains unclear.

The clinical outcomes of EGFR-TKIs are controversial. It has been shown that for NSCLC patients with sensitive *EGFR* mutations, first-line treatment with gefitinib yielded PFS of 8–13 months (55), erlotinib yielded a PFS of 9.7–13 months (5), and afatinib yielded a PFS of 13.4–15.2 months (6). The LUX-Lung 7 trial suggested that afatinib achieved superior clinical outcomes compared with gefitinib-treated patients bearing *EGFR* L858R or exon 19 deletions (56). However, other studies have shown that PFS and OS are similar in gefitinib- and afatinib-treated patients (39, 57). In a real-world study, the clinical outcomes of PFS or OS were similar among patients treated with gefitinib, erlotinib, or afatinib for NSCLC patients bearing sensitizing *EGFR* mutations (5). Therefore, the clinical outcomes were similar among the three EGFR-TKIs. However, these EGFR-TKIs have different incidences of T790M mutation.

Patients with acquired T790M can choose osimertinib treatment, whereas those without acquired T790M can only receive chemotherapy. As shown in **Figure 6**, the clinical prognosis was better for patients with acquired T790M mutations who were treated with osimertinib. PFS of NSCLC patients with acquired T790M after treatment with gefitinib, erlotinib, and afatinib was 10.4-15.6 months (13, 15, 16). The PFS of NSCLC patients with acquired T790M mutation treated with platinum-based chemotherapy was only 6 months (17). In patients without acquired T790M, PFS after platinum-based chemotherapy was worse, only 4.4–5.1 months (13, 17). Joo et al. also suggested that osimertinib treatment was independently associated with better outcomes, such as longer OS and PFS (54). A preclinical model also suggested that T790M-positive cells grow more slowly than T790M-negative cells (53). Thus, T790M appears to be a prognostic marker. As the presence of T790M is an important factor in choosing treatment and determining prognosis, assessing which population will develop T790M is vital. This should be considered when selecting EGFR-TKIs, and patients must be screened for acquired *EGFR* T790M mutations at the time of tumor progression.

The occurrence of T790M mutation has important implications for further treatment and prognosis after first- or second-generation EGFR-TKI therapy. The PFS after afatinib treatment was similar to or slightly higher than that after gefitinib and erlotinib treatments. However, the T790M mutation rate of afatinib was significantly

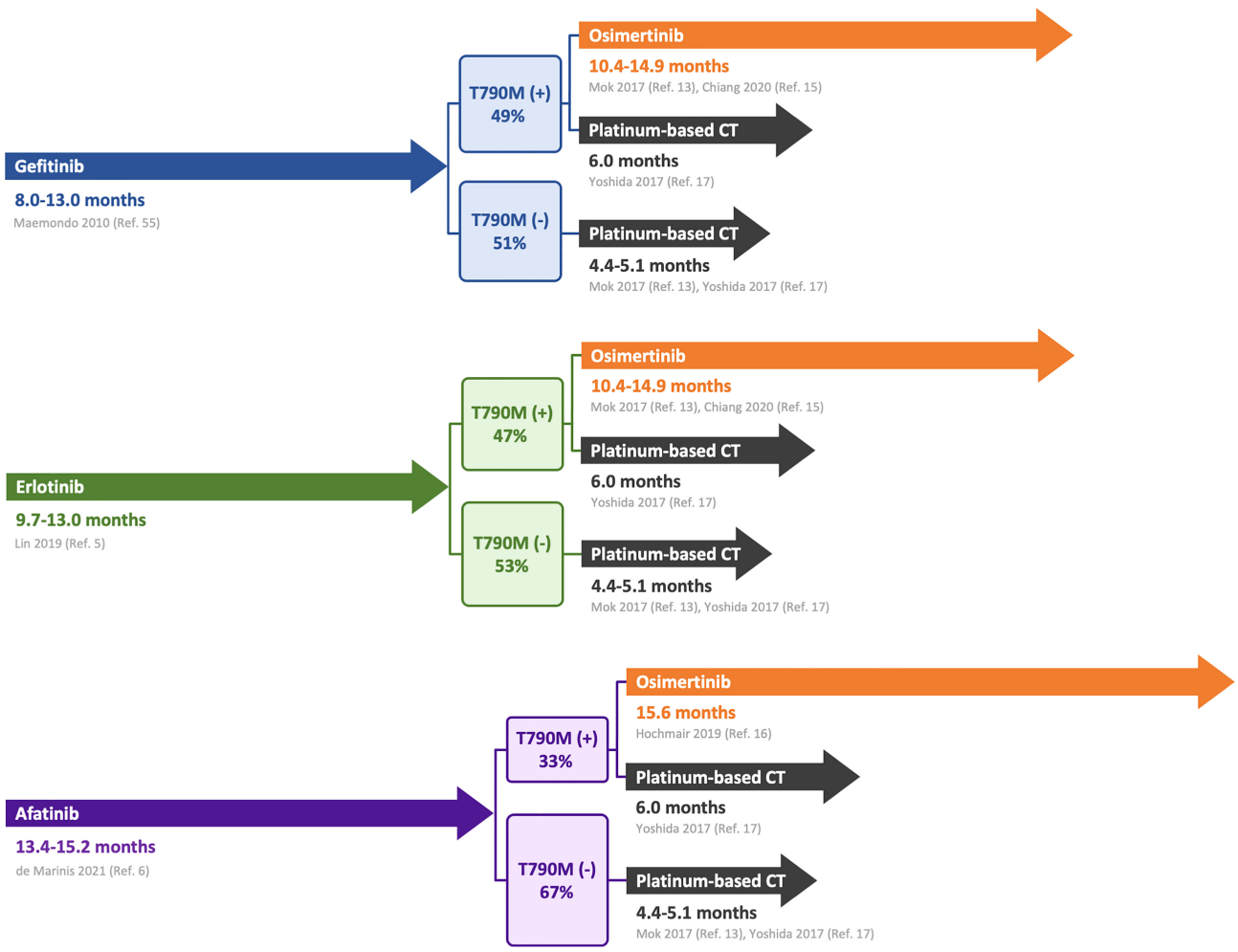

FIGURE 6 | Progression-free survival of T790M-positive and -negative patients.

lower than those of gefitinib and erlotinib. Patients with acquired T790M mutations during EGFR-TKI treatment showed better PFS and OS with osimertinib treatment. Accordingly, we suggest gefitinib and erlotinib as the first-line treatments for patients with advanced NSCLC. However, in precision medicine, selecting patients with a high probability of receiving first-generation EGFR-TKIs is a better strategy. Ouyang et al. showed that a lower body mass index (≤ 25 kg/m^2), higher levels of neuron-specific enolase (> 17.9 ng/ml), and retroperitoneal lymph node metastasis before treatment are independent risk factors for the acquired T790M mutation (58). Lin et al. revealed that the independent factors for T790M mutation were first-generation EGFR-TKIs, initial liver metastasis, male sex, and uncommon *EGFR* mutations (5).

4.1 Limitations of This Study

This meta-analysis had several limitations. First, the literature cited in this meta-analysis was retrospective but not a randomized control trial. The clinical conditions of the subjects who received the three EGFR-TKIs were unequal. Second, the study was not designed to determine the incidence of T790M mutations. Therefore, the timing of biopsy, sample collection (tissues or blood), and methods for detecting T790M were not well designed. Our analysis showed a significantly lower detection rate of acquired T790M mutations in plasma biopsy samples than that in tissue biopsy samples. There are many methods for detecting the T790M mutation. Droplet digital PCR (ddPCR) and matrix-assisted laser desorption/ionization-time of flight mass spectrometry (MALDI-TOF MS) are highly sensitive approaches capable of detecting mutations, and studies using ddPCR and MALDI-TOF MS have shown a higher incidence of detecting T790M (40, 47). The duration of exposure to EGFR-TKIs is an independent factor for the occurrence of T790M mutations. However, the time required for rebiopsy has not been standardized. Third, we included all the available first- and second-generation EGFR-TKIs. However, studies on acquired T790M in patients treated with icotinib or dacomitinib are limited. Therefore, we did not discuss the effects of icotinib or dacomitinib. Further meta-analysis should be performed with more studies on icotinib and dacomitinib.

5 CONCLUSIONS

Lung cancer is associated with significant mortality rates worldwide. Lung adenocarcinoma is the most common type of NSCLC. *EGFR* mutations occur frequently in adenocarcinoma, and oral EGFR-TKIs with good responses are promising treatments for patients with advanced NSCLC. T790M mutation is the most common mechanism of acquired resistance. Our meta-analysis of 29 studies showed that erlotinib and gefitinib had a higher OR for the T790M mutation than afatinib. The acquired T790M mutation rate was significantly lower with afatinib treatment than that with gefitinib or erlotinib in the overall population. The T790M mutation rate is of great significance because osimertinib treatment in patients with the T790M mutation shows a good prognosis.

DATA AVAILABILITY STATEMENT

The original contributions of this study are included in the article/**Supplementary Material**. Further inquiries can be directed to the corresponding author.

AUTHOR CONTRIBUTIONS

The authors confirm their contribution to the paper as follows: study conception and design: Y-KW and C-CL. Data collection: P-CH and Y-KW. Statistical analysis: P-CH, C-YK, and I-ST. Interpretation of results: Y-KW, C-YH, M-CY, and C-CL. Drafting manuscript: P-CH and C-CL. And project administration: C-CL. All authors have reviewed the results and approved the final version of the manuscript.

FUNDING

This study was supported by grants from Taipei Tzu Chi Hospital and Buddhist Tzu Chi Medical Foundation [TCRD-TPE-109-24(3/3) and TCRD-TPE-111-11].

SUPPLEMENTARY MATERIAL

The Supplementary Material for this article can be found online at: https://www.frontiersin.org/articles/10.3389/fonc.2022.869390/full#supplementary-material

REFERENCES

1. Chang YS TS, Chen YC, Liu TY, Lee YT, Yen JC, Fang HY, et al. Mutation Profile of Non-Small Cell Lung Cancer Revealed by Next Generation Sequencing. *Respir Res* (2021) 22(1):3. doi: 10.1186/s12931-020-01608-5
2. Lui NS, Benson J, He H, Imielski BR, Kunder CA, Liou DZ, et al. Sub-Solid Lung Adenocarcinoma in Asian Versus Caucasian Patients: Different Biology But Similar Outcomes. *J Thorac Dis* (2020) 12(5):2161–71. doi: 10.21037/jtd.2020.04.37
3. You JHS, Cho WCS, Ming WK, Li YC, Kwan CK, Au KH, et al. Egfr Mutation-Guided Use of Afatinib, Erlotinib and Gefitinib for Advanced Non-Small-Cell Lung Cancer in Hong Kong - a Cost-Effectiveness Analysis. *PLoS One* (2021) 16(3):e0247860. doi: 10.1371/journal.pone.0247860
4. Solassol I, Pinguet F, Quantin X. Fda- and Ema-Approved Tyrosine Kinase Inhibitors in Advanced Egfr-Mutated Non-Small Cell Lung Cancer: Safety, Tolerability, Plasma Concentration Monitoring, and Management. *Biomolecules* (2019) 9(11)1–19. doi: 10.3390/biom9110668
5. Lin YT, Chen JS, Liao WY, Ho CC, Hsu CL, Yang CY, et al. Clinical Outcomes and Secondary Epidermal Growth Factor Receptor (Egfr) T790m Mutation Among First-Line Gefitinib, Erlotinib and Afatinib-Treated Non-Small Cell Lung Cancer Patients With Activating Egfr Mutations. *Int J Cancer* (2019) 144(11):2887–96. doi: 10.1002/ijc.32025

6. de Marinis F LK, Poltoratskiy A, Egorova I, Hochmair M, Passaro A, Migliorino MR, et al. Afatinib in Egfr Tki-Naïve Patients With Locally Advanced or Metastatic Egfr Mutation-Positive Non-Small Cell Lung Cancer: Interim Analysis of a Phase 3b Study. *Lung Cancer (Amsterdam Netherlands)* (2021) 152:127–34. doi: 10.1016/j.lungcan.2020.12.011
7. Khwaja RM, Chu QS. Present and Emerging Biomarkers in Immunotherapy for Metastatic Non-Small Cell Lung Cancer: A Review. *Curr Oncol (Toronto Ont)* (2022) 29(2):479–89. doi: 10.3390/curroncol29020043
8. Herath S, Sadeghi Rad H, Radfar P, Ladwa R, Warkiani M, O'Byrne K, et al. The Role of Circulating Biomarkers in Lung Cancer. *Front Oncol* (2021) 11:801269. doi: 10.3389/fonc.2021.801269
9. Xu CW, Lei L, Wang WX, Lin L, Zhu YC, Wang H, et al. Molecular Characteristics and Clinical Outcomes of Egfr Exon 19 C-Helix Deletion in Non-Small Cell Lung Cancer and Response to Egfr Tkis. *Trans Oncol* (2020) 13(9):100791. doi: 10.1016/j.tranon.2020.100791
10. Jiang H, Zhu M, Li Y, Li Q. Association Between Egfr Exon 19 or Exon 21 Mutations and Survival Rates After First-Line Egfr-Tki Treatment in Patients With Non-Small Cell Lung Cancer. *Mol Clin Oncol* (2019) 11(3):301–8. doi: 10.3892/mco.2019.1881
11. Wagener-Ryczek S, Heydt C, Süptitz J, Michels S, Falk M, Alidousty C, et al. Mutational Spectrum of Acquired Resistance to Reversible Versus Irreversible Egfr Tyrosine Kinase Inhibitors. *BMC Cancer* (2020) 20(1):408. doi: 10.1186/s12885-020-06920-3
12. El Kadi N, Wang L, Davis A, Korkaya H, Cooke A, Vadnala V, et al. The Egfr T790m Mutation Is Acquired Through Aicda-Mediated Deamination of 5-Methylcytosine Following Tki Treatment in Lung Cancer. *Cancer Res* (2018) 78(24):6728–35. doi: 10.1158/0008-5472.Can-17-3370
13. Mok TS, Wu YL, Ahn MJ, Garassino MC, Kim HR, Ramalingam SS, et al. Osimertinib or Platinum-Pemetrexed in Egfr T790m-Positive Lung Cancer. *New Engl J Med* (2017) 376(7):629–40. doi: 10.1056/NEJMoa1612674
14. Hayashi H, Nadal E, Gray JE, Ardizzoni A, Caria N, Puri T, et al. Overall Treatment Strategy for Patients With Metastatic Nsclc With Activating Egfr Mutations. *Clin Lung Cancer* (2022) 23(1):e69–82. doi: 10.1016/j.cllc.2021.10.009
15. Chiang CL, Huang HC, Shen CI, Luo YH, Chen YM, Chiu CH. Post-Progression Survival in Secondary Egfr T790m-Mutated Non-Small-Cell Lung Cancer Patients With and Without Osimertinib After Failure of a Previous Egfr Tki. *Targeted Oncol* (2020) 15(4):503–12. doi: 10.1007/s11523-020-00737-7
16. Hochmair MJ, Morabito A, Hao D, Yang CT, Soo RA, Yang JC, et al. Sequential Afatinib and Osimertinib in Patients With Egfr Mutation-Positive Non-Small-Cell Lung Cancer: Updated Analysis of the Observational Giotag Study. *Future Oncol (London England)* (2019) 15 (25):2905–14. doi: 10.2217/fon-2019-0346
17. Yoshida T, Kuroda H, Oya Y, Shimizu J, Horio Y, Sakao Y, et al. Clinical Outcomes of Platinum-Based Chemotherapy According to T790m Mutation Status in Egfr-Positive Non-Small Cell Lung Cancer Patients After Initial Egfr-Tki Failure. *Lung Cancer (Amsterdam Netherlands)* (2017) 109:89–91. doi: 10.1016/j.lungcan.2017.05.001
18. Hutton B, Salanti G, Caldwell DM, Chaimani A, Schmid CH, Cameron C, et al. The Prisma Extension Statement for Reporting of Systematic Reviews Incorporating Network Meta-Analyses of Health Care Interventions: Checklist and Explanations. *Ann Intern Med* (2015) 162(11):777–84. doi: 10.7326/m14-2385
19. Team R. *Rstudio: Integrated Development for R*. Boston, MA: RStudio, PBC (2020).
20. König J, Krahn U, Binder H. Visualizing the Flow of Evidence in Network Meta-Analysis and Characterizing Mixed Treatment Comparisons. *Stat Med* (2013) 32(30):5414–29. doi: 10.1002/sim.6001
21. Sterne JA, Hernán MA, Reeves BC, Savović J, Berkman ND, Viswanathan M, et al. Robins-I: A Tool for Assessing Risk of Bias in Non-Randomised Studies of Interventions. *BMJ* (2016) 355:i4919. doi: 10.1136/bmj.i4919
22. Sequist LV, Waltman BA, Dias-Santagata D, Digumarthy S, Turke AB, Fidias P, et al. Genotypic and Histological Evolution of Lung Cancers Acquiring Resistance to Egfr Inhibitors. *Sci Trans Med* (2011) 3(75):75ra26. doi: 10.1126/scitranslmed.3002003
23. Yano S, Yamada T, Takeuchi S, Tachibana K, Minami Y, Yatabe Y, et al. Hepatocyte Growth Factor Expression in Egfr Mutant Lung Cancer With Intrinsic and Acquired Resistance to Tyrosine Kinase Inhibitors in a Japanese Cohort. *J Thorac Oncol* (2011) 6(12):2011–7. doi: 10.1097/JTO.0b013e31823ab0dd
24. Hata A, Katakami N, Yoshioka H, Takeshita J, Tanaka K, Nanjo S, et al. Rebiopsy of Non-Small Cell Lung Cancer Patients With Acquired Resistance to Epidermal Growth Factor Receptor-Tyrosine Kinase Inhibitor: Comparison Between T790m Mutation-Positive and Mutation-Negative Populations. *Cancer* (2013) 119(24):4325–32. doi: 10.1002/cncr.28364
25. Sun JM, Ahn MJ, Choi YL, Ahn JS, Park K. Clinical Implications of T790m Mutation in Patients With Acquired Resistance to Egfr Tyrosine Kinase Inhibitors. *Lung Cancer (Amsterdam Netherlands)* (2013) 82(2):294–8. doi: 10.1016/j.lungcan.2013.08.023
26. Li W, Ren S, Li J, Li A, Fan L, Li X, et al. T790m Mutation Is Associated With Better Efficacy of Treatment Beyond Progression With Egfr-Tki in Advanced Nsclc Patients. *Lung Cancer* (2014) 84(3):295–300. doi: 10.1016/j.lungcan.2014.03.011
27. Jin Y, Shao Y, Shi X, Lou G, Zhang Y, Wu X, et al. Mutational Profiling of Non-Small-Cell Lung Cancer Patients Resistant to First-Generation Egfr Tyrosine Kinase Inhibitors Using Next Generation Sequencing. *Oncotarget* (2016) 7(38):61755–63. doi: 10.18632/oncotarget.11237
28. Ko R, Kenmotsu H, Serizawa M, Koh Y, Wakuda K, Ono A, et al. Frequency of Egfr T790m Mutation and Multimutational Profiles of Rebiopsy Samples From Non-Small Cell Lung Cancer Developing Acquired Resistance to Egfr Tyrosine Kinase Inhibitors in Japanese Patients. *BMC Cancer* (2016) 16 (1):864. doi: 10.1186/s12885-016-2902-0
29. Matsuo N, Azuma K, Sakai K, Hattori S, Kawahara A, Ishii H, et al. Association of Egfr Exon 19 Deletion and Egfr-Tki Treatment Duration With Frequency of T790m Mutation in Egfr-Mutant Lung Cancer Patients. *Sci Rep* (2016) 6:36458. doi: 10.1038/srep36458
30. Nosaki K, Satouchi M, Kurata T, Yoshida T, Okamoto I, Katakami N, et al. Re-Biopsy Status Among Non-Small Cell Lung Cancer Patients in Japan: A Retrospective Study. *Lung Cancer (Amsterdam Netherlands)* (2016) 101:1–8. doi: 10.1016/j.lungcan.2016.07.007
31. Takahama T, Sakai K, Takeda M, Azuma K, Hida T, Hirabayashi M, et al. Detection of the T790m Mutation of Egfr in Plasma of Advanced Non-Small Cell Lung Cancer Patients With Acquired Resistance to Tyrosine Kinase Inhibitors (West Japan Oncology Group 8014ltr Study). *Oncotarget* (2016) 7 (36):58492–9. doi: 10.18632/oncotarget.11303
32. Tseng JS, Su KY, Yang TY, Chen KC, Hsu KH, Chen HY, et al. The Emergence of T790m Mutation in Egfr-Mutant Lung Adenocarcinoma Patients Having a History of Acquired Resistance to Egfr-Tki: Focus on Rebiopsy Timing and Long-Term Existence of T790m. *Oncotarget* (2016) 7(30):48059–69. doi: 10.18632/oncotarget.10351
33. Lee CK, Kim S, Lee JS, Lee JE, Kim SM, Yang IS, et al. Next-Generation Sequencing Reveals Novel Resistance Mechanisms and Molecular Heterogeneity in Egfr-Mutant Non-Small Cell Lung Cancer With Acquired Resistance to Egfr-Tkis. *Lung Cancer* (2017) 113:106–14. doi: 10.1016/j.lungcan.2017.09.005
34. Oya Y, Yoshida T, Kuroda H, Shimizu J, Horio Y, Sakao Y, et al. Association Between Egfr T790m Status and Progression Patterns During Initial Egfr-Tki Treatment in Patients Harboring Egfr Mutation. *Clin Lung Cancer* (2017) 18 (6):698–705.e2. doi: 10.1016/j.cllc.2017.05.004
35. Wang W, Song Z, Zhang Y. A Comparison of Ddpcr and Arms for Detecting Egfr T790m Status in Ctdna From Advanced Nsclc Patients With Acquired Egfr-Tki Resistance. *Cancer Med* (2017) 6(1):154–62. doi: 10.1002/cam4.978
36. Zhang Q, Ke E, Niu F, Deng W, Chen Z, Xu C, et al. The Role of T790m Mutation in Egfr-Tki Re-Challenge for Patients With Egfr-Mutant Advanced Lung Adenocarcinoma. *Oncotarget* (2017) 8(3):4994–5002. doi: 10.18632/oncotarget.14007
37. Kaburagi T, Kiyoshima M, Nawa T, Ichimura H, Saito T, Hayashihara K, et al. Acquired Egfr T790m Mutation After Relapse Following Egfr-Tki Therapy: A Population-Based Multi-Institutional Study. *Anticancer Res* (2018) 38 (5):3145–50. doi: 10.21873/anticanres.12577
38. Lee K, Kim Y, Jung HA, Lee SH, Ahn JS, Ahn MJ, et al. Repeat Biopsy Procedures and T790m Rates After Afatinib, Gefitinib, or Erlotinib Therapy in Patients With Lung Cancer. *Lung Cancer (Amsterdam Netherlands)* (2019) 130:87–92. doi: 10.1016/j.lungcan.2019.01.012
39. Yoon BW, Kim JH, Lee SH, Choi CM, Rho JK, Yoon S, et al. Comparison of T790m Acquisition Between Patients Treated With Afatinib and Fefitinib as

First-Line Therapy: Retrospective Propensity Score Matching Analysis. *Trans Oncol* (2019) 12(6):852–8. doi: 10.1016/j.tranon.2019.04.004
40. Del Re M, Petrini I, Mazzoni F, Valleggi S, Gianfilippo G, Pozzessere D, et al. Incidence of T790m in Patients With Nsclc Progressed to Gefitinib, Erlotinib, and Afatinib: A Study on Circulating Cell-Free DNA. *Clin Lung Cancer* (2020) 21(3):232–7. doi: 10.1016/j.cllc.2019.10.003
41. Dal Maso A, Lorenzi M, Roca E, Pilotto S, Macerelli M, Polo V, et al. Clinical Features and Progression Pattern of Acquired T790m-Positive Compared With T790m-Negative Egfr Mutant Non–Small-Cell Lung Cancer: Catching Tumor and Clinical Heterogeneity Over Time Through Liquid Biopsy. *Clin Lung Cancer* (2020) 21(1):1–14.e3. doi: 10.1016/j.cllc.2019.07.009
42. Oya Y, Yoshida T, Asada K, Oguri T, Inui N, Morikawa S, et al. Clinical Utility of Liquid Biopsy for Egfr Driver, T790m Mutation and Egfr Amplification in Plasma in Patients With Acquired Resistance to Afatinib. *BMC Cancer* (2021) 21(1)1–9. doi: 10.1186/s12885-020-07777-2
43. Onitsuka T, Uramoto H, Nose N, Takenoyama M, Hanagiri T, Sugio K, et al. Acquired Resistance to Gefitinib: The Contribution of Mechanisms Other Than the T790m, Met, and Hgf Status. *Lung Cancer (Amsterdam Netherlands)* (2010) 68(2):198–203. doi: 10.1016/j.lungcan.2009.05.022
44. Uramoto H, Yamada T, Yano S, Kondo N, Hasegawa S, Tanaka F. Prognostic Value of Acquired Resistance-Related Molecules in Japanese Patients With Nsclc Treated With an Egfr-Tki. *Anticancer Res* (2012) 32(9):3785–90.
45. Ji W, Choi CM, Rho JK, Jang SJ, Park YS, Chun SM, et al. Mechanisms of Acquired Resistance to Egfr-Tyrosine Kinase Inhibitor in Korean Patients With Lung Cancer. *BMC Cancer* (2013) 13:606. doi: 10.1186/1471-2407-13-606
46. Campo M, Gerber D, Gainor JF, Heist RS, Temel JS, Shaw AT, et al. Acquired Resistance to First-Line Afatinib and the Challenges of Prearranged Progression Biopsies. *J Thorac Oncol* (2016) 11(11):2022–6. doi: 10.1016/j.jtho.2016.06.032
47. Liang SK, Hsieh MS, Lee MR, Keng LT, Ko JC, Shih JY. Real-World Experience of Afatinib as a First-Line Therapy for Advanced Egfr Mutation-Positive Lung Adenocarcinoma. *Oncotarget* (2017) 8(52):90430–43. doi: 10.18632/oncotarget.19563
48. Tanaka K, Nosaki K, Otsubo K, Azuma K, Sakata S, Ouchi H, et al. Acquisition of the T790m Resistance Mutation During Afatinib Treatment in Egfr Tyrosine Kinase Inhibitor-Naïve Patients With Non-Small Cell Lung Cancer Harboring Egfr Mutations. *Oncotarget* (2017) 8(40):68123–30. doi: 10.18632/oncotarget.19243
49. Passiglia F, Rizzo S, Di Maio M, Galvano A, Badalamenti G, Listì A, et al. The Diagnostic Accuracy of Circulating Tumor DNA for the Detection of Egfr-T790m Mutation in Nsclc: A Systematic Review and Meta-Analysis. *Sci Rep* (2018) 8(1):13379. doi: 10.1038/s41598-018-30780-4
50. Li X, Zhou C. Comparison of Cross-Platform Technologies for Egfr T790m Testing in Patients With Non-Small Cell Lung Cancer. *Oncotarget* (2017) 8 (59):100801–18. doi: 10.18632/oncotarget.19007
51. Li D, Ambrogio L, Shimamura T, Kubo S, Takahashi M, Chirieac LR, et al. Bibw2992, an Irreversible Egfr/Her2 Inhibitor Highly Effective in Preclinical Lung Cancer Models. *Oncogene* (2008) 27(34):4702–11. doi: 10.1038/onc.2008.109
52. Miller VA, Hirsh V, Cadranel J, Chen YM, Park K, Kim SW, et al. Afatinib Versus Placebo for Patients With Advanced, Metastatic Non-Small-Cell Lung Cancer After Failure of Erlotinib, Gefitinib, or Both, and One or Two Lines of Chemotherapy (Lux-Lung 1): A Phase 2b/3 Randomised Trial. *Lancet Oncol* (2012) 13(5):528–38. doi: 10.1016/s1470-2045(12)70087-6
53. Chmielecki J, Foo J, Oxnard GR, Hutchinson K, Ohashi K, Somwar R, et al. Optimization of Dosing for Egfr-Mutant Non-Small Cell Lung Cancer With Evolutionary Cancer Modeling. *Sci Trans Med* (2011) 3(90):90ra59. doi: 10.1126/scitranslmed.3002356
54. Joo JW, Hong MH, Shim HS. Clinical Characteristics of T790m-Positive Lung Adenocarcinoma After Resistance to Epidermal Growth Factor Receptor-Tyrosine Kinase Inhibitors With an Emphasis on Brain Metastasis and Survival. *Lung Cancer (Amsterdam Netherlands)* (2018) 121:12–7. doi: 10.1016/j.lungcan.2018.04.013
55. Maemondo M, Inoue A, Kobayashi K, Sugawara S, Oizumi S, Isobe H, et al. Gefitinib or Chemotherapy for Non-Small-Cell Lung Cancer With Mutated Egfr. *New Engl J Med* (2010) 362(25):2380–8. doi: 10.1056/NEJMoa0909530
56. Park K, Tan EH, O'Byrne K, Zhang L, Boyer M, Mok T, et al. Afatinib Versus Gefitinib as First-Line Treatment of Patients With Egfr Mutation-Positive Non-Small-Cell Lung Cancer (Lux-Lung 7): A Phase 2b, Open-Label, Randomised Controlled Trial. *Lancet Oncol* (2016) 17(5):577–89. doi: 10.1016/s1470-2045(16)30033-x
57. Paz-Ares L, Tan EH, O'Byrne K, Zhang L, Hirsh V, Boyer M, et al. Afatinib Versus Gefitinib in Patients With Egfr Mutation-Positive Advanced Non-Small-Cell Lung Cancer: Overall Survival Data From the Phase Iib Lux-Lung 7 Trial. *Ann Oncol* (2017) 28(2):270–7. doi: 10.1093/annonc/mdw611
58. Ouyang W, Yu J, Huang Z, Chen G, Liu Y, Liao Z, et al. Risk Factors of Acquired T790m Mutation in Patients With Epidermal Growth Factor Receptor-Mutated Advanced Non-Small Cell Lung Cancer. *J Cancer* (2020) 11(8):2060–7. doi: 10.7150/jca.37991

Conflict of Interest: The authors declare that the research was conducted in the absence of any commercial or financial relationships that could be construed as potential conflicts of interest.

Publisher's Note: All claims expressed in this article are solely those of the authors and do not necessarily represent those of their affiliated organizations, or those of the publisher, the editors and the reviewers. Any product that may be evaluated in this article, or claim that may be made by its manufacturer, is not guaranteed or endorsed by the publisher.

frontiers | Frontiers in Oncology

CLINICAL TRIAL
published: 30 June 2022
doi: 10.3389/fonc.2022.891938

Whole-Exome Sequencing Uncovers Specific Genetic Variation Difference Based on Different Modes of Drug Resistance in Small Cell Lung Cancer

Ning Tang[1], Zhenzhen Li[2], Xiao Han[1], Chenglong Zhao[3], Jun Guo[1] and Haiyong Wang[1]**

[1] Department of Internal Medicine-Oncology, Shandong Cancer Hospital and Institute, Shandong First Medical University and Shandong Academy of Medical Sciences, Jinan, China, [2] Berry Oncology Corporation, Beijing, China, [3] Department of Pathology, The First Affiliated Hospital of Shandong First Medical University and Shandong Provincial Qianfoshan Hospital, Jinan, China

OPEN ACCESS

Edited by:
Michele Simbolo,
University of Verona, Italy

Reviewed by:
Emanuele Vita,
Agostino Gemelli University Polyclinic (IRCCS), Italy
Francesco Pepe,
University of Naples Federico II, Italy

***Correspondence:**
Jun Guo
jngj2005@126.com
Haiyong Wang
wanghaiyong6688@126.com

Specialty section:
This article was submitted to Thoracic Oncology, a section of the journal Frontiers in Oncology

Received: 08 March 2022
Accepted: 17 May 2022
Published: 30 June 2022

Citation:
Tang N, Li Z, Han X, Zhao C, Guo J and Wang H (2022) Whole-Exome Sequencing Uncovers Specific Genetic Variation Difference Based on Different Modes of Drug Resistance in Small Cell Lung Cancer. Front. Oncol. 12:891938. doi: 10.3389/fonc.2022.891938

The poor survival rate of small cell lung cancer (SCLC) is mainly related to the condition that patients with SCLC often have good responses to first-line chemotherapy initially, but later on, most of these patients relapse rapidly due to resistance to further treatment. In this study, we attempted to analyze whole-exome sequencing data based on the largest sample size to date, to develop a classifier to predict whether a patient will be chemorefractory or chemosensitive and to explicate the risk of recurrence that affects the prognosis of patients. We showed the different characteristics of somatic mutational signatures, somatic mutation genes, and distinct genome instability between chemorefractory and chemosensitive SCLC patients. Amplified mutations in the chemosensitive group inhibited the regulation of the cell cycle process, transcription factor binding, and B-cell differentiation. Analysis of deletion mutation also suggested that detection of the chromosomal-level variation might influence our treatment decisions. Higher PD-L1 expressions (based on TPS methods) were mostly present among chemosensitive patients (p = 0.026), while there were no differences in PD-L1 expressions (based on CPS methods) and $CD8^+$ TILs between the two groups. According to the model determined by logistic regression, each sample was endowed with a predictive probability value (PV). The samples were divided into a high-risk group (>0.55) and a low-risk group (≤0.55), and the survival analysis showed obvious differences between the two groups. This study provides a reference basis to translate this knowledge into practice, such as formulating personalized treatment plans, which may benefit Chinese patients with SCLC.

Keywords: small cell lung cancer, whole-exome sequencing, somatic mutational signature, recurrence, therapeutic strategy

INTRODUCTION

Lung cancer remains one of the most frequently diagnosed cancers and the most common cause of cancer-related mortality worldwide, with small cell lung cancer (SCLC) accounting for ~15% of all lung cancer cases (1, 2). SCLC is characterized by rapid growth, a tendency to metastasize, and poor survival rates with a median survival rate of 7 months. Patients with SCLC often have good responses to first-line chemotherapy initially; however, most of these patients relapse rapidly due to resistance to further treatment. Therefore, SCLC has been classified as a chemorefractory disease if patients develop resistance to platinum-based chemotherapy within 3 months. In a situation where the disease has been controlled for 3 months or longer, it is defined as chemosensitive (3). Thus, there is an urgent need to predict whether a patient is chemorefractory or chemosensitive and to explicate the risk of recurrence that may affect the prognosis of patients.

Recently, researchers have attempted to use single-cell sequencing of circulating tumor cells (CTCs) to develop classifiers by bioinformatics analysis of the genome-wide copy number alteration (CNA) data. Carter and colleagues (4) reported that they identified 2,281 loci from blood samples drawn from 13 patients with SCLC that indicated substantial discrepancy to generate 16 CNA profiles that stratified CTC samples into chemosensitive and chemorefractory patients. Su et al. (5) established a 10-CNA score classifier based on single CTCs from 48 patients for the prediction of prognosis, which demonstrated that a high CNA score could herald poor PFS. We have observed different results among these studies, which warrants a larger cohort. In addition, the stability of liquid biopsies could be influenced by tumor location, size, vascularity, and the detection method used (6, 7); thus, the results based on tumor tissues are expected to be seen. Moreover, immune checkpoint inhibitors (ICIs) have become the paradigm for the treatment of cancer (3, 8–11). The first-line management of extensive-stage SCLC has been platinum with etoposide; however, the addition of atezolizumab or durvalumab to chemotherapy resulted in superior overall survival compared with platinum and etoposide treatment. The influence of the tumor immune microenvironment on resistance in patients with SCLC is generally less studied.

In this study, we attempted to analyze the whole-exome sequencing (WES) data based on the tissues of 177 SCLC patients, known to be the largest sample size currently, to develop a classifier covering the clinical features, tumor immune microenvironment, gene mutation, and chromosome structure variation, in the hope of improving the precise and appropriate treatment for patients with SCLC. We hope that these endeavors would lead to the precise treatment of SCLC patients.

MATERIAL AND METHODS

Sample Collection, Processing, and Genomic DNA Extraction

We recruited histologically confirmed SCLC patients from the Shandong Cancer Hospital and Institute (SCH). All diagnoses were independently confirmed by two experienced pathologists. In addition to blood samples (2 ml), tumor tissue samples were obtained by biopsies. A strict quality inspection was carried out to remove contaminated and insufficient DNA samples. Finally, 177 patients were enrolled in our study. The overall survival (OS) time was defined as the interval between diagnosis and death, or between diagnosis and the last observation point. For surviving patients, data were censored at the last follow-up (November 26, 2020). Clinicopathological data were retrieved from the patients' medical records. This study was approved by the Ethics Committee of the Shandong Cancer Hospital and Institute. All patients included in this study provided written informed consent.

Biopsied tumor tissues were fixed in formalin and then embedded in paraffin (FFPE). The corresponding blood samples were set as controls. Genomic DNA was extracted from each FFPE sample using the GeneRead DNA FFPE Kit (Qiagen, USA) and from the blood sample using the DNA Blood Midi/Mini Kit (Qiagen, USA).

DNA Library Construction and Whole-Exome Sequencing

Genomic DNA was enzymatically digested into 200 bp fragments (5× WGS Fragmentation Mix, Qiagen, USA). T-adapters were added to both ends after repairing and A tailing. For the WES library construction, purified DNA was amplified by ligation-mediated PCR. Then, final sequencing libraries were generated using the 96 rxn xGen Exome Research Panel v1.0 (Integrated DNA Technologies, USA), according to the manufacturer's instructions. Paired-end multiplex samples were sequenced with the Illumina NovaSeq 6000 System (Illumina, USA). The sequencing depth was 200× per tissue sample and 100× per white blood cell (WBC) sample.

Sequence Data Processing and Alignment of the SCH Cohort

Raw sequencing data were preprocessed by Fastp to trim adaptor sequences (12). Then, clean reads in FastQ format were aligned to the reference human genome (hg19/GRCh37) by Burrows-Wheeler Aligner (BWA, v0.7.15) (13). SAM tools (14) and Picard (2.12.1) (http://picard.sourceforge.net/) were used to sort mapped BAM files and process PCR duplicates. To compute the sequencing coverage and depth, the final BAM files were generated by GATK (Genome Analysis Toolkit 3.8) for local realignment and base quality recalibration (15).

Mutational Signature Analysis

Somatic mutational signatures were *de-novo* analyzed from the clean WES data by the "Somatic Signatures" R package (v2.20.0) (16), according to the non-negative matrix factorization (NMF) method. Four highly confident mutational signatures were derived from the SCH cohort. Then, they were compared with the consensus signatures in the COSMIC dataset (https://cancer.sanger.ac.uk/cosmic/), based on the cosine similarity analysis to nominate each derived signature with the highest COSMIC dataset similarity [i.e., SBS4 (S4), SBS2 (S2), SBS6 (S6), and SBS5 (S5), respectively] for the SCH cohort.

To further determine the distribution of mutational signatures and the frequencies of each patient, deconstructSigs (v1.9.0) was used as previously described (17). Patients harboring the S2, S4, S5, and S6 mutations, as well as S2, S4, S5, and S6 weights, were compared using the Wilcoxon test among the two groups.

Somatic Mutation Variant Detection and Driver Gene Prediction

Somatic single nucleotide variations (SNVs) were identified from the clean sequencing data by MuTect (18), and somatic small insertions and deletions (InDels) were detected by the GATK Somatic Indel Detector. The ANNOVAR software was used for the annotation of variants based on multiple databases (19), including variant (HGVS), population frequency (1000 Genomes Project, dbSNP, ExAC), variant functional prediction (PolyPhen-2 and SIFT), and phenotype or disease (OMIM, COSMIC, ClinVar) databases. After the annotation, the retained non-synonymous SNVs were screened from disease databases for further analysis with variant allele frequency (VAF) (cutoff ≥ 3%) or VAF for cancer hotspots (cutoff ≥ 1%). Tumor mutation burden (TMB) was calculated with the total numbers of non-synonymous SNVs and indel variants per megabase of coding regions. Dominant tumor neoantigens were predicted using OptiType to infer the individual HLA type (20). Tumor neoantigen burden (TNB) was calculated with the total numbers of neoantigens per megabase of coding regions. Significant driver genes were identified by combining MutsigCV and dNdScv, as previously described (21, 22), with a false discovery rate (FDR) cutoff <5%. Genes with significantly different mutation frequencies among the two groups were determined based on the gene mutation rates in each group using a two-sided Fisher's exact test with a *p*-value of 0.05.

Copy Number Variation Identification

Copy number variations (CNVs) for all patients in the SCH cohort were first identified using the Genome Identification of Significant Targets in Cancer (GISTIC) 2.0 algorithm (23). At the chromosomal arm level, significant amplifications or deletions were screened with FDR (cutoff < 10%) for further analyses. At a focal CNV level, significant amplification was screened with FDR (cutoff < 5%) and G-score (cutoff > 0.3). Significant deletion was screened with FDR (cutoff < 5%) and G-score (cutoff < −0.2) for further analyses.

Focal CNV-related gene analysis was performed for each patient based on paired tumor-normal WES data using the GATK depth of coverage with parameters (–minBaseQuality 0 –minMappingQuality 20 –start 1 –stop 500 –nBins 200 –includeRefNSites –countType COUNT_FRAGMENTS). The amplified genes were defined by a copy number ratio of tumor vs. normal >4, while deleted genes were defined by a copy number ratio of tumor vs. normal <0.5. Then, focal CNV-related genes were filtered according to the COSMIC Cancer Gene Census database (https://cancer.sanger.ac.uk/cosmic/) to obtain a cancer-related focal CNV gene list. Genes with significantly different CNV frequencies among the two groups were determined based on the gene alteration rates in each group using a two-sided Fisher's exact test with a *p*-value of 0.05.

Pathway and Functional Enrichment Analysis

Somatic mutation and focal CNV-related genes with enriched biological functions and involved pathways were analyzed using the online tool Metascape (https://metascape.org/gp/index.html#/main/step1), based on the Gene Ontology (GO) and Kyoto Encyclopedia of Genes and Genomes (KEGG) databases (https://www.kegg.jp/kegg/kegg1.html).

Tumor Heterogeneity and Genome Instability Analysis

To investigate intratumor heterogeneity (ITH), mutant allele tumor heterogeneity (MATH) values for each tumor sample were calculated from the median absolute deviation (MAD) and the median of its mutant–allele fractions at tumor-specific mutated loci: MATH = 100 × MAD/median. These analyses were performed in R with default parameters as previously reported (24). Cancer cell fraction (CCF) and clonal and subclonal mutations in each tumor specimen were calculated based on the proportion of mutated reads (VAF) as previously reported (25).

Regarding genome instability analyses, cellular purity, ploidy, and the segmented allele-specific copy number profiles of each specimen's tumor cells were estimated using Sequenza (26). The fraction of genome altered (FGA) was defined as the percentage of a tumor genome harboring copy number variations against the whole genome. Loss-of-heterozygosity (LOH) segments or mutations were defined by the minor allele copy number or mutation ratio <0.25 (27). Whole-genome doubling (WGD) events were defined as the major allele ploidy >1.5 on at least 70% of at least 11 autosomes as the duplicated autosome number per sample (28). The Wilcoxon rank-sum test was used to compare the median values of the variables between the two groups. A *p*-value of 0.05 was considered significant.

Immunohistochemical Staining

Immunohistochemical staining was conducted using the Enhance Labelled Polymer System (ELPS). First, the tumor specimen sections were incubated with anti-PD-L1 (CST, 13684, 1:100) and anti-$CD8^+$ (CST, 85336, 1:100) at 4°C overnight. Then, they were washed three times with PBS (5 min per wash). Next, the slides were incubated with the corresponding secondary antibodies at 37°C for 30 min, and they were washed three times with PBS (5 min per wash). Furthermore, the slides reacted with 3,3-diaminobenzidine (DAB) and then washed with distilled water. Next, dehydration was conducted, followed by clearing and mounting with neutral gums. Finally, the stained tissue images were captured by the Digital Pathology Slide Scanner (KF-PRO-120, KF-BIO).

Programmed Cell Death Ligand 1 Expression

To evaluate programmed cell death ligand 1 (PD-L1) expression, a tumor proportion score (TPS) was defined as the number of PD-L1-staining tumor cells divided by the total number of viable tumor cells multiplied by 100. A combined positive score (CPS) was defined as the number of PD-L1-staining cells divided by the

total number of viable tumor cells multiplied by 100 (29). Tonsil PD-L1 staining was adopted to ensure the eligibility of the enrolled specimens. Qualified staining was defined as strong positivity for PD-L1 in the intratonsillar cleft epithelium, whereas negative staining was for PD-L1 in lymphocytes (mantle zone and germinal center B cells) and superficial epithelial cells.

$CD8^+$ T-Cell Infiltration

We also evaluated whether $CD8^+$ T cells were uniformly distributed in the tumor stroma at lower magnification. If $CD8^+$ T cells were equally distributed, they were measured in three randomly chosen areas (0.1 mm^2) at a 200-fold magnification. If unequally distributed, the corresponding areas were selected at a 200-fold magnification according to $CD8^+$ T-cell percentages in areas of different densities (0.1 mm^2), as referred from the PD-L1 expression evaluation criteria. The calculation was defined as follows: $CD8^+$ T-cell count/0.1 mm^2 × 10 or $CD8^+$ T-cell count/mm^2.

Sequencing Data Availability

Raw sequencing data were deposited in the Genome Sequencing Archive (GSA) of the China National Center for Bioinformation (CNCB) (https://ngdc.cncb.ac.cn/gsa/) under accession number subHRA001430.

Statistical Analyses

The R Foundation for Statistics Computing Package (R package, version 3.3.3) was used to perform the statistical analyses. The Fisher's exact test (for categorical variables) and the Wilcoxon rank-sum test (for continuous variables) were used to analyze the relationship between the two groups. The Kaplan–Meier method was used to estimate the effects on OS and PFS time based on the log-rank tests. A p-value <0.05 was defined as statistically significant. Hazard ratios of multiple factors on OS and PFS time were obtained from the Cox proportional hazards model.

RESULTS

Different Characteristics of Somatic Mutational Signatures Between Chemorefractory and Chemosensitive SCLC Patients

A further expedition of SCLC genomic landscape features was presented through the WES of the large SCH SCLC cohort. First, the mutation spectrum analysis showed that the two most frequent nucleic acid base substitutions of somatic mutations were transversions (C>A/G>T) followed by transitions (C>T/G>A) (**Supplementary Figure 2**), consistent with previous SCLC studies. Then, mutational signatures were *de-novo* calculated and characterized from all 177 specimens based on the 96 possible mutation types, according to a previously published method.

Two signatures showed differences between the two groups, compared to the COSMIC mutational signature database: smoking-related S4 and unknown S5 (**Figure 1**). Generally, SCLC is associated with heavy tobacco smoking. Chemosensitive patients tended to harbor smoking-related S4 mutations more than chemorefractory patients. However, smoking history did not significantly differ between the two groups. The situation had previously been reported that C>A/G>T transversions, typically prevalent in S4, have no significant correlation with the SCLC smoking status (30, 31). In turn, S5 mutations were more frequently found in the chemorefractory group. This indicated that therapeutic vulnerabilities for different SCLC subtypes may be related to molecular change during SCLC tumor development.

Driver and Recurrent Somatic Mutation Genes Between the Two Groups

SCLC is considered to be a disease of genomic alterations and relatively higher mutation rate per megabase (Mb) (1, 2). We used MutSigCV and dNdScv (FDR q < 0.1) to identify the differential somatic mutation genes between the two groups, and the genes with a mutation frequency greater than 5% were indicated in the graph (**Figure 2A**). Our results showed that *KMT2D* (30%), LRP2 (30%), *OR1N2* (17.5%), *KIAA1109* (15.83%), *LAMA4* (15%), *ZNF469* (14.17%), *GPR158* (11.67%), *NRK* (10.83%), *APBA2* (10.83%), *RNF213* (10.83%), *ABCC1* (9.17%), *GLI2* (9.17%), *RP1* (9.17%), *ADAMTS13* (8.33%), and *IQSEC2* (8.33%) were more frequently predicted in the chemosensitive group, while *FNDC1* (22.81%), *FAT2* (21.05%), *SPATA31E1* (17.54%), *AOC1* (17.54%), *SYNE2* (17.54%), *THSD7A* (17.54%), *TRIM58* (17.54%), *OGDHL* (15.79%), *NTRK3* (14.04%), *OR4C6* (14.04%), *PTPN13* (14.04%), *COL9A1* (12.28%), *MYO18A* (12.28%), and *KDM3B* (10.53%) more commonly appeared in the chemorefractory group. This suggested the relativity between the high-frequency mutations of somatic mutation genes and disease recurrence.

Further functional analysis showed that the differential genes more frequently predicted in the chemorefractory group were most significantly enriched in tight junction, lysosome, Hippo signaling pathway, and olfactory transduction. Moreover, the differential genes more frequently predicted in the chemosensitive group were most significantly enriched in neuron projection morphogenesis and localization within the membrane (**Figure 2B**). The results suggested the potential mechanisms of chemoresistance on somatic mutation levels, which warrants further study.

In addition, among the differential genes found between the chemorefractory group and the chemosensitive group, we applied survival correlation analysis and identified eight somatic mutation genes mentioned earlier that significantly reduced PFS time, compared to wild-type genotypes (**Figure 2C; Supplementary Figures 3**, **4**). Meanwhile, three somatic mutation genes that were more frequently predicted in the chemosensitive group significantly increased PFS time. This further strengthens the (**Figure 2D**) fact that they have pivotal roles in SCLC relapse and chemotherapy resistance. There was no significant difference, however, in OS time apart from *LRP2* (**Supplementary Figure 5**).

The VAF analysis reflected that VAF in the Re group was higher than that in the Se group in all gene mutations (p = 6.2e −11) and clonal gene mutations (p = 0.022), but there was no

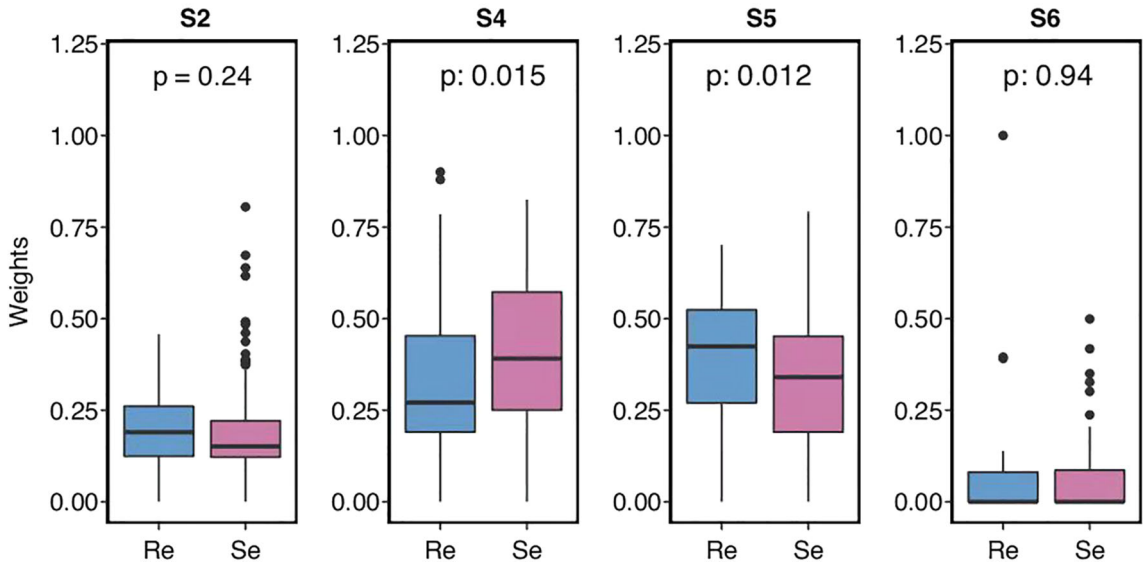

FIGURE 1 | Small cell lung cancer (SCLC) patients' mutational signature and the weights of different somatic mutational signatures in each group.

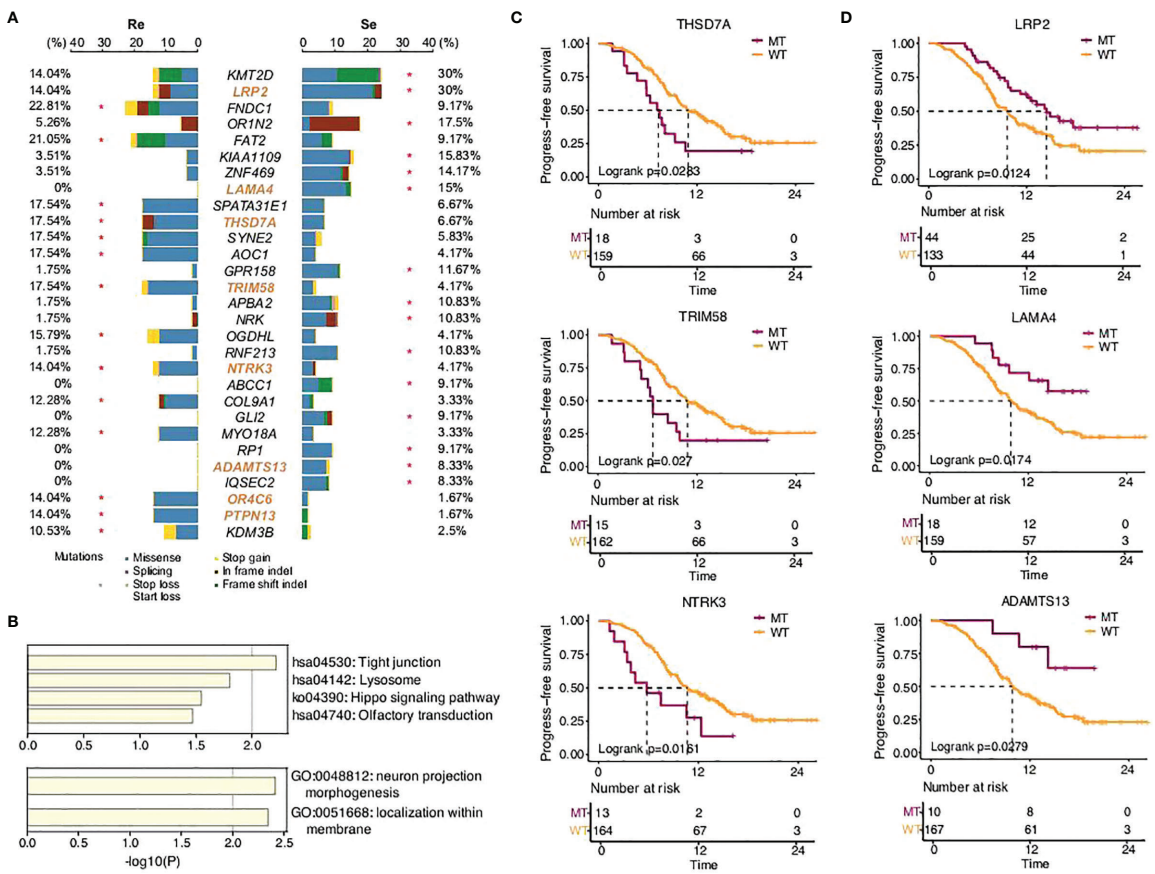

FIGURE 2 | SCLC patients' somatic mutational features in the two groups. **(A)** Comparison of somatic mutational features with a mutation frequency greater than 5%. **(B)** GO functions enriched by all the genes predicted in this study. KEGG pathways enriched by the somatic mutation genes that significantly affected PFS time in this study. **(C,D)** Progression-free survival of different gene status.

difference concerning driver mutations (p = 0.41) or LOH (p = 0.27). No difference was observed between the two groups with respect to TMB (p = 0.12) and MATH score (p = 0.28) (**Supplementary Figure 6**).

Distinct Genome Instability Between the Two Groups

CNVs, novel structural variations in human chromosomes, are extremely common in SCLC, and our results had come to similar conclusions (**Figure 3**). We identified a high frequency of significant mutations in the two groups: *C8orf82CEP72* (42.11%), *EXOC3* (28.07%), *PLEKHG4B* (24.56%), *CEP72* (22.81%), *ING1* (21.05%), *SYNGR3* (19.3%), *HAGH* (19.3%), *MAP7D1* (17.54%), *VPS28* (17.54%), *STX10* (17.54%), *HSD11B1L* (17.54%), *FAM195A* (15.79%), *BTNL3* (15.79%), *RPL8* (15.79%), *ZNF414* (15.79%), *TNFRSF12A* (15.79%), *LRRC24* (15.79%), *KIFC2* (15.79%), *FBXL16* (15.79%), and *GLI4* (14.04%) in the chemorefractory group and *CTRB2* (22.5%), *LOC101928018* (18.33%), *PQLC1* (13.33%), *CLEC18C* (11.67%), *CTIF* (10.83%), and *SIVA1* (10.83%) in the chemosensitive group. The above somatic CNV analyses showed that the chemorefractory group seemingly experienced more mutations of the CNV site compared with the chemosensitive group (**Figure 3A**). We have noted that these changes involved certain oncogenic signaling pathways (**Figure 3B**) whose alterations significantly impacted patients' PFS time (**Figure 3C; Supplementary Figures 7-11**). Similar to previous results, these changes had very little impact on OS time (**Supplementary Figures 7-12**).

Amplified or Deletion Mutations Between the Two Groups

The subsequent analysis revealed differences between the two groups. The segmented copy numbers were visualized in a heatmap and the significance of chromosome alterations was determined by GISTIC analysis (**Figures 4A, B**). The differing clones of mutations were prevalent in the two types of specimens with a few similar parts. We found more amplified mutations in the chemorefractory group, which are related to certain functions, such as transcription factor binding, regulation of hemopoiesis, leukocyte differentiation, peptidyl-tyrosine phosphorylation, positive regulation of cell death, transcription regulator complex, regulation of cellular response to stress, chromatin binding, histone modification, regulation of kinase activity, damaged DNA binding, response to radiation, homeostasis of a number of cells, positive regulation of

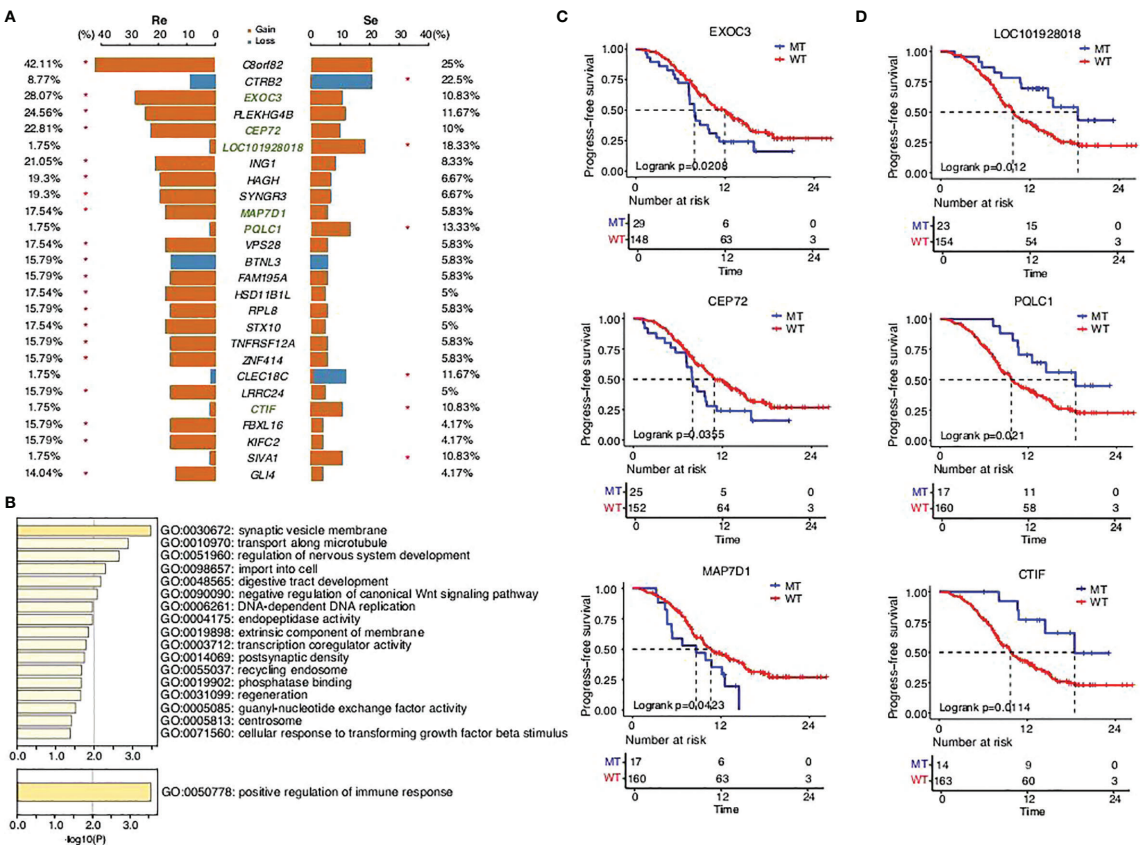

FIGURE 3 | SCLC patients' copy number variant in the two groups. **(A)** Comparison of the copy number variants with a mutation frequency greater than 5%. **(B)** GO functions enriched by all the mutations predicted in this study. KEGG pathways enriched by the mutations that significantly affected PFS time in this study. **(C,D)** Progression-free survival status of the different genes.

endothelial cell proliferation, ubiquitin protein ligase binding, rhythmic process, regulation of cellular response to growth factor stimulus, response to hypoxia, ankyrin binding, and negative regulation of catabolic process (**Figures 4C, D**). Amplified mutations in the chemosensitive group inhibited the regulation of the cell cycle process, transcription factor binding, and B-cell differentiation. Analysis of deletion mutation also suggested that the detection of the chromosomal-level variation might influence our treatment strategies (**Supplementary Figure 13**).

Immunotherapy Features Between the Two Groups

Immune checkpoint inhibitors (ICIs) have altered the treatment of SCLC (32–34). Multiple biomarkers, such as PD-L1 and $CD8^+$ tumor-infiltrating lymphocytes (TILs), have been identified to help tailor immunotherapy. According to our current study, higher PD-L1 expressions (based on TPS methods) were mostly present among chemosensitive patients (p = 0.026; **Figure 5**), while there were no differences between the two groups in terms of PD-L1 expressions (based on CPS methods) and $CD8^+$ TILs. Significantly, hyperprogressive disease (HPD), a pattern of progression in which a flare-up of tumor growth occurred during immunotherapy, was similar between the two groups. This suggests that chemosensitive patients might more likely benefit from immunotherapy.

It has been shown that some crucial genetic mutations could influence the efficiency of ICI treatments (35). However, our study suggests that there were no differences in genomic instability between the two groups. Analyses that take more factors into account are needed in our future studies (**Supplementary Figure 14**).

The Predictive Model of Drug Resistance of SCLC

There was a significant difference in the survival rates of different resistance levels in SCLC patients (**Figure 6A**). In

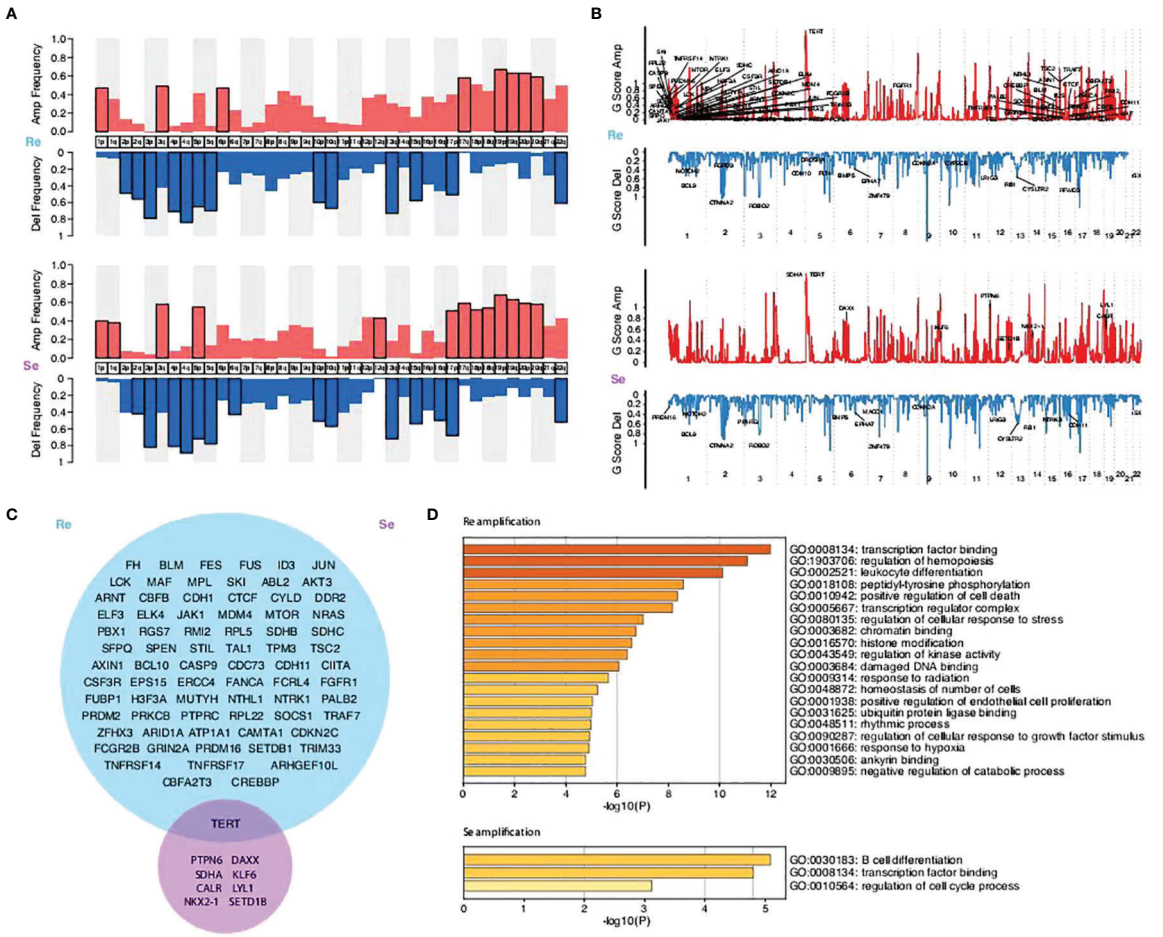

FIGURE 4 | Comparison of the copy number variations between the two groups and their enriched biological functions. **(A)** Amplification and deletion frequency of copy number variations (CNVs) on the chromosome arm level. **(B)** Scores of the significant amplification and deletion regions. **(C)** Venn graphs showing different amplification focal CNV genes between the two groups predicted by the GISTIC method (FDR q < 0.1). **(D)** KEGG pathways and GO functions enriched by focal CNV genes that significantly affected PFS time.

this study, we attempted to screen optimal subsets of features between the two groups and set up a predictive model of drug resistance of SCLC. The statistical analysis of data from three different angles offered us some clues (**Table 1**; **Supplementary Table 1**). The first part included the clinical characteristics, age, gender, stage, family history, smoking, drinking, metastasis, PD-L1 expressions, and $CD8^+$ TILs. The factors with *p*-value ≤0.2 were selected by univariate logistic regression analysis, and age, stage, family history, and $CD8^+$ TILs were chosen. Similarly, differences at the molecular level, such as *ABCC1*, *APBA2*, *GPR158*, *KMT2D*, *NTRK3*, *TRIM58*, *FNDC1*, *FAT2*, *OR1N2*, *LRP2*, and *KIAA1109*, were obtained. The same goes for features of chromosome variation that included *C8orf82*, *CTRB2*, *EXOC3*, *PQLC1*, and *BTNL3*.

There were 20 eigenvalues in total as discussed previously. Step function was used to determine multivariate logistic regression through a stepwise regression process with resistance as the target variable. Eventually, 16 eigenvalues were selected (**Figures 6B, C**).

According to the model determined by logistic regression, each sample was endowed with a predictive probability value (PV). Then, the samples were divided into a high-risk group (>0.55) and a low-risk group (≤0.55), and the survival analysis showed obvious differences between the groups. This suggests that the predictive model, to a certain extent, could predict the drug resistance of SCLC.

DISCUSSION

The treatment of lung cancer has achieved remarkable progress in the past two decades and has improved the outcomes for many patients. The in-depth study of driver genes has realized the individualized treatment of patients with NSCLC (36–39) and significantly improved the survival time. However, this advantage did not benefit patients with SCLC. At present, SCLC is divided into different subtypes (40), which had no substantial significance in clinical therapeutic decision-making. ICIs have also improved the prognosis of SCLC to a certain extent, but the treatment options are mainly refined to radiotherapy and chemotherapy. Chemotherapy resistance is one of the main reasons for the poor prognosis of SCLC. From a clinical perspective, SCLC is generally divided into chemorefractory and chemosensitive according to PFS time. In this case, there is neither an effective means to evaluate the potential benefits of patients before treatment nor a molecular mechanism to further explore effective treatment methods.

Genetic mutations are widely present in two different types of patients, which is the same as previously reported. Our SNV and CNV analyses showed a significant difference between the two groups. Further functional analysis showed that genomic instability in cancer cells may lead to the tumor's rapid growth, tendency to metastasize, immune escape, and resistance to chemotherapy. Interestingly, the mutation status of *LRP2*

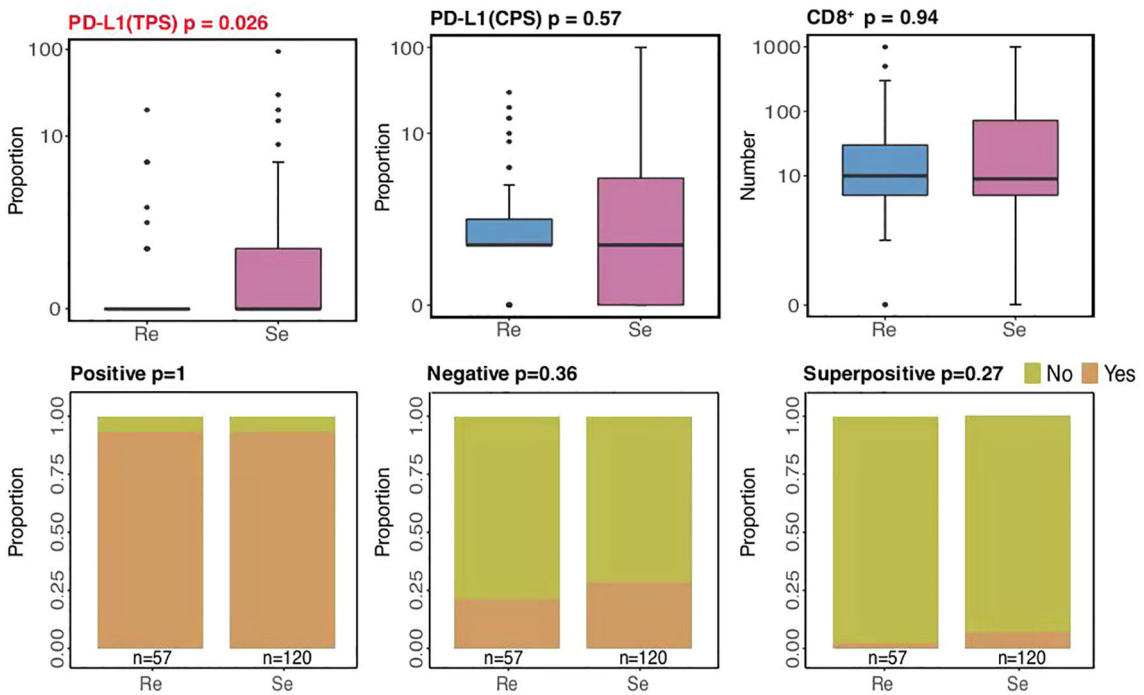

FIGURE 5 | Comparison of immunotherapy-related biomarkers.

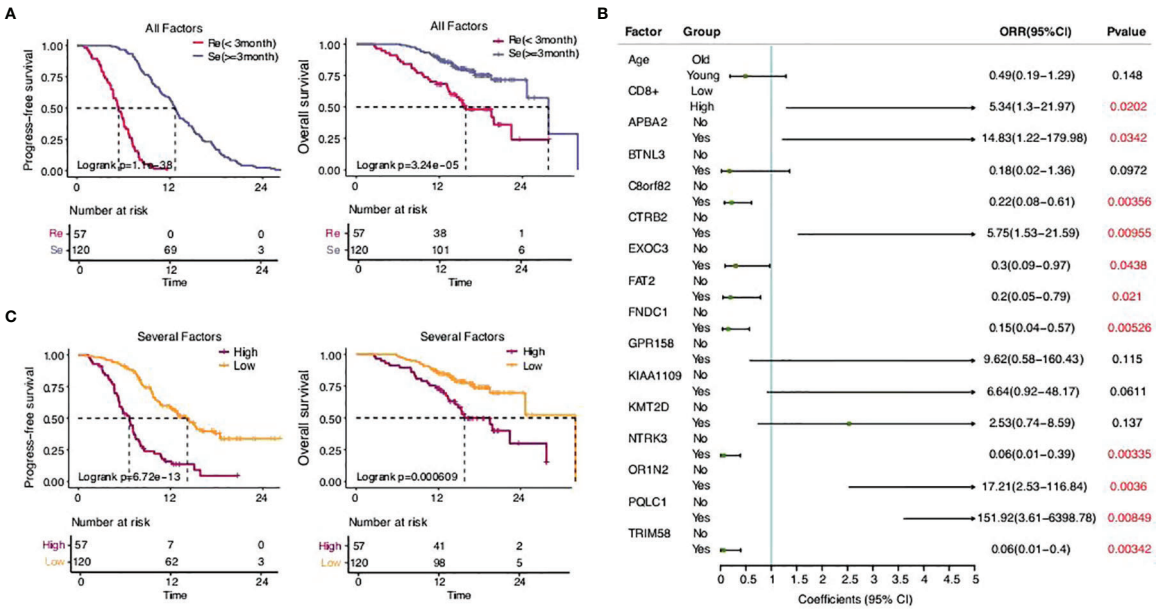

FIGURE 6 | The predictive model of drug resistance of SCLC. **(A)** Statistical analysis of the two groups. **(B)** Sixteen eigenvalues got selected through the stepwise regression process with resistance as the target variable. **(C)** Statistical analysis of the high-risk group and the low-risk group.

related to encoding for low-density lipoprotein-related protein 2 or megalin affected the OS time, while other gene mutations only affected the PFS time. The particularity of *LRP2* deserves further study. Targeted screening and evaluation by WES providing the reference criterion for individualized treatment and drug development are imperatively needed.

There have been some particular findings in chromosomal-level genomic alterations. The amplification mutation of the chemorefractory group increased significantly and was significantly related to tumor proliferation, metastasis, and immune escape. This shows that genomic heterogeneity is the main reason for the different biological behaviors. Similarly, the difference in deletion mutation between the two groups was more pronounced in cell proliferation in the chemorefractory group (41). Interestingly, it has been indicated by some studies that inactivating the *ERK1/2* signaling pathway would suppress cisplatin resistance in non-small cell lung cancer (42). It deeply supported the correlation of drug resistance and provided a basis for drug research and development.

Immunotherapy, especially with ICIs targeting PD-L1, has durably changed the treatment for SCLC. According to our current study, higher PD-L1 expressions (based on TPS methods) were mostly present among the chemosensitive patients, with HPD being similar between the two groups. Conventional markers, including PD-L1 and $CD8^+$ TILs, may not be enough to serve as clinical references (43–46). We observed that mutations in our experimental samples were related to functions and immune responses, such as leukocyte differentiation ratio, regulation of cellular response to stress, and B-cell differentiation, which warrants the prediction of immunotherapy benefits by immune-related markers and genetic background incorporation. Altogether, this suggested that chemosensitive patients might be the most appropriate subgroup for immunotherapy. However, a broader analysis of predictive biomarkers should be carried out in the future to verify our inferences.

There have been several studies establishing the corresponding classifier for clinical outcomes based on a single CTC in patients with SCLC (4, 5). We screened a wider range of features that covered clinical characteristics, molecular level, and chromosome variation. The survival analysis showed an obvious advantage in the low-risk group (p = 6.72e−13) suggesting that our model has significant potential as a predictive and prognostic method. However, it needs to be proven by further experiments using larger samples.

Overall, our study has expanded our knowledge regarding SCLC based on a total of 177 patients with SCLC, the largest Chinese SCLC cohort study to date. Our findings revealed the difference between the two groups, the genomic characteristics, and the resistance mechanism of Chinese SCLC patients, thereby laying the groundwork for improved SCLC management *via* personalized medicine development. The model established by logistic regression divided patients into high-risk and low-risk groups, so as to establish a convenient approach for clinical disease differentiation. This study provides a reference basis to translate knowledge into practice, such as formulating personalized treatment plans, which may benefit Chinese patients with SCLC.

TABLE 1 | Logisic regression models to check the differences in Re and Se groups.

Biomarkers	Group	Odds ratio	95% CI	*p*-value
Age_group	Old			
	Young	0.64	0.34–1.22	0.175
Stage	Extensive stage			
	Limited stage	2.19	1.14–4.2	0.0187
Fam. hist	No			
	Yes	0.61	0.29–1.27	0.187
Gender	Male			
	Female	1.32	0.64–2.7	0.453
Smoking	Yes			
	No	1.43	0.74–2.76	0.289
Drinking	No			
	Yes	0.7	0.37–1.33	0.28
Metastases	No			
	Yes	0.94	0.41–2.17	0.884
CD8_num_group	Low			
	High	2.13	0.91–5	0.0813
PDL1_TPS_prop_group	Low			
	High	1.6	0.6–4.25	0.347
ABCC1	No			
	Yes	22,454,206.5	0–Inf	0.988
APBA2	No			
	Yes	6.8	0.87–53.35	0.068
BTNL3	No			
	Yes	0.29	0.1–0.81	0.0182
C8orf82	No			
	Yes	0.46	0.23–0.89	0.0222
CTRB2	No			
	Yes	3.31	1.21–9.09	0.0199
EXOC3	No			
	Yes	0.31	0.14–0.7	0.00504
FAT2	No			
	Yes	0.38	0.16–0.92	0.0321
FNDC1	No			
	Yes	0.34	0.14–0.82	0.0162
GPR158	No			
	Yes	7.4	0.95–57.71	0.0563
KIAA1109	No			
	Yes	3.39	0.96–11.96	0.0581
KMT2D	No			
	Yes	2.63	1.13–6.1	0.0249
NTRK3	No			
	Yes	0.27	0.08–0.85	0.0262
OR1N2	No			
	Yes	3.82	1.09–13.38	0.0363
PQLC1	No			
	Yes	9.24	1.2–71.28	0.0329
TRIM58	No			
	Yes	0.2	0.07–0.63	0.0057
LRP2	No			
	Yes	2.63	1.13–6.1	0.0249

DATA AVAILABILITY STATEMENT

The datasets presented in this study can be found in online repositories. The names of the repository/repositories and accession number(s) can be found below: Genome Sequence Archive in Data Center of Beijing Institute of Genomics under the accession number subHRA001430.

AUTHOR CONTRIBUTIONS

HW and JG: conceptualization, writing—review and editing, supervision, and validation. NT: writing—original draft, visualization, methodology, investigation, and formal analysis. ZL, XH, and CZ: writing—methodology and formal analysis. All authors contributed to the article and approved the submitted version.

FUNDING

This study was supported jointly by special funds for Taishan Scholars Project (grant no. tsqn201812149).

SUPPLEMENTARY MATERIAL

The Supplementary Material for this article can be found online at: https://www.frontiersin.org/articles/10.3389/fonc.2022.891938/full#supplementary-material

Supplementary Figure 1 | Comparison of clinical features between the two group.

Supplementary Figure 2 | Comparison of four highly confident mutational signatures (S1, S2, S3, and S4) derived in the SCH cohort with those in the COSMIC dataset using Cosine similarity analysis.

Supplementary Figure 3 | PFS of OR4C6 different mutation status.PFS, progression-free survival.

Supplementary Figure 4 | PFS of PTPN13different mutation status.

Supplementary Figure 5 | OS of *LRP2*different mutation status.OS, overall survival.

Supplementary Figure 6 | TheVAF analysis of the two group.VAF, variant allele fraction.

Supplementary Figure 7 | PFS of CTDP1different mutation status.

Supplementary Figure 8 | PFS of KLF5different mutation status.

Supplementary Figure 9 | PFS of NFATC1different mutation status.

Supplementary Figure 10 | PFS of SYTL1different mutation status.

Supplementary Figure 11 | PFS of TTLL10different mutation status.

Supplementary Figure 12 | OS of PQLC1different mutation status.

Supplementary Figure 13 | Comparison of copy number variations between the two group and their enriched biological functions. **(A)** Venn graphs showing different deletionfocal CNV genes between the two group predicted by the GISTIC method (FDR q < 0.1). **(B)** KEGG pathways and GO functions enriched by focal CNV genes that significantly affected PFS time.

Supplementary Figure 14 | Comparison of genomic instability between two groups.

Supplementary Table 1 | Eigenvalues of the two groups in total.

REFERENCES

1. International Agency for Research on Cancer. *Global Cancer Observatory: Cancer Today* . World Health Organization. Available at: https://gco.iarc.fr/today (Accessed Jan 19, 2020).
2. Horn L, Mansfield A S, Szczęsna A, Havel L, Krzakowski M, Hochmair M J, et al. First-Line Atezolizumab Plus Chemotherapy in Extensive-Stage Small-Cell Lung Cancer. *N Engl J Med* (2018) 379:2220–29. doi: 10.1056/NEJMoa1809064
3. van Meerbeeck JP, Fennell DA, De Ruysscher DK. Small-Cell Lung Cancer. *Lancet* (2011) 378:1741–55. doi: 10.1016/S0140-6736(11)60165-7
4. Carter L, Rothwell DG, Mesquita B, Smowton C, Leong H S, Fernandez-Gutierrez F, et al. Inferring the Evolution and Progression of SmallCell Lung Cancer by Single-Cell Sequencing of Circulating Tumor Cells. *Clin Cancer Res* (2019) 25(16):5049–61.
5. Zhe S, Zhijie W, Xiaohui N, et al. Inferring the Evolution and Progression of SmallCell Lung Cancer by Single-Cell Sequencing of Circulating Tumor Cells. *Clin Cancer Res* (2019) 25(16):5049–61. doi: 10.1158/1078-0432.CCR-18-3571
6. Oxnard GR, Thress KS, Alden RS, Lawrance R, Paweletz C P, Cantarini M, et al. Association Between Plasma Genotyping and Outcomes of Treatment With Osimertinib (AZD9291) in Advanced non-Small-Cell Lung Cancer. *J Clin Oncol* (2016) 34:3375–82. doi: 10.1200/JCO.2016.66.7162
7. Sacher AG, Paweletz C, Dahlberg SE, Alden R S, O'Connell A, Feeney N, et al. Prospective Validation of Rapid Plasma Genotyping for the Detection of EGFR and KRAS Mutations in Advanced Lung Cancer. *JAMA Oncol* (2016) 2:1014–22. doi: 10.1001/jamaoncol.2016.0173
8. Reck M, Liu S, Mansfield A, Mok T.S.K., Scherpereel A., Reinmuth N., et al. IMpower133: Updated Overall Survival (OS) Analysis of First-Line (1L) Atezolizumab (Atezo)+ Carboplatin+ Etoposide in Extensive-Stage SCLC (ES-SCLC). *Ann Oncol* (2019) 30:v710–11. doi: 10.1093/annonc/mdz264
9. Paz-Ares L, Dvorkin M, Chen Y, Reinmuth N, Hotta K, Trukhin D, et al. Durvalumab Plus Platinumetoposide Versus Platinum-Etoposide in First-Line Treatment of Extensive-Stage Small-Cell Lung Cancer (CASPIAN): A Randomised, Controlled, Open-Label, Phase 3 Trial. *Lancet* (2019) 394:1929–39. doi: 10.1016/S0140-6736(19)32222-6
10. Paz-Ares LG, Dvorkin M, Chen Y, Reinmuth N, Hotta K, Trukhin D, et al. Durvalumab ± Tremelimumab + Platinum-Etoposide in First-Line Extensive-Stage SCLC (ES-SCLC): Updated Results From the Phase III CASPIAN Study. *Proc Am Soc Clin Oncol* (2020) 38(suppl):9002. doi: 10.1200/JCO.2020.38.15_suppl.9002
11. Rudin CM, Awad MM, Navarro A, Gottfried M, Peters S, Csőszi T, et al. KEYNOTE-604: Pembrolizumab (Pembro) or Placebo Plus Etoposide and Platinum (EP) as First-Line Therapy for Extensive-Stage (ES) Small-Cell Lung Cancer (SCLC). *Proc Am Soc Clin Oncol* (2020) 38(suppl):9001. doi: 10.1200/JCO.2020.38.15_suppl.9001
12. Chen S, Zhou Y, Chen Y, Gu J, et al. Fastp: An Ultra-Fast All-in-One FASTQ Preprocessor. *Bioinformatics* (2018) 34(17):i884–90. doi: 10.1093/bioinformatics/bty560
13. Li H, Durbin R. Fast and Accurate Short Read Alignment With Burrows-Wheelertransform. *Bioinformatics* (2009) 25(14):1754–60. doi: 10.1093/bioinformatics/btp324
14. Li H, Handsaker B, Wysoker A, Fennell T, Ruan J, Homer N, et al. 1000 Genome Project Data Processing Subgroup. The Sequence Alignment/Map Format and SAMtools. *Bioinformatics* (2009) 25(16):2078–9. doi: 10.1093/bioinformatics/btp352
15. McKenna A, Hanna M, Banks E, Sivachenko A, Cibulskis K, Kernytsky A, et al. The Genome Analysis Toolkit: A MapReduce Framework for Analyzing Next-Generation DNA Sequencing Data. *Genome Res* (2010) 20(9):1297–303. doi: 10.1101/gr.107524.110
16. Gehring JS, Fischer B, Lawrence M, Huber W. SomaticSignatures: Inferring Mutational Signatures From Single-Nucleotide Variants. *Bioinformatics* (2015) 31(22):3673–5. doi: 10.1093/bioinformatics/btv408
17. Rosenthal R, McGranahan N, Herrero J, Taylor BS, Swanton C. DeconstructSigs: Delineating Mutational Processes in Single Tumors Distinguishes DNA Repair Deficiencies and Patterns of Carcinoma Evolution. *Genome Biol* (2016) 17:31. doi: 10.1186/s13059-016-0893-4
18. Cibulskis K, Lawrence MS, Carter SL, Sivachenko A, Jaffe D, Sougnez C, et al. Sensitive Detection of Somatic Point Mutations in Impure and Heterogeneous Cancer Samples. *Nat Biotechnol* (2013) 31(3):213–9. doi: 10.1038/nbt.2514
19. Wang K, Li M, Hakonarson H. ANNOVAR: Functional Annotation of Genetic Variants From High-Throughput Sequencing Data. *Nucleic Acids Res* (2010) 38(16):e164. doi: 10.1093/nar/gkq603
20. Szolek A, Schubert B, Mohr C, Sturm M, Feldhahn M, Kohlbacher O. OptiType: Precision HLA Typing From Next-Generation Sequencing Data. *Bioinformatics* (2014) 30(23):3310–6. doi: 10.1093/bioinformatics/btu548

21. Lawrence MS, Stojanov P, Polak P, Kryukov GV, Cibulskis K, Sivachenko A, et al. : Mutational Heterogeneity in Cancer and the Search for New Cancer-Associated Genes. *Nature* (2013) 499(7457):214–8. doi: 10.1038/nature12213
22. Martincorena I, Raine KM, Gerstung M, Dawson KJ, Haase K, Van Loo P, et al. Universal Patterns of Selection in Cancer and Somatic Tissues. *Cell* (2017) 171(5):1029–1041.e1021. doi: 10.1016/j.cell.2017.09.042
23. Mermel CH, Schumacher SE, Hill B, et al. GISTIC2.0 Facilitates Sensitive and Confident Localization of the Targets of Focal Somatic Copy-Number Alteration in Human Cancers. *Genome Biol* (2011) 12(4):R41–1. doi: 10.1186/gb-2011-12-4-r41
24. Mroz EA, Rocco JW. MATH, a Novel Measure of Intratumor Genetic Heterogeneity,is High in Poor-Outcome Classes of Head and Neck Squamous Cell Carcinoma. *Oral Oncol* (2013) 49(3):211–5. doi: 10.1016/j.oraloncology.2012.09.007
25. Letouzé E, Shinde J, Renault V, Couchy G, Blanc JF, Tubacher E, et al. Mutational Signatures Reveal the Dynamic Interplay of Risk Factors and Cellular Processes During Liver Tumorigenesis. *Nat Commun* (2017) 8 (1):1315. doi: 10.1038/s41467-017-01358-x
26. Favero F, Joshi T, Marquard AM, Birkbak NJ, Krzystanek M, Li Q, et al. Sequenza: Allele-Specific Copy Number and Mutation Profiles From Tumor Sequencing Data. *Ann Oncol* (2015) 26(1):64–70. doi: 10.1093/annonc/mdu479
27. López S, Lim EL, Horswell S, Haase K, Huebner A, Dietzen M, et al. Interplay Between Whole-Genome Doubling and the Accumulation of Deleterious Alterations in Cancer Evolution. *Nat Genet* (2020) 52(3):283–93. doi: 10.1038/s41588-020-0584-7
28. Priestley P, Baber J, Lolkema MP, Steeghs N, de Bruijn E, Shale C, et al. Pan-Cancer Whole-Genome Analyses of Metastatic Solid Tumours. *Nature* (2019) 575(7781):210–6. doi: 10.1038/s41586-019-1689-y
29. Doroshow DB, Bhalla S, Beasley MB, Sholl LM, Kerr KM, Gnjatic S, et al. PD-L1 as a Biomarker of Response to Immune-Checkpoint Inhibitors. *Nat Rev Clin Oncol* (2021) 18(6):345–62. doi: 10.1038/s41571-021-00473-5
30. George J, Lim JS, Jang SJ, Cun Y, Ozretić L, Kong G, et al. Comprehensive Genomic Profiles of Small Cell Lung Cancer. *Nature* (2015) 524(7563):47–53. doi: 10.1038/nature14664
31. McBride D J, Meynert A, Jones D. A Small-Cell Lung Cancer Genome With Complex Signatures of Tobacco Exposure. *Nature* (2010) 463:184–90. doi: 10.1038/nature08629
32. Fukuoka M, Masuda N, Furuse K, Negoro S, Takada M, Matsui K, et al. A Randomized Trial in Inoperable non-Small-Cell Lung Cancer: Vindesine and Cisplatin Versus Mitomycin, Vindesine, and Cisplatin Versus Etoposide Andcisplatin Alternating With Vindesine and Mitomycin. *J Clin Oncol* (1991) 9:606–13. doi: 10.1200/JCO.1991.9.4.606
33. Hanna N, Bunn PAJr, Langer C, Einhorn L , Guthrie TJr , Beck T, et al. Randomized Phase III Trial Comparing Irinotecan/Cisplatin With Etoposide/Cisplatin in Patients With Previously Untreated Extensive-Stage Disease Small-Cell Lung Cancer. *J Clin Oncol* (2006) 24:2038–43. doi: 10.1200/JCO.2005.04.8595
34. Noda K, Nishiwaki Y, Kawahara M, Negoro S, Sugiura T, Yokoyama A, et al. Irinotecan Plus Cisplatin Compared With Etoposide Plus Cisplatin for Extensive Small-Cell Lung Cancer. *N Engl J Med* (2002) 346:85–91. doi: 10.1056/NEJMoa003034
35. Shen J, Ju Z, Zhao W, Wang L, Peng Y, Ge Z, et al. ARID1A Deficiency Promotes Mutability and Potentiates Therapeutic Antitumor Immunity Unleashed by Immune Checkpoint Blockade. *Nat Med* (2018) 24(5):556–62. doi: 10.1038/s41591-018-0012-z
36. Soria JC, Ohe Y, Vansteenkiste J, Reungwetwattana T, Chewaskulyong B, Lee KH, et al. Osimertinib in Untreated EGFR-Mutated Advanced non-Small-Cell Lung Cancer. *N Engl J Med* (2018) 378:113–25. doi: 10.1056/NEJMoa1713137
37. Zhou C, Wu YL, Chen G, Vergnenegre A, Massuti B, Felip E, et al. Erlotinib Versus Chemotherapy as First-Line Treatment for Patients With Advanced EGFR Mutation-Positive non-Small-Cell Lung Cancer (OPTIMAL, CTONG-0802): A Multicentre, Openlabel, Randomised, Phase 3 Study. *Lancet Oncol* (2011) 12:735–42. doi: 10.1016/S1470-2045(11)70184-X
38. Mok TS, Wu YL, Thongprasert S, Yang C-H, Chu D-T, Saijo N, et al. Gefitinib or Carboplatin-Paclitaxel in Pulmonary Adenocarcinoma. *N Engl J Med* (2009) 361:947–57. doi: 10.1056/NEJMoa0810699
39. Sequist LV, Yang JC, Yamamoto N, O'Byrne K, Hirsh V, Mok T, et al. Phase III Study of Afatinib or Cisplatin Plus Pemetrexed in Patients With Metastatic Lung Adenocarcinoma With EGFR Mutations. *J Clin Oncol* (2013) 31:3327–34. doi: 10.1200/JCO.2012.44.2806
40. Rudin CM, Brambillla E, Faivre-Finn C, Sage J, et al. Small-Cell Lung Cancer. *Nat Rev Dis Primers* (2021) 7(1):3. doi: 10.1038/s41572-020-00235-0
41. Wang K, Ji W, Yu Y, Li Z, Niu X, Xia W, et al. FGFR1-ERK1/2-SOX2 Axis Promotes Cell Proliferation, Epithelial-Mesenchymal Transition, and Metastasis in FGFR1-Amplified Lung Cancer. *Oncogene* (2018) 37 (39):5340–54. doi: 10.1038/s41388-018-0311-3
42. Xue F, Yang C, Yun K, Jiang C, Cai R, Liang M, et al. Reduced LINC00467 Elevates microRNA-125a-3p to Suppress Cisplatin Resistance in non-Small Cell Lung Cancer Through Inhibiting Sirtuin 6 and Inactivating the ERK1/2 Signaling Pathway. *Cell Biol Toxicol* (2021). doi: 10.1007/s10565-021-09637-6
43. Borghaei H, Paz-Ares L, Horn L, Spigel D R , Steins M , Ready N E, et al. Nivolumab Versus Docetaxel in Advanced Nonsquamous non-Small-Cell Lung Cancer. *N Engl J Med* (2015) 373(17):1627–39. doi: 10.1056/NEJMoa1507643
44. Herbst RS, Baas P, Kim DW, Felip E, Pérez-Gracia J L, Han J-Y, et al. Pembrolizumab Versus Docetaxel for Previously Treated, PD-L1-Positive, Advanced non-Small-Cell Lung Cancer (KEYNOTE-010): A Randomised Controlled Trial. *Lancet* (2016) 387(10027):1540–50. doi: 10.1016/S0140-6736(15)01281-7
45. Rittmeyer A, Barlesi F, Waterkamp D, Park K, Ciardiello F, von Pawel J, et al. Atezolizumab Versus Docetaxel in Patients With Previously Treated non-Small-Cell Lung Cancer (OAK): A Phase 3, Open-Label, Multicentre Randomised Controlled Trial. *Lancet* (2017) 389(10066):255–65. doi: 10.1016/S0140-6736(16)32517-X
46. Fehrenbacher L, Spira A, Ballinger M, Kowanetz M, Vansteenkiste J, Mazieres J, et al. Atezolizumab Versus Docetaxel for Patients With Previously Treated non-Small-Cell Lung Cancer (POPLAR): A Multicentre, Open-Label, Phase 2 Randomised Controlled Trial. *Lancet* (2016) 387(10030):1837–46. doi: 10.1016/S0140-6736(16)00587-0
47. Lally BE, Urbanic JJ, Blackstock AW, Miller AA, Perry MC. Small Celllung Cancer: Have We Made Any Progress Over the Last 25 Years? *Oncologist* (2007) 12:1096–104. doi: 10.1634/theoncologist.12-9-1096

Conflict of Interest: ZL was employed by Berry Oncology Corporation.

The remaining authors declare that the research was conducted in the absence of any commercial or financial relationships that could be construed as a potential conflict of interest.

Publisher's Note: All claims expressed in this article are solely those of the authors and do not necessarily represent those of their affiliated organizations, or those of the publisher, the editors and the reviewers. Any product that may be evaluated in this article, or claim that may be made by its manufacturer, is not guaranteed or endorsed by the publisher.

frontiers | Frontiers in Oncology

TYPE Original Research
PUBLISHED 14 November 2022
DOI 10.3389/fonc.2022.968064

OPEN ACCESS

EDITED BY
Iacopo Petrini,
University of Pisa, Italy

REVIEWED BY
Marcello Tiseo,
University Hospital of Parma, Italy
Chiara Ambrogio,
University of Turin, Italy

*CORRESPONDENCE
Lorenzo Antonuzzo
lorenzo.antonuzzo@unifi.it

†These authors share last authorship

SPECIALTY SECTION
This article was submitted to Thoracic Oncology, a section of the journal Frontiers in Oncology

RECEIVED 13 June 2022
ACCEPTED 17 October 2022
PUBLISHED 14 November 2022

CITATION
Fancelli S, Caliman E, Mazzoni F, Paglialunga L, Gatta Michelet MR, Lavacchi D, Berardi R, Mentrasti G, Metro G, Birocchi I, Delmonte A, Priano I, Comin CE, Castiglione F, Bartoli C, Voltolini L, Pillozzi S and Antonuzzo L (2022) KRAS G12 isoforms exert influence over up-front treatments: A retrospective, multicenter, Italian analysis of the impact of first-line immune checkpoint inhibitors in an NSCLC real-life population. *Front. Oncol.* 12:968064. doi: 10.3389/fonc.2022.968064

KRAS G12 isoforms exert influence over up-front treatments: A retrospective, multicenter, Italian analysis of the impact of first-line immune checkpoint inhibitors in an NSCLC real-life population

Sara Fancelli[1,2], Enrico Caliman[1,2], Francesca Mazzoni[3], Luca Paglialunga[2], Marta Rita Gatta Michelet[3], Daniele Lavacchi[2], Rossana Berardi[4], Giulia Mentrasti[4], Giulio Metro[5], Ilaria Birocchi[5], Angelo Delmonte[6], Ilaria Priano[6], Camilla Eva Comin[1,7], Francesca Castiglione[8], Caterina Bartoli[8], Luca Voltolini[1,9], Serena Pillozzi[3†] and Lorenzo Antonuzzo[1,2,3*†]

[1]Department of Experimental and Clinical Medicine, University of Florence, Florence, Italy, [2]Clinical Oncology Unit, Careggi University Hospital, Florence, Italy, [3]Medical Oncology Unit, Careggi University Hospital, Florence, Italy, [4]Department of Medical Oncology, Università Politecnica delle Marche, Azienda Ospedaliero Universitaria (AOU) Ospedali Riuniti di Ancona, Ancona, Italy, [5]Medical Oncology Unit, Santa Maria della Misericordia Hospital, Perugia, Italy, [6]Scientific Institute of Romagna for the Study and Treatment of Tumors (IRST) Istituto di Ricovero e Cura a Carattere Scientifico (IRCCS), Meldola, Italy, [7]Surgery, Histopathology and Molecular Pathology Unit, Careggi University Hospital, Florence, Italy, [8]Pathological Histology and Molecular Diagnostics Unit, Careggi University Hospital, Florence, Italy, [9]Thoracic Surgery Unit, Careggi University Hospital, Florence, Italy

Background: KRAS is commonly mutated in non-small cell lung cancer (NSCLC); however, the prognostic and predictive impact of each G12 substitution has not been fully elucidated. The approval of specific G12C inhibitors has modified the idea of KRAS "undruggability", and although the first-line standard consists of immune checkpoint inhibitors (ICIs) with or without chemotherapy, as suggested at ASCO 2022, the outcome in KRAS-mutated population is still controversial.

Methods: We retrospectively described the clinical and pathological characteristics of a homogeneous G12 mutated cohort of 219 patients treated in four Italian oncologic units. We evaluated the outcome (PFS at 18 months and OS at 30 months) of those who underwent standard first-line treatment according to PD-L1 status, focusing on differences across single mutations.

Results: In the study population, 47.9% of patients harbor the KRAS G12C mutation; 20.5%, G12V; 17.4%, G12D; and 8.2%, G12A. Smoking was a common behavior of patients harboring transversions and transition mutations. PD-L1 expression does not show particular distribution in the case series, although we recorded a prevalence of PD-L1 <1% in G12V (51.4%) compared to G12A (26.7%). ICIs alone was the clinician's choice in 32.7% of patients, and the chemo-immune combination in 17.3% of patients. We described the independent prognostic role of young age (p = 0.007), female gender (p = 0.016), and an ICI-based regimen (p = 0.034) regardless of mutations. Overall, our data confirm the worst prognostic value of G12V mutation apart from treatment choice unlike the other major mutations (C, D, and A) that showed a favorable trend in PFS.

Conclusions: KRAS G12 mutations are confirmed to have different characteristics, and the outcome is influenced by ICI first-line regimen. This study provides valuable information for further analysis in the future.

KEYWORDS

KRAS mutations, KRAS G12 isoforms, treatment responses, immune check-point inhibitors, PD-L1

Introduction

RAS genes encode for a family of small membrane-bound guanosine-triphosphate (GTP) binding proteins involved in the regulation of cell proliferation, growth, and mobility, as well as in apoptosis mechanisms through several downstream effectors. *RAS* mutations lead to protein conformation changes resulting in the perpetual activation of downstream pathways and a complete independence from the upstream signaling (1). Fifteen percent to 25% of non-small cell lung cancer (NSCLC) patients harbor Kras mutations that, in 95% of cases, rely on base substitution in exon 2 (2). According to the COSMIC database, G12C, G12V, G12D, and G12A mutations are the most common KRAS single-amino acid substitutions in lung adenocarcinoma (LUAD) (3), unlike the squamous cell histotype in which KRAS mutations are rare (3%–5%) (4, 5). The prognostic and predictive value of Kras mutations is still controversial. Although the prognosis appears to be correlated to the KRAS' codon damage and to the setting analyzed (6–8), the predictive value did not find a precise characterization. In fact, the clinical trials evaluating the use of different agents [TKI, chemotherapy (CT), antiangiogenics, or different combinations of these] were inconclusive in the KRAS-mutated population (9–11). Recent results from the phase 2 trials CodeBreaK 100 and KRYSTAL-1 (12, 13) led to FDA approval of KRAS G12C selective inhibitors, i.e., sotorasib in May 2021 and the new drug application for the use of adagrasib in February 2022, for patients with pretreated KRAS G12C-NSCLC (14, 15). Despite the encouraging results, neither sotorasib nor adagrasib is still recommended as a first-line treatment in advanced KRAS G12C LUAD, and results in this setting are awaited from ongoing clinical trials (e.g., KRYSTAL-7, CodeBreak201, and NCT04933695). Monoclonal antibodies targeting the PD1/PD-L1 axis and CTLA-4 (e.g., nivolumab, pembrolizumab, atezolizumab, and ipilimumab) induce T-cell reactivation in several neoplasms, although their efficacy is patchy due to existing mechanisms of immunosuppression (16, 17). However, immunotherapy has gradually become relevant in KRAS-mutated patients, both because it is currently a standard first-line treatment alone or in combination with CT (18, 19), and because of its efficacy in these patients, as described in numerous experiences including the Keynote-042 subgroup analysis (20–23). Moreover, as recently reported at ASCO 2022, the use of chemo-immune checkpoint inhibitors enhances overall survival (OS) and overall response rate (ORR) in a KRAS-mutated population (24). It is noteworthy that Kras has been reported to influence the peritumor immune microenvironment and the expression of PD-L1 (25, 26), and *in vitro* evidence suggests a difference in the enhancement of antitumor immunity caused by different punctiform mutations in KRAS (27, 28).

The above-mentioned background has inspired this Italian retrospective study to directly evaluate in an unselected KRAS G12-mutated population the real impact of the use of chemo- or immunotherapies alone or in combination, as a frontline treatment according to demographic characteristics and single-amino acid substitutions.

Materials and methods

Study population

We enrolled all NSCLC patients with a confirmed diagnosis of LUAD, detected from January 2015 to December 2021 in four Italian Cancer Units [Clinical and Medical Oncology Units, Careggi University Hospital, Florence; Department of Medical Oncology, Università Politecnica delle Marche, AOU Ospedali Riuniti di Ancona, Ancona; Medical Oncology Unit, Santa Maria della Misericordia Hospital, Perugia; and the Scientific Institute of Romagna for the Study and Treatment of Tumors (IRST) IRCCS, Meldola]. Eligibility criteria included the following: age >18 years and available KRAS G12 mutation status regardless of the expression of PD-L1, which was not mandatory. We collected demographic data in an electronic record including age, sex, ECOG PS, smoking habits, data of death or last follow-up, disease characteristics such as KRAS mutational status, and PD-L1 status (<1%; 1%–49% and >50%) when available. Details about first-line treatment [date of first and last dose treatment, and best response achieved according to the Response Evaluation Criteria in Solid Tumors (RECIST) version 1.1] were gathered. The measured clinical outcomes were progression-free survival (PFS) evaluated at 18 months and OS at 30 months. All data were collected and analyzed anonymously; all patients signed an informed consent prior to starting treatment. This study complies with the Declaration of Helsinki rules of the World Medical Association and has been reviewed and approved by the Regional Ethics Committee for Clinical Trials of the Tuscany Region (approval No.: 20039_oss).

Treatments

All patients underwent frontline therapy with anti-PD-L1, CT, or a combination of them. The drugs that were mainly used were the following: four to six cycles of cisplatin 75 mg/m^2 or carboplatin area under the concentration time curve, 5 mg per milliliter per minute intravenous (IV) D1 Q3W, pemetrexed 500 mg/m^2 IV D1 Q3W continued until the radiographically confirmed PD or toxicity, and pembrolizumab 200 mg IV D1 Q3W until the radiographically confirmed progression disease, toxicity, or the conclusion of 35 planned cycles. Pembrolizumab was administered alone or in combination with the CT regimen previously described. Few patients underwent a carboplatin-based regimen with paclitaxel 175 mg/m^2 and bevacizumab 7.5 mg/kg IV D1 Q3W.

KRAS mutation analysis

DNA was extracted from formalin-fixed paraffin-embedded tissue using a MagCore® Genomic DNA FFPE One-Step Kit on MagCore® Automated Nucleic Acid Extractor HF16Plus. Mutational analysis was performed as per local practice with the following panels: Myriapod® NGS-LT 56G Onco panel on Ion Torrent Ion S5™ system, with Myriapod® NGS Cancer panel DNA on Illumina MiSeq® and with Myriapod® Lung status on MassARRAY®. The analysis of the results of the NGS sequencing was carried out using Myriapod NGS Data Analysis Software and mutations were selected using the online genetic databases Clinvar and COSMIC [a minimum variant allele frequency (VAF) of 5% was applied for variant filtering].

PD-L1 detection

From each block, 4-µm sections were cut and stained with monoclonal antibody PD-L1 (clone SP263, Ventana Medical System, Ventana, Tucson, Arizona) on an automated staining platform (Benchmark ULTRA; Ventana). An OptiView DAB IHC detection kit (Ventana) and an OptiView Amplification kit (Ventana) were used according to the manufacturer's recommendations for visualization of the immunoreaction. Positive and negative controls were set parallel to the analyzed section. The positive control used was a tonsil section, and the negative control used was ready-to-use mouse serum with no immunization (Ventana). Partial or complete membrane staining of vital malignant cells was considered positive regardless of intensity. For each positive case, the percentage of viable stained tumor cells over total tumor cells (TPS) was used to categorize PD-L1 expression in three groups: TPS < 1% (negative), 1%–49%, and ≥50%.

Statistical analysis

Demographic and clinical data, disease and treatment characteristics, treatment exposure, and outcomes were analyzed using descriptive statistics. Continuous variables were presented as median and range, and categorical data were presented as counts and percentages. The Kaplan–Meier analysis was used to estimate PFS and OS, and log-rank test was applied to test for statistical significance. Cox proportional hazards model analysis was used to generate point estimates of the hazard ratio (HR) and the corresponding 95% confidence interval (CI) to estimate the risk of each individual KRAS isoform with outcome. Survival distributions for specific subgroups of patients has been tested with log-rank test. A p-value of 0.05 or lower has been considered statistically significant According to the class of demographic/clinical variables, suitable multivariate models were constructed, consistent with the significance of each variable (significance identified through the respective p-values relating to the Student's t-test of significance for each variable involved), as well as the possible significance of the interactions between the variables. All statistical analyses were performed using Jamovi (The Jamovi

Project, 2021), and the creation of graphs and figures was carried out with R Statistical Software (v4.1.2; R Core Team 2021).

Results

Patients' characteristics

We evaluated 219 patients with single punctiform mutation on KRAS G12 treated in four Italian oncology units with CT or immune checkpoint inhibitors (ICIs) alone or their combination as first-line therapy for stage IV NSCLC. The baseline characteristics of the enrolled patients are described in Table 1. As expected, most of the patients enrolled were male (61.2%) and older than 65 years (64.8%). The majority of patients were ECOG PS 0–1 (94%). The harboring of G12 mutations was strictly related to smoking habits (p = 0.032). G12C, G12V, G12D, and G12A isoforms were depicted in 47.9%, 20.5%,17.4%, and 8.2% of our population, respectively, while the other isoforms (S, F, and I) were rare (lower than 6%). No particular distribution was observed regarding the expression of PD-L1 in our population. CT was the most used first-line regimen in half of the G12 mutated patients, followed by ICIs alone (32.7%). The recent (2020) approval of the chemo-immune combination in Italy has negatively influenced the sample size of this subgroup (17.3%). Data about demographic characteristics analyzed by G12 single mutation highlighted in the G12V subgroup a predominance of the elderly (80%), and an equal distribution between young (50%) and elderly (50%) in G12A. No differences in gender distribution were observed, as expected, with a prevalence of men in all mutations. However, smoking habit seems to be closely related to C isoform expression (100%), even though D and V isoforms also harbor in never-smokers (13.2% and 11.1%). We described in G12V a prevalence of PD-L1 < 1% (51.4%); conversely, G12C had 43% of PD-L1 > 50% (p = 0.042). Intriguingly, G12A had a higher PD-L1 > 1% expression (73.4%) than the other isoforms (Figures 1A–D). Even when analyzed for mutation, the most commonly used therapy was CT, unlike the chemo-immune combination (data not shown).

TABLE 1 Clinical and demographic patients characteristics.

Baseline characteristics	No. of patients (n = 219)
Sex	
Female	85 (38.8%)
Male	134 (61.2%)
Age	
<65	77 (35.2%)
≥65	142 (64.8%)
ECOG PS	
0	81 (37%)
1	125 (57%)
2	13 (6%)
3	0 (0%)
Smoking habitus	
Never	11 (5%)
Current	115 (52.8%)
Former	92 (42.2%)
G12 mutations	
C	105 (47.9%)
V	45 (20.5%)
D	38 (17.4%)
A	18 (8.2%)
Others§	13 (5.9%)
PD-L1 expression*	
<1%	67 (38.5%)
1%–49%	42 (24.1%)
≥50	65 (37.4%)
First line†	
CT	104 (50%)
ICI	68 (32.7%)
CT+ICI	36 (17.3%)

§=F, S, and I; *n = 174 patients with PD-L1 status available; †n = 208 patients treated as first line.
CT, chemotherapy; ICI, immune checkpoint inhibitor.

G12 survival analysis

We investigate the prognostic role of KRAS G12 mutations according to patients and disease characteristics and treatment chosen. Median PFS and OS of the entire population were 5.0 months (4.0–6.0 months) and 16.0 months (16.0–19.0 months), respectively, with some differences, even not statistically significant among G12 isoforms (PFS p = 0.518 and OS p = 0.593). PFS at 18 months demonstrated to be better for young people (mPFS 6.0 months, 4.0–11.0 months; HR: 1.42, 95% CI 1.01–2.0, p = 0.044) and for women (mPFS 6.0 months, 4.0–11.0 months; HR: 1.54, 95% CI 1.10–2.15, p = 0.013). The advantage was preserved for gender (p = 0.020) despite age (p = 0.150) also in multivariate analysis. No significant differences in PFS were observed according to PD-L1 expression or G12 mutation; even a trend in favor of the C isoform was found compared to V (p = 0.145) and for PD-L1 ≥ 50% compared to PD-L1 <1% (p = 0.154). The subgroup of patients exposed to ICI with or without CT showed a benefit compared to chemotherapy alone (HR: 0.63, 95% CI 0.45–0.87, p = 0.005) in univariate and multivariate analysis (Table 2) (Figures 2A, B). In particular, we registered a mOS of 17.0 months (13.0–29.0 months) for the C isoform (n = 79), a mOS of 13.5 months (6.0–26.0 months) for D (n = 28), a mOS of 21.0 months (7.0–NR months) for the A substitution (n = 13), and a mOS of 12.0 months (8.0–18.0 months) for the V substitution (n = 35), which proved to be the mutation with the worst prognosis. Univariate analysis upheld a better OS for <65-year-old patients (mOS 20.5 months, 19.0–NR; HR: 1.71. 95% CI 1.15–2.55, p = 0.008) and female patients (mOS 23.0 months, 18.0–NR; HR: 1.78. 95% CI 1.21–2.64, p = 0.004) (Table 3) (Figures 2C, D). The benefit of young age and female gender was confirmed also in the multivariate analysis. As per PFS, our

10.3389/fonc.2022.968064

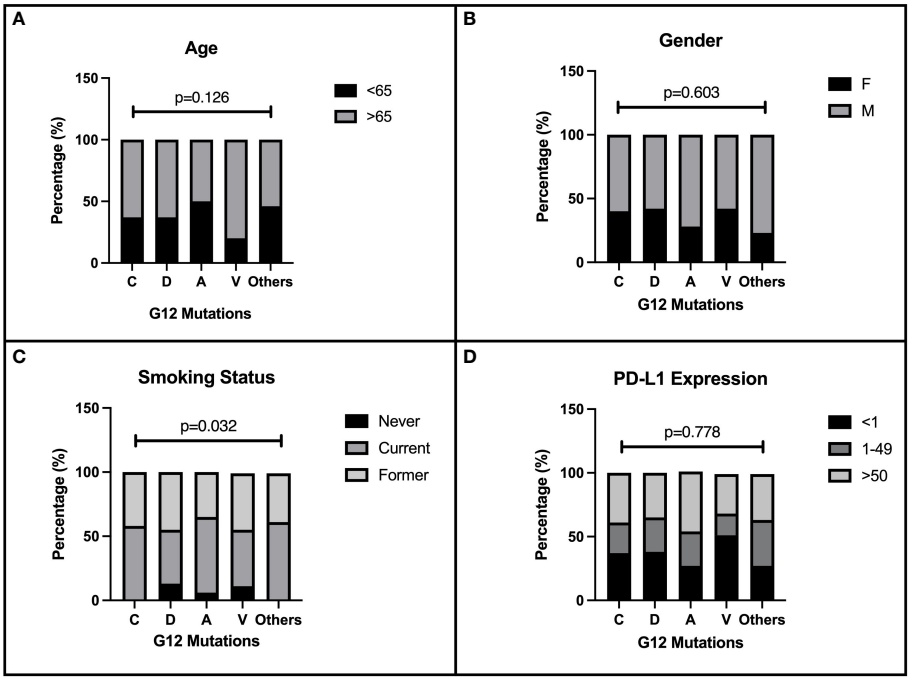

FIGURE 1
Correlation of patients' characteristics and G12 bases. Baseline characteristics of 219 NSCLC patients enrolled in the present retrospective study. The distribution of demographic and immunohistochemical properties is shown in figure according to the single amino acid mutation. The distribution of G12 isoforms was correlated to: **(A)** age of patients at diagnosis (< 65 and ≥65 years), p=0.126. **(B)** gender p=0.603. **(C)** smoking habits p=0.032. **(D)** PD-L1 expression, p=0.778.

dataset supports a trend in OS in favor of C when compared to the V isoform (p = 0.130) and in patients with a lack of PD-L1 expression (p = 0.138) when compared to patients with PD-L1 overexpression. Immunotherapy in addition or not to CT demonstrates a survival benefit in the population regardless of the G12 isoform and PD-L1 expression as shown in Table 3 (mOS of 18.5 months, 15.0–NR; HR: 0.69. 95% CI 0.47–1.00, p = 0.048) benefit we also recorded in multivariate (p = 0.034).

Treatment survival in G12 amino acid substitutions

In accordance with previous results, we decided to analyze the amino acid substitutions' outcomes according to treatments received. Among 106 CT-treated patients, global mPFS was 6.0 months (3.0–6.0 months) and no significant differences in mPFS were observed between the major mutations (A, C, D, and V)

TABLE 2 Univariate and multivariate progression-free survival analysis.

Characteristics	Univariate			Multivariate		
	HR	95% CI	*p*	HR	95% CI	*p*
Sex (female *vs.* male)	1.54	1.10–2.15	**0.013**	1.52	1.07–2.15	**0.020**
Age (<65 *vs.* ≥65)	1.42	1.01–2.00	**0.044**	1.30	0.01–1.85	0.150
PD-L1 (<1 *vs.* 1–49)	1.22	0.75–1.97	0.427			
PD-L1 (<1 *vs.* ≥50)	0.73	0.47–1.13	0.154			
G12 mutations (C *vs.* D)	1.05	0.66–1.67	0.830			
G12 mutations (C *vs.* A)	1.21	0.64–2.28	0.563			
G12 mutations (C *vs.* V)	1.34	0.90–2.00	0.145			
G12 mutations (C *vs.* Others)	1.40	0.70–2.81	0.343			
First line (ICI ± CT *vs.* CT)	0.63	0.45–0.87	**0.005**	0.62	0.45–0.87	**0.005**

Bold was used to pin point data with relevance.

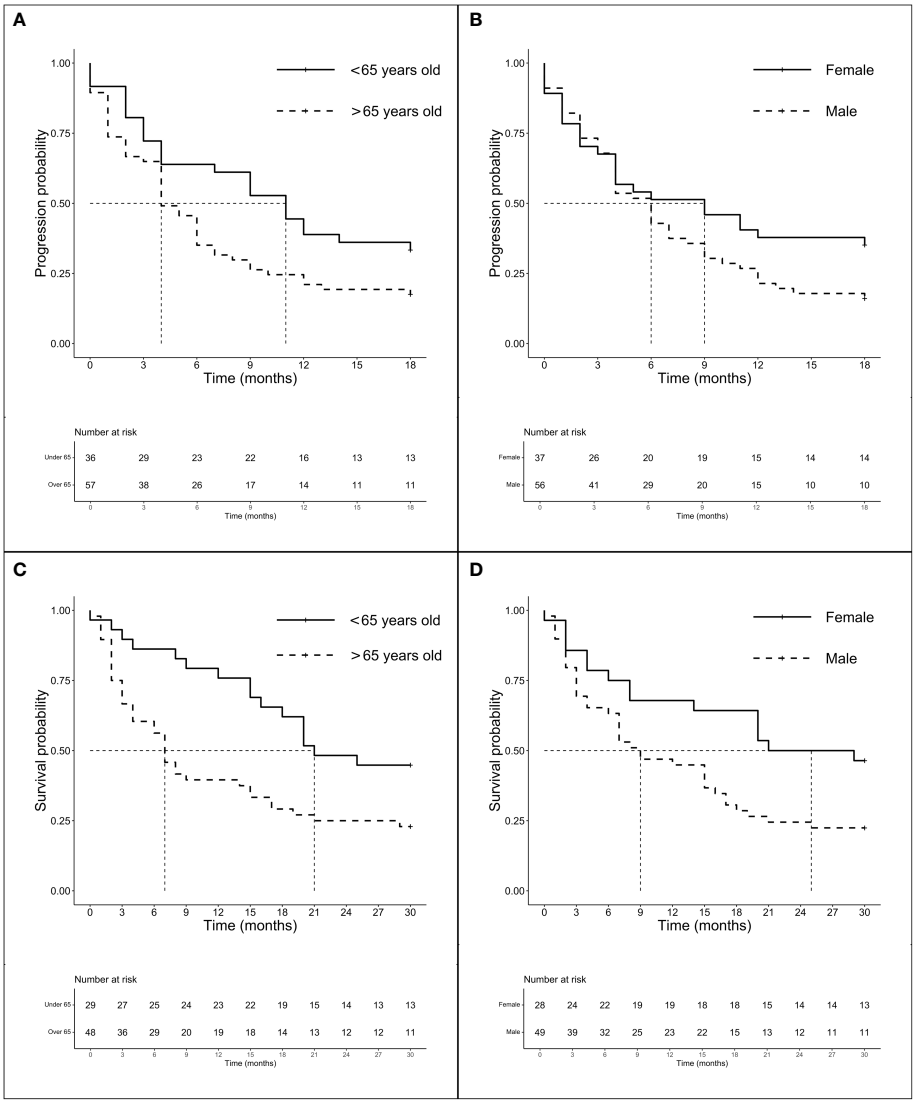

FIGURE 2
Survival analysis (PFS and OS) according to age and gender. Survival analysis (PFS and OS) of G12 patients according to age (panels A and C) and gender (panel B and D). **(A)** mPFS of patients < 65 years (n = 62) *vs*. patients > 65 years (n = 119): 6.0 months (95% CI 4.0–11.0 months) *vs*. 4.0 months (95% CI 4.0–6.0 months), p = 0.518. **(B)** mPFS of female (n = 71) *vs*. male (n = 110): 6.0 months (95% CI 4.0–11.0 months) *vs*. 4.0 months (95% CI 3.0–6.0 months), p = 0.013. **(C)** mOS of patients < 65years (n = 56) *vs*. patients > 65 years (n = 109): 20.5 months (95% CI 10.0–NR months) *vs*. 13.0 months (95% CI 9.0–17.0 months), p = 0.007. **(D)** mOS of female (n = 63) *vs*. male (n = 102): 23.0 months (95% CI 18.0–NR months) *vs*. 14.5 months (95% CI 9.0–17.0 months), p = 0.004.

ranging from 3.5 to 4 months (p = 0.591). The mOS was 16.0 months (12.0–19.0 months) and none of the main isoforms analyzed seems to benefit from CT (p = 0.800). We then evaluated the outcome of treatment including ICI both on the total population (n = 94) and according to a major single mutation. Intriguingly, although the global mPFS was 6.0 months, isoforms C and V showed the same lower median of 4.0 months (3.0–12.0 months for V and 4.0–18.0 months for C). Mutations D and A instead showed higher mPFS (8.0 months, 6.0–NR and 9.0 months, 4.0–NR, respectively). Later, we chose to compare the outcomes of the better prognosis mutations C (n = 43), D (n = 16), and A (n = 10) with isoform V (n = 19) to evaluate the importance of the individual mutations in a population homogeneously exposed to ICI (Figures 3A–C). Interestingly, despite mPFS being similar in the two groups, we highlighted a favorable trend in PFS for C compared with the V isoform (p = 0.114) (Figure 3A). As shown in the figure, a similar trend was also described for D (p = 0.165) and A (p = 0.140) mutations when compared to V (Figures 3B, C). The mOS of the ICI-exposed subgroup (n = 78) was 15 months (8.0–20.0 months). As seen for PFS, V proved to be the mutation with the

TABLE 3 Univariate and multivariate overall survival analysis.

Characteristics	Univariate			Multivariate		
	HR	95% CI	*p*	HR	95% CI	*p*
Sex (female *vs.* male)	1.78	1.21–2.64	**0.004**	1.71	1.16–2.53	**0.007**
Age (<65 *vs.* ≥65)	1.71	1.15–2.55	**0.008**	1.63	1.09–2.44	**0.016**
PD-L1 (<1 *vs.* 1–49)	1.12	0.61–2.06	0.707			
PD-L1 (<1 *vs.* ≥50)	1.47	0.88–2.44	0.138			
G12 mutations (C *vs.* D)	1.38	0.84–2–27	0.209			
G12 mutations (C *vs.* A)	1.13	0.57–2.23	0.725			
G12 mutations (C *vs.* V)	1.44	0.90–2.29	0.130			
G12 mutations (C *vs.* Others)	1.41	0.67–2.98	0.365			
First line (ICI ± CT *vs.* CT)	0.69	0.47–1.00	**0.048**	0.66	0.46–0.97	**0.034**

Bold was used to pin point data with relevance.

worst prognosis (mOS: 9.0 months, 4.0–NR) unlike the C (15.0 months, 6.0–NR), D (11.5 months, 7.0–NR), and A (20.0 months, 15.0–NR) mutations even if the comparison between better-survival mutations and the V isoform showed no significant differences. Finally, the PD-L1 expression seems to not have a prognostic role. We observed the worst outcome for those expressing PD-L1 > 50% (mOS 8.50 months, 4.0–21.0 months) who were exposed to ICI alone, while patients with PD-L1 <1% or 1%–49% who underwent CT-ICI had a mOS of 17.0 and 15.5 months, respectively ($p = 0.404$).

Discussion

The role and characteristics of intracellular membrane proteins from the RAS family as the hub for signaling of receptor tyrosine kinases (RTK) (29, 30), G-protein-coupled receptors (GPCR) (31), and members of the integrin family (32) have been known for decades. The switch between an inactive GDP-bound and an active GTP-bound state, mediated by GTPase activating protein (GAP) and guanine nucleotide exchange factors (GEFs) (33, 34), was a well-known mechanism leading to several downstream pathways' activation, especially RAF1 and PI3K (1). Somatic Ras mutations are prone to different switching times between an active and an inactive Ras state and to different GTP hydrolysis rates (27, 35), and the activation of different downstream pathways according to different single-amino acid substitutions in mutant KRAS tumors has been described (36–38). This evidence supports the renowned undruggability of KRAS directly or through several targets of up- or downstream signaling.

The recent discovery of drugs (sotorasib and adagrasib) able to selectively bind G12C with favorable efficacy/toxicity ratio has

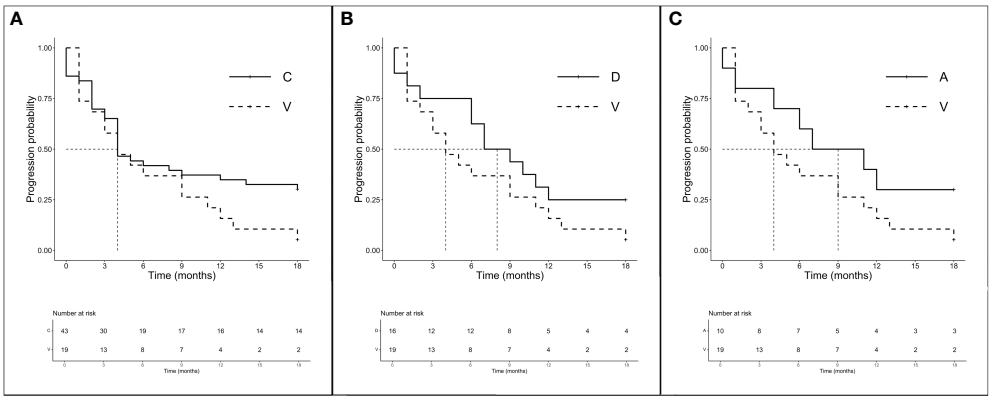

FIGURE 3
PFS according to single amino acid substitutions in patients treated with ICI ± CT ($n = 94$). **(A)** mPFS C ($n = 43$) *vs.* V ($n = 19$): 4.0 months (95% CI 4.0–18.0 months) *vs.* 4.0 months (95% CI 3.0–12.0 months), $p = 0.114$. **(B)** mPFS D ($n = 16$) *vs.* V ($n = 16$): 8.0 months (95% CI 6.0–NR months) *vs.* 4.0 months (95% CI 3.0–12.0 months), $p = 0.165$. **(C)** mPFS A ($n = 10$) *vs.* V ($n = 16$): 9.0 months (95% CI 4.0–NR months) *vs.* 4.0 months (95% CI 3.0–12.0 months), $p = 0.140$.

modified the concept of KRAS inhibition (39), and we are eager to know the results regarding their efficacy and clinical outcome (NCT04303780; NCT04685135). Despite the efforts and encouraging results of phase 2 trials in the post-first-line setting (14, 15), sotorasib and adagrasib are not recommended as frontline treatment in advanced KRAS G12C LUAD, and the final results of ongoing first-line clinical trials are still pending (e.g., KRYSTAL-7, CodeBreak201, and NCT04933695). Moreover, results on drugs targeting other mutations are still lacking even if several promising drug candidates emerge as inhibitors of other KRAS mutants as per EX185 designated to inhibit KRAS G12D, G12C, and G12V and to engage GNP-bound KRAS (40) or MRTX1133, which has shown efficacy in the KRAS G12D mutant xenograft mouse tumor model (41). Immunotherapy in combination or not with CT according to PD-L1 expression is still the standard in this wide population (18, 19, 42).

In our cohort, we analyzed a homogeneous population of KRAS G12-mutated LUAD patients ($n = 219$) undergoing first-line therapy with CT or ICI alone or their combination. The aim of the study was to characterize a possible unique profile to discriminate each single G12 mutation by treatment outcome or demographic characteristics. According to data from the COSMIC database, we observed comparable G12 amino acid substitution percentage in our population; in particular, the major detected substitutions were C (47.9%), V (20.5%), D (17.4%), and A (8.2%) (3), while the other isoforms (e.g., G, F, S, and I) were rare (less than 6%).

In accordance with Riely and colleagues (43) and preclinical evidence supporting the development of KRAS mutations due to epigenetic changes after tobacco exposure (44), we confirmed the prevalence of the KRAS G12 mutation in patients with smoking habit (95%), especially in transversions (G → T/C). Different from literature, we also described in transition mutations (G → A) a predominance of smokers (86.8%). Patients enrolled in our analysis were predominantly elderly (64.8%) and male (61.2%), which is comparable to the global LUAD distribution. Age and gender results are associated with outcome: female gender was an independent prognostic factor for longer PFS and OS and age <65 years correlated with better OS.

The different sensitivity of the specific mutant KRAS to different treatments (CT, TKIs, or anti-angiogenetics) has been widely described (45, 46), and previous *in vitro* and clinical data suggest that different KRAS mutations have different depths and durations of response to old-fashioned treatments (36, 47, 48). In addition, CT agents as platinum-derived drugs and the anti-metabolite pemetrexed have immunomodulatory properties, being able to increase MHC-I expression and recruitment of effectors (e.g., TILs, macrophages, and memory T cells) and to reduce the activity of players of the immunosuppressive microenvironment such as Tregs (49, 50). Nevertheless, in our analysis, the use of CT was globally unsatisfactory and none of the mutations analyzed had a solid benefit either in PFS or in OS. Based on the results, we investigated the efficacy of ICIs alone or in combination in our population, finding a 38% decreasing risk of disease progression and 34% death in patients receiving first-line treatment including ICI with or without CT.

Several studies attempted to determine the impact of KRAS mutations on the outcome of patients treated with ICI in the advanced setting with contradictory results (51–54). The gain from the addition of ICIs in KRAS-mutated patients is consistent with several retrospective analyses in real life (20–22) and supported by the results of the analysis of the mutated KRAS subgroup in the Keynote-042 trial, where pembrolizumab instead of CT had an ORR of 56.7% versus 18%, and similar benefits were registered in the G12C subgroup with PFS and OS similar to the entire population enrolled (23). Recently, at ASCO 2022, Nakajima and colleagues described an improved OS and ORR in a KRAS-mutated population treated with chemo-immune combination as frontline treatment, confirming our observations (24).

It should be noted that the outcome of KRAS-mutant treatments is dominated by co-occurring genetic events, as STK11/LKB1 and KEAP1 mutations define a subset of "cold" NSCLC resistant to ICI, while *TP53* alterations increase the inflammatory microenvironment, leading to an efficient immune response. However, clinical reports and retrospective gene sequencing did not identify a specific association between certain comutations and single KRAS isoforms (55, 56). Furthermore, the use of gene panels including these comutations has a patchy distribution in clinical practice; thus, information regarding this in our retrospective case series is missing.

The PD-1/PD-L1 axis is involved in the inhibition of the immune system and more specifically in the self-tolerance and regulation of T lymphocyte activity (57). Chen and colleagues described *in vitro* the ability of KRAS to upregulate PD-L1 *via* p-ERK, inducing apoptosis of CD3+ T cells and resulting in immune escape, an unfavorable condition that can be reversed by anti-PD-1 antibody (25). The involvement of other signaling pathways supporting the expression of PD-L1 as MAPK, together with STAT3, but not PI3K, has also been suggested (58). Later, the role of the Akt-mTOR axis (59) and PD-L1 miRNA stabilization (60) offered further evidence of the complexity of the influence of KRAS to PD-L1 in NSCLC. Falk and colleagues (61) described a better prognosis in patients with PD-L1 TPS ≥ 1% in $KRAS^{mut}$ than in $KRAS^{wt}$ exposed to ICI, and several other clinical retrospective examples and literature review support Falk's observations (52, 54, 62). It is evident that the KRAS mutational status could be a potential biomarker of favorable outcome for ICI treatments; however, pivotal ICI trials did not provide univocal data on either the efficacy of these treatments or the biomarker role of PD-L1. In contrast to Falk, our data suggest a trend towards a better prognosis for patients with PD-L1 <50%. These results were partially confirmed in the subgroup analysis of patients treated with ICI with/without CT where an absence or lower PD-L1 expression seems more advantageous than PD-L1 ≥50%.

According to the Italian Medicine Agency, PD-L1 TPS ≥50% is the requirement to prescribe pembrolizumab while the combination with CT is allowed only in patients with expression of PD-L1 <50%, and this could explain the benefit of the population with PD-L1 <50% seen in our analysis. Despite the promising preclinical observations, pivotal clinical trials with the ambition to demonstrate the superiority of CT-ICI combinations did not allow the enrollment of patients with KRAS mutations; therefore, there is a lack of concrete efficacy results in this population.

Even more complex is the understanding of the predictive value of response to treatments when considering individual mutations. We have previously remarked on the lack of benefit across isoforms from the use of CT, which is consistent with the observation by Wiesweg and colleagues who described that isoforms have the same intermediate prognosis (48). Thereafter, we explored the prognostic value of G12C, V, D, and A undergoing ICI ± CT and we instead noted a more unfavorable trend in PFS for G12V compared to G12C, and although mOS between mutations was almost doubled for C (9.0 months *vs*. 15.0 months), the difference was not relevant. Furthermore, V has a worse prognosis than the remaining isoforms, particularly A and D. Differences in OS are observed in these subgroups, although not statistically significant. Ihle in 2012 (36) described a poor outcome affecting patients in the BATTLE-1 trial with isoforms C and V mutated, probably due to the differences in pathway activation, which are supported by *in vitro* analysis highlighting a predominance of p-Akt activation in the D isoform, and a predominance of RalA/B for C and V isoforms. In the BATTLE-1 trial, patients were exposed to several TKIs; however, this evidence suggested a modulation of the pathways when mutations are exposed to similar treatments. Similar to our data, the mPFS of C and V isoforms exposed to ICI was 4 months, but the authors highlighted a worsening PFS in those who have *STK11/LKB1* comutations (63); unfortunately, this information is not available in our dataset. The disadvantageous weight of the V isoform has been extensively described (47, 64–66), and contrary to what has been reported in the literature (63, 67), our series was released from the high expression of PD-L1. As a matter of fact, in our case series and different from literature, the A isoform has a better outcome to ICI treatments, and this is the mutation with a higher rate of PD-L1 expression (>1%: 73.4%) and young patients, while the V mutation shows its worst prognosis in the elderly. Those results are in conflict with the study by Shen Mo et al. (68), according to which KRAS G12D and G12V mutations are better candidates for immunotherapy, whereas patients with KRAS G12A or G12C mutations are not. Intriguingly, and the same as what Jeanson and colleagues described (62), we noticed a better prognosis in those mutations as per A, which expressed a high rate of PD-L1, even if it is not possible to draw final conclusions given the small number of the subgroup.

Conclusions

Despite the limitations derived from the retrospective characteristics of the study and the relative lack of comutation assessment, we can affirm that, to our knowledge, this is the first multicenter, real-life study with this sample size aimed only at G12 mutations in first-line patients undergoing treatment including ICI. We confirmed the scarce efficacy of CT alone in this population, which instead benefits from the use of ICI alone or in combination with CT, a benefit not linked to PD-L1 overexpression. We also confirmed the benefit in some isoforms (C, D, and A) and the negative prognostic value of the V mutation, which maintains a poor prognosis regardless of the treatment chosen, probably related to an aged population and the relative lack of PD-L1 expression in the subgroup.

Data availability statement

The original contributions presented in the study are included in the article, further inquiries can be directed to the corresponding author.

Ethics statement

The studies involving human participants were reviewed and approved by Ethics Committee of Area Vasta Centro (CEAVC) part of the Regional Ethics Committee of the Tuscany Region. The patients/participants provided their written informed consent to participate in this study.

Author contributions

Conceptualization: SF, EC, and SP. Collection of data: SF, GMen, IB, MM, GMet, IP, and CB. Interpretation of data: SF, SP, and EC. Data curation: LV, CC, FC, and CB. Writing—original draft preparation: SF. Writing—review and editing: FM, SP, LA, and LP. Supervision: AD, RB, and LA. All authors have read and agreed to the published version of the manuscript. All authors contributed to the article and approved the submitted version.

Funding

The data collection and the writing of the entire project are partially supported by ERA PerMed, having participated in the call "Second Joint Transnational Call for Proposals (JTC) 2019 on Personalized Medicine: Multidisciplinary Research Towards Implementation within the framework of ERA PerMed", passed the final selection, and obtained the required funding and funds

of Professor Antonuzzo, Department of Experimental and Clinical Medicine, University of Florence.

Conflict of interest

The authors declare that the research was conducted in the absence of commercial or financial relationships that could be construed as a potential conflict of interest.

Publisher's note

References

1. Gimple RC, Wang X. RAS: Striking at the core of the oncogenic circuitry. *Front Oncol* (2019) 9:965. doi: 10.3389/fonc.2019.00965

2. Forbes SA, Beare D, Boutselakis H, Bamford S, Bindal N, Tate J, et al. COSMIC: Somatic cancer genetics at high-resolution. *Nucleic Acids Res* (2017) 45: D777–83. doi: 10.1093/nar/gkw1121

3. COSMIC database. (2022). Available at: https://cancer.sanger.ac.uk/cosmic/gene/analysis?all_data=&coords=AA%3AAA&dr=&end=190&gd=&id=398646&ln=KRAS&seqlen=190&sn=lung&start=1#ts (Accessed May 19, 2022).

4. Hammerman PS, Voet D, Lawrence MS, Voet D, Jing R, Cibulskis K, et al. Comprehensive genomic characterization of squamous cell lung cancers. *Nature* (2012) 489:519–25. doi: 10.1038/nature11404

5. Jemal A, Siegel R, Ward E, Hao Y, Xu J, Murray T, et al. Cancer statistics, 2008. *Cancer J Clin* (2008) 58:71–96. doi: 10.3322/CA.2007.0010

6. Yu HA, Sima CS, Shen R, Kass S, Gainor J, Shaw A, et al. Prognostic impact of KRAS mutation subtypes in 677 patients with metastatic lung adenocarcinomas. *J Thorac Oncol* (2015) 10:431–7. doi: 10.1097/JTO.0000000000000432

7. Shepherd FA, Domerg C, Hainaut P, Jänne PA, Pignon J-P, Graziano S, et al. Pooled analysis of the prognostic and predictive effects of KRAS mutation status and KRAS mutation subtype in early-stage resected non-Small-Cell lung cancer in four trials of adjuvant chemotherapy. *J Clin Oncol* (2013) 31:2173–81. doi: 10.1200/JCO.2012.48.1390

8. Mellema WW, Masen-Poos L, Smit EF, Hendriks LEL, Aerts JG, Termeer A, et al. Comparison of clinical outcome after first-line platinum-based chemotherapy in different types of KRAS mutated advanced non-small-cell lung cancer. *Lung Cancer* (2015) 90:249–54. doi: 10.1016/j.lungcan.2015.09.012

9. Eberhard DA, Johnson BE, Amler LC, Goddard AD, Heldens SL, Herbst RS, et al. Mutations in the epidermal growth factor receptor and in KRAS are predictive and prognostic indicators in patients with non-small-cell lung cancer treated with chemotherapy alone and in combination with erlotinib. *J Clin Oncol* (2005) 23:5900–9. doi: 10.1200/JCO.2005.02.857

10. Zhu C-Q, da Cunha Santos G, Ding K, Sakurada A, Cutz J-C, Liu N, et al. Role of KRAS and EGFR as biomarkers of response to erlotinib in national cancer institute of Canada clinical trials group study BR.21. *J Clin Oncol* (2008) 26:4268–75. doi: 10.1200/JCO.2007.14.8924

11. Schneider CP, Heigener D, Schott-Von-Römer K, Gütz S, Laack E, Digel W, et al. Epidermal growth factor receptor-related tumor markers and clinical outcomes with erlotinib in non-small cell lung cancer: An analysis of patients from german centers in the trust study. *J Thorac Oncol* (2008) 3:1446–53. doi: 10.1097/JTO.0b013e31818ddcaa

12. Li B, Skoulidis F, Falchook G, Sacher A, Velcheti V, Dy G, et al. PS01.07 registrational phase 2 trial of sotorasib in KRAS p.G12C mutant NSCLC: First disclosure of the codebreak 100 primary analysis. *J Thorac Oncol* (2021) 16:S61. doi: 10.1016/j.jtho.2021.01.321

13. Jänne PA, Riely GJ, Gadgeel SM, Heist RS, Ou S-HI, Pacheco JM, et al. Adagrasib in non–Small-Cell lung cancer harboring a KRASG12C mutation. *New Engl J Med* (2022) 33:1–12. doi: 10.1056/NEJMoa2204619

14. *FDA Grants accelerated approval to sotorasib for KRAS G12C mutated NSCLC* (2021). Available at: https://www.fda.gov/drugs/resources-information-approved-drugs/fda-grants-accelerated-approval-sotorasib-kras-g12c-mutated-nsclc.

15. *U.S. food and drug administration (FDA) accepts mirati therapeutics' new drug application for adagrasib as treatment of previously treated KRASG12C-mutated non-small cell lung cancer* (2022). Available at: https://ir.mirati.com/press-releases/press-release-details/2022/U.S.-Food-and-Drug-Administration-FDA-Accepts-Mirati-Therapeutics-New-Drug-Application-for-Adagrasib-as-Treatment-of-Previously-Treated-KRASG12C-Mutated-Non-Small-Cell-Lung-Cancer/default.asp.

16. Skoulidis F, Goldberg ME, Greenawalt DM, Hellmann MD, Awad MM, Gainor JF, et al. STK11/LKB1 mutations and PD-1 inhibitor resistance in KRAS -mutant lung adenocarcinoma. *Cancer Discovery* (2018) 8:822–36. doi: 10.1158/2159-8290.CD-18-0099

17. Helena JJ van R, Azad T, Ling M, Hao Y, Snetsinger B, Khanal P, et al. The hippo pathway component taz promotes immune evasion in human cancer through PD-L1. *Cancer Res* (2018) 78:1457–70. doi: 10.1158/0008-5472.CAN-17-3139

18. Planchard D, Popat S, Kerr K, Novello S, Smit EF, Faivre-Finn C, et al. Correction to: "Metastatic non-small cell lung cancer: ESMO clinical practice guidelines for diagnosis, treatment and follow-up". *Ann Oncol* (2019) 30:863–70. doi: 10.1093/annonc/mdy474

19. Paz-Ares L, Ciuleanu TE, Cobo M, Schenker M, Zurawski B, Menezes J, et al. First-line nivolumab plus ipilimumab combined with two cycles of chemotherapy in patients with non-small-cell lung cancer (CheckMate 9LA): an international, randomised, open-label, phase 3 trial. *Lancet Oncol* (2021) 22:198–211. doi: 10.1016/S1470-2045(20)30641-0

20. Amanam I, Mambetsariev I, Gupta R, Achuthan S, Wang Y, Pharaon R, et al. Role of immunotherapy and co-mutations on KRAS-mutant nonsmall cell lung cancer survival. *J Thorac Dis* (2020) 12:5086–95. doi: 10.21037/jtd.2020.04.18

21. Liu C, Zheng S, Jin R, Wang X, Wang F, Zang R, et al. The superior efficacy of anti-PD-1/PD-L1 immunotherapy in KRAS-mutant non-small cell lung cancer that correlates with an inflammatory phenotype and increased immunogenicity. *Cancer Lett* (2020) 470:95–105. doi: 10.1016/j.canlet.2019.10.027

22. Dietrich M, Hunis B, Raez L. P2.07-052 detection of KRAS mutation in blood predicts favorable response to immunotherapy in NSCLC. *J Thorac Oncol* (2017) 12:S2149. doi: 10.1016/j.jtho.2017.09.1308

23. Herbst RS, Lopes G, Kowalski DM, Kasahara K, Wu Y-L, de Castro G, et al. LBA4 association of KRAS mutational status with response to pembrolizumab monotherapy given as first-line therapy for PD-L1-positive advanced non-squamous NSCLC in keynote-042. *Ann Oncol* (2019) 30:xi63–4. doi: 10.1093/annonc/mdz453.001

24. Nakajima E, Ren Y, Vallejo J, Al. E. Outcomes of first-line immune checkpoint inhibitors with or without chemotherapy according to KRAS mutational status and PD-L1 expression in patients with advanced NSCLC: FDA pooled analysis. *JCO* (2022) 40:9001. doi: 10.1200/JCO.2022.40.16_suppl.9001

25. Chen N, Fang W, Lin Z, Peng P, Wang J, Zhan J, et al. KRAS mutation-induced upregulation of PD-L1 mediates immune escape in human lung adenocarcinoma. *Cancer Immunol Immunother* (2017) 66:1175–87. doi: 10.1007/s00262-017-2005-z

26. Incecco AD, Andreozzi M, Ludovini V, Rossi E, Capodanno A, Landi L, et al. PD-1 and PD-L1 expression in molecularly selected non-small-cell lung cancer patients. *British Journal of Cancer* (2015) 112:95–102. doi: 10.1038/bjc.2014.555

27. Koltun E, Cregg J, Rice MA, Whalen DM, Freilich R, Jiang J, et al. Abstract 1260: First-in-class, orally bioavailable KRAS<sup<G12V</sup<(ON) tri-complex inhibitors, as single agents and in combinations, drive profound anti-tumor activity in preclinical models of KRAS<sup<G12V</sup< mutant cancers. *Cancer Res* (1260) 2021) 81:1260. doi: 10.1158/1538-7445.AM2021-1260

28. Glorieux C, Xia X, He YQ, Hu Y, Cremer K, Robert A, et al. Regulation of PD-L1 expression in K-ras-driven cancers through ROS-mediated FGFR1 signaling. *Redox Biol* (2021) 38:101780. doi: 10.1016/j.redox.2020.101780

29. Buday L, Downward J. Epidermal growth factor regulates p21ras through the formation of a complex of receptor, Grb2 adapter protein, and sos nucleotide exchange factor. *Cell* (1993) 73:611–20. doi: 10.1016/0092-8674(93)90146-H

30. Arvidsson AK, Rupp E, Nånberg E, Downward J, Rönnstrand L, Wennström S, et al. Tyr-716 in the platelet-derived growth factor beta-receptor

kinase insert is involved in GRB2 binding and ras activation. *Mol Cell Biol* (1994) 14:6715–26. doi: 10.1128/mcb.14.10.6715

31. Wan Y, Kurosaki T, Huang X-Y. Tyrosine kinases in activation of the MAP kinase cascade by G-protein-coupled receptors. *Nature* (1996) 380:541–4. doi: 10.1038/380541a0

32. Clark EA, Hynes RO. Ras activation is necessary for integrin-mediated activation of extracellular signal-regulated kinase 2 and cytosolic phospholipase a 2 but not for cytoskeletal organization. *J Biol Chem* (1996) 271:14814–8. doi: 10.1074/jbc.271.25.14814

33. Vigil D, Cherfils J, Rossman KL, Der CJ. Ras superfamily GEFs and GAPs: validated and tractable targets for cancer therapy? *Nat Publishing Group* (2010) 10 (12):842–57. doi: 10.1038/nrc2960

34. Cherfils J, Zeghouf M. Regulation of small GTPases by GEFs, GAPs, and GDIs. *Physiol Rev* (2013) 93:269–309. doi: 10.1152/physrev.00003.2012

35. Mccormick F. Sticking it to KRAS : Covalent inhibitors enter the clinic. *Cancer Cell* (2020) 37:3–4. doi: 10.1016/j.ccell.2019.12.009

36. Ihle NT, Byers LA, Kim ES, Saintigny P, Lee JJ, Blumenschein GR, et al. Effect of KRAS oncogene substitutions on protein behavior: Implications for signaling and clinical outcome. *J Natl Cancer Inst* (2012) 104:228–39. doi: 10.1093/jnci/djr523

37. Hunter JC, Manandhar A, Carrasco MA, Gurbani D, Gondi S, Westover KD. Biochemical and structural analysis of common cancer-associated KRAS mutations. *Mol Cancer Res* (2015) 13:1325–35. doi: 10.1158/1541-7786.MCR-15-0203

38. Virtudes Céspedes M, Josep Sancho F, Guerrero S, Parreñ M, Casanova I, Angel Pavón M, et al. K-Ras Asp12 mutant neither interacts with raf, nor signals through erk and is less tumorigenic than K-ras Val12. *Carcinogenesis* (2006) 27 (11):2190-200. doi: 10.1093/carcin/bgl063

39. Ostrem JM, Peters U, Sos ML, Wells JA, Shokat KM. K-Ras (G12C) inhibitors allosterically control GTP affinity and effector interactions. *Nature* (2013) 503:548–51. doi: 10.1038/nature12796

40. Vasta JD, Peacock DM, Zheng Q, Walker JA, Zhang Z, Zimprich CA, et al. KRAS is vulnerable to reversible switch-II pocket engagement in cells. *Nat Chem Biology* (2022) 18:596–604. doi: 10.1101/2021.10.15.464544

41. Wang X, Allen S, Blake JF, Bowcut V, Briere DM, Calinisan A, et al. Identification of MRTX1133, a noncovalent, potent, and selective KRAS G12D inhibitor. *Cite This: J Med Chem* (2021) 2022:3133. doi: 10.1021/acs.jmedchem.1c01688

42. Gandhi L, Rodríguez-Abreu D, Gadgeel S, Esteban E, Felip E, de Angelis F, et al. Pembrolizumab plus chemotherapy in metastatic non–Small-Cell lung cancer. *New Engl J Med* (2018) 378:2078–92. doi: 10.1056/nejmoa1801005

43. Riely GJ, Kris MG, Rosenbaum D, Marks J, Li A, Chitale DA, et al. Frequency and distinctive spectrum of KRAS mutations in never smokers with lung adenocarcinoma. *Clin Cancer Res* (2008) 14:5731–4. doi: 10.1158/1078-0432.CCR-08-0646

44. Vaz M, Hwang SY, Kagiampakis I, Phallen J, Patil A, O'Hagan HM, et al. Chronic cigarette smoke-induced epigenomic changes precede sensitization of bronchial epithelial cells to single-step transformation by KRAS mutations. *Cancer Cell* (2017) 32:360–376.e6. doi: 10.1016/j.ccell.2017.08.006

45. Renaud S, Guerrera F, Seitlinger J, Reeb J, Voegeli C, Legrain M, et al. KRAS-specific amino acid substitutions are associated with different responses to chemotherapy in advanced non-small cell lung cancer. *Clin Lung Cancer* (2018) 1:e919-e931. doi: 10.1016/j.cllc.2018.08.005

46. Metro G, Chiari R, Duranti S, Siggillino A, Fischer MJ, Giannarelli D, et al. Impact of specific mutant KRAS on clinical outcome of EGFR-TKI-treated advanced non-small cell lung cancer patients with an EGFR wild type genotype. *Lung Cancer* (2012) 78:81–6. doi: 10.1016/J.LUNGCAN.2012.06.005

47. Garassino M, Marabese M, Rusconi P, Rulli E, Martelli O, Farina G. Different types of K-ras mutations could affect drug sensitivity and tumour behaviour in non-small-cell lung cancer. *Ann Oncol* (2011) 24:92–6. doi: 10.5791/0882-2875-24.2.92

48. Wiesweg M, Kasper S, Worm K, Herold T, Reis H, Sara L, et al. Impact of RAS mutation subtype on clinical outcome–a cross-entity comparison of patients with advanced non-small cell lung cancer and colorectal cancer. *Oncogene* (2019) 38:2953–66. doi: 10.1038/s41388-018-0634-0

49. Cavazzoni A, Digiacomo G, Alfieri R, Monica S, Fumarola C, Galetti M, et al. Pemetrexed enhances membrane PD-L1 expression and potentiates T cell-mediated cytotoxicity by anti-PD-L1 antibody therapy in non-Small-Cell lung cancer. *Cancers (Basel)* (2020) 12:666. doi: 10.3390/cancers12030666

50. de Biasi AR, Villena-Vargas J, Adusumilli PS. Cisplatin-induced antitumor immunomodulation: A review of preclinical and clinical evidence. *Clin Cancer Res* (2014) 20(21):5384–91. doi: 10.1158/1078-0432.CCR-14-1298

51. Torralvo J, Friedlaender A, Achard V, Addeo A. The activity of immune checkpoint inhibition in kras mutated non-small cell lung cancer: A single centre experience. *Cancer Genomics Proteomics* (2019) 16:577–82. doi: 10.21873/cgp.20160

52. Passiglia F, Cappuzzo F, Alabiso O, Bettini AC, Bidoli P, Chiari R, et al. ARTICLE efficacy of nivolumab in pre-treated non-small-cell lung cancer patients harbouring KRAS mutations. *Br J Cancer* (2019) 120:57–62. doi: 10.1038/s41416-018-0234-3

53. Mazieres J, Drilon A, Lusque A, Mhanna L, Cortot AB, Mezquita L, et al. Immune checkpoint inhibitors for patients with advanced lung cancer and oncogenic driver alterations: Results from the IMMUNOTARGET registry. *Ann Oncol* (2019) 30:1321–8. doi: 10.1093/annonc/mdz167

54. Kim JH, Kim HS, Kim BJ. Prognostic value of KRAS mutation in advanced non-small-cell lung cancer treated with immune checkpoint inhibitors: A metaanalysis and review. *Oncotarget* (2017) 8:48248–52. doi: 10.18632/oncotarget.17594

55. Skoulidis F, Byers LA, Diao L, Papadimitrakopoulou VA, Tong P, Izzo J, et al. Co-Occurring genomic alterations define major subsets of KRAS-mutant lung adenocarcinoma with distinct biology, immune profiles, and therapeutic vulnerabilities. *Cancer Discovery* (2015) 5:861–78. doi: 10.1158/2159-8290.CD-14-1236

56. Arbour KC, Jordan E, Kim HR, Dienstag J, Yu HA, Sanchez-Vega F, et al. Effects of co-occurring genomic alterations on outcomes in patients with KRAS-mutant non-small cell lung cancer. *Clin Cancer Res* (2018) 24:334–40. doi: 10.1158/1078-0432.CCR-17-1841

57. Pardoll DM. The blockade of immune checkpoints in cancer immunotherapy. *Nat Publishing Group* (2012) 12:252–64. doi: 10.1038/nrc3239

58. Sumimoto H, Takano A, Teramoto K, Daigo Y. RAS-Mitogen-Activated protein kinase signal is required for enhanced PD-L1 expression in human lung cancers. *PLOS ONE* (2016) 11(11):e0166626. doi: 10.1371/journal.pone.0166626

59. Lastwika KJ, Iii WW, Li QK, Norris J, Xu H, Ghazarian SR, et al. Microenvironment and immunology control of PD-L1 expression by oncogenic activation of the AKT-mTOR pathway in non-small cell lung cancer. *Cancer Res* (2016) 76(2):227–38. doi: 10.1158/0008-5472.CAN-14-3362

60. Coelho MA, de Carné Trécesson S, Rana S, Zecchin D, Moore C, Molina-Arcas M, et al. Oncogenic RAS signaling promotes tumor immunoresistance by stabilizing PD-L1 mRNA. *Immunity* (2017) 47:1083–99.e6. doi: 10.1016/j.immuni.2017.11.016

61. Falk AT, Yazbeck N, Guibert N, Chamorey E, Paquet A, Ribeyre L, et al. Effect of mutant variants of the KRAS gene on PD-L1 expression and on the immune microenvironment and association with clinical outcome in lung adenocarcinoma patients. *Lung Cancer* (2018) 121:70–5. doi: 10.1016/j.lungcan.2018.05.009

62. Jeanson A, Tomasini P, Souquet-Bressand M, Brandone N, Boucekine M, Grangeon M, et al. Efficacy of immune checkpoint inhibitors in KRAS-mutant non-small cell lung cancer (NSCLC). *J Thorac Oncol* (2019) 14:1095–101. doi: 10.1016/j.jtho.2019.01.011

63. Tamiya Y, Zenke Y, Matsumoto S, Furuya N, Sakamoto T, Kato T, et al. Therapeutic impact of mutation subtypes and concomitant STK11 mutations in KRAS–mutated non-small cell lung cancer (NSCLC): A result of nationwide genomic screening project (LC-SCRUM-Japan). *J Clin Oncol* (2020) 38:9589. doi: 10.1200/JCO.2020.38.15_suppl.9589

64. Renaud S, Falcoz PE, Schaëffer M, Guenot D, Romain B, Olland A, et al. Prognostic value of the KRAS G12V mutation in 841 surgically resected Caucasian lung adenocarcinoma cases. *Br J Cancer* (2015) 113:1206–15. doi: 10.1038/bjc.2015.327

65. Nadal E, Chen G, Prensner JR, Shiratsuchi H, Sam C, Zhao L, et al. KRAS-G12C mutation is associated with poor outcome in surgically resected lung adenocarcinoma. *J Thorac Oncol* (2014) 9:1513–22. doi: 10.1097/JTO.0000000000000305

66. Wu SG, Liao WY, Su KY, Yu SL, Huang YL, Yu CJ, et al. Prognostic characteristics and immunotherapy response of patients with nonsquamous NSCLC with kras mutation in East Asian populations: A single-center cohort study in Taiwan. *JTO Clin Res Rep* (2021) 2:100140. doi: 10.1016/j.jtocrr.2020.100140

67. Pan LN, Ma YF, Li Z, Hu JA, Xu ZH. KRAS G12V mutation upregulates PD-L1 expression *via* TGF-β/EMT signaling pathway in human non-small-cell lung cancer. *Cell Biol Int* (2021) 45:795–803. doi: 10.1002/cbin.11524

68. Shen M, Qi R, Ren J, Lv D, Yang H. Characterization with KRAS mutant is a critical determinant in immunotherapy and other multiple therapies for non-small cell lung cancer. *Front Oncol* (2022) 11:780655. doi: 10.3389/fonc.2021.780655

frontiers | Frontiers in Oncology

TYPE Review
PUBLISHED 22 November 2022
DOI 10.3389/fonc.2022.1004669

OPEN ACCESS

EDITED BY
Michele Simbolo,
University of Verona, Italy

REVIEWED BY
Marina Trombetta Lima,
University of Groningen, Netherlands
Sriram Chandrasekaran,
University of Michigan, United States
Linchong Sun,
Guangdong Academy of Medical Sciences, China

*CORRESPONDENCE
Ren-Wang Peng
renwang.peng@insel.ch
Patrick Dorn
patrick.dorn@insel.ch

SPECIALTY SECTION
This article was submitted to Thoracic Oncology, a section of the journal Frontiers in Oncology

RECEIVED 27 July 2022
ACCEPTED 31 October 2022
PUBLISHED 22 November 2022

CITATION
Ning W, Marti TM, Dorn P and Peng R-W (2022) Non-genetic adaptive resistance to KRAS^{G12C} inhibition: EMT is not the only culprit. *Front. Oncol.* 12:1004669. doi: 10.3389/fonc.2022.1004669

Non-genetic adaptive resistance to KRAS^{G12C} inhibition: EMT is not the only culprit

Wenjuan Ning[1,2], Thomas M. Marti[1,2], Patrick Dorn[1,2]* and Ren-Wang Peng[1,2]*

[1]Division of General Thoracic Surgery, Inselspital, Bern University Hospital, University of Bern, Bern, Switzerland, [2]Department for BioMedical Research (DBMR), University of Bern, Bern, Switzerland

Adaptions to therapeutic pressures exerted on cancer cells enable malignant progression of the tumor, culminating in escape from programmed cell death and development of resistant diseases. A common form of cancer adaptation is non-genetic alterations that exploit mechanisms already present in cancer cells and do not require genetic modifications that can also lead to resistance mechanisms. Epithelial-to-mesenchymal transition (EMT) is one of the most prevalent mechanisms of adaptive drug resistance and resulting cancer treatment failure, driven by epigenetic reprogramming and EMT-specific transcription factors. A recent breakthrough in cancer treatment is the development of KRAS^{G12C} inhibitors, which herald a new era of therapy by knocking out a unique substitution of an oncogenic driver. However, these highly selective agents targeting KRAS^{G12C}, such as FDA-approved sotorasib (AMG510) and adagrasib (MRTX849), inevitably encounter multiple mechanisms of drug resistance. In addition to EMT, cancer cells can hijack or rewire the sophisticated signaling networks that physiologically control cell proliferation, growth, and differentiation to promote malignant cancer cell phenotypes, suggesting that inhibition of multiple interconnected signaling pathways may be required to block tumor progression on KRAS^{G12C} inhibitor therapy. Furthermore, the tumor microenvironment (TME) of cancer cells, such as tumor-infiltrating lymphocytes (TILs), contribute significantly to immune escape and tumor progression, suggesting a therapeutic approach that targets not only cancer cells but also the TME. Deciphering and targeting cancer adaptions promises mechanistic insights into tumor pathobiology and improved clinical management of KRAS^{G12C}-mutant cancer. This review presents recent advances in non-genetic adaptations leading to resistance to KRAS^{G12C} inhibitors, with a focus on oncogenic pathway rewiring, TME, and EMT.

KEYWORDS

non-genetic adaptive resistance, KRAS G12C inhibitors, EMT, symbiosis, TME

Introduction

Lung cancer is the most commonly diagnosed malignancies and the leading cause of cancer death worldwide, with 5-year survival rates still below 15% (1). The majority of patients with lung cancer are diagnosed with non-small cell lung cancer (NSCLC), which has benefited significantly from biomarker-guided targeted therapies (2). For example, EGFR tyrosine kinase inhibitors (e.g., gefitinib, erlotinib, and afatinib) and ALK tyrosine kinase inhibitors (e.g., crizotinib, ceritinib) have demonstrated superior objective response rates and significant better progression-free survival in NSCLC patients harboring epidermal growth factor receptor (EGFR) mutations or anaplastic lymphoma kinase (ALK) rearrangements than conventional one-fit-all chemotherapy (3, 4).

KRAS is the most frequently mutated oncoprotein in human cancers, affecting 25% to 30% of patients with NSCLC (5). Ironically, unlike the oncoproteins EGFR and ALK, which are less prevalently altered in NSCLC, there are few targeted therapies for *KRAS*-mutant NSCLC, and few clinical studies have specifically addressed this largest NSCLC subpopulation (6, 7). To date, direct inhibition of various mutant KRAS proteins has been a clinical challenge (7). Farnesyl transferase inhibitors designed to specifically inhibit KRAS by disrupting the protein's association with the plasma membrane, showed little clinical efficacy, as did agents targeting effector proteins downstream of KRAS, such as the coveted RAF-MEK-ERK (MAPK) signaling pathway (8, 9).

The revolution in the fighting against KRAS-mutant cancers occurred in 2012 when a breakthrough study showed that KRAS with G12C (glycine to cysteine) substitution can be targeted by a group of small molecules that bind covalently to the substituted cysteine in the Switch-II pocket of the protein (10) (Table 1). This finding provided the impetus for further studies that eventually culminated in the FDA approval of the first KRAS inhibitor, sotorasib (AMG510), for the treatment of locally advanced or metastatic lung cancer with $KRAS^{G12C}$ mutation, putting an end to the legend of "undruggable RAS proteins" (11). Since these inhibitors preferentially target GDP-bound KRAS (inactive form), a prerequisite for their efficacy is that $KRAS^{G12C}$ retains GTPase activity, which converts the allosteric switch of $KRAS^{G12C}$ from a GTP-bound to a GDP-bound conformation with assistance of GTPase-activating proteins (GAPs) such as neurofibromin 1 (NF1) (12, 13).

Despite this milestone, there is still an unmet need to target other KRAS-mutant alleles (e.g., G12D, G12V, G13D, and Q61H). In addition, $KRAS^{G12C}$ inhibitors are confronted with low response rates (intrinsic resistance) and development of resistant disease (acquired resistance) (14–17). While intrinsic resistance occurs due to preexisting clonal cancer cells that are refractory to and outgrow upon treatment, cancer cells can also develop the phenotype of adaptive or acquired resistance during treatment. The general concept of intrinsic and acquired resistance to anticancer therapy Has been very recently reviewed elsewhere (18).

Cancer cells can develop drug resistance by acquiring novel genetic alterations that promote tumor growth, such as a novel missense mutation of the KRAS protein other than $KRAS^{G12C}$ or at a site that affects the Switch-II pocket (S-IIP) conformation, or amplification of upstream receptor tyrosine kinases (RTKs) (19). Here, we focus on the mechanisms of resistance to $KRAS^{G12C}$ inhibitor therapy driven by phenotypic plasticity and the identification of alternative strategies to overcome resistance. First, cancer cells can use non-genetic adaptions to counteract targeted inhibition of $KRAS^{G12C}$ because oncogenic pathways are woven into intricate signaling circuits, allowing alternative pathways to assume the role of maintaining proliferating activities upon the inhibition of one pathway. Second, the tumor microenvironment (TME) of cancer cells, such as tumor-infiltrating lymphocytes (TILs), contribute significantly to immune escape and tumor progression, suggesting a therapeutic approach that targets not only cancer cells but also the TME. Third, EMT, an important phenotypic plasticity program, has been identified as a major cause of both intrinsic and acquired resistance to $KRAS^{G12C}$ inhibitors, as well as inhibition of the MAPK pathway (20–22). This type of

TABLE 1 $KRAS^{G12C}$ inhibitors.

$KRAS^{G12C}$ inhibitor	Chemical name	Drug name	Trade name(s)
1st generation	ARS853	–	–
2nd generation	ARS1620	–	–
In clinical trial	AMG510	Sotorasib	Lumakras, Lumykras
	MRTX849	Adagrasib	–
	HBI-2438	–	–
	JAB-21822	–	–
	JDQ443	–	–
	D-1553	–	–
	HS-10370	–	–

adaption take advantage of mechanism already present in cancer cells and does not require genetic modifications.

Recent evidence has shown that cancer cells can employ multiple mechanisms driven by non-genetic adaptations to counteract therapeutic pressure. Fully deciphering these mechanisms will provide new approaches to prevent cancer cells from escaping programmed cell death and to restore their susceptibility to $KRAS^{G12C}$-targeted therapy (23). Interestingly, the adaptive response of cells to cancer therapy has in part in common with the phenotypic plasticity by which cancer cells evolve during metastasis (reviewed in (24)). In this context, it has been proposed that the biological pathways underlying the phenotypic plasticity of scattered tumor cells during metastasis can be classified into five categories, e.g., EMT, stemness, metabolism, dormancy, and host-organ mimicry (25). In this review, we extend this concept of phenotypic plasticity and specifically addresses therapy-induced plasticity of cancer cells (e.g., rewiring of oncogenic signaling pathways, phenotypic switching, and remodeling of the TME) in the context of resistance to $KRAS^{G12C}$ inhibitors. In particular, we focus on the causal contribution of oncogenic signaling bypass, the symbiotic interaction between cancer cells and TME and EMT, and strategies to improve $KRAS^{G12C}$ inhibitor therapy.

Non-genetic adaptive resistance to $kras^{G12C}$ inhibition: bypassing oncogenic signaling pathways

RAS proteins (KRAS, NRAS, and HRAS) transduce extracellular signals from upstream RTKs to downstream signaling pathways, with the mitogen-activated protein kinase (MAPK) cascade RAF-MEK-ERK and the PI3K-AKT-mTOR pathway being best studied (26). Although both pathways play critical roles in cell proliferation and survival, the MAPK pathway is considered the major downstream effector of RAS proteins (Figure 1).

The RAF-MEK-ERK and PI3K-AKT-mTOR pathways negatively interact with each other and thus may compensate when one of them is inhibited (27). Indeed, ARS1620, a second-generation covalent inhibitor of $KRAS^{G12C}$, has been reported to synergize *in vitro* and *in vivo* with several PI3K inhibitors in $KRAS^{G12C}$ mutant cancer cells (e.g., HCC44, H2122 and SW1573) that exhibit intrinsic resistance to ARS1620 (28). That RAF/MEK/ERK and PI3K/AKT/mTOR are tightly intertwined and compensate for each other has been further confirmed by the combinatorial effects of MEK and AKT inhibitors in RAS-mutated multiple myeloma, which significantly increased apoptotic cell death compared with single agents (29).

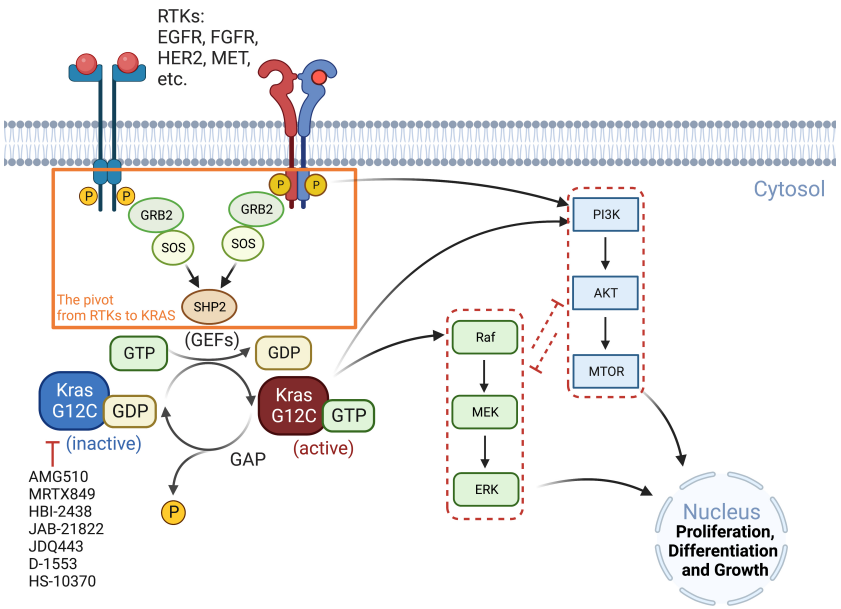

FIGURE 1
Oncogenic KRAS signaling pathway. KRAS switches between the GDP-bound inactive form and the GTP-bound active state, which is facilitated by GEFs and GAP, respectively. Activated RTKs relay extracellular signals from GRB2 to SOS, one of the major GEFs, to SHP2 and to KRAS. $KRAS^{G12C}$ inhibitors (AMG510, MRTX849, etc.) preferentially target the GDP-bound inactive form of the KRAS protein and prevent its conversion to the active form (GTP-bound). The major signaling cascades upstream and downstream of KRAS are also highlighted. GAP, GTPase-activating protein; GEFs, guanine nucleotide exchange factors; GRB2, growth factor receptor-bound protein 2; P, phosphorylation; SHP2, Src homology region 2 domain-containing phosphatase-2; SOS, son of sevenless protein.

Inhibition of RAS-RAF-MEK-ERK signaling may also adaptively activate upstream RTKs by eliminating negative feedback loops, thereby activating other KRAS downstream effectors such as mTOR signaling and bypassing RAS-RAF-MEK-ERK, and promoting resistance to $KRAS^{G12C}$ inhibitors. Indeed, it has been shown that ARS1620 downregulates the phosphorylation sites of EGFR that is inhibitory for EGFR activity. Moreover, ARS1620 could downregulate multiple inhibitory phosphorylation sites of HER2/3 and increased the total level of HER2/3 (30), suggesting that $KRAS^{G12C}$ inhibition can abrogate EGFR/HER2/3 blockage and facilitate their activation. As a result, the combination of adagrasib (MRTX849) with EGFR or ERBB inhibitors was significantly better than single agents in xenograft models of $KRAS^{G12C}$-mutant H2122 (NSCLC) and KYSE-410 (esophageal carcinoma) (31). Moreover, the anti-tumor efficacy of sotorasib is enhanced by the EGFR inhibitor cetuximab, as the drug combination significantly reduces cell viability *in vitro* and potently suppresses tumor growth in a patient-derived xenograft (PDX) model (32).

FGFR1 has also been reported to influence the response to $KRAS^{G12C}$ inhibitors. In $KRAS^{G12C}$ models, combined FGFR inhibitors with ARS1620 showed synergistic effects in mesenchymal subsets (30). MET, also known as hepatocyte growth factor receptor (HGFR), may play a similar role: it can activate RAS *via* GEFs. Independent of RAS, MET induces AKT activation, and its amplification has been shown to lead to AMG510 resistance in NSCLC cells. The combination of MET and $KRAS^{G12C}$ inhibitors was able to limit tumor growth in xenograft models (33).

Inhibition of other nodes of the RAS-RAF-MEK-ERK axis also has the potential to increase the efficacy of $KRAS^{G12C}$ inhibitors. A synergistic effect has been observed by dual inhibition of MEK and FGFR1 in genetically engineered mouse models, and an increase in FRS2, the FGFR adaptor protein, has been reported to promote $KRAS^{G12C}$ inhibitor resistance (9, 34). Combined inhibition of BRAF and EGFR effectively improves the response of BRAF(V600E) colon cancers to BRAF inhibitors (35). Upregulation of EGFR and platelet-derived growth factor receptor (PDGFRβ) by TGF-β signaling leads to resistance to BRAF and MEK inhibitors (36), and upregulation of PDGFRα by the Sonic Hedgehog Homolog (Shh) pathway confers resistance to BRAF inhibition in metastatic BRAF(V600E) melanoma (37). Similarly, co-targeting MEK and SHP2 intensively blocks RTK-RAS signaling and is superior to inhibiting individual RTKs as RTKs phosphorylate and activate SHP2 and promote signaling from SOS1/2 to RAS (38).

$KRAS^{G12C}$ inhibitors bind to the GDP-bound inactive KRAS protein, so upstream signaling molecules that promote the allosteric switch from the inactive to the active conformation of the protein also promote resistance to $KRAS^{G12C}$ inhibitors. SOS1 is a guanine nucleotide exchange factor (GEF) that activates RAS, and SHP2 (SH2 containing protein tyrosine phosphatase-2) is a tyrosine phosphatase that activates SOS1-regulated RAS-GTP loading. As an overlapped node in RTKs to RAS cycle, it is not surprisingly that these factors are now being targeted as a new therapeutic framework, with improved anti-tumor efficacy observed by co-targeting SHP2 and $KRAS^{G12C}$, regardless of ARS1620, AMG510, or MRTX849 (19, 39, 40).

Several novel signaling pathways have been shown to compensate for KRAS signaling. Polo-like kinase 1 (PLK1) is a serine/threonine kinase with pleiotropic functions in mitosis and in response to DNA damages by regulating ataxia-telangiectasia mutated (ATM) and ATM- and Rad3-Related (ATR) checkpoint activity. Inhibition of PLK1 leads to synthetic lethality in RAS-mutant cells because RAS mutations are associated with mitotic stress, rendering RAS-mutant cells more dependent upon on PLK1 activity for proper mitotic progression (41). We have recently shown that dual inhibition of PLK1 and FGFR1 has synergistic anticancer effects in KRAS-mutant cancer cells, as FGFR1 and PLK1 cooperate control the metabolic stress associated with KRAS mutation (42). We summarize recently identified targets and strategies that improve $KRAS^{G12C}$ inhibitor therapy in Table 2.

Non-genetic adaptive resistance $kras^{G12C}$ inhibition: symbiosis of cancer cells with the TME

The tumor microenvironment (TME), the niche surrounding the cancer cells, consists of normal resident cells, immune cells, fibroblasts, stromal cells, blood vessels, signaling molecules, metabolites, and the extracellular matrix (ECM). Tumor and the TME co-exist as a symbiotic unit and constantly interact, which plays a critical role in defense against external stimuli such as anticancer drugs (Figure 2). Tumor cells even recruit immune cells as "partners in crime". Although the mechanisms underlying immune escape are not fully understood, it has been shown that tissue-resident macrophages protect cancer cells from immune surveillance by upregulating regulatory T-cell (Treg) responses (43).

Remodeling TME significantly affects tumor response to anticancer drugs, which involves not only immune cells but also other symbiotic components such as coagulation and angiogenesis. RAS/PI3K promotes the expression of angiogenic factors, e.g., vascular endothelial growth factor A (VEGFA), *via* cyclooxygenase 2 (COX2) (44) and activation of tumor angiogenesis and coagulation pathways leads to adaption to sotorasib (45). Consequently, COX2 inhibition *via* PI3K impairs anti-angiogenesis.

The programmed death-1 (PD-1)/PD-1 ligand 1 (PD-L1) axis expressed on activated T cells and cancer cells functions as an immune checkpoint. The interaction of PD-L1 with PD-1 silences the T cells, resulting in so-called tumor-induced

TABLE 2 Targets and strategies to improve the efficacy of $KRAS^{G12C}$ inhibitors.

RAS signaling nodes		Combination target	Reference
KRAS-G12C		PI3K/AKT/mTOR	Misale, S., et al. (28)
		SHP2/SOS	Lou, K., et al. (40), Fedele, C., et al. (39), Hallin, J., et al. (31), Solanki, H.S., et al. (30)
		EGFR	Hallin, J., et al. (31), Amodio, V., et al. (32)
		HER2/HER3	Solanki, H.S., et al.(30), Ho, C.S.L., et al.(2021)
		FGFR	Solanki, H.S., et al.(30)
		MET	Suzuki, S., et al. (33)
MAPK	BRAF MEK	EGFR	Prahallad, A., et al. (35)
		PDGFRα/PDGFRβ	Sun, C., et al. (36), Sabbatino, F., et al. (37)
		FGFR	Manchado, E., et al. (9), Lu, H., et al. (34)
		SHP2/SOS	Fedele, C., et al. (38)

immunosuppression (46). PD-1/PD-L1 inhibitors prevent the interaction, reactivate T cell function, and kill cancer cells. Other immune checkpoints such as T-cell immunoglobulin mucin-3 (Tim-3) and transmembrane glycoprotein NMB (GPNMB), increase sharply after PD-1/PD-L1 blockade, and inhibition of Tim-3 or GPNMB can reverse anti-PD-1 treatment failure (47, 48). After 24-h exposure to an anti-PD-1 antibody (10 μg/ml) on tumor-infiltrating lymphocytes (TILs), Tim-3 expression was increased by 50% and 40% in $CD8^+$ T cells and in $CD4^+CD25^{low/-}$ effector T cells, respectively (49). It was reported that Tim-3 activation is mediated by PI3K/AKT/mTOR, which plays a key role in inflammatory response (50), and that SHP2 inhibition increases the ratio of $CD8^+$/Treg cells and sensitize tumors to PD-1 inhibition in pancreatic ductal adenocarcinoma (PDAC) and NSCLC models (39).

In a syngeneic $KRAS^{G12C}$ colon cancer model, the number of total and proliferating $CD3^+$ T cells as well as $CD8^+$ T cells increased after AMG510 treatment, suggesting remodeling of the TME by AMG510. AMG510 plus PD-1 inhibitors resulted in long-term tumor-specific T cell responses (51, 52). However, a reduction of adaptive immune responses was also observed in sotorasib-resistant tumors, and immune escape may be a crucial factor contributing to $KRAS^{G12C}$ inhibition resistance (45).

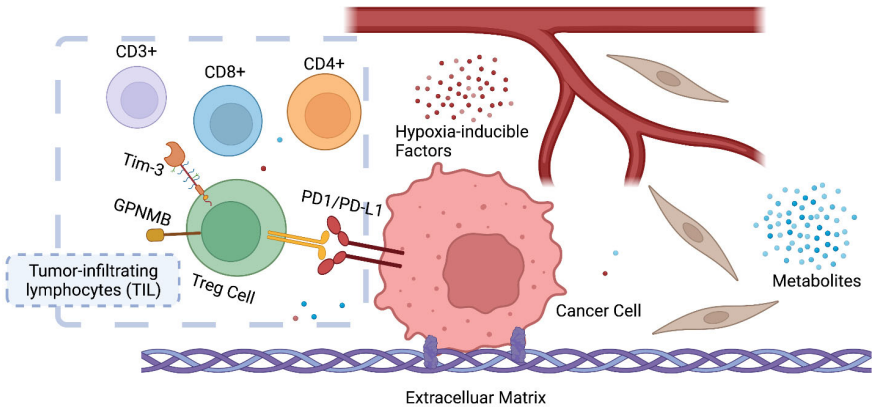

FIGURE 2
Symbiosis between cancer cells and the tumor microenvironment (TME). The infiltration and ratio of different lymphocytes are determined by the antigen presentation of cancer cells, which in return influences tumor growth and response to therapy. Hypoxia-inducible factors (HIF) and metabolites (e.g., lactate) also play a key role in reprogramming the TME of cancer. $CD3^+$ T-lymphocyte: T cells that mediate the activation of tumor-reactive T cells, e.g., $CD8^+$ naive T cells and $CD4^+$ naive T cells. $CD4^+$ T lymphocyte: also called T helper cell, which remodels TME by releasing cytokines and mediates the anti-tumor response of $CD8^+$ T cells by cross-presentation of dendritic cells. $CD8^+$ T lymphocytes: also called cytotoxic T cell, the specific killer that targets the surveilled cancer cells. Treg cells: also called suppressor T cells, a subpopulation of T cells that modulate the immune system, maintain tolerance to self-antigens, and prevent autoimmune disease. Treg cells are immunosuppressive and generally suppress or downregulate the induction and proliferation of effector T cells. Treg cells express CD4, FOXP3, and CD25 and are thought to be derived from the same lineage as naïve $CD4^+$ cells. Since effector T cells also express CD4 and CD25, it is difficult to effectively distinguish Treg cells from effector $CD4^+$ cells, making them difficult to study.

Non-genetic adaptive resistance kras^{G12C} inhibition: EMT and other transcriptional/post-transcriptional adaptions

Epithelial-to-mesenchymal transition (EMT) is the manifestation of a series of epigenetic and biochemical alterations that enable the phenotypic change from an epithelial to a mesenchymal cell phenotype (53). A variety of biochemical drivers can lead to this progression, e.g., transforming growth factor-beta (TGF-β), tumor necrosis factor-alpha (TNF-α), hypoxia-inducible factor-alpha (HIF-α), Wnt signaling, Interleukins (IL-1β, IL-6), Hedgehog, and the Hippo pathway (54–56), and impart cancer cells with properties of mesenchymal stem cells, drug resistance and invasiveness (Figure 3).

Long-term exposure to TGF-β increased the ratio of GTP-bound KRAS protein level in KRAS^{G12C} mutant malignancies, as did in Twist- or Snail-expressing mesenchymal cells. In KRAS^{G12C} mutant cancers, the amount of GTP-bound KRAS proteins determines the sensitivity to KRAS^{G12C} inhibitors, which interacts with and blocks KRAS^{G12C} when it is in the inactive GDP-bound state (Figure 1), so an increased ratio of KRAS-GTP versus KRAS-GDP cause resistance to KRAS^{G12C} inhibitors (20, 57).

Regardless of inhibiting KRAS itself or the downstream MAPK pathway, EMT is blameworthy for drug resistance (45). Activation of the PI3K pathway in mesenchymal-like KRAS^{G12C} mutant cancer cells could be the molecular basis for EMT-mediated resistance or, alternatively, could be due to a cell cycle alteration leading to CDK4-dependent growth (58). Cells expressing high levels of CSNK2A1 (Casein Kinase 2 Alpha 1) were found to have an increased mesenchymal gene signature, and reduction of CSNK2A1 converted the cells to the epithelial type and restored their sensitivity to KRAS^{G12C} or MEK inhibitors (59). Therefore, strategies that promote mesenchymal-to-epithelial transition (MET) are promising to overcome resistance to KRAS^{G12C} inhibitors.

The KRAS-MAPK axis has been shown to be associated with immune checkpoint activity through a mechanism that controls the post-transcriptional functions of immune checkpoint proteins. PD-L1 is encoded by *CD274* and MAPK signaling has been shown to play a critical role in stabilizing *CD274* mRNA, increasing PD-L1 protein levels and consequently promoting peripheral immune tolerance (60). As a result, inhibition of the RAS-MAPK pathway prevents EGF- and IFNγ-induced PD-L1 expression by suppressing *CD274* mRNA and augments the efficacy of immunotherapy (51, 52, 61). More importantly, tumor cells undergoing EMT can escape immune surveillance, suggesting that EMT is involved in the acquisition of resistance to immunotherapy (62). Indeed, Snail has been associated with the induction of immunosuppressive cytokines, activation of regulatory T cells (Treg), and the generation of impaired dendritic cells (63). EMT in tumor cells

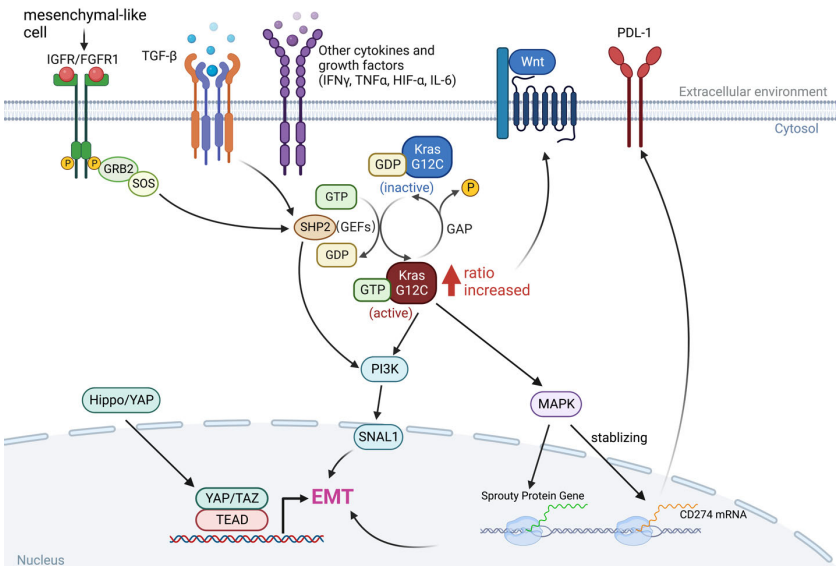

FIGURE 3
The interaction between KRAS signaling and EMT. The KRAS-MAPK pathway is important for the stability of CD274 (PD-L1) mRNAs. KRAS signaling and YAP/TAZ converge to activate transcriptional programs that regulates EMT and EMT is a key driver of tumor immune evasion. IGFR, insulin-like growth factor receptor; FGFR1, fibroblast growth factor receptor 1; TGF-β, transforming growth factor-beta; IFN-γ, interferon gamma; TNF-α, tumor necrosis factor-alpha; HIF-α, hypoxia-inducible factor-alpha; IL-6, interleukins 6; SNAI1, snail family transcriptional repressor 1.

that have undergone phenotypic changes has significant effects on the recognition of cancer cells by the native and adaptive immune systems. Both down- and up-regulation of cell surface molecules with immunological significance have been described (64). In general, these changes are accompanied by immune resistance and evasion, although exceptions to this rule have also been reported (Figure 3).

Yes-associated protein (YAP) and TEA domain 2 (TEAD2) are a transcriptional co-regulator and a downstream effector of Hippo signaling pathway, respectively, that play critical roles in controlling the expression of several EMT-related genes and have been reported to confer resistance to multiple drugs (65, 66). The relationship between YAP and the RAF/MEK/ERK cascade was discovered by genetic screens, which showed that the inhibitory combination of RAF or MEK with YAP has increased efficacy not only in BRAF-mutant cancers but also in KRAS-mutant cancers (67). In a $KRAS^{G12C}$ mutant PDAC model, inhibition of YAP1 improves the efficacy of KRAS blockade (68).

c-MYC is another oncogenic transcription factor being involved in crucial processes such as metabolic reprograming, extracellular matrix remodeling, inflammation, and regulation of a variety of malignant features in cancer (69). KRAS controls c-MYC by stabilizing the protein stability and activation of c-MYC in turn promotes KRAS-driven oncogenic potential. For example, $KRAS^{G12C}$ promotes cap-dependent translation initiation and c-MYC is an indirect indicator of the process (70). Further, KRAS and c-MYC cooperate to drive an immunosuppressive TME in cancer development, leading to increase in macrophage infiltration of tumours and decrease in CD3+ T cells, B cells and natural killer (NK) cells. These changes in the TME precede an increase in tumour size and are promoted by tumour cell-derived CC-chemokine ligand 9 (CCL9) and interleukin−23 (IL−23). Depletion of these cytokines can reduce tumour development as CCL9 is crucial for infiltration of macrophages, angiogenesis and T cell loss, and IL−23 is crucial for loss of T, B and NK cells. Infiltrating macrophages also express PD-L1, which is required for loss of T cells. Consequently, Myc deactivation rapidly reverse the observed stromal changes and induce tumour cell apoptosis and NK cell-dependent regression of Kras-driven lung adenocarcinoma in mice (71).

Overexpression of c-MYC in cancers leads to extracellular matrix (ECM) degradation and promotes angiogenesis, which in turn contributes to malignant invasion and metastasis. Overall, deregulation of c-MYC not only drives an oncogenic signaling in cancer cells, but also impinges on the TME by linking cellular signaling pathways, EMT, and the TME (72, 73). Thus, it is not surprising that amplification of the MYC gene results in drug resistance to $KRAS^{G12C}$ inhibition (70).

Conclusion

The development of covalent inhibitors that effectively and selectively target $KRAS^{G12C}$ represents an unprecedented breakthrough in the personalized treatment of patients with KRAS-mutant cancers. This advance has ushered in a new era of targeted therapy that distinguishes the G12C mutation from other KRAS mutations (e.g., G12D, G12S, G12V, Q61H), resulting in selective eradication of $KRAS^{G12C}$-mediated oncogenic signaling without affecting other KRAS substitutions and normal tissues. However, the perennial problem of resistance to targeted therapies also apply here, pointing to the pressing need to explore and therapeutically exploit the underlying mechanisms to overcome resistance to and maximize the efficacy of $KRAS^{G12C}$ inhibitor therapy.

Current evidence suggests a multifaceted mechanism of resistance to $KRAS^{G12C}$ inhibitor therapy that involves both tumor-intrinsic and -extrinsic processes. In addition to resistance mechanisms driven by genetic alterations in cancer cells, non-genetic adaptations mediated by rewiring of oncogenic signaling pathways, reciprocal interactions between cancer cells and TME, and phenotypic plasticity such as EMT are among the key strategies used by cancer cells to acquire a stem cell phenotype, an immunosuppressive niche, and, in particular, drug resistance.

Because the central role of KRAS is mediated by diverse cellular processes that not only occur in cancer cells but also involve the TME, this versatility of KRAS effector pathways is destined to dictate diverse adaptions that can be undertaken under treatment pressure. A comprehensive and in-depth understanding of resistance mechanisms will ultimately and profoundly transform the therapeutic landscape of $KRAS^{G12C}$ inhibitors, although neither a universal solution nor limited versatility of mode of action is likely. This underscores the heterogeneity of $KRAS^{G12C}$-mutant tumors and the need to consider other factors, such as genetic alterations co-occurring with $KRAS^{G12C}$ that contribute to drug resistance, in developing precision medicine. Combination therapy holds the potential to increase efficacy and selectivity, reduce single-drug dosing, decrease the development of drug resistance, and possibly avoid toxicity, and thus has emerged as an effective strategy for the treatment of refractory cancers. Nevertheless, the advent of potent and selective inhibitors for $KRAS^{G12C}$ is definitely not the beginning of the end, but the end of the beginning for the era of precision medicine, as this breakthrough has spurred the search for mutation-specific targeted therapies, as evidenced by the most recent development of $KRAS^{G12D}$ inhibitors (74).

Author contributions

WN reviewed existing literature, prepared the figure and table, and wrote the manuscript; TM and PD edited and revised the manuscript; R-WP conceived the study, edited, and revised the manuscript; All authors contributed to the article and approved the submitted version.

Funding

This study was supported by a grant from Swiss National Science Foundation (SNSF #310030_192648; to R-WP). WN is supported by a PhD fellowship from China Scholarship Council (WN).

Conflict of interest

The authors declare that the research was conducted in the absence of any commercial or financial relationships that could be construed as a potential conflict of interest.

Publisher's note

References

1. Bray F, Ferlay J, Soerjomataram I, Siegel RL, Torre LA, Jemal A. Global cancer statistics 2018: GLOBOCAN estimates of incidence and mortality worldwide for 36 cancers in 185 countries. *CA Cancer J Clin* (2018) 68(6):394–424. doi: 10.3322/caac.21492

2. Kris MG, Johnson BE, Berry LD, Kwiatkowski DJ, Iafrate AJ, Wistuba II, et al. Using multiplexed assays of oncogenic drivers in lung cancers to select targeted drugs. *Jama* (2014) 311(19):1998–2006. doi: 10.1001/jama.2014.3741

3. Mok TS, Wu YL, Thongprasert S, Yang CH, Chu DT, Saijo N, et al. Gefitinib or carboplatin-paclitaxel in pulmonary adenocarcinoma. *N Engl J Med* (2009) 361 (10):947–57. doi: 10.1056/NEJMoa0810699

4. Solomon BJ, Mok T, Kim DW, Wu YL, Nakagawa K, Mekhail T, et al. First-line crizotinib versus chemotherapy in ALK-positive lung cancer. *N Engl J Med* (2014) 371(23):2167–77. doi: 10.1056/NEJMoa1408440

5. Prior IA, Lewis PD, Mattos C. A comprehensive survey of ras mutations in cancer. *Cancer Res* (2012) 72(10):2457–67. doi: 10.1158/0008-5472.CAN-11-2612

6. Cox AD, Fesik SW, Kimmelman AC, Luo J, Der CJ, et al. Drugging the undruggable RAS: Mission possible? *Nat Rev Drug Discov* (2014) 13(11):828–51. doi: 10.1038/nrd4389

7. Yang H, Liang SQ, Schmid RA, Peng RW. New horizons in KRAS-mutant lung cancer: Dawn after darkness. *Front Oncol* (2019) 9:953. doi: 10.3389/fonc.2019.00953

8. Samatar AA, Poulikakos PI. Targeting RAS-ERK signalling in cancer: promises and challenges. *Nat Rev Drug Discov* (2014) 13(12):928–42. doi: 10.1038/nrd4281

9. Manchado E, Weissmueller S, Morris JP 4th, Chen CC, Wullenkord R, Lujambio A, et al. A combinatorial strategy for treating KRAS-mutant lung cancer. *Nature* (2016) 534(7609):647–51. doi: 10.1038/nature18600

10. Lito P, Solomon M, Li LS, Hansen R, Rosen N. Allele-specific inhibitors inactivate mutant KRAS G12C by a trapping mechanism. *Science* (2016) 351 (6273):604–8. doi: 10.1126/science.aad6204

11. FDA approves first KRAS inhibitor: Sotorasib. *Cancer Discov* (2021) 11(8): OF4. doi: 10.1158/2159-8290.CD-NB2021-0362

12. Kim D, Xue JY, Lito P. Targeting KRAS(G12C): From inhibitory mechanism to modulation of antitumor effects in patients. *Cell* (2020) 183 (4):850–9. doi: 10.1016/j.cell.2020.09.044

13. Herbst RS, Schlessinger J. Small molecule combats cancer-causing KRAS protein at last. *Nature* (2019) 575(7782):294–5. doi: 10.1038/d41586-019-03242-8

14. Hong DS, Fakih MG, Strickler JH, Desai J, Durm GA, Shapiro GI, et al. KRAS(G12C) inhibition with sotorasib in advanced solid tumors. *N Engl J Med* (2020) 383(13):1207–17. doi: 10.1056/NEJMoa1917239

15. Skoulidis F, Li BT, Dy GK, Price TJ, Falchook GS, Wolf J, et al. Sotorasib for lung cancers with KRAS p.G12C mutation. *N Engl J Med* (2021) 384(25):2371–81. doi: 10.1056/NEJMoa2103695

16. Riely GJ, Kris MG, Rosenbaum D, Marks J, Li A, Chitale DA, et al. Frequency and distinctive spectrum of KRAS mutations in never smokers with lung adenocarcinoma. *Clin Cancer Res an Off J Am Assoc Cancer Res* (2008) 14 (18):5731–4. doi: 10.1158/1078-0432.CCR-08-0646

17. Johnson ML, Ou SHI, Barve M, Rybkin II, Papadopoulos KP, Lea TA, et al. KRYSTAL-1: activity and safety of adagrasib (MRTX849) in patients with colorectal cancer (CRC) and other solid tumors harboring a KRAS G12C mutation. *Eur J Cancer* (2020) 138(S2):S1-2. doi: 10.1016/S0959-8049(20)31077-7

18. Labrie M, Brugge JS, Mills GB, Zervantonakis IK. Therapy resistance: opportunities created by adaptive responses to targeted therapies in cancer. *Nat Rev Cancer* (2022) 22(6):323–39. doi: 10.1038/s41568-022-00454-5

19. Awad MM, Liu S, Rybkin II, Arbour KC, Dilly J, Zhu VW, et al. Acquired resistance to KRAS(G12C) inhibition in cancer. *N Engl J Med* (2021) 384(25):2382–93. doi: 10.1056/NEJMoa2105281

20. Adachi Y, Ito K, Hayashi Y, Kimura R, Tan TZ, Yamaguchi R, et al. Epithelial-to-Mesenchymal transition is a cause of both intrinsic and acquired resistance to KRAS G12C inhibitor in KRAS G12C-mutant non-small cell lung cancer. *Clin Cancer Res* (2020) 26(22):5962–73. doi: 10.1158/1078-0432.CCR-20-2077

21. Arner EN, Du W, Brekken RA. Behind the wheel of epithelial plasticity in KRAS-driven cancers. *Front Oncol* (2019) 9:1049. doi: 10.3389/fonc.2019.01049

22. Kitai H, Ebi H, Tomida S, Floros KV, Kotani H, Adachi Y, et al. Epithelial-to-Mesenchymal transition defines feedback activation of receptor tyrosine kinase signaling induced by MEK inhibition in KRAS-mutant lung cancer. *Cancer Discovery* (2016) 6(7):754–69. doi: 10.1158/2159-8290.CD-15-1377

23. Ning W, Yang Z, Kocher GJ, Dorn P, Peng RW. A breakthrough brought about by targeting KRAS(G12C): Nonconformity is punished. *Cancers (Basel)* (2022) 14(2):390. doi: 10.3390/cancers14020390

24. Weiss F, Lauffenburger D, Friedl P. Towards targeting of shared mechanisms of cancer metastasis and therapy resistance. *Nat Rev Cancer* (2022) 22(3):157–73. doi: 10.1038/s41568-021-00427-0

25. Jehanno C, Vulin M, Richina V, Richina F, Bentires-Alj M. Phenotypic plasticity during metastatic colonization. *Trends Cell Biol* (2022) 32(10):854–67. doi: 10.1016/j.tcb.2022.03.007

26. Abankwa D, Gorfe AA. Mechanisms of ras membrane organization and signaling: Ras rocks again. *Biomolecules* (2020) 10(11):1522. doi: 10.3390/biom10111522

27. Ersahin T, Tuncbag N, Cetin-Atalay R. The PI3K/AKT/mTOR interactive pathway. *Mol Biosyst* (2015) 11(7):1946–54. doi: 10.1039/C5MB00101C

28. Misale S, Fatherree JP, Cortez E, Li C, Bilton S, Timonina D, et al. KRAS G12C NSCLC models are sensitive to direct targeting of KRAS in combination with PI3K inhibition. *Clin Cancer Res* (2019) 25(2):796–807. doi: 10.1158/1078-0432.CCR-18-0368

29. Steinbrunn T, Stühmer T, Sayehli C, Chatterjee M, Einsele H, Bargou RC, et al. Combined targeting of MEK/MAPK and PI3K/Akt signalling in multiple

myeloma. *Br J Haematol* (2012) 159(4):430–40. doi: 10.1111/bjh.12039

30. Solanki HS, Welsh EA, Fang B, Izumi V, Darville L, Stone B, et al. Cell type-specific adaptive signaling responses to KRAS(G12C) inhibition. *Clin Cancer Res* (2021) 27(9):2533–48. doi: 10.1158/1078-0432.CCR-20-3872

31. Hallin J, Engstrom LD, Hargis L, Calinisan A, Aranda R, Briere DM, et al. The KRASG12C inhibitor MRTX849 provides insight toward therapeutic susceptibility of KRAS-mutant cancers in mouse models and patients. *Cancer Discovery* (2020) 10(1):54–71. doi: 10.1158/2159-8290.CD-19-1167

32. Amodio V, Yaeger R, Arcella P, Cancelliere C, Lamba S, Lorenzato A, et al. EGFR blockade reverts resistance to KRAS(G12C) inhibition in colorectal cancer. *Cancer Discov* (2020) 10(8):1129–39. doi: 10.1158/2159-8290.CD-20-0187

33. Suzuki S, Yonesaka K, Teramura T, Takehara T, Kato R, Sakai H, et al. KRAS inhibitor resistance in MET-amplified KRAS (G12C) non-small cell lung cancer induced by RAS- and non-RAS-Mediated cell signaling mechanisms. *Clin Cancer Res* (2021) 27(20):5697–707. doi: 10.1158/1078-0432.CCR-21-0856

34. Lu H, Liu C, Velazquez R, Wang H, Dunkl LM, Kazic-Legueux M, et al. SHP2 inhibition overcomes RTK-mediated pathway reactivation in KRAS-mutant tumors treated with MEK inhibitors. *Mol Cancer Ther* (2019) 18(7):1323–34. doi: 10.1158/1535-7163.MCT-18-0852

35. Prahallad A, Sun C, Huang S, Di Nicolantonio F, Salazar R, Zecchin D, et al. Unresponsiveness of colon cancer to BRAF(V600E) inhibition through feedback activation of EGFR. *Nature* (2012) 483(7387):100–3. doi: 10.1038/nature10868

36. Sun C, Wang L, Huang S, Heynen GJ, Prahallad A, Robert C, et al. Reversible and adaptive resistance to BRAF(V600E) inhibition in melanoma. *Nature* (2014) 508(7494):118–22. doi: 10.1038/nature13121

37. Sabbatino F, Wang Y, Wang X, Flaherty KT, Yu L, Pepin D, et al. PDGFRα up-regulation mediated by sonic hedgehog pathway activation leads to BRAF inhibitor resistance in melanoma cells with BRAF mutation. *Oncotarget* (2014) 5 (7):1926–41. doi: 10.18632/oncotarget.1878

38. Fedele C, Ran H, Diskin B, Wei W, Jen J, Geer MJ, et al. SHP2 inhibition prevents adaptive resistance to MEK inhibitors in multiple cancer models. *Cancer Discovery* (2018) 8(10):1237–49. doi: 10.1158/2159-8290.CD-18-0444

39. Fedele C, Li S, Teng KW, Foster CJR, Peng D, Ran H, et al. SHP2 inhibition diminishes KRASG12C cycling and promotes tumor microenvironment remodeling. *J Exp Med* (2020) 218(1):e20201414. doi: 10.1084/jem.20201414

40. Lou K, Steri V, Ge AY, Hwang YC, Yogodzinski CH, Shkedi AR, et al. KRAS (G12C) inhibition produces a driver-limited state revealing collateral dependencies. *Sci Signal* (2019) 12(583):eaaw9450. doi: 10.1126/scisignal.aaw9450

41. Luo J, Emanuele MJ, Li D, Creighton CJ, Schlabach MR, Westbrook TF, et al. A genome-wide RNAi screen identifies multiple synthetic lethal interactions with the ras oncogene. *Cell* (2009) 137(5):835–48. doi: 10.1016/j.cell.2009.05.006

42. Yang Z, Liang SQ, Saliakoura M, Yang H, Vassella E, Konstantinidou G, et al. Synergistic effects of FGFR1 and PLK1 inhibitors target a metabolic liability in KRAS-mutant cancer. *EMBO Mol Med* (2021) 13(9):e13193. doi: 10.15252/emmm.202013193

43. Casanova-Acebes M, Dalla E, Leader AM, LeBerichel J, Nikolic J, Morales BM, et al. Tissue-resident macrophages provide a pro-tumorigenic niche to early NSCLC cells. *Nature* (2021) 595(7868):578–84. doi: 10.1038/s41586-021-03651-8

44. Cuesta C, Arévalo-Alameda C, Castellano E. The importance of being PI3K in the RAS signaling network. *Genes (Basel)* (2021) 12(7):1094. doi: 10.3390/genes12071094

45. Tsai YS, Woodcock MG, Azam SH, Thorne LB, Kanchi KL, Parker JS, et al. Rapid idiosyncratic mechanisms of clinical resistance to KRAS G12C inhibition. *J Clin Invest* (2022) 132(4):e155523. doi: 10.1172/JCI155523

46. Alsaab HO, Sau S, Alzhrani R, Tatiparti K, Bhise K, Kashaw SK, et al. PD-1 and PD-L1 checkpoint signaling inhibition for cancer immunotherapy: Mechanism, combinations, and clinical outcome. *Front Pharmacol* (2017) 8:561. doi: 10.3389/fphar.2017.00561

47. Koyama S, Akbay EA, Li YY, Herter-Sprie GS, Buczkowski KA, Richards WG, et al. Adaptive resistance to therapeutic PD-1 blockade is associated with upregulation of alternative immune checkpoints. *Nat Commun* (2016) 7:10501. doi: 10.1038/ncomms10501

48. Xu X, Xie K, Li B, Xu L, Huang L, Feng Y, et al. Adaptive resistance in tumors to anti-PD-1 therapy through re-immunosuppression by upregulation of GPNMB expression. *Int Immunopharmacol* (2021) 101(Pt B):108199. doi: 10.1016/j.intimp.2021.108199

49. Shayan G, Srivastava R, Li J, Schmitt N, Kane LP, Ferris RL. Adaptive resistance to anti-PD1 therapy by Tim-3 upregulation is mediated by the PI3K-akt pathway in head and neck cancer. *Oncoimmunology* (2017) 6(1):e1261779. doi: 10.1080/2162402X.2016.1261779

50. Stark AK, Sriskantharajah S, Hessel EM, Okkenhaug K. PI3K inhibitors in inflammation, autoimmunity and cancer. *Curr Opin Pharmacol* (2015) 23:82–91. doi: 10.1016/j.coph.2015.05.017

51. Canon J, Rex K, Saiki AY, Mohr C, Cooke K, Bagal D, et al. The clinical KRAS(G12C) inhibitor AMG 510 drives anti-tumour immunity. *Nature* (2019) 575 (7781):217–23. doi: 10.1038/s41586-019-1694-1

52. Briere DM, Li S, Calinisan A, Sudhakar N, Aranda R, Hargis L, et al. The KRAS(G12C) inhibitor MRTX849 reconditions the tumor immune microenvironment and sensitizes tumors to checkpoint inhibitor therapy. *Mol Cancer Ther* (2021) 20(6):975–85. doi: 10.1158/1535-7163.MCT-20-0462

53. Kalluri R, Weinberg RA. The basics of epithelial-mesenchymal transition. *J Clin Invest* (2009) 119(6):1420–8. doi: 10.1172/JCI39104

54. Yang H, Hall SRR, Sun B, Zhao L, Gao Y, Schmid RA, et al. NF2 and canonical hippo-YAP pathway define distinct tumor subsets characterized by different immune deficiency and treatment implications in human pleural mesothelioma. *Cancers* (2021) 13(7):1561. doi: 10.3390/cancers13071561

55. Ricciardi M, Zanotto M, Malpeli G, Bassi G, Perbellini O, Chilosi M, et al. Epithelial-to-mesenchymal transition (EMT) induced by inflammatory priming elicits mesenchymal stromal cell-like immune-modulatory properties in cancer cells. *Br J Cancer* (2015) 112(6):1067–75. doi: 10.1038/bjc.2015.29

56. Butti R, Gunasekaran VP, Kumar TVS, Banerjee P, Kundu GC. Breast cancer stem cells: Biology and therapeutic implications. *Int J Biochem Cell Biol* (2019) 107:38–52. doi: 10.1016/j.biocel.2018.12.001

57. Du B, Shim JS. Targeting epithelial-mesenchymal transition (EMT) to overcome drug resistance in cancer. *Molecules* (2016) 21(7):965. doi: 10.3390/molecules21070965

58. Padhye A, Konen JM, Rodriguez BL, Fradette JJ, Ochieng JK, Diao L, et al. Targeting CDK4 overcomes EMT-mediated tumor heterogeneity and therapeutic resistance in KRAS mutant lung cancer. *JCI Insight* (2021) 6(17):e148392. doi: 10.21203/rs.3.rs-355354/v1

59. Wang H, Lv Q, Xu Y, Cai Z, Zheng J, Cheng X, et al. An integrative pharmacogenomics analysis identifies therapeutic targets in KRAS-mutant lung cancer. *EBioMedicine* (2019) 49:106–17. doi: 10.1016/j.ebiom.2019.10.012

60. Frydenlund N, Mahalingam M. PD-L1 and immune escape: insights from melanoma and other lineage-unrelated malignancies. *Hum Pathol* (2017) 66:13–33. doi: 10.1016/j.humpath.2017.06.012

61. Stutvoet TS, Kol A, de Vries EG, de Bruyn M, Fehrmann RS, Terwisscha van Scheltinga AG, et al. MAPK pathway activity plays a key role in PD-L1 expression of lung adenocarcinoma cells. *J Pathol* (2019) 249(1):52–64. doi: 10.1002/path.5280

62. Knutson KL, Lu H, Stone B, Reiman JM, Behrens MD, Prosperi C, et al. Immunoediting of cancers may lead to epithelial to mesenchymal transition. *J Immunol* (2006) 177(3):1526–33. doi: 10.4049/jimmunol.177.3.1526

63. Kamei D, Murakami M, Sasaki Y, Nakatani Y, Majima M, Ishikawa Y, et al. Microsomal prostaglandin e synthase-1 in both cancer cells and hosts contributes to tumour growth, invasion and metastasis. *Biochem J* (2010) 425(2):361–71. doi: 10.1042/BJ20090045

64. Topper MJ, Vaz M, Chiappinelli KB, DeStefano Shields CE, Niknafs N, Yen RC, et al. Epigenetic therapy ties MYC depletion to reversing immune evasion and treating lung cancer. *Cell* (2017) 171(6):1284–1300.e21. doi: 10.1016/j.cell.2017.10.022

65. Diepenbruck M, Waldmeier L, Ivanek R, Berninger P, Arnold P, van Nimwegen E, et al. Tead2 expression levels control the subcellular distribution of yap and taz, zyxin expression and epithelial-mesenchymal transition. *J Cell Sci* (2014) 127(7):1523–36. doi: 10.1242/jcs.139865

66. Heng BC, Zhang X, Aubel D, Bai Y, Li X, Wei Y, et al. An overview of signaling pathways regulating YAP/TAZ activity. *Cell Mol Life Sci* (2021) 78 (2):497–512. doi: 10.1007/s00018-020-03579-8

67. Lin L, Sabnis AJ, Chan E, Olivas V, Cade L, Pazarentzos E, et al. The hippo effector YAP promotes resistance to RAF- and MEK-targeted cancer therapies. *Nat Genet* (2015) 47(3):250–6. doi: 10.1038/ng.3218

68. Yan H, Yu CC, Fine SA, Youssof AL, Yang YR, Yan J, et al. Loss of the wild-type KRAS allele promotes pancreatic cancer progression through functional activation of YAP1. *Oncogene* (2021) 40(50):6759–71. doi: 10.1038/s41388-021-02040-9

69. Dong Y, Tu R, Qing G, Dong Y. Regulation of cancer cell metabolism: oncogenic MYC in the driver's seat. *Signal Transduct Target Ther* (2020) 5(1):124. doi: 10.1038/s41392-020-00235-2

70. Zhao Y, Murciano-Goroff YR, Xue JY, Ang A, Lucas J, Mai TT, et al. Diverse alterations associated with resistance to KRAS(G12C) inhibition. *Nature* (2021) 599(7886):679–83. doi: 10.1038/s41586-021-04065-2

71. Kortlever RM, Sodir NM, Wilson CH, Burkhart DL, Pellegrinet L, Brown Swigart L, et al. Myc cooperates with ras by programming inflammation and immune suppression. *Cell* (2017) 171(6):1301–1315.e14. doi: 10.1016/j.cell.2017.11.013

72. Ciribilli Y, Borlak J. Oncogenomics of c-myc transgenic mice reveal novel regulators of extracellular signaling, angiogenesis and invasion with clinical significance for human lung adenocarcinoma. *Oncotarget* (2017) 8(60):101808–31. doi: 10.18632/oncotarget.21981

73. Kim JH, Cho EB, Lee J, Jung O, Ryu BJ, Kim SH, et al. Emetine inhibits migration and invasion of human non-small-cell lung cancer cells via regulation of ERK and p38 signaling pathways. *Chem Biol Interact* (2015) 242:25–33. doi: 10.1016/j.cbi.2015.08.014

74. Hallin J, Bowcut V, Calinisan A, Briere DM, Hargis L, Engstrom LD, et al. Anti-tumor efficacy of a potent and selective non-covalent KRAS(G12D) inhibitor. *Nat Med* (2022) 28(10):2171–82. doi: 10.1038/s41591-022-02007-7

frontiers | Frontiers in Oncology

TYPE Original Research
PUBLISHED 09 February 2023
DOI 10.3389/fonc.2023.1115156

OPEN ACCESS

EDITED BY
Mohamed Rahouma,
NewYork-Presbyterian, United States

REVIEWED BY
Lorenzo Belluomini,
University of Verona, Italy
Stephen Swisher,
University of Texas MD Anderson Cancer Center, United States

*CORRESPONDENCE
Gabriella Fontanini
gabriella.fontanini@unipi.it

SPECIALTY SECTION
This article was submitted to Thoracic Oncology, a section of the journal Frontiers in Oncology

RECEIVED 03 December 2022
ACCEPTED 31 January 2023
PUBLISHED 09 February 2023

CITATION
Alì G, Poma AM, Di Stefano I, Zirafa CC, Lenzini A, Martinelli G, Romano G, Chella A, Baldini E, Melfi F and Fontanini G (2023) Different pathological response and histological features following neoadjuvant chemotherapy or chemo-immunotherapy in resected non-small cell lung cancer. *Front. Oncol.* 13:1115156. doi: 10.3389/fonc.2023.1115156

Different pathological response and histological features following neoadjuvant chemotherapy or chemo-immunotherapy in resected non-small cell lung cancer

Greta Alì[1], Anello Marcello Poma[2], Iosè Di Stefano[2], Carmelina Cristina Zirafa[3], Alessandra Lenzini[3], Giulia Martinelli[2], Gaetano Romano[3], Antonio Chella[4], Editta Baldini[5], Franca Melfi[3] and Gabriella Fontanini[2]*

[1]Unit of Pathological Anatomy, University Hospital of Pisa, Pisa, Italy, [2]Department of Surgical, Medical, Molecular Pathology and Critical Area, University of Pisa, Pisa, Italy, [3]Multispecialty Centre for Surgery, Minimally Invasive and Robotic Thoracic Surgery, University Hospital of Pisa, Pisa, Italy, [4]Unit of Pneumology, University Hospital of Pisa, Pisa, Italy, [5]Medical Oncology, San Luca Hospital, Lucca, Italy

Introduction: Non-small cell lung cancer (NSCLC) is the leading cause of cancer incidence and mortality worldwide. Neoadjuvant chemo-immunotherapy has led to clinical benefits in resectable NSCLC in comparison to chemo-therapy alone. Major pathological response (MPR) and pathological complete response (pCR) have been used as surrogates of neoadjuvant therapy response and clinical outcomes. However, the factors affecting the pathological response are still controversial. Therefore, in this study we retrospectively examined MPR and pCR in two different cohorts of NSCLC patients, 14 treated by chemotherapy and 12 by chemo-immunotherapy in the neoadjuvant setting.

Methods: In resected tumor specimens, different histological characteristics were evaluated: necrosis, fibrosis, inflammation, presence of organizing pneumonia, granuloma, cholesterol cleft, and reactive epithelial alterations. In addition, we evaluated how MPR impacts on event-free survival (EFS) and overall survival (OS). In a small group of patients treated by chemo-immunotherapy, a gene expression analysis of the Hippo pathway was performed both in preoperative biopsies and matched post-surgical specimens.

Results: We observed a better pathological response in the chemo-immunotherapy treated cohort: 6/12 patients (50.0%) achieved a MPR ≤10% and 1/12 (8.3%) achieved pCR both on primary tumor and on lymph nodes. On the contrary, no patient treated with chemotherapy alone achieved pCR or MPR ≤10%. A higher amount of stroma in the neoplastic bed was observed in patients treated with immuno-chemotherapy. Moreover, patients achieving better MPR (including pCR) had significantly improved overall survival (OS) and event-free survival (EFS). After neoadjuvant chemo-immunotherapy, residual tumors showed a remarkable upregulation of genes consistent with the activation of YAP/TAZ. Also, alternative checkpoint, such as CTLA-4, were enhanced.

10.3389/fonc.2023.1115156

Discussion: Our findings showed that neoadjuvant chemo-immunotherapy treatment improves MPR and pCR thus resulting in better EFS and OS. Moreover, a combined treatment could induce different morphological and molecular changes in comparison to chemotherapy alone, thus giving new insights in the assessment of pathological response.

KEYWORDS

non-small cell lung cancer, neoadjuvant therapy, chemo-immunotherapy, pathological response, prognosis, biomarkers

1 Introduction

Non-small cell lung cancer (NSCLC) is the greatest cause of cancer death. Despite recent improvements in the treatment of advanced NSCLC, little is known about therapy efficacy in resectable tumors (1, 2). Although the advances in staging, surgical techniques, and the introduction of adjuvant chemotherapy for stage II and III NSCLC, a large number of operated patients experience disease recurrence (3). In particular, patients with resectable NSCLC at high risk of recurrence may benefit from neoadjuvant or adjuvant chemotherapy, but the 5-year overall survival is reached only in 5% of cases (4). In recent years, immunotherapy emerged as a therapeutic option for lung cancer, and neoadjuvant immunotherapy can be a good alternative for patients with resectable NSCLC. In the neoadjuvant setting immunotherapy, a combination of chemotherapy and immunotherapy, and targeted therapies are currently under investigation (5–7).

However, there are no established guidelines about the assessment of response to neoadjuvant therapy on resected lung cancer specimens. Over the years, different approaches have been used to assess pathological response, including pathological complete response (pCR) and major pathological response (MPR) (8, 9). Previous studies have suggested a positive association between pathological response, mainly pCR, and clinical outcome of patients. It has been demonstrated that patients with NSCLC showing a MPR of 10% or less have a significantly better outcome after neoadjuvant chemotherapy (10–12). As regards immunotherapy alone data are still limited.,. However, a neoadjuvant chemo-immunotherapy may increase the proportion of patients achieving a major pathological response (MPR) (13, 14). Indeed, available studies (15) showed that neoadjuvant chemo-immunotherapy can be more effective than chemotherapy alone in patients with resectable NSCLC. However, a considerable percentage of tumors do not completely respond to neoadjuvant chemo-immunotherapy, and patients may develop early disease progression (16). Thus, the identification of patients without a substantial pathological response is crucial to adjust treatment. To date, no studies have compared the pathological response to chemotherapy and to chemo-immunotherapy in NSCLC. In this study we retrospectively examined the efficacy of neoadjuvant chemotherapy and chemo-immunotherapy in patients with NSCLC comparing the MPR and several histological characteristics such as necrosis, fibrosis, and inflammation both in the tumor and in the collateral lung parenchyma. In addition, we evaluated how MPR impacts on event-free survival (EFS) and overall survival (OS). Moreover, in a small group of patients treated with chemo-immunotherapy, we performed a gene expression analysis of the Hippo pathway, crucial for tissue repair and associated with treatment resistance, both in preoperative biopsies and matched post-surgical specimens.

2 Materials and methods

2.1 Patient selection

We retrospectively enrolled 26 NSCLC patients, including 14 who had received chemotherapy and 12 who had received chemo-immunotherapy in the neoadjuvant setting, from April 2017 to January 2021 and from December 2018 to October 2021, respectively. In detail, Surgical specimens of patients were collected from the archives of the Operative Unit of Pathological Anatomy III of the University Hospital of Pisa. In detail, tumors included 14 adenocarcinoma (ADC), 8 squamous cell carcinoma (SCC), 1 adenosquamous carcinoma, 1 pleomorphic carcinoma, and 2 large cell neuroendocrine carcinoma obtained from patients who underwent surgical resection at the Department of Cardiothoracic Surgery of the University Hospital of Pisa. For 5 patients treated with combined chemo-immunotherapy, we also collected pre-surgical biopsies. Participation in this study required informed consent. Treatment regimens and indications for surgery were determined by a multidisciplinary team. All patients received surgery within 4-6 weeks after neoadjuvant chemo-immunotherapy or chemotherapy. In detail, 14 patients received 2-4 cycles of a conventional platinum-based doublet chemotherapy regimen, whereas 12 patients received 2-6 cycles of a conventional platinum-based doublet chemotherapy regimen combined with PD-1 (pembrolizumab, n=4) or PD-L1 inhibitors, (atezolizumab in 6 cases and durvalumab in 2 cases). As per standard institutional procedures, all surgical resections were performed with thoracotomy, video-assisted thoracoscopic surgery, or robotic-assisted pulmonary resection.

Clinical information including patient sex, age, molecular status, PD-L1 immunohistochemical expression, EFS, and OS, were reviewed for each patient. EFS was considered as the time from the start of neoadjuvant treatment until disease progression. OS was considered from the start of therapy to the date of death or censored at the last

follow-up. This study was approved by the ethics committee "Comitato Etico di Area Vasta Nord Ovest" (CEAVNO) for Clinical Experimentation (Protocol Number: ID19211).

2.2 Pathological response evaluation

Information on neoadjuvant therapy, such as medication and course of treatment, was documented. Tumors were staged according to the American Joint Committee on Cancer Lung Cancer Staging, 8th edition (17). The pathological response was assessed independently by two pathologists (GA and IDS) that evaluated both pCR and MPR. MPR was defined as residual viable tumor cells in the primary tumor bed and sampled lymph nodes. MPR was reported both as a continuous variable and using the 10% cut-off, whereas pCR was defined as the complete absence of residual viable tumor cells in the primary tumor (8, 9).

In detail, according to the recommendations of The International Association for the Study of Lung Cancer (IASLC) (9), if the tumor bed was small (≤ 3 cm) the tumor was entirely sampled. If the tumor bed was larger than 3 cm, the tumor was cut in serial sections approximately 0.5 cm thick and after gross inspection the most representative cross section showing viable tumor was sampled (at least one cross section of the entire tumor). If no viable tumor was identified in the cross sections, the remaining tumor tissue was examined histologically to see if any viable tumor was present. Besides tumor cells, the percentages of major components of the tumor bed such as necrosis and stroma (which includes inflammatory cells and fibrosis) were calculated with the total adding up to 100%, as previously described (9). The percentage of residual viable tumor was estimated by comparing the estimated cross-sectional area of the viable tumor foci with estimated cross-sectional areas of necrosis, fibrosis, and inflammation on each hematoxylin and eosin slide. The results for all slides were averaged together to determine the mean values for each patient (10). For lymph node pathological response, the same approach was used for histological evaluation that was used for the resected lung cancer.

Moreover, we calculated the pathological regression (PR) evaluated as 100 - the percentage of residual viable tumor cells. Finally, we evaluated other histological features in the tumor microenvironment such as inflammation, fibrosis, presence of organizing pneumonia, granuloma, cholesterol cleft, and reactive epithelial alterations.

PD-L1 expression before treatment was detected by using the rabbit monoclonal primary antibody SP263 and the expression was evaluated by tumor proportion score (TPS).

2.3 Gene expression analysis

For all samples, tumor cell percentage was estimated independently by two expert pathologists and tumor component was enriched by manual macrodissection before nucleic acid extraction. In detail, total RNA was purified from three-to-four unstained formalin-fixed paraffin embedded (FFPE) sections (10 µm-thick) using the Qiagen RNeasy FFPE kit (Qiagen, Hilden, Germany), and according to the manufacturer's suggestions. RNA quality and concentration were assessed using an Xpose spectrophotometer (Trinean, Gentbrugge, Belgium). About 150 ng of total RNA were used for gene expression analysis using the nCounter system (nanoString Technologies, Seattle, WA, USA). A custom panel of 88 genes was designed including 10 housekeeping genes (i.e., *CLTC*, *EDC3*, *GAPDH*, *GUSB*, *HPRT1*, *MRPS5*, *NUBP1*, *PGK1*, *PRPF38A*, *SF3A3*), 4 genes encoding for immune checkpoint proteins (i.e., *CD274*, *CTLA4*, *PDCD1*, *VSIR*) and 74 genes belonging to the Hippo pathway. The complete list of genes is reported in Supplementary Table S1. Total RNA was hybridized with capture and reporter probes at 60°C for 20 hours; cleanup of samples and counts of digital reports were performed as described by the manufacturer (nanoString Technologies).

2.4 Data analyses and statistics

Continuous variables are presented as median and interquartile range (IQR) and were tested by the Mann-Whitney test or by the Kruskal-Wallis test followed by the Dunn test. Categorical variables were tested by the Fisher exact test. Correlations between continuous variables were evaluated by Pearson correlation.

For gene expression analysis, raw counts were normalized using the nCounter Advanced Analysis (nanoString Technologies). Differentially expressed genes were computed following the procedures of the nCounter Advanced Analysis. *P*-values were adjusted by the Benjamini-Hochberg method, and a false discovery rate (FDR) of 0.05 was considered significant. Principal component analysis (PCA) was performed using PCAtools v.2.10.0 package, while hierarchical clustering was carried out using heatmap3 v. 1.1.9 package. Optimal cut-off for MPR was assessed by the Contal and O'Quigley's method and using the survMisc v.0.5.6 package. Survival curves were estimated by the Kaplan-Meier method following the procedures of survival v.3.4-0 package and plotted using survminer v.0.4.9 package. Hazard ratio (HR) was estimated using the Cox regression method.

All analysis and plots were generated in R environment v.4.1.2 (https://www.r-project.org/, last accessed November 14, 2022) unless otherwise specified.

3 Results

3.1 Patient clinico-pathological characteristics and different treatment regimens

Clinico-pathological characteristics of patients are summarized in Table 1. Twenty-three patients with resectable NSCLC were included: 8 were females and 18 males aged from 41 to 78 years old (median age of 66 years). Twelve patients were treated with combined chemo-immunotherapy and 14 with chemotherapy. Most patients (50.8%) had stage IA to IB disease, 5 (19.2%) had stage IIB, 7 (26.2%) had stage IIIA and IIIB, and one (3.8%) patient had stage IVA. For the combined immuno-chemotherapy treated patients, 10 (83.3%) had a PD-L1 TPS of 1% or higher and 2 (16.7%) had TPS of 50% or higher. For chemotherapy treated patients, 3 (21.4%) had PD-L1 negative, 9

TABLE 1 Clinicopathological characteristics and pathological response of NSCLC patients according to treatment regimens.

Features	All Patients (n = 26)	CIT Patients (n = 12)	CT Patients (n = 14)	P value
Age (years), median (IQR)	69 (57-71)	67 (58.5-70.5)	69 (59.5-71.75)	0.55
Sex, n (%) *female* *male*	8 (30.8) 18 (69.2)	3 (25) 9 (75)	5 (35.7) 9 (64.3)	0.43
Size of tumor (cm), median (IQR)	4.35 (2.50-6.22)	4.35 (2.87-6.00)	4.15 (2.42-6.45)	0.88
Histology, n (%) *ADC* *SCC* *Others*	14 (53.8) 8 (30.8) 4 (15.4)	7 (58.3) 3 (25.0) 2 (16.7)	7 (50.0) 5 (35.6) 2 (14.4)	0.87
pT, n (%) *T1 (a+b+c)* *T2 (a+b)* *T3* *T4*	7 (26.2) 6 (23.1) 8 (30.8) 4 (15.4)	5 (41.8) 3 (25.0) 5 (41.8) 1 (8.3)	3 (21.4) 5 (35.7) 3 (21.4) 3 (21.4)	0.26
pN, n (%) *N0* *N1* *N2*	16 (61.5) 6 (23.1) 4 (15.4)	8 (66.6) 2 (16.7) 2 (16.7)	8 (57.2) 4 (28.6) 2 (14.3)	0.86
Clinical Stage (8th edition), n (%) *IA (IA1, IA2, IA3) - IB* *IIB* *IIIA - IIIB* *IVA*	13 (50.8) 5 (19.2) 7 (26.2) 1 (3.8)	6 (50) 2 (16.7) 4 (33.3) 0	7 (50.0) 3 (21.4) 3 (21.4) 1 (7.2)	0.82
Grade, n (%) *G2* *G3*	(n = 23) 9 (39.1) 14 (60.9)	(n = 11) 4 (36.4) 7 (63.6)	(n = 12) 5 (41.7) 7 (58.3)	0.67
MPR, median (IQR)	36.5 (9-59.5)	6 (2.75-34.75)	56 (12-72)	**0.001**
MPR, n (%) *≤ 10%* *> 10%*	7 (26.9) 19 (73.1)	7 (58.2) 5 (41.8)	0 14 (100)	**0.001**
PD-L1 expression, n (%) *Negative (< 1%)* *Positive (≥ 1% - 49%)* *(≥ 50%)*	3 (11.5) 19 (73.1) 4 (15.4)	0 11 (91.7) 1 (8.3)	3 (21.4) 8 (57.2) 3 (21.4)	0.20
Mutational status, n (%) *WT* *KRAS mutation* *RET rearrangement* *NA*	14 (53.9) 6 (23.1) 1 (3.8) 5 (19.2)	6 (50.0) 4 (33.4) 1 (8.3) 1 (8.3)	8 (49.9) 2 (14.4) 0 4 (35.7)	0.36

CIT, chemo-immunotherapy; CT, chemotherapy; IQR, interquartile range; ADC, adenocarcinoma; SCC, squamous cell carcinoma; Others comprise: 1 adenosquamous cell carcinoma; 1 pleomorphic carcinoma; and 2 large cell neuroendocrine carcinoma; WT, wild-type; NA, not available.
Bold *p*-value: value below 0.05 was considered significant.

(64.2%) had tumor with low PD-L1 expression (TPS 1-49%), and 2 (14.4%) had tumor with high PD-L1 (TPS ≥ 50%).

No significant differences between the two neoadjuvant therapy groups were observed in terms of age, sex, histological tumor type, size of tumors, TNM stage, grade, PD-L1 expression, and mutational status (Table 1).

3.2 Pathological response and morphological data

Major pathological response was different between the two cohorts of patients both as continuous variable ($p < 0.0001$) and considering the 10% cut-off ($p < 0.0001$) (Table 1). In detail, 7 patients treated with combined immuno-chemotherapy (58.3%) achieved a MPR ≤10% and one patient (3.8%) pCR in the primary tumor and sampled lymph nodes. On the other hand, no chemotherapy treated patients achieved MPR ≤10% or pCR (Figure 1). The waterfall plot shows pathological regression in the resected primary lung tumor after neoadjuvant treatment (Figure 2).

To further explore the pathological response after treatment, we evaluated also several histological features on tumor specimens and in the surrounding lung parenchyma (Figures 3A–F). We observed a significantly higher amount of stroma in the neoplastic bed in the cohort of patients treated with immuno-chemotherapy ($p = 0.004$) (Figure 1). The evaluation of stroma included fibrosis and

10.3389/fonc.2023.1115156

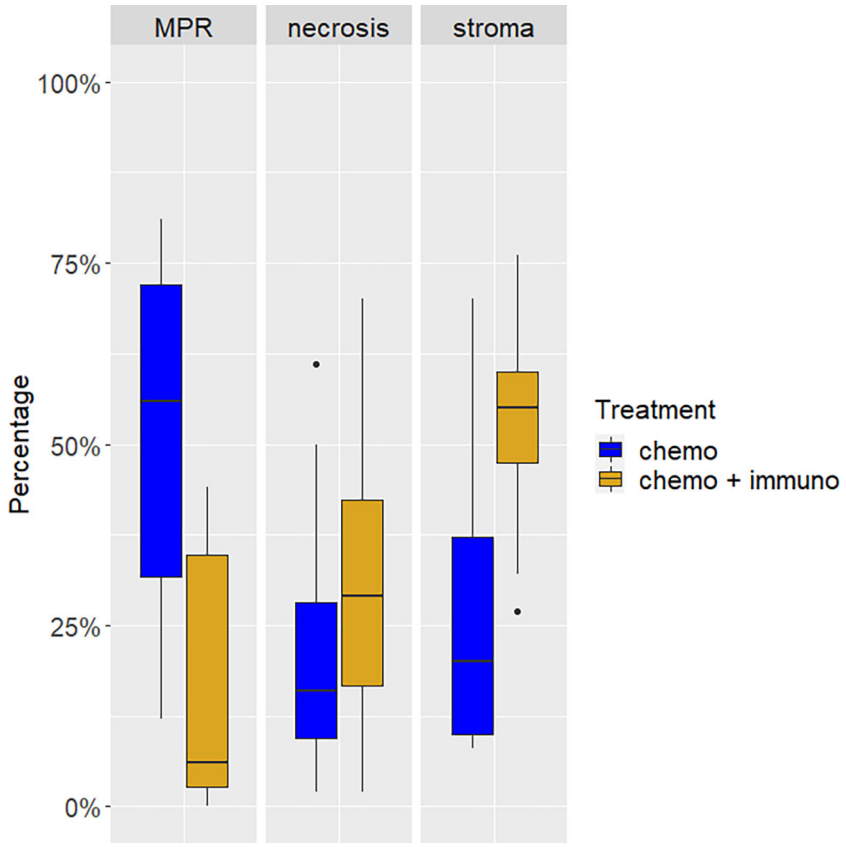

FIGURE 1
Tumor composition after neoadjuvant treatment with chemo- or chemo-immunotherapy. The proportion of viable tumor cells (major pathological response, MPR) was lower in tumors from patients of the chemo-immunotherapy cohort. These cases showed also a higher proportion of necrosis and stroma.

inflammation in the tumor bed. However, we did not observe statistically significant differences in terms of fibrosis and inflammation as well as the presence of organizing pneumonia, granuloma, cholesterol cleft, and reactive epithelial alterations. Although these morphological characteristics did not reach statistical significance in the two different treatment cohorts, they were less prominent or absent in patients treated with chemotherapy alone. The complete list of histological features is summarized in Table 2.

Although no significant correlations were found between PD-L1 immunohistochemical expression and MPR, necrosis, and stroma, we observed a trend showing that PD-L1 levels positively correlated with MPR both in the general cohort and in patients treated with combination therapy. On the contrary, the amount of stroma positively correlated with PD-L1 expression levels only in the combined treated patients (Figures 4A–F).

3.3 Survival analyses

The last follow-up was in June 2022. For all patients, the overall median follow-up was 23 months (interquartile range, IQR, 16 – 32 months). In the chemotherapy treated patient cohort, the median follow-up was 16 months (IQR, 16 – 26). In the combined immuno-chemotherapy cohort, the median follow-up was 29 months (IQR, 22 – 35 months).

In univariate analysis and considering the entire cohort of patients, MPR was predictive of long-term OS (p = 0.04) and EFS (p = 0.04) after neoadjuvant therapy. In particular the best cut-off was 33% of viable tumor cells, which significantly stratified patients according to EFS (p = 0.02), and OS (p = 0.01) (Figures 5A–D).

Regarding histopathological features of tumors, the amount of necrosis was associated with a longer EFS (p = 0,02), whereas no association was observed between necrosis and OS.

We observed also a trend for a better overall survival of patients treated with chemo-immunotherapy (p = 0.07) and, as expected, a trend for a better outcome of patients with stage I or II disease both in EFS (p = 0.12) and OS (p = 0.12).

Finally, we performed a multivariate analysis including MPR, stage and treatment. While higher disease stage was predictive of poor EFS (p = 0.02) and OS (p = 0.05), MPR was associated with EFS independently of stage and treatment regimen (p = 0.02) (Table 3).

3.4 Gene expression analysis

Gene expression analysis was performed in a small set of samples, namely 5 tumors from patients treated with neoadjuvant chemo-immunotherapy. For each case, both pre- and post-surgical tissue samples were analyzed to observe changes of Hippo gene expression. Differences between pre- and post-surgical samples were remarkable at unsupervised analyses. In fact, pre- and post-surgical samples were

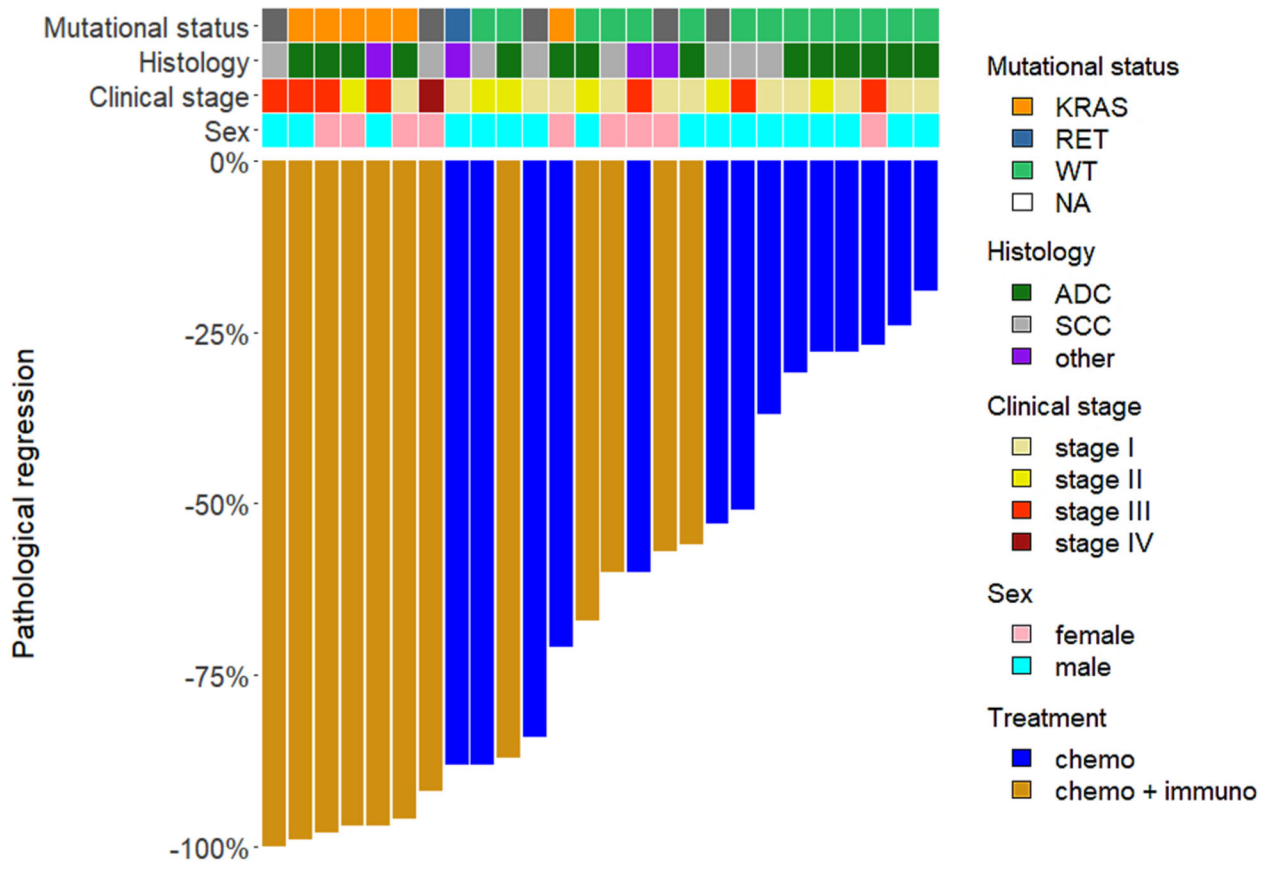

FIGURE 2
Waterfall plot of pathological response. The bars represent patients according to the different neoadjuvant treatments, chemotherapy alone (chemo) and chemo-immunotherapy (chemo-immuno). The upper rows show clinic-pathological characteristics of patients (mutational status, histology, clinical stage, sex). WT, wild-type; NA, not available; ADC, adenocarcinoma; SCC, squamous cell carcinoma.

clearly separated at PCA (Figure 6A) and heatmap (Figure 6B), with only one exception in the latter. Six genes were significantly upregulated in post-surgical samples (Figure 6C), namely *ETS1*, *FAT4*, *STAT5A*, *ETS2*, *CTLA4* and *LATS2*. In Table 4 are reported genes with an FDR below 0.15.

To evaluate the activation of YAP and TAZ (encoded by *YAP1* and *WWTR1* genes respectively) two approaches were used. First, a YAP-TAZ target score was built by averaging the expression level of 3 validated targets (i.e., *AMOTL2*, *LATS2* and *PTPN14*, DOI: 10.1016/j.celrep.2018.10.001). Second, the mRNA expression of *YAP1* and *WWTR1* were evaluated. As presented in Figure 6D, YAP-TAZ target score was always higher in post-surgical samples with one exception. These results were confirmed by the pre- and post-surgical levels of *YAP1* and *WWTR1*. In fact, after neoadjuvant immunotherapy, both genes were upregulated, especially *WWTR1* (Figure 6E).

4 Discussion

In resectable NSCLC preoperative treatments, including immunotherapy, can improve clinical outcomes and patients survival (6).

To date, there are limited data establishing the prognostic relationship between pathological response after neoadjuvant therapy in resectable NSCLC and clinical outcome, making it an interesting research area. Pathological response has been proposed as a surrogate indicator of benefit to neoadjuvant therapy in order to evaluate the effectiveness of agents tested in clinical trial (18). Numerous studies showed that neoadjuvant chemotherapy treated patients with lung cancer that achieve a MPR ≤10% have a significantly improved survival (10, 12, 19). Therefore, pathological response, including pCR and MPR, can be relevant to assess the impact of neoadjuvant chemo-immunotherapy (10).

Studies evaluating the effect of neoadjuvant immunotherapy in resectable NSCLC have shown a median pathological response of 50-92.5%. In particular, a MPR defined as 10% or less of residual viable tumor cells in the resected primary tumor was reported in 40.5-56.7% of cases, while cPR, defined as no viable tumor within the resected specimen, was reported in 15-33% and 8.1-10% for primary lesions and lymph nodes respectively. These responses are better than those reported for patients treated with neoadjuvant chemotherapy (5, 13, 20–23).

In the present study, we retrospectively analyzed 26 NSCLC patients treated with neoadjuvant therapy of which 14 with chemotherapy alone and 12 with chemo-immunotherapy. In agreement with literature data (5, 13, 20–23), we observed a better pathological response in the chemo-immunotherapy cohort: six patients (50.0%) achieved a MPR and one patient a pCR both on

10.3389/fonc.2023.1115156

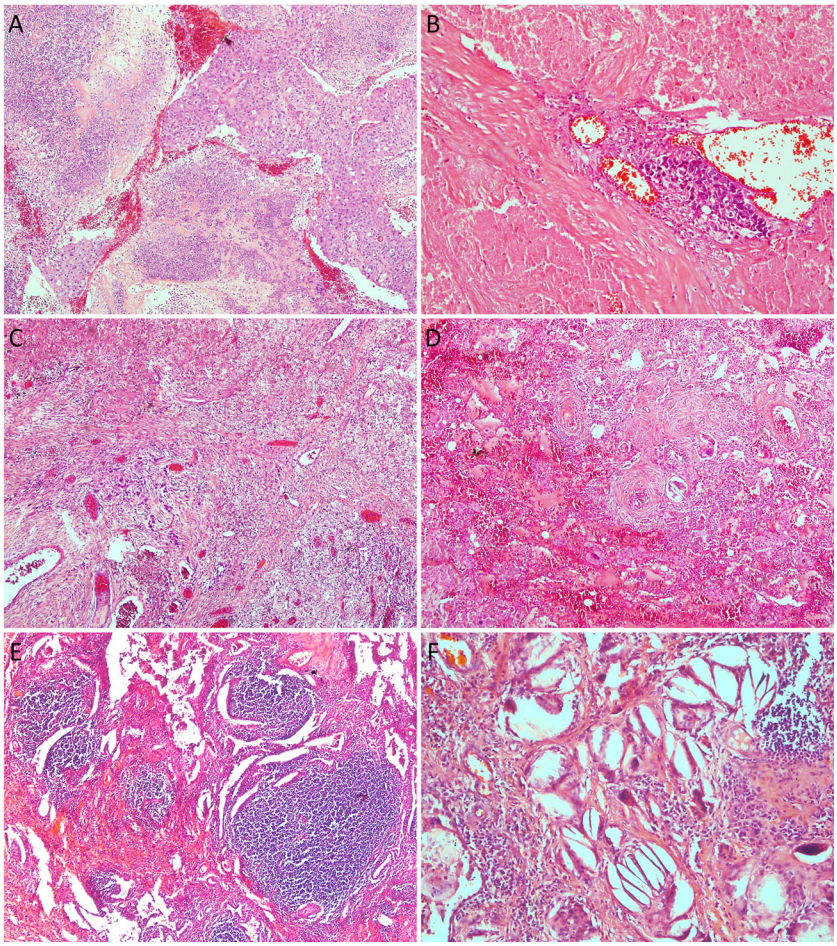

FIGURE 3
Histologic features after neoadjuvant therapy: **(A)**, area of solid nests of chemotherapy treated squamous cell carcinoma surrounded by necrotic areas (magnification x 10); **(B)**, chemo-immunotherapy treated tumor with a large area of necrosis showing a single focus of viable adenocarcinoma (magnification x 20); **(C)**, focus of atypical cells of chemo-immunotherapy treated tumor with adenocarcinoma histology surrounded by dense fibrosis (magnification x 4); **(D)**, chemotherapy treated tumor with larger area of dense fibrosis with abundant foamy histiocytes (magnification x 4); **(E)**, this area of chemo-immunotherapy treated tumor shows fibrosis with extensive inflammatory infiltrate of lymphocytes and plasma cells (magnification x 4); **(F)**, high power of the same tumor showing chronic inflammation, cholesterol clefts, foamy histiocytes, and fibrosis.

TABLE 2 Morphological characteristics of tumors after neoadjvant treatment.

Morphological Features	All Patients (N = 26)	Treated CIT Patients (N = 12)	Treated CT Patients (N = 14)	P value
Necrosis, median (IQR)	20 (11.5-40)	29 (16.75-42.25)	16 (9.5-28.25)	0.28
Stroma (fibrosis and inflammation), median (IQR)	39 (20-56.5)	20 (10-37.25)	55 (47.5-60)	**0.004**
Tumor inflammation, n (%) *Yes* *No*	17 (65.4) 9 (34.6)	10 (83.3) 2 (16.7)	7 (50.0) 7 (50.0)	0.11
Tumor fibrosis, n (%) *Yes* *No*	19 (73.1) 7 (26.9)	11 (91.7) 1 (8.3)	8 (57.1) 6 (42.9)	0.08
Parenchyma inflammation, n (%) *Yes* *No*	15 (57.7) 11 (42.3)	5 (41.7) 7 (58.3)	10 (71.4) 4 (28.6)	0.23
Parenchyma fibrosis, n (%) *Yes* *No*	18 (69.2) 8 (30.8)	10 (83.3) 2 (16.7)	8 (57.1) 6 (42.9)	0.22

(Continued)

10.3389/fonc.2023.1115156

TABLE 2 Continued

Morphological Features	All Patients (N = 26)	Treated CIT Patients (N = 12)	Treated CT Patients (N = 14)	P value
Organizing pneumonia, n (%) *Yes* *No*	18 (69.2) 8 (30.8)	9 (75) 3 (25)	9 (64.3) 5 (35.7)	0.68
Cholesterol cleft, granuloma, n (%) *Yes* *No*	17 (65.4) 9 (34.6)	10 (83.3) 2 (16.7)	7 (50.0) 7 (50.0)	0.11
Reactive epithelial alterations, n (%) *Yes* *No*	15 (57.7) 11 (42.3)	9 (75) 3 (25)	6 (42.9) 8 (57.1)	0.13

CIT, chemo-immunotherapy; CT, chemotherapy; bold p-value: value below 0.05 was considered significant.

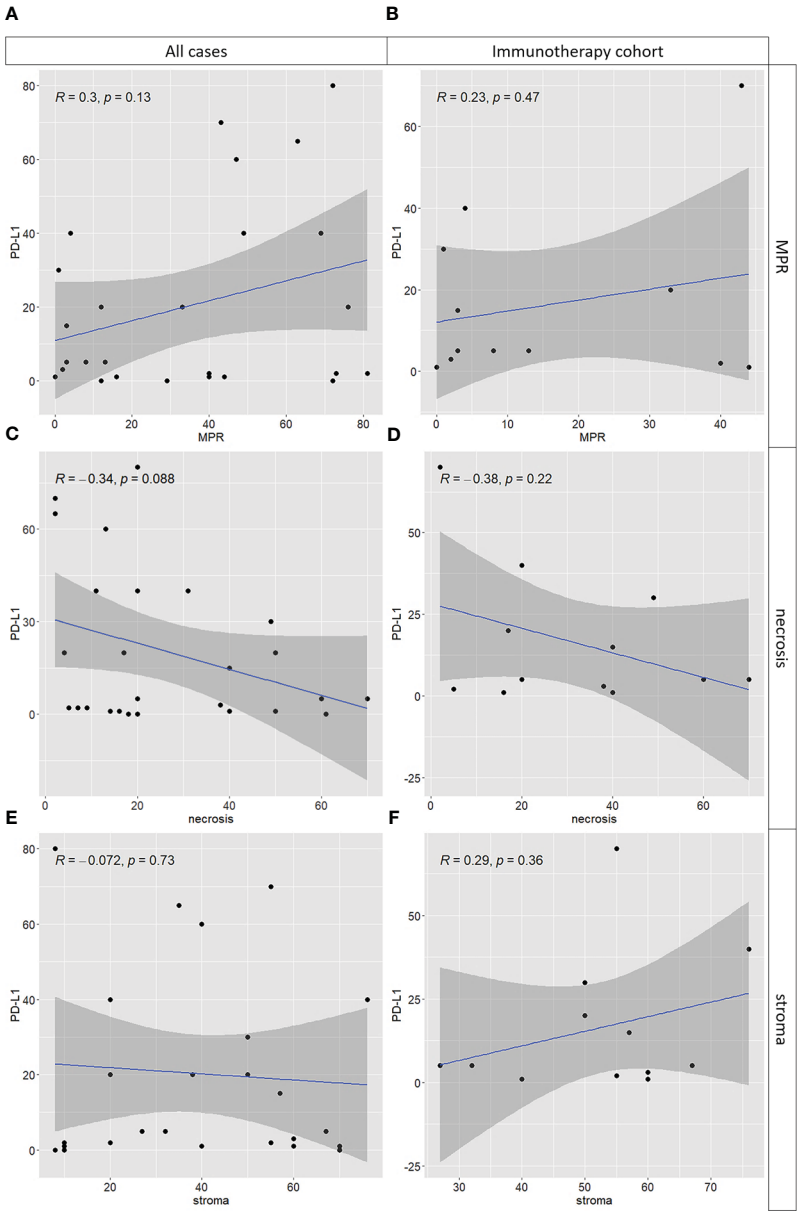

FIGURE 4
Correlations between PD-L1 tumor proportion score in naïve tumor and tumor components after neoadjuvant treatment including major pathological response (MPR), necrosis and stroma (i.e, inflammatory cells and fibrosis). On the left (i.e., panels **A**, **C**, **E**) the entire cohort of cases was used; on the right (i.e., panels **B**, **D**, **F**) only cases treated with chemo-immunotherapy were used. While for MPR **(A, B)** and necrosis **(C, D)** the results are consistent, a mild positive correlation between PD-L1 levels and stroma is observed in the chemo-immunotherapy cohort only **(F)**, not in the entire cohort **(E)**.

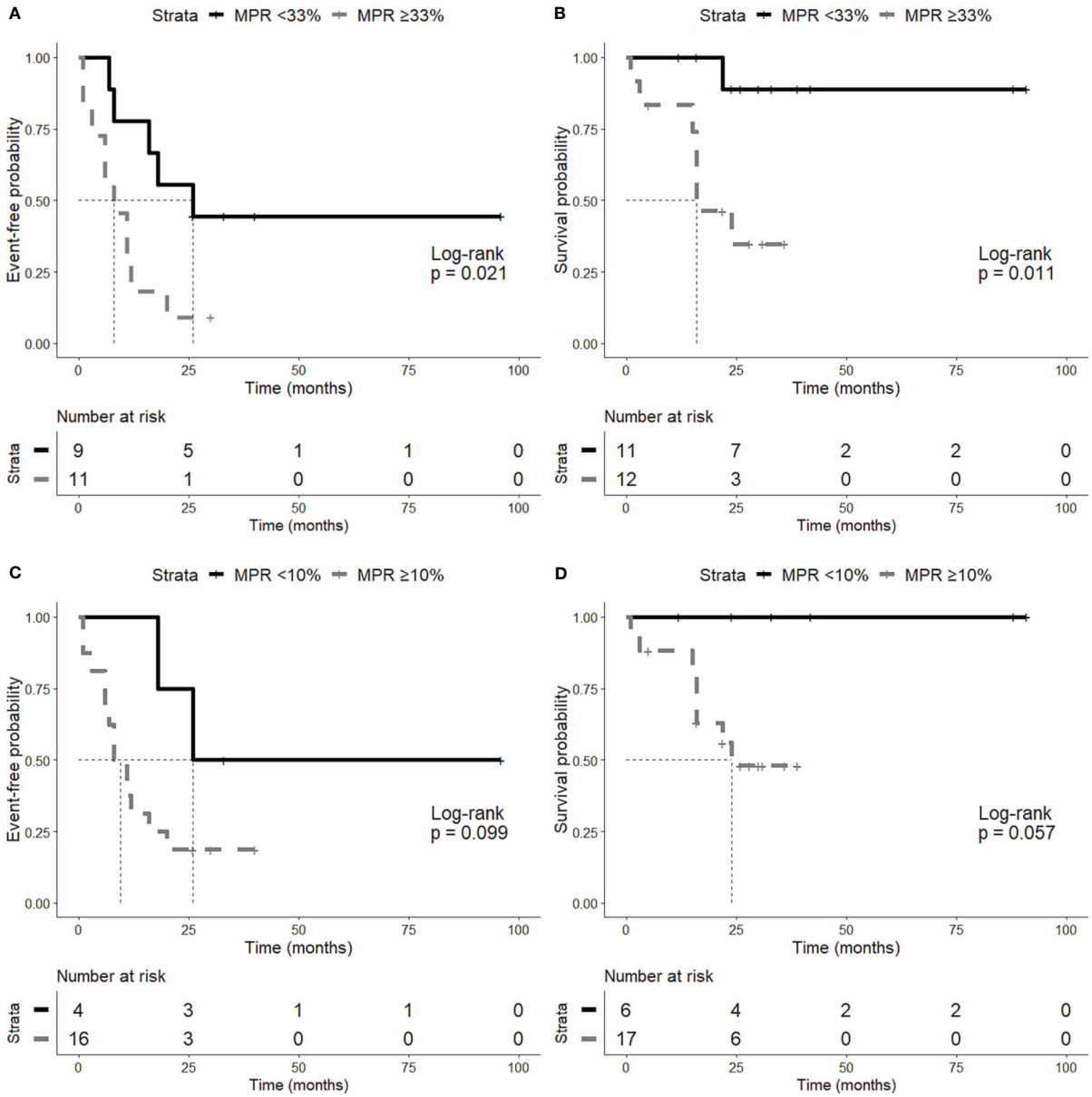

FIGURE 5
Time-to-event analyses. Patients were stratified according to the best cut-off of major pathological response (MPR) (i.e., 33% of viable tumor cells). Patients with less than 33% of viable tumor cells showed a better event-free survival (EFS) **(A)** and overall survival (OS) **(B)**. The classic 10% MPR cut-off was also tested and showed the same trend both on EFS **(C)** and OS **(D)**.

primary tumor and on lymph nodes (8.3%). On the contrary, no patient treated with chemotherapy alone achieved pCR or MPR.

In comparison to our results, Shi L and collaborators reported a higher pathological response in squamous cell lung carcinoma treated with neoadjuvant chemo-immunotherapy (24), with 66.7% of patients achieving MPR and 39.7% cases achieving a pCR. This discrepancy could be due to the different type of specimens included in the study. In fact, they analyzed only squamous histology, whereas we analyzed also adenocarcinoma, large cell neuroendocrine carcinoma, and adenosquamous carcinoma. Previous data showed that squamous cell carcinoma demonstrates a different response to immunotherapy in comparison to non-squamous cell carcinoma, with much more infiltration of immune cells and higher expression of PD-L1 (25–27). Even after neoadjuvant chemotherapy, squamous cell carcinoma shows a greater MPR than adenocarcinoma (28).

Recently, new clinical trials showed an improved EFS in patients treated with neoadjuvant chemo-immunotherapy or immunotherapy alone, as compared to chemotherapy treated patients (5, 6, 29). CheckMate-816 clinical trial compared neoadjuvant nivolumab plus chemotherapy versus neoadjuvant chemotherapy showing longer EFS in patients who achieved pathological response (5). In the present study, we observed a significant association between MPR after neoadjuvant treatment and prognosis. In particular, we observed an association between MPR and both EFS ($p = 0.04$) and OS ($p = 0.04$). These findings were also confirmed by multivariate analysis showing that MPR was associated with EFS independently of stage and treatment regimen ($p = 0.02$). We observed also a trend for a better

10.3389/fonc.2023.1115156

TABLE 3 Univariate and multivariate time-to-event analyses.

	OS		EFS	
	HR (95% CI)	*P-value*	*HR (95% CI)*	*P-value*
Univariate Analysis				
MPR*	1.03 (1.00-1.05)	**0.04**	1.02 (1.00-1.04)	**0.04**
Necrosis	0.97 (0.93-1.01)	0.16	0.96 (0.93-0.99)	**0.02**
Stroma	0.97 (0.93-1.01)	0.18	1 (0.97-1.02)	0.84
Stage				
I-II	1	0.12	1	0.12
III-IV	3.09 (0.76-12.59)		2.31 (0.81-6.60)	
Treatment				
CT	1	0.07	1	0.36
CIT	0.14 (0.02-1.19)		0.61 (0.22-1.74)	
Multivariate Analysis				
MPR*	1.02 (0.99-1.05)	0.27	1.03 (1.00-1.06)	**0.02**
Stage				
I-II	1	**0.05**	1	**0.02**
III-IV	4.56 (1.02-20.39)		4.10 (1.20-13.99)	
Treatment				
CT	1	0.20	1	0.94
CIT	0.20 (0.02-2.31)		1.05 (0.28-3.94)	

MPR, major pathological response; MPR*: MPR was used as continuous variable; OS, overall survival; EFS, event free survival; CIT, chemo-immunotherapy; CT, chemotherapy.
Patients were stratified according to MPR, stage and treatment to evaluate differences in OS and EFS.
Bold *p*-value: value below 0.05 was considered significant.

overall survival of patients treated with chemo-immunotherapy (p = 0.07) and, as expected, a trend for a better outcome of patients with stage I and II disease both in EFS (p = 0.12) and OS (p = 0.12). However, these results did not reach statistical significance probably due to the small number of cases.

Although promising, our results show that a considerable percentage of neoadjuvant chemo-immunotherapy treated patients (40%–75%) still do not achieve MPR or pCR, presenting a higher risk of relapse (5, 23, 30). Thus, the identification of predictive biomarkers of pathological response in resectable NSCLC is needed.

Cottrell and collaborators suggested that immunotherapy responsive tumors showed specific histological changes reflecting a state of immune activation (31). This finding could explain lack of correlation between pathological and radiological responses reported after neoadjuvant immunotherapy, related to the increased size of tumor on imaging caused by the infiltration of T-cells and macrophages, neovascularization and fibrosis (32).

In our study, we evaluated other histological features of tumor bed including necrosis and stroma. Regarding the amount of necrosis, we didn't observe any significant difference between the two treatment cohorts, whereas we observed a significantly higher amount of stroma in the neoplastic bed in the immuno-chemotherapy treated patients. This observation agrees with previous studies showing a greater amount of fibrosis in patients treated with chemo plus immunotherapy compared to patients treated with chemotherapy alone (18).

Regarding the identification of predictive factors for neoadjuvant treatments, we evaluated immunohistochemical PD-L1 expression since it is a critical marker to guide patient selection for immunotherapy in advanced NSCLC. However, we did not find associations between PD-L1 expression and pathological response or other histological features. We observed only a trend showing that PD-L1 levels positively correlated with MPR both in the general cohort and with MPR and stroma in patients treated with combination therapy. Although some studies reported a greater benefit from the combined chemo-immunotherapy in patients with a high PD-L1 immunohistochemical expression (33, 34), others suggested a lack of correlation between PD-L1 expression of pre-treatment specimens and patients' response (24, 30). Therefore, PD-L1 expression should not be considered a good predictive marker for neoadjuvant chemo-immunotherapy. Probably an optimal approach should not be based on the analysis of a single marker, but it should be more comprehensive evaluating not only the tumor but also its microenvironment.

In this study, after neoadjuvant chemo-immunotherapy, residuals tumors showed the upregulation of *YAP1* and *WWTR1*, which encode for YAP and TAZ respectively. Consistently, YAP/TAZ target expression was enhanced. These findings are consistent with high levels of fibrosis in these tumors since the activation of YAP/TAZ is crucial in regulating tissue repair (doi: 10.1038/s41573-020-0070-z). However, this activation could suggest also the selection of cells

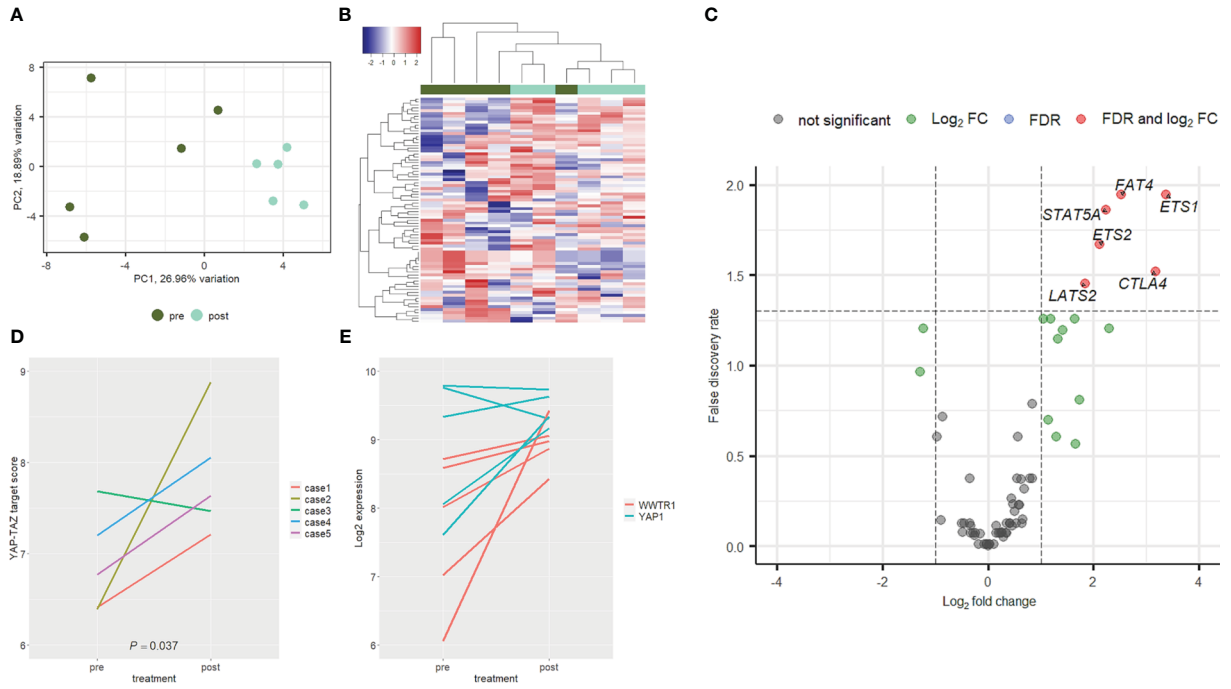

FIGURE 6
Expression profile of Hippo genes. Paired naïve (green) and post-surgical (cyan) tumors from the chemo-immunotherapy cohort clearly separated at PCA **(A)** and hierarchical clustering **(B)** analyses. In post-surgical specimens a trend towards gene upregulation was observed **(C)**, with six genes significantly deregulated (red dots). YAP-TAZ target score was significantly upregulated in post-surgical samples **(D)**. This was consistent with a trend towards upregulation of genes encoding for YAP and TAZ (i.e., YAP1 and WWTR1 respectively, especially the latter) **(E)**.

resistant to treatment (doi: 10.1016/j.cell.2014.06.004), and could open new perspectives in further lines of treatment. Similarly, the enhanced expression of *CTLA4* after treatment with PD-1 or PD-L1 agonists, could be a resistance mechanism that should be considered after progression to PD-1/PD-L1 blockade.

Several limitations associated with the present study should be mentioned. First, the small sample size made it difficult to obtain robust statistical results and a further validation is warranted. Second, this was a retrospective, non-randomized single-center study needing to be confirmed in prospective cohorts. Moreover, our study lacks

TABLE 4 Genes deregulated after adjuvant chemo-immunotherapy.

Gene symbol	Gene name	Log2 FC	FDR
ETS1	ETS proto-oncogene 1, transcription factor	3.38	0.0113
FAT4	FAT atypical cadherin 4	2.52	0.0113
STAT5A	signal transducer and activator of transcription 5A	2.24	0.0137
ETS2	ETS proto-oncogene 2, transcription factor	2.11	0.0214
CTLA4	cytotoxic T-lymphocyte associated protein 4	3.17	0.0303
LATS2	large tumor suppressor kinase 2	1.84	0.0351
DCHS1	dachsous cadherin-related 1	1.65	0.0552
YWHAB	tyrosine 3-monooxygenase/tryptophan 5-monooxygenase activation protein beta	1.06	0.0552
SMAD7	SMAD family member 7	1.19	0.0552
TEAD1	TEA domain transcription factor 1	2.29	0.0623
AJUBA	ajuba LIM protein	-1.22	0.0623
MYC	MYC proto-oncogene, bHLH transcription factor	1.41	0.0638
RASSF5	Ras association domain family member 5	1.32	0.0715
SCRIB	scribble planar cell polarity protein	-1.29	0.1080

FC, fold change; FDR, false discovery rate.

long-term follow up that will be necessary to evaluate the efficacy of neoadjuvant chemo-immunotherapy on recurrence and survival in resectable NSCLC.

In conclusion, despite these limitations, our study demonstrated that the combination of immunotherapy and chemotherapy in neoadjuvant setting significantly improves pathological response in comparison to chemotherapy alone. At the same time, we suggested that chemo-immunotherapy could induce different morphological and molecular changes of treated specimens, both of the tumor and of the collateral lung parenchyma, in comparison to chemotherapy alone. These differences can impact on specimens processing and scoring in the evaluation of pathological response, and can increase our knowledge of biological and histological features of responders and non-responders to different neoadjuvant therapies.

Data availability statement

The datasets presented in this study can be found in online repositories. The names of the repository/repositories and accession number(s) can be found in the article/Supplementary Material.

Ethics statement

The studies involving human participants were reviewed and approved by "Comitato Etico di Area Vasta Nord Ovest" (CEAVNO) for Clinical Experimentation (Protocol Number: ID19211). The patients/participants provided their written informed consent to participate in this study.

Author contributions

GA, EB, FM, and GF contributed to conception and design of the study. AL, AC, and GM organized the database. AP performed the statistical analysis. GA and IS wrote the first draft of the manuscript. GA, GR, and CZ wrote sections of the manuscript. All authors contributed to manuscript revision, read, and approved the submitted version.

Conflict of interest

The authors declare that the research was conducted in the absence of any commercial or financial relationships that could be construed as a potential conflict of interest.

Publisher's note

All claims expressed in this article are solely those of the authors and do not necessarily represent those of their affiliated organizations, or those of the publisher, the editors and the reviewers. Any product that may be evaluated in this article, or claim that may be made by its manufacturer, is not guaranteed or endorsed by the publisher.

Supplementary material

The Supplementary Material for this article can be found online at: https://www.frontiersin.org/articles/10.3389/fonc.2023.1115156/full#supplementary-material

References

1. Arriagada R, Bergman B, Dunant A, Le Chevalier T, Pignon JP, Vansteenkiste J. Cisplatin-based adjuvant chemotherapy in patients with completely resected non-small-cell lung cancer. *N Engl J Med* (2004) 350:351–60. doi: 10.1056/NEJMoa031644

2. Burdett S, Pignon JP, Tierney J, Tribodet H, Stewart L, Le Pechoux C, et al. Adjuvant chemotherapy for resected early-stage non-small cell lung cancer. *Cochrane Database Syst Rev* (2015) 3:CD011430. doi: 10.1002/14651858.CD011430

3. Martin J, Ginsberg RJ, Venkatraman ES, Bains MS, Downey RJ, Korst RJ, et al. Long-term results of combined-modality therapy in resectable non– small-cell lung cancer. *J Clin Oncol* (2002) 20:1989–95. doi: 10.1200/JCO.2002.08.092

4. Arriagada R, Dunant A, Pignon JP, Bergman B, Chabowski M, Grunenwald D, et al. Long-term results of the international adjuvant lung cancer trial evaluating adjuvant cisplatin-based chemotherapy in resected lung cancer. *J Clin Oncol* (2010) 28:35–42. doi: 10.1200/JCO.2009.23.2272

5. Forde PM, Spicer J, Lu S, Provencio M, Mitsudomi T, Awad MM, et al. Neoadjuvant nivolumab plus chemotherapy in resectable lung cancer. *N Engl J Med* (2022) 386:1973–85. doi: 10.1056/NEJMoa2202170

6. Cascone T, William WN, Weissferdt A, Leung CH, Lin HY, Pataer A, et al. Neoadjuvant nivolumab or nivolumab plus ipilimumab in operable non-small cell lung cancer: the phase 2 randomized NEOSTAR trial. *Nat Med* (2021) 27:504–14. doi: 10.1038/s41591-020-01224-28

7. Bott MJ, Yang SC, Park BJ, Adusumilli PS, Rusch VW, Isbell JM, et al. Initial results of pulmonary resection after neoadjuvant nivolumab in patients with resectable non-small cell lung cancer. *J Thorac Cardiovasc Surg* (2019) 158:269–76. doi: 10.1016/j.jtcvs.2018.11.124

8. Rojas F, Parra ER, Wistuba II, Haymaker C, Solis Soto LM. Pathological response and immune biomarker assessment in non-Small-Cell lung carcinoma receiving neoadjuvant immune checkpoint inhibitors. *Cancers (Basel)* (2022) 14:2775. doi: 10.3390/cancers14112775

9. Travis WD, Dacic S, Wistuba I, Sholl L, Adusumilli P, Bubendorf L, et al. IASLC multidisciplinary recommendations for pathologic assessment of lung cancer resection specimens after neoadjuvant therapy. *J Thorac Oncol* (2020) 15:709–40. doi: 10.1016/j.jtho.2020.01.005

10. Pataer A, Kalhor N, Correa AM, Raso MG, Erasmus JJ, Kim ES, et al. Histopathologic response criteria predict survival of patients with resected lung cancer after neoadjuvant chemotherapy. *J Thorac Oncol* (2012) 7:825–32. doi: 10.1097/JTO.0b013e318247504a

11. Chaft JE, Rusch V, Ginsberg MS, Paik PK, Finley DJ, Kris MG, et al. Phase II trial of neoadjuvant bevacizumab plus chemotherapy and adjuvant bevacizumab in patients with resectable nonsquamous non-small-cell lung cancers. *J Thorac Oncol* (2013) 8:1084–90. doi: 10.1097/JTO.0b013e31829923ec

12. Junker K, Thomas M, Schulmann K, Klinke F, Bosse U, Müller KM. Tumour regression in non-small-cell lung cancer following neoadjuvant therapy. histological assessment. *J Cancer Res Clin Oncol* (1997) 123:469–477. doi: 10.1007/BF01192200

13. Shu CA, Gainor JF, Awad MM, Chiuzan C, Grigg CM, Pabani A, et al. Neoadjuvant atezolizumab and chemotherapy in patients with resectable non-small-cell lung cancer: An openlabel, multicentre, single-arm, phase 2 trial. *Lancet Oncol* (2020) 21:786–95. doi: 10.1016/S1470-2045(20)30140-6

14. Rothschild SI, Zippelius A, Eboulet EI, Savic Prince S, Betticher D, Bettini A, et al. Durvalumab in addition to neoadjuvant chemotherapy in patients with stage IIIA(N2) non-small-cell lung cancer-a multicenter single-arm phase II trial. *J Clin Oncol* (2021) 39:2872–80. doi: 10.1200/JCO.21.00276

15. Chen X, MA K. Neoadjuvant therapy in lung cancer: What is most important: Objective response rate or major pathological response? *Curr Oncol* (2021) 28:4129–38. doi: 10.3390/curroncol28050350

16. Mouillet G, Monnet E, Milleron B, Puyraveau M, Quoix E, David P, et al. Pathologic complete response to preoperative chemotherapy predicts cure in early-

stage non-small-cell lung cancer: combined analysis of two IFCT randomized trials. *J Thorac Oncol* (2012) 7:841–9. doi: 10.1097/JTO.0b013e31824c7d92

17. Rusch VW, Chansky K, Kindler HL, Nowak AK, Pass HI, Rice DC, et al. Staging and prognostic factors committee, advisory boards, and participating institutions. prognostic factors committee, the IASLC mesothelioma staging project: Proposals for the m descriptors and for revision of the TNM stage groupings in the forthcoming (eighth) edition of the TNM classification for mesothelioma. *J Thorac Oncol* (2016) 11:2112–9. doi: 10.1016/j.jtho.2016.09.124

18. Weissferdt A, Pataer A, Vaporciyan AA, Correa AM, Sepesi B, Moran CA, et al. Agreement on major pathological response in NSCLC patients receiving neoadjuvant chemotherapy. *Clin Lung Cancer* (2020) 21:341–8. doi: 10.1016/j.cllc.2019.11.003

19. Hellmann MD, Chaft JE, William WNJr., Rusch V, Pisters KM, Kalhor N, et al. Pathological response after neoadjuvant chemotherapy in resectable non-small-cell lung cancers: Proposal for the use of major pathological response as a surrogate endpoint. *Lancet Oncol* (2014) 15:e42–50. doi: 10.1016/S1470-2045(13)70334-6

20. Cao C, Guo A, Chen C, Chakos A, Bott M, Yang CJ, et al. Systematic review of neoadjuvant immunotherapy for patients with non-small cell lung cancer. *Semin Thorac Cardiovasc Surg* (2021) 33:850–7. doi: 10.1053/j.semtcvs.2020.12.012

21. Gao S, Li N, Gao S, Xue Q, Ying J, Wang S, et al. Neoadjuvant PD-1 inhibitor (Sintilimab) in NSCLC. *J Thorac Oncol* (2020) 15:816–26. doi: 10.1016/j.jtho.2020.01.017

22. Pignon JP, Tribodet H, Scagliotti GV, Douillard JY, Shepherd FA, Stephens RJ, et al. Lung adjuvant cisplatin evaluation: A pooled analysis by the LACE collaborative group. *J Clin Oncol* (2008) 26:3552–9. doi: 10.1200/JCO.2007.13.9030

23. Provencio M, Nadal E, Insa A, García-Campelo MR, Casal-Rubio J, Dómine M, et al. Neoadjuvant chemotherapy and nivolumab in resectable non-small-cell lung cancer (NADIM): An open-label, multicentre, single-arm, phase 2 trial. *Lancet Oncol* (2020) 21:1413–22. doi: 10.1016/S1470-2045(20)30453-8

24. Shi L, Meng Q, Tong L, Li H, Dong Y, Su C, et al. Pathologic response and safety to neoadjuvant PD-1 inhibitors and chemotherapy in resectable squamous non-small-cell lung cancer. *Front Oncol* (2022) 12:956755. doi: 10.3389/fonc.2022.956755

25. Chen Q, Fu YY, Yue QN, Wu Q, Tang Y, Wang WY, et al. Distribution of PD-L1 expression and its relationship with clinicopathological variables: An audit from 1071 cases of surgically resected non-small cell lung cancer. *Int J Clin Exp Pathol* (2019) 12:774–86.

26. Shen D, Wang J, Wu J, Chen S, Li J, Liu J, et al. Neoadjuvant pembrolizumab with chemotherapy for the treatment of stage IIB-IIIB resectable lung squamous cell carcinoma. *J Thorac Dis* (2021) 13:1760–8. doi: 10.21037/jtd-21-103

27. Ling Y, Li N, Li L, Guo C, Wei J, Yuan P, et al. Different pathologic responses to neoadjuvant anti-PD-1 in primary squamous lung cancer and regional lymph nodes. *NPJ Precis Oncol* (2020) 4:32. doi: 10.1038/s41698-020-00135-2

28. Qu Y, Emoto K, Eguchi T, Aly RG, Zheng H, Chaft JE, et al. Pathologic assessment after neoadjuvant chemotherapy for NSCLC: Importance and implications of distinguishing adenocarcinoma from squamous cell carcinoma. *J Thorac Oncol* (2019) 14:482–93. doi: 10.1016/j.jtho.2018.11.017

29. Lee JM, Kim AW, Marjanski T, Falcoz PE, Tsuboi M, Wu YL, et al. Important surgical and clinical end points in neoadjuvant immunotherapy trials in resectable NSCLC. *JTO Clin Res Rep* (2021) 2:100221. doi: 10.1016/j.jtocrr.2021.100221

30. Provencio M, Serna-Blasco R, Nadal E, Insa A, García-Campelo MR, Casal Rubio J, et al. Overall survival and biomarker analysis of neoadjuvant nivolumab plus chemotherapy in operable stage IIIA non-Small-Cell lung cancer (NADIM phase II trial). *J Clin Oncol* (2022) 40:2924–33. doi: 10.1200/JCO.21.02660

31. Cottrell TR, Thompson ED, Forde PM, Stein JE, Duffield AS, Anagnostou V, et al. Pathologic features of response to neoadjuvant anti-PD-1 in resected non-small-cell lung carcinoma: A proposal for quantitative immune-related pathologic response criteria (irPRC). *Ann Oncol* (2018) 29:1853–60. doi: 10.1093/annonc/mdy218

32. Nishino M, Hatabu H, Hodi FS. Imaging of cancer immunotherapy: Current approaches and future directions. *Radiology* (2019) 290:9–22. doi: 10.1148/radiol.2018181349

33. Wang J, Yu X, Barnes G, Leaw S, Bao Y, Tang B. The effects of tislelizumab plus chemotherapy as first-line treatment on health-related quality of life of patients with advanced squamous non-small cell lung cancer: Results from a phase 3 randomized clinical trial. *Cancer Treat Res Commun* (2021) 30:100501. doi: 10.1016/j.ctarc.2021.100501

34. Zhou C, Wang Z, Sun Y, Cao L, Ma Z, Wu R, et al. Sugemalimab versus placebo, in combination with platinum-based chemotherapy, as first-line treatment of metastatic non-small-cell lung cancer (GEMSTONE-302): Interim and final analyses of a double-blind, randomised, phase 3 clinical trial. *Lancet Oncol* (2022) 23:220–33. doi: 10.1016/S1470-2045(21)00650-1

frontiers | Frontiers in Oncology

TYPE Brief Research Report
PUBLISHED 21 March 2023
DOI 10.3389/fonc.2023.1012783

OPEN ACCESS

EDITED BY
Michele Simbolo,
University of Verona, Italy

REVIEWED BY
Lorenzo Belluomini,
University of Verona, Italy
Alessandro Morabito,
G. Pascale National Cancer Institute Foundation (IRCCS), Italy

*CORRESPONDENCE
Richa Dawar
richa.dawar@med.miami.edu

SPECIALTY SECTION
This article was submitted to Thoracic Oncology, a section of the journal Frontiers in Oncology

RECEIVED 05 August 2022
ACCEPTED 08 February 2023
PUBLISHED 21 March 2023

CITATION
Kareff SA, Gawri K, Khan K, Kwon D, Rodriguez E, Lopes GdL and Dawar R (2023) Efficacy and outcomes of ramucirumab and docetaxel in patients with metastatic non-small cell lung cancer after disease progression on immune checkpoint inhibitor therapy: Results of a monocentric, retrospective analysis. *Front. Oncol.* 13:1012783. doi: 10.3389/fonc.2023.1012783

Efficacy and outcomes of ramucirumab and docetaxel in patients with metastatic non-small cell lung cancer after disease progression on immune checkpoint inhibitor therapy: Results of a monocentric, retrospective analysis

Samuel A. Kareff[1], Kunal Gawri[2], Khadeja Khan[3], Deukwoo Kwon[4], Estelamari Rodriguez[5], Gilberto de Lima Lopes[5] and Richa Dawar[5]*

[1]Department of Graduate Medical Education, University of Miami Sylvester Comprehensive Cancer Center/Jackson Memorial Hospital, Miami, FL, United States, [2]Department of Medicine, State University of New York-Buffalo, Buffalo, NY, United States, [3]Department of Undergraduate Medical Education, University of Miami Miller School of Medicine, Miami, FL, United States, [4]Department of Population Health Science and Policy, Icahn School of Medicine at Mount Sinai, New York, NY, United States, [5]Department of Medical Oncology, University of Miami Sylvester Comprehensive Cancer Center, Miami, FL, United States

Current first-line standard therapy for metastatic non-small cell lung cancer without driver mutations involves chemotherapy and immunotherapy combination. Prior to the advent of immune checkpoint inhibition, REVEL, a randomized phase III trial demonstrated improved progression-free and overall survival with ramucirumab and docetaxel (ram+doc) in patients who failed platinum-based first-line therapy. Long-term outcomes related to second-line ramucirumab and docetaxel after first-line immunotherapy exposure remain unknown. We analyzed outcomes for 35 patients from our center whom received ramucirumab and docetaxel following disease progression on chemotherapy and immunotherapy combination. Median progression-free survival among patients who received ram+doc after exposure to immunotherapy was 6.6 months (95% CI = 5.5 to 14.9 months; $p<0.0001$), and median overall survival was 20.9 months (95% CI = 13.4 months to infinity; $p<0.0001$). These outcomes suggest that there may a synergistic benefit to combining chemotherapy with anti-angiogenic therapy after immunotherapy exposure. Future analyses should be evaluated prospectively and among a larger patient subset.

KEYWORDS

ramucirumab, docetaxel, platinum-based treatment resistance, metastatic NSCLC, REVEL

Introduction

Non-small cell lung cancer (NSCLC) is the most common type of lung cancer, accounting for nearly 80% of all cases, and often presents in the locally advanced or metastatic settings (1). Currently, a combination of chemotherapy and/or immunotherapy (IO) is considered standard first-line treatment for metastatic NSCLC (mNSCLC) without driver mutations, often tailored based on a patient's programmed death-ligand 1 (PD-L1) status (2). Before the advent of IO as first-line therapy, REVEL, a randomized, multicenter, phase III clinical trial, demonstrated improved progression-free survival (PFS), overall survival (OS), and quality of life (QoL) with ramucirumab and docetaxel (ram+doc) chemotherapy and antiangiogenic combination in patients whose disease progressed after platinum-based doublet first-line chemotherapy compared with docetaxel alone (3, 4). This combination was proposed utilizing ramucirumab as a complete human monoclonal IgG1 antibody with direct vascular endothelial growth factor receptor 2 (VEGFR2) antagonism given already known improved outcomes with docetaxel in platinum-resistant disease (5). Indeed, this biological rationale of overcoming the demonstrated immunosuppressive effect of VEGF has been proven in other lines of therapy and in combination with immunotherapy, such as the IMPOWER150 study which demonstrated improved outcomes for nonsquamous mNSCLC when combining atezolizumab, bevacizumab, and platinum-doublet chemotherapy in the first-line setting (6). There have been studies that have shown promising results in other forms of platinum-resistant tumor histologies, namely, urothelial and gastric cancers (7, 8). There exist data mostly limited to retrospective cohort analyses in East Asia and Europe discussing responses to ram+doc treatment in patients pretreated with IO-based therapy; however, any synergistic benefit has not been proven for patients with mNSCLC (9). Therefore, our study aims to clarify the efficacy and outcomes of this combined therapeutic approach in patients with paclitaxel-resistant mNSCLC.

Materials and methods

We performed a retrospective cohort study among all patients with mNSCLC treated at the University of Miami Sylvester Comprehensive Cancer Center. We retrospectively identified all patients with mNSCLC whose disease demonstrated progression after IO-based therapy and then received ram+doc as a subsequent line of therapy between January 1st, 2010 and March 1st, 2020. A total of thirty-nine patients were identified whom met these inclusion criteria. We subsequently excluded 4 patients with EGFR or ALK driver mutations from our analysis. As such, thirty-five ($n = 35$) patients were included in our final analysis. We assessed patients' PFS and OS after ram+doc treatment utilizing the Kaplan-Meier method as primary outcomes. We compared our center's retrospective data with those from REVEL data utilizing a simulation study *via* Wilcoxon test. Since REVEL data was not available for reproduction, we used median PFS and median OS and corresponding 95% CIs to estimate the distribution of median survival time for our dataset compared to that of REVEL using an approximate Bayesian computation (ABC) approach. We also collected information on adverse events (AEs) during ram+doc treatment as a secondary outcome. This study was approved by the University of Miami Institutional Review Board eProst #20170427.

Results

Patient characteristics

Of a total 44 patients treated with ramucirumab and docetaxel at our center, we excluded 6 patients with *EGFR* mutation, 1 with *ALK* mutation, and 2 without previous exposure to IO. We report the patient demographics as well as some treatment characteristics for the 35 included patients in Table 1. Patients' age ranged from 45 to 76 years (median 65 years). There were a total 17 females (48.6%) and 18 males (51.4%) represented in the sample. 19 patients identified as Hispanic/Latinx (54.3%), 12 as white (34.3%), and 1

TABLE 1 Demographics of patients whom received ramucirumab and docetaxel, and characteristics of treatment, at the University of Miami.

Demographic/Treatment Category	Sub-Category	*n* (%)
Race/Ethnicity	Black	1 (2.9)
	Hispanic/Latinx	19 (54.3)
	White	12 (34.3)
	Other/Multiple	3 (8.6)
Gender	Female	17 (48.6)
	Male	18 (51.4)
Age	40-49	1 (2.9)
	50-59	7 (20)
	60-69	18 (51.4)
	70-79	9 (25.7)
History of Tobacco Use	Yes	28 (80)
	No	7 (20)
Histology	Adenocarcinoma	33 (94.3)
	Squamous Cell Carcinoma	2 (5.7)
PDL1 Percentage	0%	14 (40)
	<50%	7 (20)
	>50%	5 (14.3)
	Unknown	9 (25.7)
Number of Metastatic Sites	<3	1 (2.9)
	>3	34 (97.1)
Sites of Metastases	Bone	24 (68.9)
	Liver	11 (31.4)
	Brain	7 (20)
First Line of Treatment	Platinum-doublet + IO	20 (57.1)
	Platinum-doublet chemo	11 (31.4)
	Platinum-doublet + anti-VEGF	2 (5.7)
	IO alone	1 (2.9)
	Other chemo	1 (2.9)
Ram+Doc Line of Therapy	Second	20 (57.1)
	Third	11 (31.4)
	Fourth or Beyond	4 (11.4)

as African American (2.8%). 28 were tobacco users (80%), while 7 were never-tobacco users (20%). All 35 patients received ICI as first-, second-, or third-line therapy for mNSCLC, which was followed immediately by ram+doc upon disease progression. 33 patients' tumor histology was adenocarcinoma (94.3%), while 2 patients' tumor histology was squamous cell carcinoma (5.7%). All patients had disease with at least 3 metastatic sites, listed in the following order of frequency: 1) bone, 2) liver, and 3) brain.

Primary and secondary patient outcomes

Median PFS (mPFS) among patients whom received ram+doc therapy after IO exposure was 6.6 months (95% confidence interval [CI] = 5.5 to 14.9 months; $p<0.0001$] (Figure 1A) and median OS (mOS) was 20.9 months (95% CI = 13.4 months to infinity; $p<0.0001$) (Figure 1B). There were no statistically significant differences detected among tumor histology. Since the REVEL data were not available for independent reproduction, we utilized the ABC approach to estimate how many *p*-values are less than 0.0001 in 1,000 tests for simulated two datasets; this approach has been validated elsewhere (10). Given that all 1,000 p-values were less than 0.0001, we found these results to be statistically significant in estimating our CIs. Moreover, since the 95% CIs of our cohort versus that of REVEL did not overlap, we considered these improved mPFS and mOS outcomes to be statistically significant as well.

We observed six patients with treatment-related adverse events related to ramucirumab: two patients with Grade 1 hypertension; two patients with proteinuria (one Grade 1 and one Grade 2); one patient with Grade 3 hemoptysis, and one with Grade 2 fatigue. Three of these patients experiencing adverse events ($n = 3/7$; 42.8%) required dose reduction. Docetaxel use led to 31 adverse events: 15 patients with fatigue, with at least one Grade 3, three patients with skin/nail changes, one patient with Grade 3 myalgias, 2 patients with neutropenia (1 Grade 3), 4 patients with anemia, 4 patients with neuropathy (1 Grade 3), and 2 patients with cough/COPD exacerbation. Three of the patients with Grade 3 adverse events ($n = 3/4$; 75%) required dose reduction of docetaxel. An additional patient demonstrated Grade 2 arthritis that was attributed to previous IO exposure, and it is unclear how ram+doc subsequent therapy mediated this toxicity. In total, seven patients ($n = 7/35$; 20%) required treatment discontinuation during the course of therapy. Further detailed results are available in Table 2.

Discussion

In our retrospective analysis, we found a statistically longer mPFS and mOS for patients with mNSCLC treated with ram+doc after progression on IO at our center compared to the original cohort reported in the REVEL study, which first analyzed this combination chemotherapy and antiangiogenic-therapy regimen in 2014 (Figures 1A, B). Our results did not show a difference in these primary outcomes based on tumor histology.

These findings are striking in that they demonstrate a possible synergy between IO pre-treatment and exposure to second-line (or beyond) antiangiogenic-therapy, namely, ramucirumab, in combination with docetaxel. These findings have been echoed in other retrospective cohorts in East Asia. For example, a retrospective review of 99 patients in multiple Japanese centers found a statistically significant mPFS response of 5.9 months in those pre-treated with IO compared to those who did not have IO exposure (2.6 months) (11). These findings were further bolstered in a *post-hoc* sub-group analysis of the original REVEL study in which East Asian patients demonstrated a mPFS of 4.88 months and mOS of 15.4 months (12).

Furthermore, our cohort did not demonstrate unexpected and/or significant adverse events, thereby supporting the safety of ram+doc as combination therapy. This observation also mirrors outcomes in other retrospective cohorts, such as a review of 77 patients in Germany that did not demonstrate unexpected toxicities, i.e., no more than 9.09% febrile neutropenia, fatigue, mucositis, stomatitis, or ileus (13). Similarly, another retrospective analysis in Japan estimated up to 16.7% total (and 11.1% Grade 3 or more) pneumonitis, which is more frequent than the 2.9% of pneumonitis as well as COPD exacerbation observed in our cohort (14).

Our findings also echo activity among a similar combination of docetaxel with nintedanib, a tyrosine kinase inhibitor that has activity against multiple kinases including VEGF. This

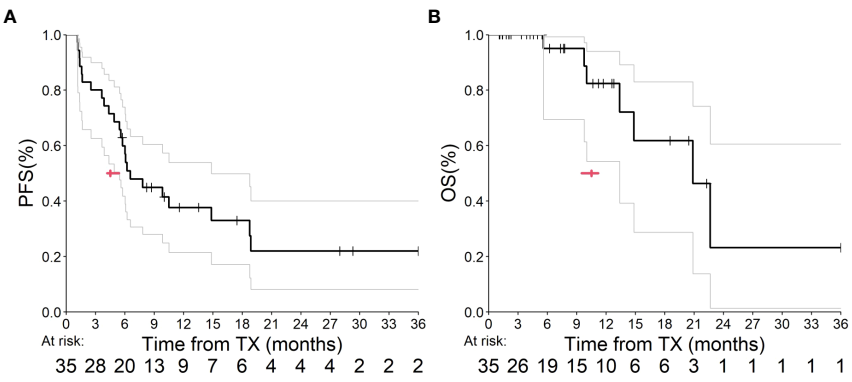

FIGURE 1
(A, B) This graph depicts PFS **(A)** and OS **(B)** from our UM outcomes. The bold line indicates our Kaplan-Meier analysis, and the gray lines represent our 95% CI estimates. The red arrow indicates median estimates within both graphs.

10.3389/fonc.2023.1012783

TABLE 2 Treatment-related adverse events related to ramucirumab and docetaxel among patients in the UM Cohort.

Toxicity Variable	All Grades (%)	Grade 3+ (%)
Hypertension (Ram)	2 (5.7)	–
Proteinuria (Ram)	2 (5.7)	–
Bleeding (Ram)	1 (2.9)	1 (2.9)
Fatigue (Ram)	1 (2.9)	–
Dose-reduction of Ram	1 (2.9)	1 (2.9)
Fatigue (Doc)	15 (42.9)	1 (2.9)
Skin/nail changes (Doc)	3 (8.6)	–
Myalgias (Doc)	1 (2.9)	1 (2.9)
Neutropenia (Doc)	2 (5.7)	1 (2.9)
Anemia (Doc)	4 (11.4)	–
Neuropathy (Doc)	4 (11.4)	1 (2.9)
Cough/COPD Exacerbation (Doc)	2 (5.7)	–
Dose-reduction of Doc	2 (5.7)	2 (5.7)
Dose-reduction of Ram + Doc	2 (5.7)	2 (5.7)
Arthralgia (IO)	1 (2.9)	–

This symbol means no value.

combination was originally approved based on the LUME-Lung1 study which demonstrated improved PFS and OS compared to docetaxel alone, particularly in adenocarcinoma histology, compared to docetaxel alone in the second-line setting (15). Real-world outcomes mirror those reported at our institution after treatment with chemo- and immunotherapy. Specifically, the VARGADO cohort demonstrated a mPFS of 6.4 months, with a 1-year OS rate of 52% in the third-line setting (16). Furthermore, another German cohort reported a mOS of 8.4 months in adenocarcinoma histology specifically (17).

Two strengths of our study are its location and demographics. Specifically, we report herein the first such retrospective analysis consisting of North American patients, with a majority of patients whom identified ethnically as Hispanic/LatinX. Additionally, our cohort's outcomes rank among the longest PFS and OS benefits recorded with post-IO ram+doc exposure to date. This result will require additional study with similar ethnic and geographic cohorts.

Our analysis has several limitations. First, this is a single-center, retrospective analysis, and as such these observations should be confirmed in a prospective fashion. The Phase II Lung-Map S1800A study evaluated ramucirumab with pembrolizumab combination therapy compared to standard of care chemotherapy, of which two-thirds of the control arm received ram+doc, and was found to demonstrate an OS benefit (17). *Post-hoc* analyses will be required to understand the true PFS and OS estimates seen in this sub-group, however. Additionally, the TREAT-LUNG observational study reported preliminary data for second- and third-line docetaxel vs. ram+doc in patients previously treated with both platinum-based chemotherapy and IO with a subset of patients demonstrating long-term responses (i.e., plateaus in Kaplan-Meier plots) (18). These findings merit closer attention once presented formally in the literature. The greatest limitation of our study is its small size. For example, a larger Japanese cohort of 1,439 patients utilized a propensity score analysis and did not find a PFS or OS advantage with this treatment strategy (19).

Overall, our institution's experience with this combination chemo- and antiangiogenic-therapy strategy adds to the data related to ram+doc after IO exposure in mNSCLC. Interpretation should be limited given its retrospective timeframe and single-center patient population.

Resource identification initiative

Ramucirumab RRID: AB_2911024.

Data availability statement

The raw data supporting the conclusions of this article will be made available by the authors, without undue reservation.

Ethics statement

The studies involving human participants were reviewed and approved by University of Miami IRB Eprost 20170427. Written informed consent for participation was not required for this study in accordance with the national legislation and the institutional requirements.

Author contributions

First authorship: SK. Equal contribution: KG, KK, DK, GL, ER. Senior/last authorship: RD. All authors contributed to the article and approved the submitted version.

Acknowledgments

We would like to acknowledge our patients; their families and caretakers; as well as our study collaborators for participating in the care necessary to perform this retrospective analysis. This study was presented in part at the virtual International Association for the Study of Lung Cancer 2020 World Conference on Lung Cancer.

Conflict of interest

The authors declare that the research was conducted in the absence of any commercial or financial relationships that could be construed as a potential conflict of interest.

Publisher's note

References

1. Molina JR, Yang P, Cassivi SD, Schild SE, Adjei AA. Non-small cell lung cancer: epidemiology, risk factors, treatment, and survivorship. *Mayo Clin Proc* (2008) 83(5):584–94. doi: 10.1016/S0025-6196(11)60735-0

2. Paz-Ares L, Luft A, Vicente D, Tafreshi A, Gümüş M, Mazières J, et al. Pembrolizumab plus chemotherapy for squamous non–Small-Cell lung cancer. *New Engl J Med* (2018) 379(21):2040–51. doi: 10.1056/NEJMoa1810865

3. Pérol M, Ciuleanu TE, Arrieta O, Prabhash K, Syrigos KN, Goksel T, et al. Quality of life results from the phase 3 REVEL randomized clinical trial of ramucirumab-plus-docetaxel versus placebo-plus-docetaxel in advanced/metastatic non-small cell lung cancer patients with progression after platinum-based chemotherapy. *Lung Cancer* (2016) 93:95–103. doi: 10.1016/j.lungcan.2016.01.007

4. Garon EB, Ciuleanu TE, Arrieta O, Prabhash K, Syrigos KN, Goksel T, et al. Ramucirumab plus docetaxel versus placebo plus docetaxel for second-line treatment of stage IV non-small-cell lung cancer after disease progression on platinum-based therapy (REVEL): a multicentre, double-blind, randomised phase 3 trial. *Lancet* (2014) 384(9944):665–73. doi: 10.1016/S0140-6736(14)60845-X

5. Fossella FV, DeVore R, Kerr RN, Crawford J, Natale RR, Dunphy F, et al. Randomized phase III trial of docetaxel versus vinorelbine or ifosfamide in patients with advanced non-small-cell lung cancer previously treated with platinum-containing chemotherapy regimens. the TAX 320 non-small cell lung cancer study group. *J Clin Oncol* (2000) 18(12):2354–62. doi: 10.1200/JCO.2000.18.12.2354

6. Socinski MA, Jotte RM, Cappuzzo F, Orlandi F, Stroyakovskiy D, Nogami N, et al. Atezolizumab for first-line treatment of metastatic nonsquamous NSCLC. *N Eng J Med* (2018) 378:2288–301. doi: 10.1056/NEJMoa1716948

7. Petrylak DP, de Wit R, Chi KN, Drakaki A, Sternberg CN, Nishiyama H, et al. Ramucirumab plus docetaxel versus placebo plus docetaxel in patients with locally advanced or metastatic urothelial carcinoma after platinum-based therapy (RANGE): overall survival and updated results of a randomised, double-blind, phase 3 trial. *Lancet Oncol* (2020) 21(1):105–20. doi: 10.1016/S1470-2045(19)30668-0

8. Wilke H, Muro K, Van Cutsem E, Oh SC, Bodoky G, Shimada Y, et al. Ramucirumab plus paclitaxel versus placebo plus paclitaxel in patients with previously treated advanced gastric or gastro-oesophageal junction adenocarcinoma (RAINBOW): a double-blind, randomised phase 3 trial. *Lancet Oncol* (2014) 15 (11):1224–35. doi: 10.1016/S1470-2045(14)70420-6

9. Kawachi H, Tamiya M, Matsumoto K, Tamiya A, Yanase T, Tanizaki S, et al. Efficacy and safety of ramucirumab and docetaxel in previously treated patients with squamous cell lung cancer: a multicenter retrospective cohort study. *Invest New Drugs* (2022) 40(3):634–42. doi: 10.1007/s10637-022-01214-w

10. Kwon D, Reis IM. Simulation-based estimation of mean and standard deviation for meta-analysis *via* approximate Bayesian computation (ABC). *BMC Med Res Methodol* (2015) 12(15):61. doi: 10.1186/s12874-015-0055-5

11. Tozuka T, Kitazono S, Sakamoto H, Yoshida H, Amino Y, Uematsu S, et al. Addition of ramucirumab enhances docetaxel efficacy in patients who had received anti-PD-1/PD-L1 treatment. *Lung Cancer* (2020) 144:71–5. doi: 10.1016/j.lungcan.2020.04.021

12. Park K, Kim JH, Cho EK, Kang JH, Shih JY, Zimmermann AH, et al. East Asian Subgroup analysis of a randomized, double-blind, phase 3 study of docetaxel and placebo in the treatment of stage IV non-small cell lung cancer following disease progression after one prior platinum-based therapy (REVEL). *Cancer Res Treat* (2016) 48(4):1177–86. doi: 10.4143/crt.2015.401

13. Brueckl WM, Reck M, Rittmeyer A, Kollmeier J, Wesseler C, Wiest GH, et al. Efficacy of docetaxel plus ramucirumab as palliative second-line therapy following first-line chemotherapy plus immune-checkpoint-inhibitor combination treatment in patients with non-small cell lung cancer (NSCLC) UICC stage IV. *Transl Lung Cancer Res* (2021) 10(7):3093–105. doi: 10.21037/tlcr-21-197

14. Harada D, Takata K, Mori S, Kozuki T, Takechi Y, Moriki S, et al. Previous immune checkpoint inhibitor treatment to increase the efficacy of docetaxel and ramucirumab combination chemotherapy. *Anticancer Res* (2019) 39(9):4987–93. doi: 10.21873/anticanres.13688

15. Reck M, Kaiser R, Mellemgaard A, Douillard J-Y, Orlov S, Krzakowski M, et al. Docetaxel plus nintedanib versus docetaxel plus placebo in patients with previously treated non-small-cell lung cancer (LUME-Lung1): a phase 3, double-blind, randomised control trial. *Lancet Oncol* (2014) 15(2):143–55. doi: 10.1016/S1470-2045(13)70586-2

16. Grohé C, Blau W, Gleiber W, Haas S, Hammerschmidt S, Krüger S, et al. Real-world efficacy of nintedanib plus docetaxel after progression on immune checkpoint inhibitors: results from the ongoing, non-interventional VARGADO study. *Clin Oncol (R Coll Radiol)* (2022) 34(7):459–68. doi: 10.1016/j.clon.2021.12.010

17. Metzenmacher M, Rizzo F, Kambartel K, Panse J, Schaufler D, Scheffler M, et al. Real-world efficacy of docetaxel plus nintedanib after chemo-immunotherapy failure in advanced pulmonary adenocarcinoma. *Future Oncol* (2021) 17(30):3965–76. doi: 10.2217/fon-2021-0424

18. Reckamp KL, Redman MW, Dragnev KH, Minichiello K, Villaruz LC, Faller B, et al. Phase II randomized study of ramucirumab and pembrolizumab versus standard of care in advanced non-small-cell lung cancer previously treated with immunotherapy-Lung-MAP S1800A. *J Clin Oncol* (2022) 40(21):2295–306. doi: 10.1200/JCO.22.00912

19. Pennell N, Clarke J, Liu SV, Gutierrez M, Batus M, Bauman JR, et al. CO145 ramucirumab+ docetaxel post immune checkpoint inhibitors (ICIS) and platinum-based chemotherapy (CHEMO) in advanced or metastatic non-small cell lung cancer (ANSCLC): Learning from the TREAT-LUNG observational study. *Poster presented at International Society for Pharmacoeconomics and Outcomes Research (ISPOR) 27th Annual Meeting*; Washington, DC; May 15-18, 2022. (2022). Available at: https://statinmed.com/presentations/checkpoint-inhibitors-platinum-based-chemotherapy-nsclc-treat-lung-observational-study/.

frontiers | Frontiers in Oncology

TYPE Review
PUBLISHED 20 April 2023
DOI 10.3389/fonc.2023.1137384

OPEN ACCESS

EDITED BY
Michele Simbolo,
University of Verona, Italy

REVIEWED BY
Francesco Pepe,
University of Naples Federico II, Italy
Jin-Yuan Shih,
National Taiwan University, Taiwan

*CORRESPONDENCE
Federico Pio Fabrizio
fp.fabrizio@operapadrepio.it
Lucia Anna Muscarella
l.muscarella@operapadrepio.it

SPECIALTY SECTION
This article was submitted to Thoracic Oncology, a section of the journal Frontiers in Oncology

RECEIVED 04 January 2023
ACCEPTED 06 April 2023
PUBLISHED 20 April 2023

CITATION
Fabrizio FP, Sparaneo A and Muscarella LA (2023) Monitoring *EGFR*-lung cancer evolution: a possible beginning of a "methylation era" in TKI resistance prediction. *Front. Oncol.* 13:1137384. doi: 10.3389/fonc.2023.1137384

Monitoring *EGFR*-lung cancer evolution: a possible beginning of a "methylation era" in TKI resistance prediction

Federico Pio Fabrizio*, Angelo Sparaneo and Lucia Anna Muscarella*

Laboratory of Oncology, Fondazione IRCCS Casa Sollievo della Sofferenza, San Giovanni Rotondo (FG), Italy

The advances in scientific knowledge on biological therapies of the last two decades have impressively oriented the clinical management of non-small-cell lung cancer (NSCLC) patients. The treatment with tyrosine kinase inhibitors (TKIs) in patients harboring Epidermal Growth Factor Receptor (*EGFR*)-activating mutations is dramatically associated with an improvement in disease control. Anyhow, the prognosis for this selected group of patients remains unfavorable, due to the innate and/or acquired resistance to biological therapies. The methylome analysis of many tumors revealed multiple patterns of methylation at single/multiple cytosine-phosphate-guanine (CpG) sites that are linked to the modulation of several cellular pathways involved in cancer onset and progression. In lung cancer patients, ever increasing evidences also suggest that the association between DNA methylation changes at promoter/intergenic regions and the consequent alteration of gene-expression signatures could be related to the acquisition of resistance to biological therapies. Despite this intriguing hypothesis, large confirmatory studies are demanded to consolidate and finalize many preliminary observations made in this field. In this review, we will summarize the available knowledge about the dynamic role of DNA methylation in *EGFR*-mutated NSCLC patients.

KEYWORDS

lung cancer, tyrosine kinase inhibitors, resistance, methylation, epigenetic markers

1 Introduction

The paradigm of cancer has evolved in the last years and conveyed into the concept of cancer "epigenome", strictly linked to cancer "genome" (1). Many epigenetic regulatory players are involved in the transcription modulation of multiple tumor suppressor genes (TSG); DNA methylation, histone modifications, aberrant expression of microRNAs (miRNAs) and long non-coding RNAs (lncRNAs) participate in many neoplastic steps,

such as dysregulation of cell growth, malignant cell transformation, invasion and metastatization (2–5).

Among all epigenetic alterations, DNA methylation represents one of the most studied chemical modifications in human disease. It occurs when methyl groups are covalently attached to the carbon at 5' position of the cytosine residue of DNA by the DNA methyltransferase (DNMT) enzymes (6, 7).

The recent implementation of high-throughput approaches for methylation analysis gives a more detailed and dynamic overview of the DNA methylation perturbation in human disease and provides new important insights on the understanding of both temporal and spatial related gene expression modification and chromatin remodeling (8–10). This enhances, by consequence, to better explain the role of this class of epigenetic changes in cancer biology, unveiling novel epigenetic predictive and prognostic molecular biomarkers for neoplastic disease monitoring and outcome prediction in patients (11, 12).

The human cancer cells are characterized by the presence of a complex aberrant methylation signature, which takes place either as a hypo- or hyper-methylation events at single interspersed CpGs and/or CpG islands located both in the promoter and intergenic regions of genes. These epigenetic modifications may represent an early event in cancer development and progression, as well as they could cooperate with genetic lesions to guide the heterogeneity of response/resistance to therapies in patients (13, 14).

In lung cancer, the association between aberrant methylation profiles and resistance to anti-EGFR therapy is still understudied. More attention is required, since changes in methylation levels may help to explain the observed heterogeneity of lung tumor response to multiple targeted therapies (14). Here we detailed and updated the most recent advances in DNA methylation modifications linked to TKI resistance mechanisms in *EGFR*-mutated patients and their related cellular pathways (15, 16).

Scientific evidences on the role of miRNA signature alterations as players in TKI of EGFR resistance was also briefly discussed. All available scientific evidences about the prognostic value of epigenetic alterations as primary/intrinsic and secondary/acquired mechanisms of resistance were summarized. Publications in English language, peer-reviewed international journals were identified on PubMed. All scientific knowledges were updated until October 2022.

2 Primary and secondary mechanisms of resistance to EGFR-TKIs in NSCLC

One of the most frequent distinctive outcome of NSCLC patients is linked to the activation of *EGFR* mutations. Somatic mutations at exons 19-21, codifying for the tyrosine kinase domain, actually represent the main molecular condition to predict a good EGFR-TKIs response in upfront therapy (17, 18). First-generation TKIs, erlotinib and gefitinib, can compete in a reversible manner with adenosine triphosphate (ATP) at EGFR binding site, whereas the second-generation (e.g. afatinib, neratinib and dacomitinib) and third generation (e.g. osimertinib) TKIs can irreversibly block the ATP pocket of EGFR receptor, thereby inhibiting its phosphorylation and downstream signal transduction activity by covalently binding the ATP binding pocket mutations. As consequence, EGFR-TKI administration frequently allows a higher overall response rate (ORR) and progression-free survival (PFS) in *EGFR*-mutated metastatic patients compared with upfront chemotherapy (19, 20). In addition, osimertinib also received in recent years the approval for the administration in patients who acquired p.T790M mutation of *EGFR* as first/second-TKI generation resistance mechanism (21, 22).

In all cases, however, all therapies administered to inhibit oncogenic kinases activity are unable to completely eradicate tumors, so the *EGFR*-mutated patients invariably develop acquired resistance after 9-12 months of treatment initiation or they do not respond to TKIs treatment at all (23, 24). Several biological mechanisms of resistance have been reported to date, such as secondary *EGFR* mutations, bypass track signaling pathways and histologic transformation, not all strictly related to TKIs affinity (23, 25). All just reported mechanisms can be classified as primary or acquired resistance events, even if some of these, such as the co-expression of other ErbB receptors or the constitutive activation of other downstream pathways, remained ambiguous and are unlikely to be located in one of the two types of resistance.

Intrinsic or primary resistance refers to patients who either do not achieve stable disease or who progress within 6 months after an initial clinical response, according to the RECIST (Response Evaluation Criteria in Solid Tumor) criteria, with a consequent worsening of clinical conditions as well as response rate and disease control rates (LDCR), approximately in 20-30% EGFR-TKIs treated patients (26). Host-related mechanisms, such as defective immune system activity, rapid metabolism, or poor absorption, are predominantly responsible for intrinsic/primary resistances. Moreover, non-sensitive *EGFR* mutations, which contribute to an inconsistent drug activity, such as the naïve threonine-to-methionine substitution at the "gatekeeper" amino acid position 790 (p.T790M) in exon 20 and some mutations in exon 19 (p.L747S/p.D761Y), p.T854A or p.L868R in exon 21 of *EGFR*, can be included in this category (27, 28).

Apart from these, other molecular mechanisms could be the activation of different pathways by mutations in *HGF* (hepatocyte growth factor) gene (29), *IGF1R* (insulin growth factor 1 receptor) gene (30), *MET* (MET proto-oncogene, receptor tyrosine kinase) gene (31), and/or *PI3K/AKT* (phosphatidylinositol-3-kinase and protein kinase B) pathway genes (32, 33). All above listed mechanisms of primary resistance generally arise after the administration of first- and second-generation TKIs in patients with NSCLC. There is also an emerging literature on primary resistance to the third-generation TKI osimertinib used in up-front therapy in *EGFR* mutated NSCLC, although data are actually in progress. The most compelling studies came from intrinsic resistance to osimertinib as second-line option: *KRAS* (Kirsten rat sarcoma virus) p.G12D mutation (co-occurring with the loss of *PTEN*, Phosphatase and tensin homolog, gene), *BRAF* (B-Raf Proto-Oncogene, Serine/Threonine Kinase mutation) mutations, *ALK* (Anaplastic lymphoma kinase) gene translocation, *HER2* (Human epidermal growth factor receptor-2)

and *MET* (tyrosine-protein kinase Met) amplifications were reported (15, 34).

Acquired or secondary resistance to TKIs typically occurs in lung cancer patients after an initial response or stable disease to EGFR-TKIs (≥ 6 months), according to the RECIST criteria. In 50-60% of NSCLC patients who developed resistance to first/second-generation TKIs, the occurrence of p.T790M in exon 20 of *EGFR* is a fixed point for lung cancer management. In NSCLC patients with a pre-existent *EGFR* activating mutation, this last condition confers resistance to TKIs by sterically blocking the binding of drugs to the receptor pocket, thus giving an advantage to cancer cells by activating signaling pathways associated with tumor progression and metastasis (35). In this specific context, the administration of osimertinib as second line of treatment in patients harboring p.T790M mutation can re-block the tumor expansion, until additional resistance mechanisms occur as a result of the loss of the p.T790M mutation and the acquisition of novel resistance to second-line osimertinib, such as p.C797S mutation at exon 20 of *EGFR* (15, 34).

Other secondary mutations, in addition to the already mentioned p.T790M which are involved in EGFR-TKI acquired resistance, are represented by p.D761Y or p.L747S (exon19 of *EGFR*), and p.T854A (exon 21 of *EGFR*) (36). Uncommon and combined *EGFR* mutations, intratumoral heterogeneity beyond *EGFR* alterations, drug inefficacy due to adaptive mechanisms exploited by cancer to convey resistance, such as histological transformation of lung adenocarcinoma into small cell lung cancer (SCLC) (37), squamous cell carcinoma (SCC), as well as the activation of alternative pro-oncogenic signaling pathways are also reported (38). The epithelial-to-mesenchymal transformation (EMT) can be also included among these resistance mechanisms, as well as the consequent loss of cell adhesion and polarity and promote the formation of tumor stem cells and decreasing the EGFR signaling addiction (39).

Variations in methylation levels and deregulation of miRNA and lncRNA machinery are widely associated with neoplastic transformation, carcinogenesis, and cancer progression. Anyway, the fluctuations of cancer methylome, both at DNA and RNA levels, remain the less investigated epigenetic changes in the context of target therapy resistance and TKI resistance in NSCLC (Figure 1).

3 The dynamic evolution of DNA methylation in TKI resistance of NSCLC: the state of art

Starting from the molecular profiling of epigenetic marks across the genome, a new focus on the methylome evolution of lung cancer may help to more clearly understand how cell biology contributes to TKI drugs resistance in NSCLC patients (38, 40). The most interesting findings in this field are summarized in Table 1 and detailed below. A representative scheme that depicts methylated genes and their associations with TKI resistance in NSCLC is also illustrated in Figure 2.

3.1 Methylated genes with STRONG evidence of association to TKI resistance in NSCLC

3.1.1 *EGFR*

A new research front is opening up to explore a potential correlation between variation in methylation levels of specific CpG sites located at promoter and/or gene body regions of *EGFR* gene and response to EGFR-TKIs in lung cancer patients (14).

The first evidence of these links comes from *Li and colleagues*' studies. By performing *in vitro* assays on mutated (H1650 and PC-9) and wild-type (H1299) *EGFR* lung cancer cell lines, they showed that *EGFR* promoter hypermethylation enhanced the antitumor effect of TKI gefitinib and modulated the expression of EGFR both at transcript and protein level. Moreover, the resistance to gefitinib in unmethylated PC-9 tumor cells having *EGFR* exon19 deletion was bypassed by using a combined treatment of 5-aza-2'-deoxy cytidine (5-aza-CdR) and gefitinib, thus boosting the growth inhibitory effects and leading to the activation of caspases (42).

The most significant support to this first evidence came from the integrative multi-omics analysis by *Xu Z and colleagues*, who investigated the *EGFR* genes in terms of CpGs methylation (49 CpG sites), somatic mutations, copy number variations (CNVs), transcriptional and protein expression level fluctuations in 535 lung adenocarcinoma (LUAD), available from The Cancer Genome Atlas (TCGA). A large number of *EGFR* CpGs located at the promotor region was identified by Illumina HumanMethylation450K and RNA-seq data analysis, whose methylation levels showed an inverse correlation with the transcription level variations, protein expression and CNVs of *EGFR* gene. By contrast, the aberrant methylation of CpGs located at the gene body regions was found to positively correlate with the EGFR protein expression. In LUAD patients having *EGFR* mutations, the Authors found that most CpG sites were hypomethylated and about 30% of these were predictive of a good prognosis for patients. In addition, promoter *EGFR* hypermethylation was found to be associated with the immune cell infiltration and increased IFN-γ signature, while an opposite correlation was found for methylation of the CpGs at gene body region. Finally, the hypermethylation of cg27637738, cg16751451, cg02316066, cg22396409, cg03046247, cg02166842, cg21901928, cg07311521 and cg06052090 CpG sites was associated to a poor prognosis in lung adenocarcinoma patients ($p<0.05$). In particular, cg02316066 and cg03046247 were the most strongly associated ones and showed a high degree of co-methylation with cg02316066 and cg03046247 ($p<0.001$) (41).

3.1.2 *PTEN*

PTEN (phosphatase and tensin homolog) is a lipid phosphatase that is involved in the negative regulation of phosphatidylinositol 3-kinase (PI3K)-AKT signaling and radio-chemotherapy in tumors. Genetic aberrations of *PTEN* are not frequent in NSCLC; by contrast, in about 35% of early stage NSCLC samples the lack of PTEN protein expression observed was reported to correlate with hypermethylation at the promoter gene region. Moreover, *PTEN*

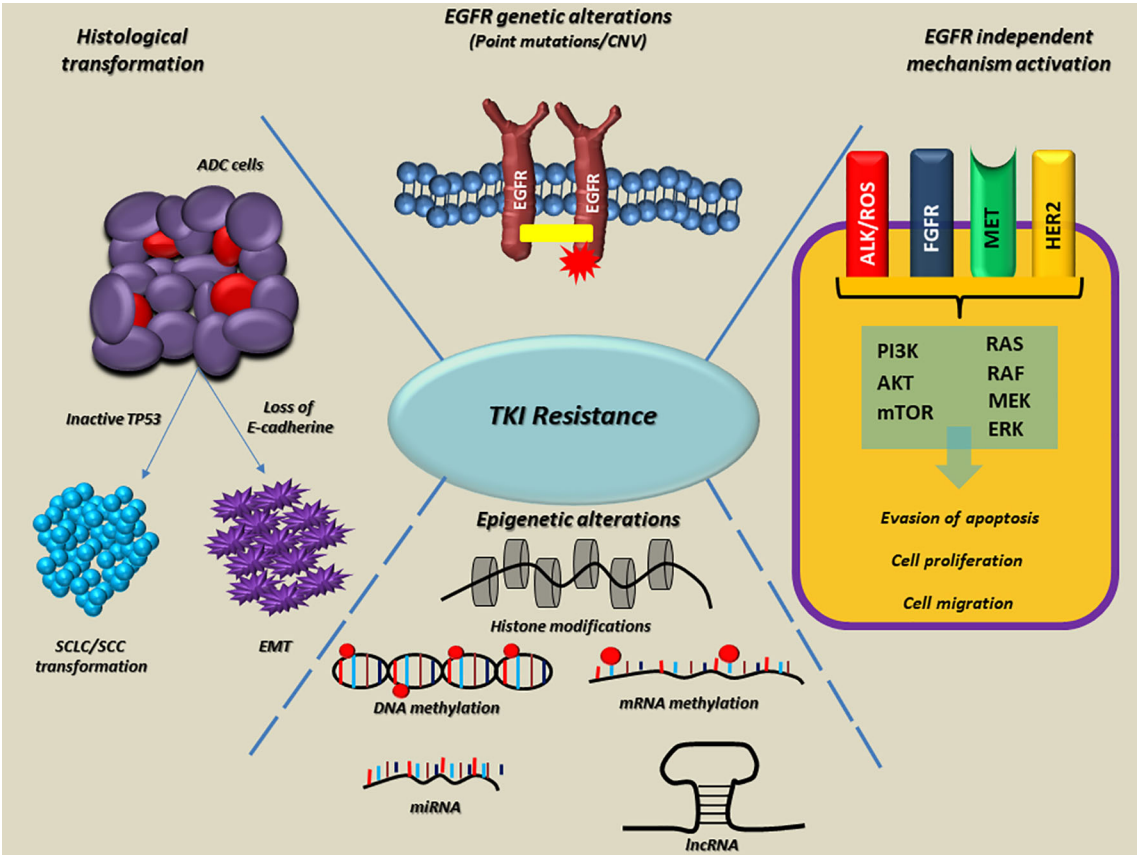

FIGURE 1
Overview of the main molecular mechanisms linked to EGFR-TKI resistance in NSCLC. On the top, *EGFR* alterations, as point mutations and copy number variations (CNVs) are involved both in intrinsic and acquired resistance to TKI. On the right side, the EGFR-independent mechanisms bypass RTK signaling through *ALK, ROS, FGFR, MET, HER2* alterations onset, thus promoting the activation of alternative and downstream pathways (e.g., PI3K/AKT/mTOR and RAS/RAF/MEK/ERK). At the bottom, epigenetic alterations such as histone modifications, DNA and RNA hypo/hypermethylation, aberrant expression of miRNAs and lncRNA frequently occur in several genes, which are able to promote tumor progression, metastasis and resistance to TKIs. Finally, on the left side, histological modifications such as SCLC or SCC transformation and EMT lead to the loss of sensitivity to EGFR TKIs in lung tumors. The dotted blue lines indicate interconnections among mechanisms linked to the EGFR-TKI resistance. EGFR, epidermal growth factor receptor; TKI, Tyrosine kinase inhibitors; Ex, exon; ins, insertion; amp, amplification; RTK, receptor tyrosine kinase; ALK, Anaplastic lymphoma kinase; ROS, ROS Proto-Oncogene, Receptor Tyrosine Kinase; FGFR, fibroblast growth factor receptor; MET, hepatocyte growth factor receptor; HER2, human epidermal growth factor receptor 2; PI3K, Phosphoinositide 3-kinase; AKT, Protein kinase B; mTOR, mammalian target of rapamycin; RAS, rat sarcoma virus; RAF, proto-oncogene c-RAF; MEK, Mitogen-activated protein kinase kinase; ERK, Extracellular signal-regulated kinase; miRNA, microRNA; lncRNA, long non-coding RNA; SCLC, small cell lung cancer; SCC, squamous cell carcinoma; EMT, epithelial –mesenchymal transition; ADC, adenocarcinoma; TP53, Tumor protein P53.

aberrant methylation was observed in NSCLC cell lines and was correlated to transcript and protein level fluctuations under *in vitro* treatment with the 5-aza-2'-deoxycytidine (43).

Consistent with data by *Soria and colleagues*, Maeda and his team explored a possible correlation between hypermethylation of CpGs located at the *PTEN* gene promoter region and resistance to gefitinib or erlotinib in the two lung cancer cell sublines GEF1-1 and GEF2-1 (obtained from cell line harboring the *EGFR* mutation p.E746_A750del). It was observed that the region located 329 to 124 nucleotide upstream from the translation initiation site of the *PTEN* promoter region was hypermethylated only in resistant cell lines. This condition inversely correlated with PTEN protein expression. *PTEN* suppression enhances the AKT phosphorylation, thus switching on the expression of cyclin D1 and ICAM-1 (intracellular adhesion molecule-1) and accelerating the migration of the cancerous cells (54). These evidences support the suggestion of an alternative approach for TKIs in combination with demethylating 5-aza/HDAC (Histone deacetylases) inhibitors or Trichostatin A (TSA) to hinder lung tumor growth, whose efficacy was observed on gefitinib-resistant PC9/f9 and PC9/f14 cells by Noro T et al. (44).

3.1.3 *HOXB9*

HOXB9 (Homeobox B9) gene codified for a sequence-specific transcription factor that is implicated in several processes from cell development to cell proliferation by enhancing the EMT, the expression of angiogenic factors (VEGF, IL-8, and/or TGFβ), and *EGFR* and *ErbB2* pathways activation, through the AKT/NF-κB/Snail pathway (55). The effects of epigenetic *HOXB9* regulation on

TABLE 1 Methylated genes and their functional and biological effects on acquired EGFR-TKI resistance in different lung cancer models.

Gene Symbol	Methylated region	Functional and biological effects	Detection methods	Cancer model	References
EGFR	49 CpGs of which six located in the promoter region (cg16751451, cg07311521, cg03860890, cg22396409, cg05064645, cg14094960). 43 CpGs along the gene body and in the 3' UTR region.	✓ An inverse correlation between methylated CpGs of *EGFR* and mRNA/protein expression was observed. ✓ Promoter hypermethylation was found to be associated with immune cell infiltration and increased IFN-γ signature, while the opposite was found for methylation of the gene body region. ✓ Hypermethylation of cg02316066 and cg03046247 was strongly associated with lung adenocarcinoma prognosis.	Human methylation 450K array (TCGA dataset); qMSP	535 LUAD patients from TCGA and 20 paired LUAD/non-cancerous lung tissue samples.	(41)
EGFR	Promoter	✓ CpG island hypermethylation at the *EGFR* promoter enhances the sensitivity to gefitinib in NSCLC cells.	MSP	NSCLC cell lines: H1650, H1299 and PC-9.	(42)
PTEN	Promoter	✓ Aberrant methylation at promoter region may partially explain the lack of PTEN expression.	MSP	NSCLC cell lines and tissues from 125 patients with early-stage NSCLC.	(43)
PTEN	Promoter	✓ Hypermethylation of CpGs located at the *PTEN* gene promoter region inversely correlates with protein expression during acquired resistance to gefitinib or erlotinib. ✓ It enhances the Akt signaling pathway.	MSP	ADC, SqCC and SCLC cell lines (PC9, GEF1-1, GEF2-1).	(44)
HOXB9	cg13643585(enhancer region)	✓ Hypermethylation of cg13643585 in *HOXB9* correlates with intrinsic resistance to EGFR-TKI.	InfiniumHuman Methylation 450K array; Pyrosequencing	79 ADC from patients with *EGFR* mutations.	(45)
PD-L1	Promoter	✓ Promoter hypermethylation inversely correlates with expression levels. ✓ High methylation levels at the *PD-L1* promoter region are linked to the resistance to anti-PD-1 therapy in both chemotherapy or EGFR-TKI treated lung cancer patients.	Bisulfite sequencing	384 NSCLC patients divided in three sub-groups (EGFR wild type, n=214; EGFR p.L858R mutated, n=108; EGFR p.T790M mutated, n=62).	(46)
GABBR2	Exons 2 and 3	✓ High levels of *GABBR2* methylation at CpG islands negatively regulate GABBR expression and ERK1/2 pathway in NSCLC tumors and cell lines having *EGFR* 19 deletions.	MSCC sequencing Sequenom EpiTYPER	NSCLC cell lines (A549, HCC4006, HCC827) and lung ADC/non-neoplastic paired tissues from locally advanced stage IIIa patients.	(47)
FRP5	Unspecified CpGs	✓ Increased levels of methylation of *SFRP5* correlate to PFS reduction in NSCLC patients under EGFR-TKI treatment.	MSP	Tumor samples from 155 patients with stages IIIB to IV NSCLC, who received EGFR-TKI therapy.	(48)
DAPK	Promoter	✓ Hypermethylation of *DAPK* promoter induces gene silencing and is related to the acquired drug resistance in NSCLCs under erlotinib treatment.	MethDet-56 array qMSP	HNSCC and NSCLC (H226, SCC-1) cell lines treated with erlotinib/cetuximab.	(49)
KL and ***S100P***	Interspersed CpG sites	✓ Promoter hypermethylation inversely correlates with expression levels. ✓ A possible role in acquired resistance to EGFR–TKI (gefitinib) is suggested.	Infinium Human Methylation 27 Bead Array	Human NSCLC cell line PC9 (EGFR exon 19 p.E746-A750del) and their gefitinib-resistant derivatives (PC9 GR, gr1, and gr3).	(50)
SPP1 and ***CD44***	cg00088885(*SPP1*) cg20971158 (*CD44*)	✓ CD44 and SSP1 methylation are prognostic factors in LUAD patients. ✓ SPP1 methylation modulates its expression and is related to 1st and 2nd	DNMIVD	GEO database (NSCLC): GSE122005: 3 resistant samples and 3 sensitive samples to gefitinib	(51)

(Continued)

TABLE 1 Continued

Gene Symbol	Methylated region	Functional and biological effects	Detection methods	Cancer model	References
		EGFR-TKI resistance of NSCLC. ✓ CD44-SSP1 axis is implicated in the trasformation of ADC in SCLC under EGFR-TKI selettive pressure.		GSE31625: 28 samples and 18 sensitive samples to erlotinib; TKI-resistant NSCLC cell lines.	
RASSF1A and ***GADD45β***	Promoter	✓ Aberrant methylation at the promoter region of *RASSF1A* and *GADD45β* inversely correlates with protein expression and is linked to the acquisition of TKI resistance in lung cancer cells. ✓ Cell treatment with 5-Aza-CdR could partially restore the sensitivity of cells to EGFR-TKI.	NimbleGen Human DNA Methylation 3x720K Promoter Plus CpG Island Array; qMSP	Gefitinib-sensitive/resistant lung ADC cell lines (PC9, PC9/GR).	(52)
Nine gene set: ***APC, BRMS1, WIF-1, FOXA1, RARb, RASSF1A, RASSF10, SHISA3, SLFN11***	Promoter	✓ DNA methylation inversely correlates with mRNA expression in lung ADC tissues for all genes. ✓ Positive patients for almost one methylated marker showed a faster progression compared to negative patients for DNA methylation in all tested genes markers.	Data TCGA Research Network WBA; MSP	PB samples from 42 NSCLC patients.	(53)

NSCLC, Non Small Cell Lung Cancer; HNSCC, Head and neck squamous cell carcinomas; LUAD, lung adenocarcinoma; SCLC, small cell lung cancer; ADC, adenocarcinoma; SCC, squamous cell carcinoma; TKI, tyrosine kinase inhibitor; CpG, cytosine-phosphate-guanine; TR, Untranslated region; TCGA, The Cancer Genome Atlas; DMBs, differentially methylated blocks; MSP, methylation-specific PCR; qMSP, quantitative methylation-specific PCR; MSCC, Methyl-sensitive cut counting; DNMIVD, DNA methylation interactive visualization database; WBA, whole bisulfite amplification; PB, Peripheral blood. PFS, progression-free survival; GEO, Gene Expression Omnibus; DAPK, death-associated protein kinase; EGFR, Epidermal Growth Factor Receptor; MET, tyrosine-protein kinase Met; HER2, Human epidermal growth factor receptor-2; GABBR2, Gamma-Aminobutyric Acid Type B Receptor Subunit 2; CGI, CpG island; ERK1/2, extracellular-signal-regulated kinase; KL, Klotho; S100P, S100 Calcium Binding Protein P; PD-L1, Programmed death-ligand 1; PD-1, Programmed cell death protein 1; PTEN, Phosphatase And Tensin Homolog; 5-Aza-CdR, 5-aza-2′-deoxycytidine; HDAC, Histone deacetylases; RASSF1A, Ras association domain family 1 isoform A; GADD45β, DNA damage-inducible 45 beta; qPCR, Real-Time Quantitative PCR; SFRP5, Secreted Frizzled Related Protein 5; SPP1, Secreted Phosphoprotein 1; CD44, cluster of differentiation; BRMS1, Human breast carcinoma metastasis-suppressor 1; FOXA1, Forkhead Box A1; RARb, Retinoic Acid Receptor Beta; RASSF10, Ras Association Domain Family Member 10; SHISA3, Shisa Family Member 3; SLFN11, Schlafen Family Member 11; WIF-1, WNT Inhibitory Factor 1; APC, adenomatous polyposis coli; IFN, interferon; HOXB9, Homeobox B9.

intrinsic and acquired TKI resistance in NSCLC patients are actually debated. A possible correlation between methylation profiling of 216 CpG sites (islands and S-shores) by Illumina Infinium Human Methylation 450K array and gene expression profile was investigated in stage III and IV *EGFR*-mutated NSCLC patients. A critical role of cis-regulation of expression by methylation in lung adenocarcinoma and intrinsic resistance to EGFR-TKIs were found both in the discovery (79 tumors sampled from patients with advanced lung adenocarcinoma before receiving EGFR-TKI) and in the validation cohort (163 patients with *EGFR*-activating mutations) of NSCLC patients. Specifically, *HOXB9* aberrant methylation at cg1364358 site, located in the enhancer region of gene, was found to be strictly related to disease progression of patients after TKI treatments and to disease monitoring, since it was able to predict a disease control rate with 88% sensitivity in patients having *EGFR* activating mutations (45).

In addition to these evidences, novel genome-wide studies using liquid biopsy samples of 122 NSCLC patients under erlotinib (67.2%), gefitinib (11.5%) or afatinib (2.5%) treatment demonstrated a correlation between hypermethylation of regulatory regions of *HOX* genes and TKI resistance in those patients also having *MET* or *HER2* amplifications. Such consistent findings indicated that the hypermethylation status of *HOX* genes could be exploited not only to monitor EGFR-TKI resistance in NSCLC patients, but also to predict and treat *MET* or *HER2* amplification mediated resistance (56).

3.2 Methylated genes with LOW evidence of association to TKI resistance in NSCLC

3.2.1 *PD-L1*

Zhang Y et al. gave an interesting indication about the role of *PD-L1* (programmed cell death ligand 1) promoter aberrant methylation in mediating the mechanisms of resistance to the anti-PD1 treatment in *EGFR* mutated NSCLC patients. A total of 384 surgical NSCLCs, previously profiled for the *EGFR* mutation status (three groups as follows: wild-type group, n=214; p.L858R group, n=108 and p.T790M group, n=62) were tested by PCR bisulfite sequencing to measure the ratio of CpGs methylation level at the *PD-L1* gene promoter region. After cancer recurrence, the PD-L1 was found to be up-regulated in patients treated with chemotherapy or EGFR-TKI therapy, but decreased in the patients with anti-PD1 therapy. Promoter methylation analysis showed that the secondary NSCLC after cancer recurrence with anti-PD1 therapy had higher levels of *PD-L1* methylation compared to those naive cancers and/or normal tissues (46).

The *in vivo* experimental validation performed by the same Authors in mice model showed that the increase of *PD-L1* promoter methylation levels reflected the reduction in PD-L1 expression after nivolumab therapy, irrespective of *EGFR* mutation status. This may be due to a pre-existent heterogeneity in *PD-L1* methylation patterns in tumor cells or to a tumor cell evolution and switch-off the PD-L1 expression through epigenetic modulation induced by

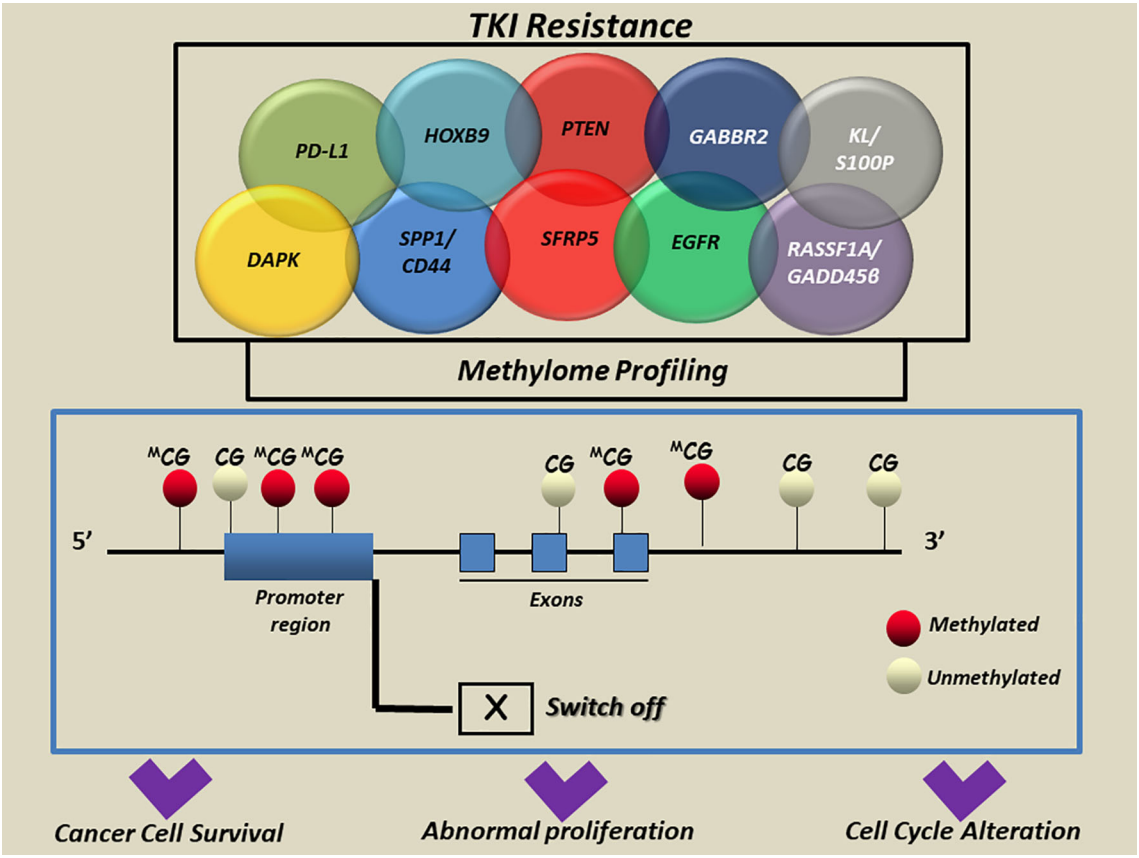

FIGURE 2
A simplified scheme of aberrant methylated genes associated with TKI resistance in NSCLC. Aberrant methylation of cytosine residues at the CpG islands in the promoter regions and/or interspersed CpGs mainly located in multiple genes was reported to modulate the transcription and induce aberrant regulation of genes implicated in cell-cycle alteration, abnormal proliferation and apoptosis escape in cancer cells. CG, cytosine guanine; DAPK, death-associated protein kinase; EGFR, Epidermal Growth Factor Receptor; GABBR2, Gamma-Aminobutyric Acid Type B Receptor Subunit 2; HOXB9, Homeobox B9; KL, Klotho; S100P, S100 Calcium Binding Protein; PD-L1, Programmed death-ligand 1; PTEN, Phosphatase And Tensin Homolog; RASSF1A, Ras association domain family 1 isoform A; GADD45β, DNA damage-inducible 45 beta; SFRP5, Secreted Frizzled Related Protein 5; SPP1, Secreted Phosphoprotein 1; CD44, cluster of differentiation 44; APC, adenomatous polyposis coli; BRMS1, Human breast carcinoma metastasis–suppressor 1; FOXA1, Forkhead Box A1; RARb, Retinoic Acid Receptor Beta; RASSF1A, Ras association domain family 1 isoform A; RASSF10, Ras Association Domain Family Member 10; SHISA3, Shisa Family Member 3; SLFN11, Schlafen Family Member 11; WIF-1, WNT Inhibitory Factor 1.

the selective pressure of the drug. Anyway, both hypotheses remain unconfirmed and need to be supported by further investigations (46).

3.2.2 *GABBR2*

GABBR2 (Gamma-Aminobutyric Acid Type B Receptor Subunit 2) gene encodes a multi-pass membrane protein that belongs to the G-protein coupled receptor 3 family and GABA-B receptor subfamily. The GABA-B receptors inhibit neuronal activity through G protein-coupled second-messenger system, which regulates the release of neurotransmitters, and the activity of ion channels and adenylyl cyclase (57). The role of GABBR2 in cancer progression was firstly supposed in thyroid carcinomas, but an elevated expression of this gene was also reported as a specific feature of lung cancerous lesions and linked to a better prognosis of patients (58, 59).

The first suggestion of a correlation between DNA methylation of *GABBR2* and resistance to TKI erlotinib in NSCLC patients comes from the study by *Niu X et al.* who investigated the variations of methylation patterns by whole-genome DNA high-throughput assays in a small cohort of NSCLC patients under erlotinib treatment (47). Specifically, the epigenetic profile of *GABBR2* gene at promoter region prior to and following erlotinib treatment were compared in two IIIa stage NSCLC patients having *EGFR* activating mutations (exon19 p.E746-A750del and p.A750-E758del). As result, the same differentially methylated region (DMR), located between exon 2 and exon 3 of *GABBR2* gene, was found in both patients, with an average of methylation changes of 42.35% and 23.50% in the two patients, respectively. Lung cancer tissues of patients tested by IHC before and after induction to erlotinib treatment in the two patients showed a consistent decrease of GABBR2 expression after erlotinib treatment. The following *in vitro* experiments also demonstrated a direct role of erlotinib in *GABBR2* methylation and the consequent downregulation of its expression in *EGFR*-mutated lung tumor cells. Conversely, the upregulation of GABBR2 may

restore TKI-induced cell apoptosis through ERK1/2 and its crosstalk pathway signaling.

Taking all together, the above findings provide a new theoretical basis for expanding this epigenetic investigations to a more large cohort of *EGFR*-mutated NSCLCs and suggest a possible role of *GABBR2* in improving clinical outcomes of TKI treated patients with locally advanced NSCLC (47).

3.2.3 *SFRP5*

SFRP5 (Secreted Frizzled Related Protein 5) gene codifies for one of the soluble Wnt signaling modulators that are involved in the regulation of cell proliferation and cancer progression (60, 61). *Zhu J and colleagues* reported that hypermethylation of *SFRP5* gene was able to predict a worse outcome in EGFR-TKI advanced adenocarcinoma patients. In their study, the Authors quantified the DNA methylation levels of a selected group of Wnt antagonist genes, after the administration of EGFR-TKI in a cohort of 155 NSCLCs of IIIB to IV patients. The correlation between the methylation status of *SFRP5* gene prior to treatment and progression-free survival (PFS) showed that the Wnt antagonist genes tend to be simultaneously methylated, as well as methylation of *SFRP5* reversely correlated with *EGFR* mutation status of patients (p= 0.011). Moreover, the subgroup of TKI-treated patients with higher *SFRP5* methylation levels showed a worse OS and PFS compared to the group with low or absent *SFRP5* methylation, independently from the *EGFR* genotype.

Finally, it was observed that patients without methylation in *SFRP1* have a longer PFS compared with patients with its methylation (9.7 months *vs* 2.0 months, p = 0.05), thus suggesting the intriguing hypothesis that activation of Wnt signaling by antagonist methylation could confer staminal properties linked to the EGFR TKIs resistance in lung cancer patients (48).

3.2.4 *DAPK*

DAPK (death-associated protein kinase) protein belongs to the calcium/calmodulin (CaM)-regulated serine/threonine protein kinase family with pro-apoptotic function through the interferon-γ, TGF, TNFα and Fas ligand mediators (62–64). Variations in DAPK expression are observed in NSCLC and in many other cancer types, at times due to DNA hypermethylation at the promoter region (65, 66).

The link between *DAPK* (death-associated protein kinase) promoter methylation and acquired resistance to anti-EGFR TKIs was investigated for the first time by *Ogawa T and collaborators* in a collection of cancer cell lines. To experimentally validate their hypothesis, a 56 genes panel methylation (MethDet-56) array was used to assess differences in methylation profile of a collection of head and neck squamous cell carcinoma (HNSCC) and NSCLC cell lines before and after acquired resistance to erlotinib and cetuximab treatments. An hypermethylation of *DAPK* gene at the promoter region linked to a decrease in its expression was exclusively observed in resistant lung cancer lines of both types of drugs and not in the parental cells. Taking into account that *DAPK* appeared to be silenced in HNSCC cells through DNA methylation long before the treatment with EGFR inhibitors, the Authors suggested *DAPK* as an epigenetic mediator in acquired resistance only in NSCLC but not in HNSCC cells (49). Even if of great interest, further studies are demanded to corroborate these results on tumor samples from NSCLC patients under TKI treatment.

3.2.5 *KL* and *S100P*

To clarify the role of epigenetic regulatory mechanisms in the resistance to gefitinib, *Terai H et al.* compared variations of global DNA methylation profile in gefitinib-sensitive and resistant lung cancer cell lines. The comprehensive DNA methylation and mRNA expression analyses performed allowed the identification of 640 genes associated with secondary resistance to EGFR-TKI. Among these, experiments of silencing by siRNA and 5-aza-dC treatment highlighted the potential role of methylation in *KL* (Klotho) and *S100P* (S100 Calcium Binding Protein P) genes in the acquisition of resistance to gefitinib (50). Anyhow, no additional studies on patients 'cohorts were conducted to date.

3.2.6 *SPP1* and *CD44*

SPP1 (Secreted Phosphoprotein 1) encodes the osteopontin (67), which has been found to abnormally express in a variety of cancers, and induces drug resistance, progression, recurrence, and metastasis in breast, ovarian, and colon cancer (68–70). Together with *CD44* (cluster of differentiation), it also contributes to early pathogenesis and metastatic potential in lung cancer (71).

Both *SPP1* and *CD44* genes were suggested by *Wang et al.* as molecular drivers that might contribute to EGFR-TKI resistance in NSCLC (51).

This interesting scientific evidence resulted from the evaluation of the transcriptional activity of the two genes in resistant NSCLC samples EGFR-TKI treated of GEO (Gene Expression Omnibus) database, which was found to be increased *versus* the sensitive ones. Data analysis on resistant NSCLCs to the 1st or 2nd TKI generation revealed that high methylation of CpGs at *SPP1* (cg00088885) and *CD44* (cg20971158) promoters could be considered a potential, independent indicator of the worst prognosis in lung adenocarcinoma patients. The upregulation of SPP1 due to hypermethylation induces resistance to the 1st and 2nd generation EGFR-TKI and influences tumor immune infiltration in tumor tissues and cell lines. Moreover, co-expression studies revealed that SSP1-CD44 axis deregulation identifies the same group of miRNA involved in transforming NSCLC into SCLC mediated by a multidrug-resistant cancer stem cells acquisition, thus modulating the cancer phenotypes transition in acquiring resistance to TKI process (51).

3.2.7 *RASSF1A* and *GADD45β*

RASSF1A (Ras association domain family protein1 isoform A) encodes for a tumor suppressor protein that exerts several anti-tumoral effects by modulating tumor growth and dissemination through several biological functions as well as cell cycle arrest, migration inhibition, and/or apoptosis induction (72). The *GADD45β* (Growth Arrest And DNA Damage-Inducible Protein GADD45 Beta) belongs to a list of genes involved in stressful growth arrest conditions and treatment with DNA damaging

molecules (73). *Hou and colleagues* assessed the methylation status at the promoter region of *RASSF1A* and *GADD45β* genes in acquired gefitinib-resistant lung adenocarcinoma PC9 (harboring *EGFR* exon19 deletion) and PC9/GR (harboring *EGFR* exon19 deletions and acquired *EGFR* exon20 p.T790M mutation) cell lines. Using Nimble Gen Human DNA Methylation 3x720K Promoter Plus CpG Island Array, they found that the promoter regions of both genes were hypermethylated only in PC9/GR cell line and that the epigenetic silencing induced by methylation was able to induce a downregulation of RASSF1A and GADD45β expression. To confirm the link between the observed methylation in both genes and resistance to gefitinib in PC9/GR cells, the Authors showed that this process could be partially reversed by using the demethylating agent 5-Aza-CdR (52). No confirmative studies on patients 'cohorts were conducted to date.

3.3 Multi-gene and Genome-wide global methylation profile and EGFR-TKI resistance

Increasing evidences about the role of DNA methylation in the molecular pathology of lung cancer highlights the need for robust technologies able to establish if whole methylome, and not only methylation changes in single or few genes, could be associated with EGFR-TKI resistance (9, 74). To date, multiple high-throughput techniques are available for assessing genome methylation and determining DMRs, both at tissue and at liquid biopsy levels, for real-time monitoring of disease load in advanced lung cancer patients (8, 75–77). Despite this, a few original studies underlined the association between whole methylome fluctuations and therapeutic resistance to first/second/third-TKI treatments in NSCLC patients.

One of the earliest evidence was provided by *Xia S and colleagues*' work, which reported that a concomitant evaluation of molecular profile and whole methylation status in lung tumors was useful to early predict response to second-line osimertinib in NSCLC patients (78). Plasma samples from n=8 stage IV osimertinib-treated *EGFR* p.T790M-positive patients with lung adenocarcinoma were longitudinally collected and analyzed using capture-based targeted DNA and methylated DNA sequencing. A significant inverse correlation between allele fraction rate and methylation status was observed (p=0.0002), which was absent in those patients who did not have any somatic mutations (78).

The link between DNA methylation profile and TKI treatment in NSCLCs was also reported in a prospective study on 36 *EGFR* mutant NSCLC patients. Tumor tissues were obtained from 10 patients prior to the TKI treatment, of which 4 matched with post-TKI re-biopsies (3 p.T790M+, 1 p.T790M-). The remaining tissues from post-TKI patients were divided into 17 positive and 9 negative for p.T790M mutation groups. The epigenetic profiling by Illumina Infinium EPIC array allowed the identification of a correlation between *EGFR* p.T790M and the epi-methylated group of patients. All post-TKI p.T790M+ samples fell within epi-group 2, whereas most of p.T790M- samples were found within epi-group 1. The report suggested that the acquisition of resistance to EGFR-TKIs could already occur at baseline and could be related to a specific multigene DNA methylation pattern, which includes probes mapping in the *EGFR* gene (79).

Nguyen HN and colleagues published a fascinating study suggesting how TKI resistance mechanisms could be associated with important changes in epigenetic profiles of lung tumors. The Authors tested plasma cell-free DNA (cfDNA) samples of 122 Vietnamese advanced NSCLC patients at stage III or IV of the disease, who had a clinical story of acquired resistance, following gefitinib/erlotinib or afatinib treatment. Using ultra-deep massively parallel sequencing targeting 450 genomic regions and covering 9593 CpG sites in nine genes (*EGFR, KRAS, NRAS, BRAF, ALK, ROS1, MET, HER2* and *PIK3CA*), it was observed that the heterogeneity of methylation patterns occurred in those cases that have different mutation profiles of acquired resistance to TKI drugs (56). Of those, genetic alterations in *EGFR*, particularly *EGFR* amplification (n = 6), showed an associated genome-wide hypomethylation. Interestingly, the level of hypomethylation was associated with the duration of response to TKI treatment.

Novel important preliminary evidences came from *Shi and colleagues* investigations, who constructed a DNA methylation-based risk score (RS) to better predict survival in *EGFR* mutated NSCLC patients after TKIs treatment. Forty mutated (Ex19del or L858R) and 21 *EGFR* wild-type blood samples of NSCLC patients were profiled by targeted bisulfite sequencing using a panel with 80,672 CpG sites, covering more than 1 million bases of the human genome. A total of 56 differentially methylated blocks appeared to be significantly downregulated in *EGFR* mutated group under TKI treatment. A four-DMB based prognostic RS model involving 4 cancer-related genes was developed to predict poor PFS, independently from their clinical factors (p<0.001) (80).

A recent study conducted by *Ntzifa A et al.* suggested that variations in DNA methylation levels of a group of nine genes (*RASSF1A, RASSF10, APC, WIF-1, BRMS1, SLFN11, RARβ, SHISA3 and FOXA1*) may play a direct role in resistance to osimertinib as second line treatment. Eighty cell-free DNA samples and 74 circulating paired tumor cells (CTCs) were collected from a total of 42 NSCLC patients, before osimertinib treatment and at the time of disease progression. The Authors proved a direct and strong correlation between *RASSF1A* and *APC* methylation levels at promoter regions. In addition, methylation rates of *APC*, *WIF-1* and *SLFN11* were found to be higher at PD. Positive NSCLC patients for at least one methylated marker had a more rapid progression than the full negative ones.

Although it was not evident a correlation between methylation and PD comparing cfDNA and paired CTC groups in 42 NSCLC patients, a concordance trend was found for 6 methylated genes (*APC, BRMS1, RASSF1A, RASSF10, SLFN11, WIF-1*). More interestingly, positive patients for almost one methylated marker showed a faster progression than patients negative for DNA methylation for all tested markers (p=0.031) (53).

4 Role of miRNA in EGFR-TKI resistance-brief overview

MicroRNAs (miRNAs) are 18-25 nucleotides single-stranded non-coding RNAs which are able to turn on and off the expression of their targeted genes (81). The deregulation of miRNA machinery is linked to the acquisition of cancer hallmarks that lead to genome instability and impact on tumor growth, invasion and metastatization (82). Recent findings have shown that miRNAs could modulate as post-transcriptional regulators the response to EGFR TKIs in overcoming resistance in NSCLC patients, as summarized in Table 2 (92, 93). The first evidence of this derived from *Hashida S and colleagues*' work, whom investigated the EGFR-TKI resistance mechanisms in a total of 10 afatinib-resistant cell lines from parental NSCLC cells with activating *EGFR* mutations (83). In particular, they found that these *EGFR*-mutant lung cancer cell lines mainly acquired *MET* amplification as a mechanism of resistance and become sensitive to afatinib plus crizotinib. The acquired *MET* amplification was co-occurrent with miR200c epigenetic silencing and the acquisition of EMT and stem cell-like features. Moreover, it was demonstrated that the acquisition of EMT and other associated features was also due to a downregulation of epithelial markers as well as E-cadherin that was observed in this group of afatinib-resistant cell lines. These findings were consistent with previous observations by *Shien et al.* (84), who reported a downregulation of miR200c by methylation in a group of NSCLC cell lines gefitinib resistant having acquired *MET* amplification and stem cell-like features (83).

Many other reports are providing evidences about the contribution of miRNAs in the complex and heterogeneous mechanisms of EGFR-TKI drug resistance in NSCLC. A role in EMT promotion linked to acquired osimertinib resistance in NSCLC was also attributed to Let-7c (85), whereas miR-7 was demonstrated to enhance TKI-induced cytotoxicity by gefitinib through the suppression of both *IGF1R* (Insulin like growth factor1 receptor) and *EGFR* signaling pathways (86).

A critical role of miR-130a in overcoming acquired resistance to EGFR-TKIs via *MET* signaling was highlighted in two separate studies. A first study demonstrated that the overexpression of miR-130a enhanced apoptosis and suppressed NSCLC cells proliferation after gefitinib treatment. Otherwise, a down-regulation of this miRNA triggered cell apoptosis with rapid proliferation in both

TABLE 2 Functional and biological role of miRNAs related to EGFR-TKI resistance in lung cancer models.

miRNA	Functional and biological effects	Cancer models	Refs
miR-200c	✓ miR200c epigenetic silencing and downregulation co-occurred with *MET* amplification in *EGFR*-mutant cells after acquired afatinib resistance and makes them more sensite to afatinib plus crizotinib. ✓ miR200c epigenetic silencing are related to the acquisition of EMT and stem cell-like features in the afatinib-resistant lung cell lines.	✓ Afatinib-resistant lung cell lines obtained from parental NSCLC cells with activating *EGFR* mutations.	(83)
miR-200c	✓ miR200c hypermethylation was associated to acquired resistance to gefitinib in lung cancer cells having *MET* amplification by promoting EMT features. ✓ miR200c epigenetic silencing are related to the acquisition of stem cell-like features in the gefitinib-resistant lung cell lines.	✓ *EGFR*-mutant lung cell lines and sublines resistant to gefitinib.	(84)
Let-7c	✓ Let-7c acts as a regulator of EMT as well as affects CSC phenotype. ✓ Its expression was correlated with resistance to osimertinib in p.T790M NSCLC cells.through the EMT modulation.	✓ H1975 (endogenous p.T790M mutation) and HCC827-T790M (with acquired p.T790M mutation) lung cancer cell lines.	(85)
miR-7	✓ miR7 enhances gefitinib cytotoxicity by suppressing both *EGFR* and *IGF1R* signaling.	✓ Adenocarcinoma lung cell (A549).	(86)
miR-130a	✓ miR-130a overexpression enhanced apoptosis and suppressed NSCLC cells proliferation before and after gefitinib treatment via MET signaling. ✓ Overexpression of MET could rescue the functions of this miRNA regarding cell apoptosis and proliferation after treatment with gefitinib.	✓ Gefitinib-sensitive and resistant NSCLC cell lines.	(87)
miR-200a	✓ miR-200a is downregulated in NSCLC cells, where it directly targets the *3′-UTR* of both *EGFR* and *MET* mRNA. ✓ Its overexpression significantly downregulates both *EGFR* and *MET* signaling pathways and severely inhibits cell migration, invasion in gefitinib resistant lung cells.	✓ Gefitinib-sensitive and resistant NSCLC cell lines.	(88)
miR-133b	✓ The increase of miR-133b expression led to a decrease in lung cancer cell growth. ✓ Variations in its expression could help to discriminated responder from non-responder patients to TKI erlotinib. ✓ High levels of miR-133b in NSCLCs were associated with longer progression-free survival time of NSCLC patients.	✓ NSCLC cell lines (A549 and H1299) and 32 patients with advanced lung ADC who received erlotinb as second- or third-line therapy.	(89)
miR-497	✓ miR-497 overexpression can reverse drug resistance of NSCLC cells to EGFR-TKI by inhibiting the expression of IGF1R protein and blocking the activation of its downstream *AKT1* signaling pathway.	✓ Gefitinib resistant lung adenocarcinoma A549 cell line (A549/GR).	(90)
miR-30a-5p	✓ Gefitinib combined with miR-30A-5p mimics, could suppress the growth in acquired TKI resistance lung cancer cells via IGF1R and HGFR signaling.	✓ H1650-acquired gefitinib-resistant cell (H1650GR), H1975, and H460 cell lines.	(91)

miRNA, microRNA; MET, MET Proto-Oncogene, Receptor Tyrosine Kinase; EGFR, epidermal growth factor receptor; EMT, epithelial-to-mesenchymal transition; CSC, Cancer stem cells; IGF1R, Insulin-like growth factor1 receptor; AKT, Protein kinase B; PI3K, phosphoinositide 3-kinase; ADC, adenocarcinoma; NSCLC, Non Small Cell Lung Cancer.

gefitinib-sensitive and resistant NSCLC cell lines. It was also demonstrated that miR-130a binds to the *3'-UTR* of *MET* and significantly suppresses its expression, so the overexpressing of MET could rescue the functions of miR-130a regarding cell apoptosis and proliferation after cells are treated with gefitinib (87). These results are in line with those published in 2015, when it has been shown that the decrease of cell invasion and migration due to miR-200a overexpression leds to gefitinib resistance in NSCLC cells via *EGFR* and *MET* signaling (88).

Bisagni A et al. was able to prove how the increase expression levels of miR-133b significantly correlated with a better PFS and OS and allowed to better discriminate NSCLC responder patients to erlotinib from non-responder. Similarly, they found a direct relationship between the upregulation of miR-200c and improved gefitinib sensitivity in NSCLC (89).

Finally, increased miR-497 level was seen to have a significant impact in enhancing sensitivity to EGFR-TKI in NSCLC cells via *IGF1R* targeting and *AKT* activation (90), whereas *in vitro* experiments and *in vivo* models were useful to demonstrate that the combination of gefitinib plus a microRNA mimic, miR-30a-5p, could overcome acquired EGFR-TKI resistance in NSCLC via a direct regulation of *IGF1R* and *HGFR* (hepatocyte growth factor receptor) signaling (91).

5 Concluding Remarks

Worldwide, lung cancer represents one of the most common types of cancer and, by far, the leading cause of cancer deaths (94, 95). Among these cases, 80-85% have an NSCLC histology, which includes adenocarcinoma, squamous cell carcinoma, and large cell carcinoma subtypes (96, 97). Changes in DNA methylation may largely underpin lung cancer in several processes as well as the capability of growth, invasion and spreading of cancer cells (98, 99). A special attention is now drowning toward DNA methylation patterns of drug-treated tumor cells that could change and support the acquisition of resistance to treatments.

The double interaction between epigenetic alterations and therapy resistance of tumors is progressively emerging and is looking for answers as to why it happens. In solid tumors and in EGFR-TKI treated NSCLC patients there are little translational evidences about the occurrence and role of DNA methylation at different regions of single/multiple genes (promoter and other regulatory regions) or CpG islands (14, 100).

To bridge the gap in this specific field is actually demanded. Specifically, it is necessary to understand how methylome could be modified and which methylated regions or specific CpG sites are affected in order to translate relevant epigenome associations into clinically personalized treatment in lung cancer patients (101). Next to this, the definition of methodological high-throughput approaches to study changes in methylation will improve the advances in this field, since measuring global or single CpG methylation will help to construct a more robust and integrated algorithm to predict and monitor disease evolution in a non-invasive manner for lung cancer patients (102–104). In recent years, there has been a growing interest in liquid biopsy to identify and monitor epigenomic drivers, also in the context of primary and acquired resistance in lung cancer (105). There are many reasons why circulating tumor DNA (ctDNA) methylation may rapidly emerge in this clinical settings. The first point leads to the fact that DNA methylation occurred as an early event in the etiology and progression of lung carcinogenesis, besides it could be strictly dependent both on tissue location and type of cancer (106). Second, it should be taken into consideration that DNA methylation profiling provides a deep characterization of ctDNA which contains important information about longitudinal changes in CpG islands across genomic regions (107). Third, the heterogeneity of CpG methylation patterns in different regions of multiple genes (promoter and other regulatory regions) is significantly associated with a poor outcome that might allow for accurate discrimination among lung cancer subtypes in liquid biopsies samples (108). Moreover, starting from the track of tumor evolution in serial ctDNA, it could be possible to identify minimal residual disease and manage early cancer progression, overcome temporally and spatially intratumor heterogeneity aiming at stratifying lung cancer patients according to recurrence risk and response to therapy (109). Although it remains to define several methodological strategies as well as optimize ctDNA extraction step to ensure a high-quality cfDNA or establish the gold standard for setting a better sensitivity and specificity of ctDNA methylation assay detection (110), a systematic analysis of liquid biopsy samples could provide important insights into the heterogeneity of TKI resistance mechanisms in NSCLC patients, thus providing essential information to better predict resistance and help the selection of subsequent treatments.

Ongoing research studies are also focused on single-cell DNA-methylation profiling that may contribute to the examination of cell-of-origins and cancer cell type heterogeneity by which becomes possible to clarify the correlation between DNA methylation and the expression fluctuations of cancer driver genes sets in different subtypes.

Author contributions

Conceptualization, FPF and LM. Data curation, FPF and AS. Writing—original draft preparation, FPF. Writing—review and editing, LM. Visualization, AS. Supervision, LM. All authors contributed to the article and approved the submitted version.

Funding

This research was funded by the Italian Ministry of Health, Ricerca Corrente 2022, by the "5x1000"voluntary contributions to Fondazione IRCCS Casa Sollievo della Sofferenza.

Conflict of interest

The authors declare that the research was conducted in the absence of any commercial or financial relationships that could be construed as a potential conflict of interest.

Publisher's note

References

1. Shen H, Laird PW. Interplay between the cancer genome and epigenome. *Cell* (2013) 153(1):38–55. doi: 10.1016/j.cell.2013.03.008

2. Cheng Y, He C, Wang M, Ma X, Mo F, Yang S, et al. Targeting epigenetic regulators for cancer therapy: mechanisms and advances in clinical trials. *Signal Transduct Target Ther* (2019) 4:62. doi: 10.1038/s41392-019-0095-0

3. Feinberg AP, Koldobskiy MA, Gondor A. Epigenetic modulators, modifiers and mediators in cancer aetiology and progression. *Nat Rev Genet* (2016) 17(5):284–99. doi: 10.1038/nrg.2016.13

4. Qian Y, Shi L, Luo Z. Long non-coding RNAs in cancer: implications for diagnosis, prognosis, and therapy. *Front Med (Lausanne)* (2020) 7:612393. doi: 10.3389/fmed.2020.612393

5. Si W, Shen J, Zheng H, Fan W. The role and mechanisms of action of microRNAs in cancer drug resistance. *Clin Epigenetics* (2019) 11(1):25. doi: 10.1186/s13148-018-0587-8

6. Greenberg MVC, Bourc'his D. The diverse roles of DNA methylation in mammalian development and disease. *Nat Rev Mol Cell Biol* (2019) 20(10):590–607. doi: 10.1038/s41580-019-0159-6

7. Villicana S, Bell JT. Genetic impacts on DNA methylation: research findings and future perspectives. *Genome Biol* (2021) 22(1):127. doi: 10.1186/s13059-021-02347-6

8. Barros-Silva D, Marques CJ, Henrique R, Jeronimo C. Profiling DNA methylation based on next-generation sequencing approaches: new insights and clinical applications. *Genes (Basel)* (2018) 9(9):429. doi: 10.3390/genes9090429

9. Beck D, Ben Maamar M, Skinner MK. Genome-wide CpG density and DNA methylation analysis method (MeDIP, RRBS, and WGBS) comparisons. *Epigenetics* (2022) 17(5):518–30. doi: 10.1080/15592294.2021.1924970

10. Consortium B. Quantitative comparison of DNA methylation assays for biomarker development and clinical applications. *Nat Biotechnol* (2016) 34(7):726–37. doi: 10.1038/nbt.3605

11. Locke WJ, Guanzon D, Ma C, Liew YJ, Duesing KR, Fung KYC, et al. DNA Methylation cancer biomarkers: translation to the clinic. *Front Genet* (2019) 10:1150. doi: 10.3389/fgene.2019.01150

12. Mancarella D, Plass C. Epigenetic signatures in cancer: proper controls, current challenges and the potential for clinical translation. *Genome Med* (2021) 13(1):23. doi: 10.1186/s13073-021-00837-7

13. Ortiz-Barahona V, Joshi RS, Esteller M. Use of DNA methylation profiling in translational oncology. *Semin Cancer Biol* (2022) 83:523–35. doi: 10.1016/j.semcancer.2020.12.011

14. Romero-Garcia S, Prado-Garcia H, Carlos-Reyes A. Role of DNA methylation in the resistance to therapy in solid tumors. *Front Oncol* (2020) 10:1152. doi: 10.3389/fonc.2020.01152

15. Leonetti A, Sharma S, Minari R, Perego P, Giovannetti E, Tiseo M. Resistance mechanisms to osimertinib in EGFR-mutated non-small cell lung cancer. *Br J Cancer* (2019) 121(9):725–37. doi: 10.1038/s41416-019-0573-8

16. Santoni-Rugiu E, Melchior LC, Urbanska EM, Jakobsen JN, Stricker K, Grauslund M, et al. Intrinsic resistance to EGFR-tyrosine kinase inhibitors in EGFR-mutant non-small cell lung cancer: differences and similarities with acquired resistance. *Cancers (Basel)* (2019) 11(7):923. doi: 10.3390/cancers11070923

17. Meador CB, Sequist LV, Piotrowska Z. Targeting EGFR exon 20 insertions in non-small cell lung cancer: recent advances and clinical updates. *Cancer Discov* (2021) 11(9):2145–57. doi: 10.1158/2159-8290.CD-21-0226

18. Rosell R, Moran T, Queralt C, Porta R, Cardenal F, Camps C, et al. Screening for epidermal growth factor receptor mutations in lung cancer. *N Engl J Med* (2009) 361 (10):958–67. doi: 10.1056/NEJMoa0904554

19. Abourehab MAS, Alqahtani AM, Youssif BGM, Gouda AM. Globally approved EGFR inhibitors: insights into their syntheses, target kinases, biological activities, receptor interactions, and metabolism. *Molecules* (2021) 26(21):6677. doi: 10.3390/molecules26216677

20. Vaid AK, Gupta A, Momi G. Overall survival in stage IV EGFR mutation –positive NSCLC: comparing first–, second– and third–generation EGFR–TKIs (Review). *Int J Oncol* (2021) 58(2):171–84. doi: 10.3892/ijo.2021.5168

21. Nagasaka M, Zhu VW, Lim SM, Greco M, Wu F, Ou SI. Beyond osimertinib: the development of third-generation EGFR tyrosine kinase inhibitors for advanced EGFR+ NSCLC. *J Thorac Oncol* (2021) 16(5):740–63. doi: 10.1016/j.jtho.2020.11.028

22. Tan CS, Kumarakulasinghe NB, Huang YQ, Ang YLE, Choo JR, Goh BC, et al. Third generation EGFR TKIs: current data and future directions. *Mol Cancer* (2018) 17 (1):29. doi: 10.1186/s12943-018-0778-0

23. Tumbrink HL, Heimsoeth A, Sos ML. The next tier of EGFR resistance mutations in lung cancer. *Oncogene* (2021) 40(1):1–11. doi: 10.1038/s41388-020-01510-w

24. Westover D, Zugazagoitia J, Cho BC, Lovly CM, Paz-Ares L. Mechanisms of acquired resistance to first- and second-generation EGFR tyrosine kinase inhibitors. *Ann Oncol* (2018) 29(suppl_1):i10–i9. doi: 10.1093/annonc/mdx703

25. Johnson M, Garassino MC, Mok T, Mitsudomi T. Treatment strategies and outcomes for patients with EGFR-mutant non-small cell lung cancer resistant to EGFR tyrosine kinase inhibitors: focus on novel therapies. *Lung Cancer* (2022) 170:41–51. doi: 10.1016/j.lungcan.2022.05.011

26. Wang J, Wang B, Chu H, Yao Y. Intrinsic resistance to EGFR tyrosine kinase inhibitors in advanced non-small-cell lung cancer with activating EGFR mutations. *Onco Targets Ther* (2016) 9:3711–26. doi: 10.2147/OTT.S106399

27. Lovly CM, Shaw AT. Molecular pathways: resistance to kinase inhibitors and implications for therapeutic strategies. *Clin Cancer Res* (2014) 20(9):2249–56. doi: 10.1158/1078-0432.CCR-13-1610

28. Suryavanshi M, Jaipuria J, Mattoo S, Dhandha S, Khatri M. Audit of molecular mechanisms of primary and secondary resistance to various generations of tyrosine kinase inhibitors in known epidermal growth factor receptor-mutant non-small cell lung cancer patients in a tertiary centre. *Clin Oncol (R Coll Radiol)* (2022) 34(11):e451–e62. doi: 10.1016/j.clon.2022.06.003

29. Pao W, Chmielecki J. Rational, biologically based treatment of EGFR-mutant non-small-cell lung cancer. *Nat Rev Cancer* (2010) 10(11):760–74. doi: 10.1038/nrc2947

30. Sharma SV, Lee DY, Li B, Quinlan MP, Takahashi F, Maheswaran S, et al. A chromatin-mediated reversible drug-tolerant state in cancer cell subpopulations. *Cell* (2010) 141(1):69–80. doi: 10.1016/j.cell.2010.02.027

31. Turke AB, Zejnullahu K, Wu YL, Song Y, Dias-Santagata D, Lifshits E, et al. Preexistence and clonal selection of MET amplification in EGFR mutant NSCLC. *Cancer Cell* (2010) 17(1):77–88. doi: 10.1016/j.ccr.2009.11.022

32. Skoulidis F, Heymach JV. Co-Occurring genomic alterations in non-small-cell lung cancer biology and therapy. *Nat Rev Cancer* (2019) 19(9):495–509. doi: 10.1038/s41568-019-0179-8

33. Tan CS, Gilligan D, Pacey S. Treatment approaches for EGFR-inhibitor-resistant patients with non-small-cell lung cancer. *Lancet Oncol* (2015) 16(9):e447–e59. doi: 10.1016/S1470-2045(15)00246-6

34. Wu L, Ke L, Zhang Z, Yu J, Meng X. Development of EGFR TKIs and options to manage resistance of third-generation EGFR TKI osimertinib: conventional ways and immune checkpoint inhibitors. *Front Oncol* (2020) 10:602762. doi: 10.3389/fonc.2020.602762

35. Ko B, Paucar D, Halmos B. EGFR T790M: revealing the secrets of a gatekeeper. *Lung Cancer (Auckl)* (2017) 8:147–59. doi: 10.2147/LCTT.S117944

36. Wu SG, Yu CJ, Yang JC, Shih JY. The effectiveness of afatinib in patients with lung adenocarcinoma harboring complex epidermal growth factor receptor mutation. *Ther Adv Med Oncol* (2020) 12:1758835920946156. doi: 10.1177/1758835920946156

37. Leonetti A, Minari R, Mazzaschi G, Gnetti L, La Monica S, Alfieri R, et al. Small cell lung cancer transformation as a resistance mechanism to osimertinib in epidermal growth factor receptor-mutated lung adenocarcinoma: case report and literature review. *Front Oncol* (2021) 11:642190. doi: 10.3389/fonc.2021.642190

38. Yang Y, Li S, Wang Y, Zhao Y, Li Q. Protein tyrosine kinase inhibitor resistance in malignant tumors: molecular mechanisms and future perspective. *Signal Transduct Target Ther* (2022) 7(1):329. doi: 10.1038/s41392-022-01168-8

39. Weng CH, Chen LY, Lin YC, Shih JY, Lin YC, Tseng RY, et al. Epithelial-mesenchymal transition (EMT) beyond EGFR mutations per se is a common mechanism for acquired resistance to EGFR TKI. *Oncogene* (2019) 38(4):455–68. doi: 10.1038/s41388-018-0454-2

40. Reita D, Pabst L, Pencreach E, Guerin E, Dano L, Rimelen V, et al. Molecular mechanism of EGFR-TKI resistance in EGFR-mutated non-small cell lung cancer: application to biological diagnostic and monitoring. *Cancers (Basel)* (2021) 13 (19):4926. doi: 10.3390/cancers13194926

41. Xu Z, Qin F, Yuan L, Wei J, Sun Y, Qin J, et al. EGFR DNA methylation correlates with EGFR expression, immune cell infiltration, and overall survival in lung adenocarcinoma. *Front Oncol* (2021) 11:691915. doi: 10.3389/fonc.2021.691915

42. Li XY, Wu JZ, Cao HX, Ma R, Wu JQ, Zhong YJ, et al. Blockade of DNA methylation enhances the therapeutic effect of gefitinib in non-small cell lung cancer cells. *Oncol Rep* (2013) 29(5):1975–82. doi: 10.3892/or.2013.2298

43. Soria JC, Lee HY, Lee JI, Wang L, Issa JP, Kemp BL, et al. Lack of PTEN expression in non-small cell lung cancer could be related to promoter methylation. *Clin Cancer Res* (2002) 8(5):1178–84.

44. Noro R, Gemma A, Miyanaga A, Kosaihira S, Minegishi Y, Nara M, et al. PTEN inactivation in lung cancer cells and the effect of its recovery on treatment with epidermal growth factor receptor tyrosine kinase inhibitors. *Int J Oncol* (2007) 31 (5):1157–63. doi: 10.3892/ijo.31.5.1157

45. Su SF, Liu CH, Cheng CL, Ho CC, Yang TY, Chen KC, et al. Genome-wide epigenetic landscape of lung adenocarcinoma links HOXB9 DNA methylation to intrinsic EGFR-TKI resistance and heterogeneous responses. *JCO Precis Oncol* (2021) 5:418–31. doi: 10.1200/PO.20.00151

46. Zhang Y, Xiang C, Wang Y, Duan Y, Liu C, Zhang Y. PD-L1 promoter methylation mediates the resistance response to anti-PD-1 therapy in NSCLC patients with EGFR-TKI resistance. *Oncotarget* (2017) 8(60):101535–44. doi: 10.18632/oncotarget.21328

47. Niu X, Liu F, Zhou Y, Zhou Z, Zhou D, Wang T, et al. Genome-wide DNA methylation analysis reveals GABBR2 as a novel epigenetic target for EGFR 19 deletion lung adenocarcinoma with induction erlotinib treatment. *Clin Cancer Res* (2017) 23 (17):5003–14. doi: 10.1158/1078-0432.CCR-16-2688

48. Zhu J, Wang Y, Duan J, Bai H, Wang Z, Wei L, et al. DNA Methylation status of wnt antagonist SFRP5 can predict the response to the EGFR-tyrosine kinase inhibitor therapy in non-small cell lung cancer. *J Exp Clin Cancer Res* (2012) 31(1):80. doi: 10.1186/1756-9966-31-80

49. Ogawa T, Liggett TE, Melnikov AA, Monitto CL, Kusuke D, Shiga K, et al. Methylation of death-associated protein kinase is associated with cetuximab and erlotinib resistance. *Cell Cycle* (2012) 11(8):1656–63. doi: 10.4161/cc.20120

50. Terai H, Soejima K, Yasuda H, Sato T, Naoki K, Ikemura S, et al. Long–term exposure to gefitinib induces acquired resistance through DNA methylation changes in the EGFR–mutant PC9 lung cancer cell line. *Int J Oncol* (2015) 46(1):430–6. doi: 10.3892/ijo.2014.2733

51. Wang Z, Zhang L, Xu W, Li J, Liu Y, Zeng X, et al. The multi-omics analysis of key genes regulating EGFR-TKI resistance, immune infiltration, SCLC transformation in EGFR-mutant NSCLC. *J Inflammation Res* (2022) 15:649–67. doi: 10.2147/JIR.S341001

52. Hou T, Ma J, Hu C, Zou F, Jiang S, Wang Y, et al. Decitabine reverses gefitinib resistance in PC9 lung adenocarcinoma cells by demethylation of RASSF1A and GADD45beta promoter. *Int J Clin Exp Pathol* (2019) 12(11):4002–10.

53. Ntzifa A, Londra D, Rampias T, Kotsakis A, Georgoulias V, Lianidou E. DNA Methylation analysis in plasma cell-free DNA and paired CTCs of NSCLC patients before and after osimertinib treatment. *Cancers (Basel)* (2021) 13(23):5974. doi: 10.3390/cancers13235974

54. Maeda M, Murakami Y, Watari K, Kuwano M, Izumi H, Ono M. CpG hypermethylation contributes to decreased expression of PTEN during acquired resistance to gefitinib in human lung cancer cell lines. *Lung Cancer* (2015) 87 (3):265–71. doi: 10.1016/j.lungcan.2015.01.009

55. Shostak K, Chariot A. EGFR and NF-kappaB: partners in cancer. *Trends Mol Med* (2015) 21(6):385–93. doi: 10.1016/j.molmed.2015.04.001

56. Nguyen HN, Cao NT, Van Nguyen TC, Le KND, Nguyen DT, Nguyen QT, et al. Liquid biopsy uncovers distinct patterns of DNA methylation and copy number changes in NSCLC patients with different EGFR-TKI resistant mutations. *Sci Rep* (2021) 11(1):16436. doi: 10.1038/s41598-021-95985-6

57. Terunuma M. Diversity of structure and function of GABA(B) receptors: a complexity of GABA(B)-mediated signaling. *Proc Jpn Acad Ser B Phys Biol Sci* (2018) 94(10):390–411. doi: 10.2183/pjab.94.026

58. Stein L, Rothschild J, Luce J, Cowell JK, Thomas G, Bogdanova TI, et al. Copy number and gene expression alterations in radiation-induced papillary thyroid carcinoma from chernobyl pediatric patients. *Thyroid* (2010) 20(5):475–87. doi: 10.1089/thy.2009.0008

59. Zhang X, Zhang R, Zheng Y, Shen J, Xiao D, Li J, et al. Expression of gamma-aminobutyric acid receptors on neoplastic growth and prediction of prognosis in non-small cell lung cancer. *J Transl Med* (2013) 11:102. doi: 10.1186/1479-5876-11-102

60. Katoh M. WNT/PCP signaling pathway and human cancer (review). *Oncol Rep* (2005) 14(6):1583–8. doi: 10.3892/or.14.6.1583

61. Liu D, Sun C, Kim N, Bhan C, Tuason JPW, Chen Y, et al. Comprehensive analysis of SFRP family members prognostic value and immune infiltration in gastric cancer. *Life (Basel)* (2021) 11(6):522. doi: 10.3390/life11060522

62. Cohen O, Inbal B, Kissil JL, Raveh T, Berissi H, Spivak-Kroizaman T, et al. DAP-kinase participates in TNF-alpha- and fas-induced apoptosis and its function requires the death domain. *J Cell Biol* (1999) 146(1):141–8. doi: 10.1083/jcb.146.999.141

63. Deiss LP, Feinstein E, Berissi H, Cohen O, Kimchi A. Identification of a novel serine/threonine kinase and a novel 15-kD protein as potential mediators of the gamma interferon-induced cell death. *Genes Dev* (1995) 9(1):15–30. doi: 10.1101/gad.9.1.15

64. Jang CW, Chen CH, Chen CC, Chen JY, Su YH, Chen RH. TGF-beta induces apoptosis through smad-mediated expression of DAP-kinase. *Nat Cell Biol* (2002) 4 (1):51–8. doi: 10.1038/ncb731

65. Li Y, Zhu M, Zhang X, Cheng D, Ma X. Clinical significance of DAPK promoter hypermethylation in lung cancer: a meta-analysis. *Drug Des Devel Ther* (2015) 9:1785–96. doi: 10.2147/DDDT.S78012

66. Zhang Y, Wu J, Huang G, Xu S. Clinicopathological significance of DAPK promoter methylation in non-small-cell lung cancer: a systematic review and meta-analysis. *Cancer Manag Res* (2018) 10:6897–904. doi: 10.2147/CMAR.S174815

67. Anborgh PH, Mutrie JC, Tuck AB, Chambers AF. Role of the metastasis-promoting protein osteopontin in the tumour microenvironment. *J Cell Mol Med* (2010) 14(8):2037–44. doi: 10.1111/j.1582-4934.2010.01115.x

68. Gothlin Eremo A, Lagergren K, Othman L, Montgomery S, Andersson G, Tina E. Evaluation of SPP1/osteopontin expression as predictor of recurrence in tamoxifen treated breast cancer. *Sci Rep* (2020) 10(1):1451. doi: 10.1038/s41598-020-58323-w

69. Amilca-Seba K, Sabbah M, Larsen AK, Denis JA. Osteopontin as a regulator of colorectal cancer progression and its clinical applications. *Cancers (Basel)* (2021) 13 (15):3793. doi: 10.3390/cancers13153793

70. Qian J, LeSavage BL, Hubka KM, Ma C, Natarajan S, Eggold JT, et al. Cancer-associated mesothelial cells promote ovarian cancer chemoresistance through paracrine osteopontin signaling. *J Clin Invest* (2021) 131(16):e146186. doi: 10.1172/JCI146186

71. Shirasaki T, Honda M, Yamashita T, Nio K, Shimakami T, Shimizu R, et al. The osteopontin-CD44 axis in hepatic cancer stem cells regulates IFN signaling and HCV replication. *Sci Rep* (2018) 8(1):13143. doi: 10.1038/s41598-018-31421-6

72. Dubois F, Bergot E, Zalcman G, Levallet G. RASSF1A, puppeteer of cellular homeostasis, fights tumorigenesis, and metastasis-an updated review. *Cell Death Dis* (2019) 10(12):928. doi: 10.1038/s41419-019-2169-x

73. Hou XJ, Zhao QD, Jing YY, Han ZP, Yang X, Wei LX, et al. Methylation mediated Gadd45beta enhanced the chemosensitivity of hepatocellular carcinoma by inhibiting the stemness of liver cancer cells. *Cell Biosci* (2017) 7:63. doi: 10.1186/s13578-017-0189-8

74. Tse OYO, Jiang P, Cheng SH, Peng W, Shang H, Wong J, et al. Genome-wide detection of cytosine methylation by single molecule real-time sequencing. *Proc Natl Acad Sci USA* (2021) 118(5):e2019768118. doi: 10.1073/pnas.2019768118

75. Fabrizio FP, Castellana S, Centra F, Sparaneo A, Mastroianno M, Mazza T, et al. Design and experimental validation of OPERA_MET-a panel for deep methylation analysis by next generation sequencing. *Front Oncol* (2022) 12:968804. doi: 10.3389/fonc.2022.968804

76. Li S, Tollefsbol TO. DNA Methylation methods: global DNA methylation and methylomic analyses. *Methods* (2021) 187:28–43. doi: 10.1016/j.ymeth.2020.10.002

77. Rauluseviciute I, Drablos F, Rye MB. DNA Methylation data by sequencing: experimental approaches and recommendations for tools and pipelines for data analysis. *Clin Epigenetics* (2019) 11(1):193. doi: 10.1186/s13148-019-0795-x

78. Xia S, Ye J, Chen Y, Lizaso A, Huang L, Shi L, et al. Parallel serial assessment of somatic mutation and methylation profile from circulating tumor DNA predicts treatment response and impending disease progression in osimertinib-treated lung adenocarcinoma patients. *Transl Lung Cancer Res* (2019) 8(6):1016–28. doi: 10.21037/tlcr.2019.12.09

79. O'Kane AL G, Shabir M, Law J, Bradbury P, Liu G, Sacher A, et al. P35.03 methylation signatures associated with T790M status in progressive NSCLC. *J Thorac Oncol* (2021) 16(3):S420. doi: 10.1016/j.jtho.2021.01.704

80. Shi D, Qin J, Liu B, Yin Y, Zhao B, Feng X, et al. 1222P a blood-based DNA methylation risk score (RS) for predicting the prognosis of EGFR mutation positive (EGFRm) advanced non-small cell lung cancer (NSCLC) after first-line TKI treatment. *Front Oncol* (2021) 11:691915. doi: 10.1016/j.annonc.2021.08.1827

81. O'Brien J, Hayder H, Zayed Y, Peng C. Overview of MicroRNA biogenesis, mechanisms of actions, and circulation. *Front Endocrinol (Lausanne)* (2018) 9:402. doi: 10.3389/fendo.2018.00402

82. Reda El Sayed S, Cristante J, Guyon L, Denis J, Chabre O, Cherradi N. MicroRNA therapeutics in cancer: current advances and challenges. *Cancers (Basel)* (2021) 13(11):2680. doi: 10.3390/cancers13112680

83. Hashida S, Yamamoto H, Shien K, Miyoshi Y, Ohtsuka T, Suzawa K, et al. Acquisition of cancer stem cell-like properties in non-small cell lung cancer with acquired resistance to afatinib. *Cancer Sci* (2015) 106(10):1377–84. doi: 10.1111/cas.12749

84. Shien K, Toyooka S, Yamamoto H, Soh J, Jida M, Thu KL, et al. Acquired resistance to EGFR inhibitors is associated with a manifestation of stem cell-like properties in cancer cells. *Cancer Res* (2013) 73(10):3051–61. doi: 10.1158/0008-5472.CAN-12-4136

85. Li XF, Shen WZ, Jin X, Ren P, Zhang J. Let-7c regulated epithelial-mesenchymal transition leads to osimertinib resistance in NSCLC cells with EGFR T790M mutations. *Sci Rep* (2020) 10(1):11236. doi: 10.1038/s41598-020-67908-4

86. Zhao JG, Men WF, Tang J. MicroRNA-7 enhances cytotoxicity induced by gefitinib in non-small cell lung cancer via inhibiting the EGFR and IGF1R signalling pathways. *Contemp Oncol (Pozn)* (2015) 19(3):201–6. doi: 10.5114/wo.2015.52655

87. Zhou YM, Liu J, Sun W. MiR-130a overcomes gefitinib resistance by targeting met in non-small cell lung cancer cell lines. *Asian Pac J Cancer Prev* (2014) 15(3):1391–6. doi: 10.7314/APJCP.2014.15.3.1391

88. Zhen Q, Liu J, Gao L, Liu J, Wang R, Chu W, et al. MicroRNA-200a targets EGFR and c-met to inhibit migration, invasion, and gefitinib resistance in non-small cell lung cancer. *Cytogenet Genome Res* (2015) 146(1):1–8. doi: 10.1159/000434741

89. Bisagni A, Pagano M, Maramotti S, Zanelli F, Bonacini M, Tagliavini E, et al. Higher expression of miR-133b is associated with better efficacy of erlotinib as the second or third line in non-small cell lung cancer patients. *PLoS One* (2018) 13(4): e0196350. doi: 10.1371/journal.pone.0196350

90. Ma W, Feng W, Tan J, Xu A, Hu Y, Ning L, et al. miR-497 may enhance the sensitivity of non-small cell lung cancer cells to gefitinib through targeting the insulin-

like growth factor-1 receptor. *J Thorac Dis* (2018) 10(10):5889–97. doi: 10.21037/jtd.2018.10.40

91. Wang F, Meng F, Wong SCC, Cho WCS, Yang S, Chan LWC. Combination therapy of gefitinib and miR-30a-5p may overcome acquired drug resistance through regulating the PI3K/AKT pathway in non-small cell lung cancer. *Ther Adv Respir Dis* (2020) 14:1753466620915156. doi: 10.1177/1753466620915156

92. Maharati A, Zanguei AS, Khalili-Tanha G, Moghbeli M. MicroRNAs as the critical regulators of tyrosine kinase inhibitors resistance in lung tumor cells. *Cell Commun Signal* (2022) 20(1):27. doi: 10.1186/s12964-022-00840-4

93. Yan H, Tang S, Tang S, Zhang J, Guo H, Qin C, et al. miRNAs in anti-cancer drug resistance of non-small cell lung cancer: recent advances and future potential. *Front Pharmacol* (2022) 13:949566. doi: 10.3389/fphar.2022.949566

94. Ferlay J, Ervik M, Lam F, Colombet M, Mery L, Piñeros M, et al. *global cancer observatory: cancer today*. Lyon: International Agency for Research on Cancer (2020). Available at: https://gcoiarcfr/today.

95. Islami F, Guerra CE, Minihan A, Yabroff KR, Fedewa SA, Sloan K, et al. American Cancer society's report on the status of cancer disparities in the united states, 2021. *CA Cancer J Clin* (2022) 72(2):112–43. doi: 10.3322/caac.21703

96. Nicholson AG, Tsao MS, Beasley MB, Borczuk AC, Brambilla E, Cooper WA, et al. The 2021 WHO classification of lung tumors: impact of advances since 2015. *J Thorac Oncol* (2022) 17(3):362–87. doi: 10.1016/j.jtho.2021.11.003

97. Thai AA, Solomon BJ, Sequist LV, Gainor JF, Heist RS. Lung cancer. *Lancet* (2021) 398(10299):535–54. doi: 10.1016/S0140-6736(21)00312-3

98. Chatterjee A, Rodger EJ, Eccles MR. Epigenetic drivers of tumourigenesis and cancer metastasis. *Semin Cancer Biol* (2018) 51:149–59. doi: 10.1016/j.semcancer.2017.08.004

99. Guo M, Peng Y, Gao A, Du C, Herman JG. Epigenetic heterogeneity in cancer. *biomark Res* (2019) 7:23. doi: 10.1186/s40364-019-0174-y

100. Lu Y, Chan YT, Tan HY, Li S, Wang N, Feng Y. Epigenetic regulation in human cancer: the potential role of epi-drug in cancer therapy. *Mol Cancer* (2020) 19(1):79. doi: 10.1186/s12943-020-01197-3

101. Oliver J, Garcia-Aranda M, Chaves P, Alba E, Cobo-Dols M, Onieva JL, et al. Emerging noninvasive methylation biomarkers of cancer prognosis and drug response prediction. *Semin Cancer Biol* (2022) 83:584–95. doi: 10.1016/j.semcancer.2021.03.012

102. Chen X, Gole J, Gore A, He Q, Lu M, Min J, et al. Non-invasive early detection of cancer four years before conventional diagnosis using a blood test. *Nat Commun* (2020) 11(1):3475. doi: 10.1038/s41467-020-17316-z

103. Farooq M, Herman JG. Noninvasive diagnostics for early detection of lung cancer: challenges and potential with a focus on changes in DNA methylation. *Cancer Epidemiol Biomarkers Prev* (2020) 29(12):2416–22. doi: 10.1158/1055-9965.EPI-20-0704

104. Shen SY, Singhania R, Fehringer G, Chakravarthy A, Roehrl MHA, Chadwick D, et al. Sensitive tumour detection and classification using plasma cell-free DNA methylomes. *Nature* (2018) 563(7732):579–83. doi: 10.1038/s41586-018-0703-0

105. Angeles AK, Janke F, Bauer S, Christopoulos P, Riediger AL, Sultmann H. Liquid biopsies beyond mutation calling: genomic and epigenomic features of cell-free DNA in cancer. *Cancers (Basel)* (2021) 13(22):5615. doi: 10.3390/cancers13225615

106. Kanwal R, Gupta K, Gupta S. Cancer epigenetics: an introduction. *Methods Mol Biol* (2015) 1238:3–25. doi: 10.1007/978-1-4939-1804-1_1

107. Keller L, Belloum Y, Wikman H, Pantel K. Clinical relevance of blood-based ctDNA analysis: mutation detection and beyond. *Br J Cancer* (2021) 124(2):345–58. doi: 10.1038/s41416-020-01047-5

108. Nunes SP, Diniz F, Moreira-Barbosa C, Constancio V, Silva AV, Oliveira J, et al. Subtyping lung cancer using DNA methylation in liquid biopsies. *J Clin Med* (2019) 8(9):1500. doi: 10.3390/jcm8091500

109. Guibert N, Pradines A, Favre G, Mazieres J. Current and future applications of liquid biopsy in nonsmall cell lung cancer from early to advanced stages. *Eur Respir Rev* (2020) 29(155):190052. doi: 10.1183/16000617.0052-2019

110. Luo H, Wei W, Ye Z, Zheng J, Xu RH. Liquid biopsy of methylation biomarkers in cell-free DNA. *Trends Mol Med* (2021) 27(5):482–500. doi: 10.1016/j.molmed.2020.12.011

Frontiers in Oncology

Advances knowledge of carcinogenesis and tumor progression for better treatment and management

The third most-cited oncology journal, which highlights research in carcinogenesis and tumor progression, bridging the gap between basic research and applications to imrpove diagnosis, therapeutics and management strategies.

Discover the latest Research Topics

See more →

Frontiers

Avenue du Tribunal-Fédéral 34
1005 Lausanne, Switzerland
frontiersin.org

Contact us

+41 (0)21 510 17 00
frontiersin.org/about/contact